GIAC
39
OGJ Articoli su giacimenti

CONTENTS

$N = \frac{N_p B_o + (W_p - W_e)}{B_o (c_e \Delta p)}$

CONTENTS

CONTENTS

Part 1

How to determine effective porosity

(a) Using a Washburn-Bunting porosimeter

GIVEN: Data obtained on a sandstone sample using a Washburn-Bunting porosimeter and calipers were as follows:

Volume of air removed from the interconnected pores and surfaces, cc.	3.3
Volume of air adsorbed on glass and core surfaces, cc.	0.6
Diameter of core, cm.	1.9
Length of core, cm.	3.8

FIND: Effective porosity of the core.

METHOD OF SOLUTION: The following equations are used:

$$\text{Per cent porosity} = \frac{\text{Pore volume}}{\text{Bulk volume}} \times 100 \quad (1)$$

$$\text{Pore volume} = \text{total volume air removed} - \text{volume air adsorbed on surfaces} \quad (2)$$

$$\text{Bulk volume} = \pi r^2 L \quad (3)$$

Where:

r = radius of core, cm.

L = length of core, cm.

SOLUTION:

Pore volume = 3.3 − 0.6 = 2.7 cc.

Bulk volume = (3.14) (1.9/2)² (3.8)

= 10.8 cc.

Per cent porosity = (2.7/10.8) × 100

= 25.0

DISCUSSION: This method of effective porosity determination is based on the ability of the apparatus to directly measure the gas contained by the pores of a sample. The gas is expanded from the pores and measured at atmospheric conditions.[1,2] Results obtained are considered accurate when care is taken to properly calibrate the apparatus for gas adsorbed on the glass and sample surfaces. Since the apparatus is constructed of glass, the method is restricted to laboratory use. The measurements are made fairly rapidly and the sample is contaminated with mercury during the test. Fairly small samples (½, ¾, or ⅞ in.) are used in the procedure.

(b) Using flood-pot data

GIVEN: A sample taken from the Bartlesville sand in Greenwood County, Kansas, was placed in a flood pot and water flooded for 12 hours. At the end of this period it was placed in a high-pressure container and subjected to 1,000 psig. mercury pressure. By means of a mercury pump it was observed that 1.5 cc. of mercury entered the core and that the bulk volume was 72.0 cc. The core was then placed in a retort and the following data obtained:

Volume of water extracted	11.0 cc.
Volume of oil extracted	3.0 cc.

FIND: Effective porosity and fluid saturations after flooding.

METHOD OF SOLUTION: Applying Equation 1 to the recovered fluids:

$$\text{Per cent porosity} = \frac{\text{Vol. gas} + \text{vol. oil} + \text{vol. water}}{\text{Bulk volume}} \times 100 \quad (4)$$

For each of the three fluids, the per cent saturation is found by:

$$\frac{\text{Volume of fluid}}{\text{Pore volume}} \times 100$$

SOLUTION:

$$\text{Per cent porosity} = \frac{1.5 \text{ cc.} + 3.0 \text{ cc.} + 11.0 \text{ cc.}}{72.0 \text{ cc.}} \times 100 = 21.5$$

Per cent oil saturation

$$= \frac{3.0 \text{ cc.}}{15.5 \text{ cc.}} \times 100 = 19.3$$

Per cent water saturation

$$= \frac{11.0 \text{ cc.}}{15.5 \text{ cc.}} \times 100 = 71.0$$

Per cent gas saturation

$$= \frac{1.5 \text{ cc.}}{15.5 \text{ cc.}} \times 100 = 9.7$$

DISCUSSION: Flood-pot tests are performed to determine the ability of water to displace additional oil from a partially or primary depleted sand. The test involves the radial injection of water into a core with fluid production obtained from a hole drilled in the center and throughout the entire length of the core. Provisions are made to trap and measure any oil displaced. After a flood-pot test is completed, most of the pore space in the core is filled with water and residual oil. A small amount of pore space may also be filled with gas. The latter can readily be measured by means of mercury injection under high pressure. Subsequent retorting of the sample will yield the fraction of the pore volume occupied by oil and water.

This method of porosity and fluid-saturation determination is considered reliable if the retorts are carefully calibrated for oil losses due to coking and water losses and/or gains due to evaporation, and water of crystallization. Care must also be taken not to loose liquids from the core in the mercury chamber and to calibrate the chamber and mercury pump for expansion under pressure.

(c) Using retort and mercury injection data

GIVEN: Two test samples were taken from adjacent positions of fresh Oklahoma Squirrel sandstone cores. Mercury was injected into sample No. 1 while sample No. 2 was retorted. The following data were obtained on the two samples:

Sample No. 1:	
Bulk volume, cc.	13.68
Weight, g. (before mercury injection)	32.50
Vol. mercury injected, cc.	0.73
Sample No. 2:	
Weight, g.	120

Corrected volume of liquids extracted:

Oil, cc.	1.00
Water, cc.	3.80

FIND: Effective porosity and fluid saturations of the fresh core.

METHOD OF SOLUTION: Additional equations needed for this method are:

$$\text{Bulk density of core} = \frac{\text{Wt. of sample}}{\text{Bulk vol. of sample}} \quad (5)$$

$$\text{Bulk volume of sample} = \frac{\text{Wt. of sample}}{\text{Bulk density of core}} \quad (6)$$

SOLUTION:

$$\text{Bulk density of core} = \frac{32.50 \text{ g.}}{13.68 \text{ cc.}} = 2.38 \text{ g./cc.}$$

$$\text{Bulk volume Sample 2} = \frac{120}{2.38} = 50.4 \text{ cc.}$$

$$\text{Volume of gas in Sample 2} = 0.73 \text{ cc.} \times \frac{120 \text{ g.}}{32.5 \text{ g.}} = 2.70 \text{ cc.}$$

$$\text{Per cent porosity (Sample 2)} = \frac{2.70 + 1.00 + 3.80}{50.4} \times 100 = 14.9$$

$$\text{Oil saturation (Sample 2)} = \frac{1.00}{7.50} \times 100 = 13.3\%$$

$$\text{Gas saturation (Sample 2)} = \frac{2.70}{7.50} \times 100 = 36.0\%$$

$$\text{Water saturation (Sample 2)} = \frac{3.80}{7.50} \times 100 = 50.7\%$$

DISCUSSION: Fluid saturation and porosity can be determined by this method in the field as well as in laboratory and is widely used.[3] It measures pore volume from a summation of the fluids contained in the pores. Volume occupied by oil and water is determined by retort extraction while volume occupied by gas is determined by mercury injection into a fresh sample obtained at a point adjacent to the sample used for retort extraction. Corrections are applied to retort readings for coking and cracking of the oil and for combined water recovered.

Samples several times the size of those used by most other methods are used and thus should give more representative formation porosity and fluid saturations. This procedure has been found to be of particular advantage in determining the porosity of samples containing shale which normally undergo shrinkage upon drying. Porosity determinations are claimed to be within 2% accuracy while the fluid-saturation-determination accuracy varies from 2% (water) to 5% (oil).

The method is accurate enough for almost any application. No error is involved due to salt deposition from the water content of the samples or due to loss of sand grains in handling. It should be noted, however, that the combined data of two adjacent samples are used. It is apparent that in some formations appreciable variations in porosity and fluid saturations will occur even between adjacent samples.

References

1. "Engineering Fundamentals on Petroleum Reservoirs," manual, The Oil and Gas Journal, pp. 29-30.
2. Pirson, S. J., "Elements of Oil Reservoir Engineering," McGraw-Hill Publishing Co., second edition, 1958, pp. 36-37.
3. Core Laboratories, Inc., "Summary of Core-Analysis Procedures" prepared for API Subcommittee on Standardization of Core-Analysis Procedures.

Part 2

More on how to determine effective porosity

By large core analysis

OBJECT: To determine the porosity of large-diameter core samples using laboratory measurements on large cores.

GIVEN: Various measurements were made using micrometer calipers and the apparatus schematically pictured:

Equilibrium pressure with billet, 139.7 cm. Hg.
Equilibrium pressure without billet, 38.1 cm. Hg.
Equilibrium pressure with core, 114.3 cm. Hg.
Equilibrium pressure without core, 38.1 cm. Hg.
Diameter of core, 8.80 cm.
Length of core, 19.00 cm.
Diameter of steel billet, 9.00 cm.
Length of steel billet, 20.00 cm.

METHOD OF SOLUTION: (A) **Bulk volume** is computed from micrometer measurements of diameter and length, provided the core sample is a smooth cylinder. If the core is irregular in shape, the bulk volume is calculated using a mercury-submergence procedure similar to that used for small cores.

Bulk volume $= \pi r^2 L$ (for cylinders)
r = radius of core
L = length of core.

(B) **Grain volume** is computed from the following formula using measurements made with air-expansion-type apparatus:

$$C = \frac{P_b - P_e}{\text{billet volume}}$$

$$\text{Grain volume} = \frac{P_c - P_e}{C}$$

C = calibration factor
P_b = pressure with steel billet
P_e = pressure without billet, i.e., empty
P_c = pressure with core
P_e = pressure without core

Apparatus for Grain Volume Determination

The apparatus for determining grain volume is shown schematically in the figure. It consists of a dry air supply, a surge tank of approximately 10 gal. capacity, a primary pressure cell, core chamber, and mercury manometers on the inlet and outlet sides. The core chamber is made of steel pipe, approximately 5½ in. i.d. A set of concentric steel sleeves is provided for adjustment of the effective core cham-

$$\text{(C) Porosity, \%} = \frac{\text{bulk volume of core} - \text{grain volume}}{\text{bulk volume of core}} \times 100$$

SOLUTION:

Steel billet volume $= \pi r^2 L = 3.1416 \times (4.50)^2 \times 20.0 = 1272.3$ cu. cm.

Bulk volume of core $= \pi r^2 L = 3.1416 \times (4.40)^2 \times 19.0 = 1155.6$ cu. cm.

$$C = \frac{P_b - P_e}{\text{billet volume}} = \frac{139.7 - 38.1}{1272.3} = .07986$$

$$\text{Grain volume} = \frac{P_c - P_e}{C} = \frac{114.3 - 38.1}{.07986} = 954.2$$

$$\text{Porosity} = \frac{1155.6 - 954.2}{1155.6} \times 100 = 17.4\%$$

ber diameter to a value slightly greater than the diameter of the core sample to be tested. End plugs are used to reduce the annular space in the core chamber after the core is in place.

Calibration and Test Procedure

Because of the sensitivity of pressure-volume measurements of air to temperature, room temperature must be maintained constant. The inlet dry air supply is regulated to approximately 230 cm. Hg. The air space volume of the primary pressure cell is adjusted by the addition of mercury until the space occupied by air is approximately equal to the average volume of the annular space in the core chamber plus the volume of the void space within the core.

After inserting an appropriate sleeve and end plugs and adjusting the volume of primary cell, air is admitted at test pressure to the primary pressure cell, the pressure recorded, and the air supply cut off. The core chamber is then closed and the valve between the core chamber and primary pressure cell is opened, allowing air to expand from the primary pressure cell into the core chamber. After equilibrium between the two cells is attained, the equilibrium pressure is read on the downstream manometer. The valve connecting the primary pressure cell with the core chamber is then closed and the core chamber depressured to atmospheric. A steel billet approximately the size of the core to be tested is placed in the chamber and the procedure repeated, with the equilibrium pressure again noted. Lastly, the core to be tested is placed in the chamber, the procedure repeated, and equilibrium pressure observed. The three equilibrium pressures, together with the volume of the steel billet, are used to calculate the grain volume as previously described.

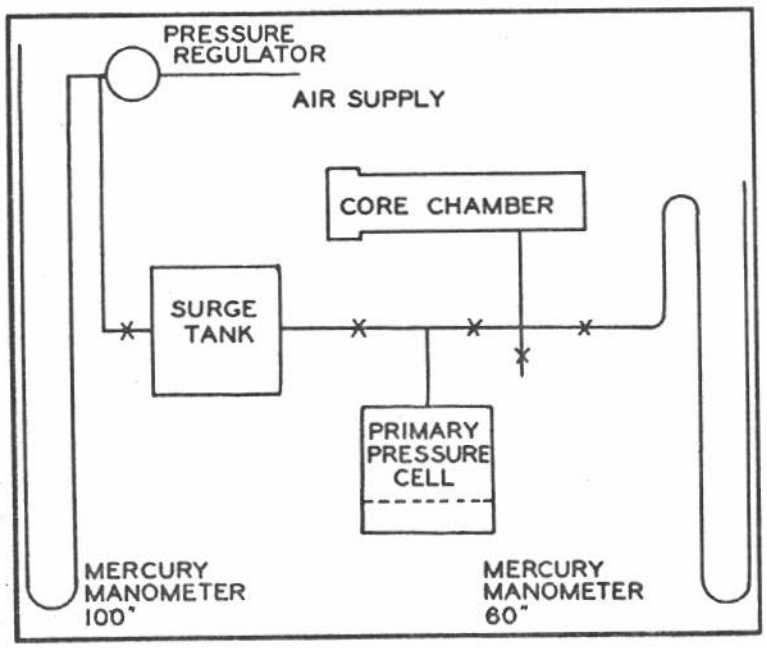

APPARATUS for determining grain volume.

DISCUSSION: Porosity determined by this method is obviously the effective porosity, being the connected void space into which the expanding air may flow. Disconnected pores which do not receive air are not included in the computed porosity.

As in most other methods of determining porosity on large or small core samples, the coring, sampling, handling, and cleaning procedures may affect the results. Because of the much larger size of the sample, errors in porosity determination introduced through coring, sampling, and handling are likely to be less on large cores than on plugs.

As expected, it is more difficult to obtain reliable porosity values on low-permeability samples, either on limestones and dolomites, or "tight" or shaly sandstones. Much more time and care are required in the testing of such samples to make sure that equilibrium has been gained between pressure in primary cell and core chamber.

As an example, some of the gas-producing sandstones of Cretaceous age in the San Juan basin of New Mexico and Colorado are quite shaly. On one well porosity reported on cores obtained by coring with gas averaged around 4%. However, water saturation on companion samples was reported at 70 to 100%, which appeared too high. In rechecking laboratory data and retesting some samples, it was found that equilibrium pressure had not been attained in most cases. Permeability was on the order of only a few tenths of a millidarcy. The average porosity as rerun was about 8%.

On this type sample, too, the effects of other factors are likely to be greater: air adsorption, because of greater surface area; shrinkage of clays or removal of water of crystallization or fine particles during cleaning; and incomplete cleaning. In addition, the porosity of the sample as tested may be different from that which existed in place before the core was cut. Such differences are due to the changes in conditions surrounding the core in removing it from the formation and getting it in the laboratory ready for testing.

Part 3

Effective porosity from MicroLog and Microlaterolog data

(a) OBJECT: To determine effective porosity using MicroLog data.

GIVEN: MicroLog obtained with hydraulic pad (also referred to as contact log and micropetrograph) for well completed in a sand formation. The resistivities of the mud cake and mud filtrate were measured as 1.20 ohm m^2/m and 1.00 ohm m^2/m respectively at the bottom-hole temperature of 150° F. The residual-oil saturation in the flushed zone was estimated to be 20%.

METHOD OF SOLUTION:

$$\phi = \frac{1}{1 - S_{or}} (0.62\, R_{mf}/R_{xo})^{1/2.15} \quad (1)$$

Where

ϕ = porosity, fraction

S_{or} = residual-oil saturation in flushed zone

R_{mf} = resistivity of mud filtrate, ohms m^2/m

R_{xo} = resistivity of flushed zone, ohm m^2/m

SOLUTION:

From Fig. 1

$R_{1''\times 1''}$ = 3.0 ohm m^2/m = micro-inverse resistivity reading.

$R_{2''}$ = 4.7 ohm m^2/m = micro normal resistivity reading.

d = 8″ = diameter of hole.

$$\frac{R_{1\times 1}}{R_{mc}} = \frac{3.0}{1.2} = 2.5$$

$$\frac{R_2}{R_{mc}} = \frac{4.7}{1.2} = 3.9$$

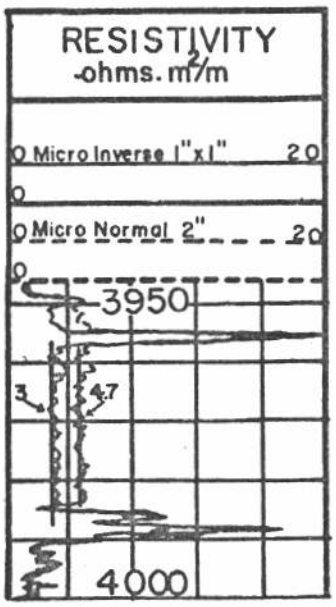

TYPICAL MicroLog for a sand formation. Fig. 1.

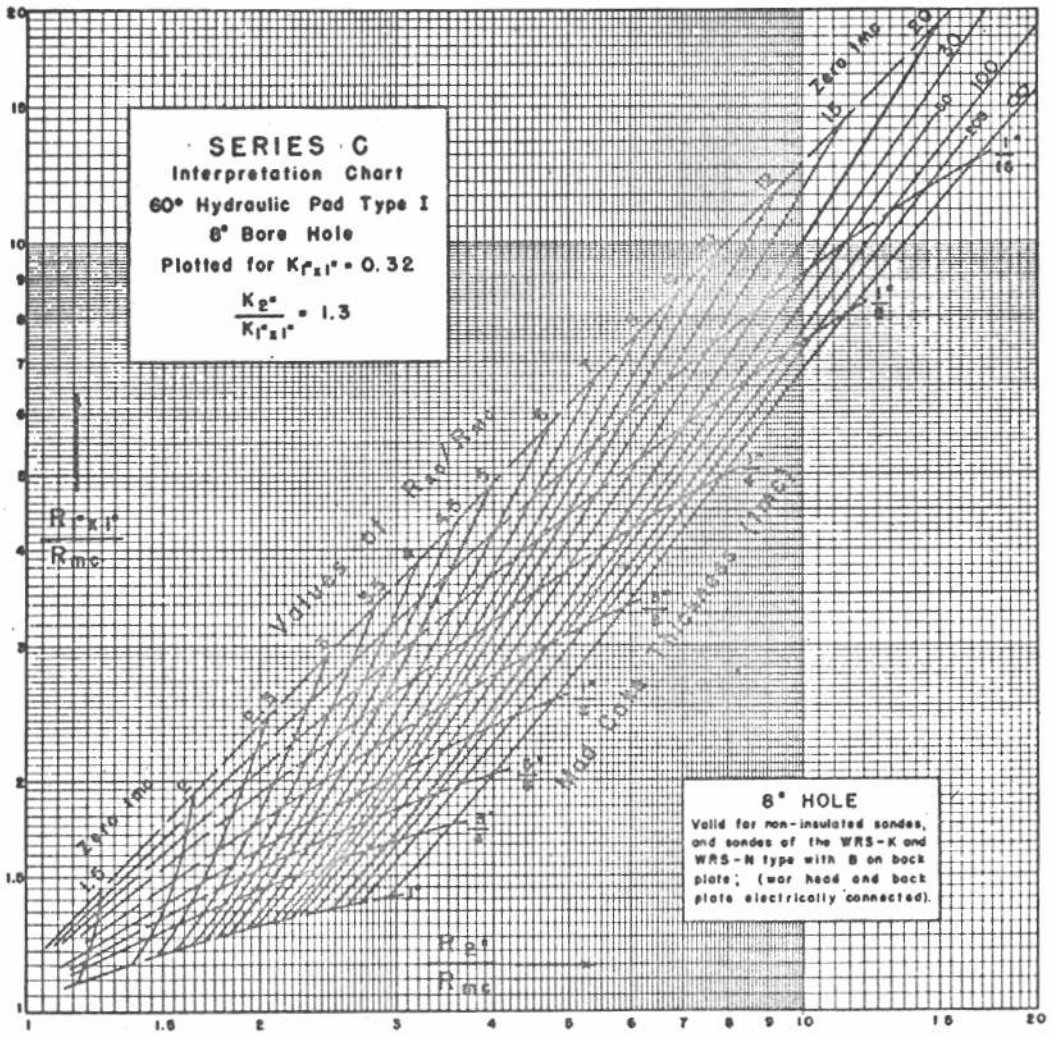

RELATION between MicroLog resistivity readings, resistivity of invaded zone, and thickness of mud cake. Reproduced by permission from Schlumberger Well Surveying Corp. Log Interpretation Charts manual, p. C-4. Fig. 2.

From Fig. 2

$$\frac{R_{xo}}{R_{mc}} = 17$$

Therefore:

$$R_{xo} = 17 \times R_{mc}$$

$$= 17 \times 1.2$$

$$= 20.4 \text{ ohm m}^2/\text{m}$$

$$\phi = \frac{1}{1-0.2}(0.62 \times 1.0/20.4)^{1/2.15}$$

$$= 0.246$$

or, porosity is 24.6%.

DISCUSSION: The determination of porosity from resistivity measurements depends upon the relationship of formation factor and porosity. This relationship in its most general form is:[1]

$$F = \frac{a}{\phi^m} \qquad (2)$$

Where:

F = resistivity of a rock saturated with a conductive fluid divided by the resistivity of the saturating conductive fluid
a = constant
m = cementation factor

The value of m has been found to vary from 1.3 to 2.3. The form of Equation 2 most used for clean formations (very little or no shale) is as follows:

$$\phi = (0.62/F)^{1/2.15}$$

$$= (0.62\, R_{mf}/R_{xo})^{1/2.15} \qquad (3)$$

Equation 3 applies to formations fully saturated with water. For formations that contain hydrocarbons in addition to water Equation 3 is modified to Equation 1. In order to solve Equation 1, S_{or} must be known. Statistical analysis of flood-pot laboratory tests indicate that S_{or} varies from 0.10 to 0.25, with most clean formations having values of approximately 0.20. Consequently, using a value of 0.20 generally gives good results in clean formations with granular porosity. Greater residual-oil saturations may occur in the cases of low-gravity (viscous) oil and low-permeability formations where the flushing action of the mud filtrate is less efficient.

Fig. 2 used in the solution of this problem is a chart drawn from laboratory measurements. It relates the MicroLog resistivity readings to both the flushed zone resistivity, R_{xo}, and the mud cake thickness. As noted, R_{mc} is used as a base. The graph applies for MicroLog measurements made with a hydraulic pad and for 8-in.-diameter holes. Readings can be corrected for application to holes of other sizes. This method of porosity determination gives the best results for formations having porosities greater than 15%. For lower porosities the mud cake becomes thick (greater than ½ in.), the R_{xo}/R_{mf} ratio becomes large (greater than 25) and readings from the chart become less reliable.

Porosity determination using MicroLogs has an advantage over core analysis in that a much larger sample is involved.

(b) OBJECT: To determine effective porosity using Microlaterolog data.

GIVEN: Microlaterolog resistivity measurements and other data for a clean low-porosity sand as follows:

Resistivity from Microlaterolog = 25 ohm m²/m.

Thickness of mud cake from filter-press measurements less than ¼ in.

Estimated residual-oil saturation = 20% of pore volume.

Resistivity of mud filtrate = 0.06 ohm m²/m.

METHOD OF SOLUTION: Equation 1 from (a) applies to this problem.

SOLUTION: It has been established that for thin mud cakes (thicknesses less than ¼ in.) the Microlaterolog reading is a reliable value of the flushed-zone resistivity (R_{xo}). Therefore,

$$R_{xo} = R_{MLL} = 25$$

$$R_{mf} = 0.06$$

$$S_{or} = 0.20$$

and

$$\phi = \frac{1}{1-0.20}(0.62 \times 0.06/25)^{1/2.15}$$

$$= 0.06$$

or, porosity is 6.0%.

DISCUSSION: In formations having porosities of 15% or less the survey currents of the MicroLog (also referred to as contact log or micropetrograph) flow mostly in the mud cake and thus reflect little of the character of the formation beyond the mud cake.[2] Under such conditions the MicroLog fails to give reliable information from which the resistivity and porosity of the invaded zone can be determined. In order to obtain reliable values in low-porosity formations, the Microlaterolog was developed. It consists of a micro device involving a focusing system in which the effect of the mud cake on the measurements obtained is reduced. In fact, for mud-cake thicknesses of less than ¼ in. this tool measures directly the resistivity of the invaded zone. For mud-cake thicknesses greater than ¼ in., it is necessary to correct the measurements for deviations caused by the mud cake. This can be done by referring to Microlaterolog departure curves.[3]

This method of effective porosity determination is especially convenient where thin mud cakes prevail. As a rule, wells drilled with high-salinity muds have thin mud cakes. The same is true of wells drilled in hard-rock country.

References

1. Martin, Maurice, "With the MicroLog You Can Be Sure," Part 2, The Oil and Gas Journal, October 24, 1955.

2. Tixier, M. P., "MicroLog and Microlaterolog," Fundamentals of Logging, University of Kansas Bookstore, pp. 57-65.

3. Wyllie, M. R. J., The Fundamentals of Electric Log Interpretation, Academic Press, Inc., Second Edition.

4. Schlumberger Well Surveying Corp., Log Interpretation Charts.

Part 4

Development of neutron-derived porosity curve

GIVEN: Core-analysis porosity measurements and neutron log for a 53-ft. interval in a limestone formation.

FIND: Neutron - derived porosity curve.

METHOD OF SOLUTION: The following describes the stepwise procedure of solution:

1. Establish an instrument zero line on the log. Fig. 1.

2. Plot gamma-ray and neutron curves on 10 by 10 cross-section paper. Fig. 1.

3. Plot core porosities on 10 by 10 cross-section paper using a scale arranged opposite to that of the neutron log. That is to say high-porosity readings will correlate with low neutron values. Fig. 1.

4. Correlate the plotted porosity curve with the neutron curve and note core-depth adjustment to neutron curve. Fig. 1 and Table 1.

5. Record opposite each core depth and corresponding porosity the actual depth and neutron deflection in inches. Table 1.

6. Plot neutron deflection on two-cycle semilog paper versus porosity. Fig. 2.

7. Draw a straight line through the plotted points. Fig. 2.

The initial gamma-ray and neutron curves are plotted on 10 by 10 cross-section paper. Core porosities are plotted on similar paper with porosities increasing from right to left, and correlated with the neutron-log plot by adjusting vertical scale upward or downward as required. When the correlation has been made, all data are transferred to a single sheet of cross-section paper, as in Fig. 1. This adjustment in depth is necessary because log depths and core depths usually do not coincide, and the log depth is considered the more accurate of the two.

Once this correlation is made, the neutron deflection corresponding to each core porosity is read (in inches or any other convenient unit) from the instrument zero line and recorded in Table 1. From these data a plot of core porosity and neutron deflection is constructed as shown in Fig. 2. The same neutron deflections can then be used to read porosity values from the curve, Fig. 2, to give the neutron-derived porosity correlation shown in Fig. 1, the data for which are tabulated in Table 1.

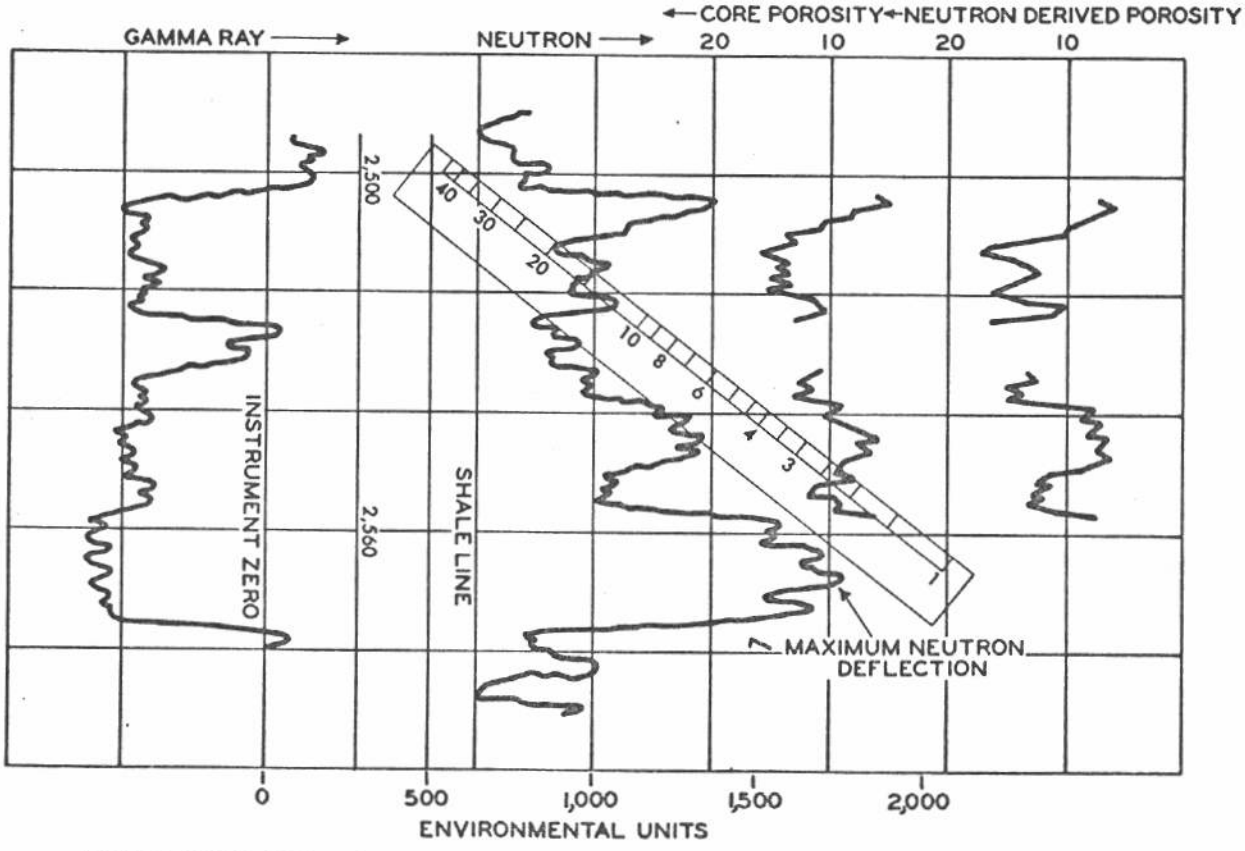

RADIOACTIVITY LOG with core and neutron-derived porosities for limestone formation. Fig. 1.

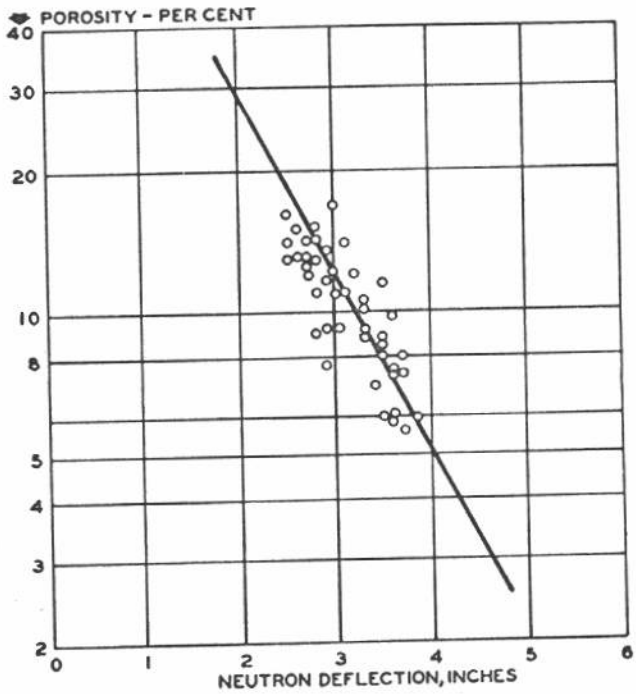

NEUTRON-DERIVED porosity curve. Fig. 2.

DISCUSSION: Research technologists have well established that the response recorded by the neutron curve is inversely proportional to the number of hydrogen atoms present in the vicinity of the instrument. Hydrogen atoms are contained in oil, gas, distillate, and water. The amount of these fluids present in clean formations traversed by a borehole is in turn dependent on the existing porosity. A high porosity (30 to 40%) would mean a high fluid and hydrogen-atom content and the neutron log would record a low value. A low porosity (5 to 10%) would mean a small fluid and hydrogen-atom content and the neutron log would record a high value. Presence of borehole fluid also affects the neutron values. However, if this is kept constant, variations in formation porosities can be detected.

The neutron response is affected by both chemically combined (water of crystallization) and free fluids. Shales normally exhibit the greatest amount of chemically combined and free fluids and thus show the lowest values on the neutron curves. Limestones and dolomites often have very low porosities and show high values on the neutron curve.

This method of porosity determination depends on the interrelationships that normally exist among neutron deflection, fluid content, and porosities. It also depends strongly on good core recovery and analysis. The idea is to select a representative well or wells in a field or area and to develop a neutron-derived porosity curve that can, in turn, be used for porosity determinations in subsequent wells. Thus in any subsequent well in which a neutron log was obtained, the neutron deflections (in the formations of interest) could be referred to the neutron-derived porosity curve and the respective porosities noted. It is apparent from this that the neutron-derived porosity curve must be representative of the field or area under study. Furthermore, the neutron logs from any subsequent wells must have been obtained under conditions of the same hole size; same casing type, and size; and in the same type of mud used in the base well. Wherever any or all of these conditions differ, then a new base curve would be required. Consequently, following the procedure outlined, several base curves (to satisfy varying conditions of hole size, casing size, and type of drilling fluid used) may be required for a field or area.

Statistically, an average porosity for medium to thick intervals of similar rock characteristics derived by this method should be fairly reliable. However, porosity determination is quite sensitive to several factors as discussed above, particularly hole size. Since hole size can vary considerably within a given well or from well to well even when the same size bit is used, the porosity determination for a point or a thin layer by this method may be subject to considerable error unless corrections for these variations are taken into account.

It is possible, by using a simplified procedure, to refer all neutron logs to base curve although well hole and casing sizes may have varied. The technique here is to use a logarithmic scale reading from 1 to 44. From the base curve establish a representative porosity value for the shale line (35.0% for the example given) and a representative porosity value for the maximum neutron deflection value (2.5% for the example given). Thus placing the 35% reading of the scale on the shale line and the 2.5% reading on the maximum deflection line, Fig. 1, porosity values can be read for any deflection in between.

And for the neutron logs of any subsequent wells in the area it would only be necessary to locate a shale line that is equivalent to shale used in the base well and similarly maximum neutron deflection line. On these the scale would be used as described for the base log. Any differences caused by hole size, casing size, or type of fluid would be compensated for by the slope assumed by the scale.

Porosity determination from neutron logs has been found to have good applicability in carbonate-type formations and for clean sandstones. In formations containing shale and other similar impurities, the method is less reliable because of the chemically held water that is characteristic of these formations.

Study of neutron-derived porosity curves indicates that they actually may be S-shaped instead of straight lines with the deviations from a straight line occurring above 25% porosity and below 5% porosity. This would tend to make the shale-line porosity higher and the maximum-deflection porosity lower than indicated by the straight line. In the normal usage of a neutron porosity scale shales are frequently assigned a porosity value of 40% and the maximum neutron deflections a porosity value of 1 to 2%.

TABLE 1—CORE ANALYSIS AND NEUTRON-LOG DATA

Actual depth, ft.	Core depth, ft.	Porosity %	Neutron deflection, in.	Neutron derived porosity, per cent
2504	2498	6.0	3.5	7.3
05	99	6.0	3.8	5.7
06	2500	8.1	3.7	6.2
07	01	8.6	3.5	7.3
08	02	10.3	3.3	8.6
2509	2503	11.0	3.1	10.2
10	04	14.0	3.1	10.2
11	05	13.0	2.8	13.0
12	06	14.0	2.5	16.6
13	07	16.0	2.5	16.6
2553	47	11.8	2.9	12.0
54	48	9.3	2.9	12.0
55	49	9.0	2.8	13.0
2556	2550	9.3	3.0	11.1
57	51	5.9	3.6	6.8

Acknowledgement . . . The authors thank S. W. McGaha, Lane Wells Co., Tulsa, for his assistance and review of this problem.

Bibliography

Hamilton, R. G. and Charrin, P., "How to Find Porosity From Normal Curve and Neutron Log," Contained in Manual "How To Interpret Electric Logs . . . Quantitative Log Analysis," published by The Oil and Gas Journal.

Bush, R. E. and Murdock, E. S., "The Quantitative Interpretation of Radioactivity Logs," Petroleum Transactions, AIME, Vol. 192, 1951.

Part 5

Effective porosity and water saturation from electric and MicroLog data

GIVEN: Electric and MicroLogs for a well showing a shaly sand lying in the subsurface interval of 1,562-76 ft. Other data obtained were as follows:

Hole size, 7⅞ in.

Resistivity of mud = 0.9 ohm m²/m at 67° F.

Resistivity of mud = 0.65 ohm m²/m at 95° F.

Resistivity of mud filtrate = 0.6 ohm m²/m at 95° F.

Resistivity of mud cake = 1.45 ohm m²/m at 95° F.

$S_{xo} = S_w^{1/5}$ (from laboratory tests on numerous cores).

K = 72.

FIND: Effective porosity and water saturation of the shaly sand.

METHOD OF SOLUTION: The following equations are used:

$$\frac{1}{R_t} = \frac{p}{R_{sh}} + \frac{(1-p)\,S_w^2}{F R_w} \quad (1)$$

$$\frac{1}{R_{xo}} = \frac{p}{R_{sh}} + \frac{(1-p)\,S_{xo}^2}{F R_{mf}} \quad (2)$$

$$PSP = -K \log \frac{R_{xo}}{R_t}$$

$$-2\,a\,K \log \frac{S_{xo}}{S_w} \quad (3)$$

$$F = 0.62/\phi^{2.15} \text{ (Humble formula)} \quad (4)$$

Where:

R_t = true resistivity of bulk sand and shale

p = shale, fraction of bulk

R_{sh} = resistivity of shale

S_w = connate-water saturation in effective pore volumes

F = formation factor of a clean sand = R_o/R_w

R_w = resistivity of connate water

R_{xo} = resistivity of the invaded zone adjacent to the borehole

S_{xo} = mud-filtrate saturation adjacent to borehole in effective pore volumes

PSP = self-potential reading opposite thick shaly bed

SSP = self-potential reading opposite thick clean bed

K = coefficient of the SP formula

a = ratio of PSP and SSP

ϕ = effective porosity

R_o = resistivity of bed fully saturated with connate water

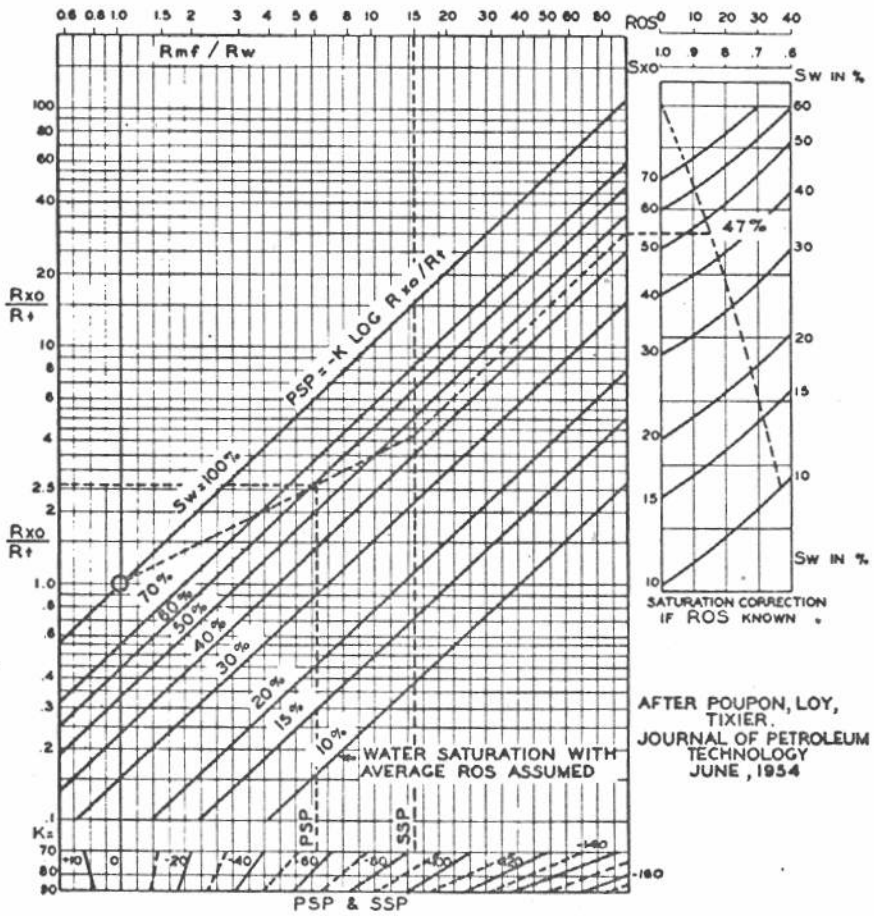

NOMOGRAPH for determination of water saturation from log data. Fig. 1.

SOLUTION:

Fig. 1 is a nomograph which represents a rigorous solution of Equation 3. Similarly, Fig. 2 is a solution of Equations 1, 2, 3, and 4. These figures and the equations represent two possible solutions to the problem. Water saturation can be obtained from Fig. 1 or by the solution of Equation 3. Porosity can be gotten from Fig. 2 or by the simultaneous solution of the four equations. Both methods of solution will be considered.

In the four equations, the unknowns are p, S, F, and ϕ. Since there is an equation for each unknown, an analytical solution is possible. Equation 3 will first be solved for the water saturation. From the two logs (Figs. 3 and 4) we obtain the following data:

PSP = −55 mv

SSP = −82 mv (from nearby clean sand)

R_t = 4 ohm m²/m

$R_{1''\times1''}$ = 3.6 ohm m²/m

$R_{2''}$ = 4.6 ohm m²/m

$$\frac{R_{1''\times1''}}{R_{mc}} = \frac{3.6}{1.45} = 2.5$$

$$\frac{R_{2''}}{R_{mc}} = \frac{4.6}{1.45} = 3.2$$

Using these two ratios and Fig. 2, page 5, a value for R_{xo}/R_{mc} = 7.25 is obtained. From this R_{xo} = 7.25 R_{mc} = (7.25) (1.45) = 10.5.

Also

$$a = \frac{PSP}{SSP} = \frac{-55}{-82} = 0.67$$

Now solving Equation 3,

$$-55 = -72 \log \frac{10.5}{4}$$

$$-- (2)(0.67)(72)\log\frac{S_w^{1/5}}{S_w}$$

then

$$\log\frac{1}{S_w^{4/5}} = \frac{25.0}{96.5} = 0.26$$

$$\frac{1}{S_w^{0.8}} = 1.82$$

$$S_w = 0.472, \text{ or } 47.2\%$$

Note on Fig. 1 that using $R_{xo}/R_t = 2.6$, PSP, SSP, and $S_{xo} = S_w^{1/5}$ that a value of S_w of 47% is obtained.

Equations 1, 2, and 4 will next be solved for porosity.

$$S_{xo} = (S_w)^{1/5} = (0.472)^{0.2} = 0.860$$

or 86.0%

From Fig. 1 for SSP = −82,

$$\frac{R_{mf}}{R_w} = 15 \text{ and}$$

$$R_w = \frac{(0.6)}{15} = 0.04$$

Then,

$$\frac{1}{4} = \frac{p}{3} + \frac{(1-p)(0.472)^2}{F(0.04)} \quad (1)$$

from which,

$$p = \frac{0.25F - 5.6}{0.33F - 5.6} \quad (5)$$

And,

$$\frac{1}{10.5} = \frac{p}{3} + \frac{(1-p)(0.86)^2}{F(0.6)} \quad (2)$$

from which,

$$0.095F = 0.33pF + 1.23 - 1.23p \quad (6)$$

Substitution of Equation 5 into 6 gives

$$0.095F = 0.33F\left(\frac{0.25F - 5.6}{0.33F - 5.6}\right) + 1.23 - 1.23\left(\frac{0.25F - 5.6}{0.33F - 5.6}\right)$$

and,

$$F = 23.9$$

Now substituting into Equation 4 and solving for porosity,

$$23.9 = \frac{0.62}{\phi^{2.15}}$$

$$\phi = 0.183 \text{ or } 18.3\%$$

From Fig. 2, using $R_{xo}/R_t = 2.6$, $a = 0.67$, $R_{xo}/R_{mf} = 10.5/0.6 = 17.5$, and $S_{xo} = 0.86$ a value of 17.0% is obtained for the porosity.

DISCUSSION: Equations 1 and 2 express the parallel flow of electricity in a sand containing shale laminations.[1] Equation 3 expresses the influence of the respective parameters involved on the self-potential obtained from a similar shaly sand.[2] Although a large number of shaly sands are of this type, there are also many that contain the shale in a dispersed state. Equations somewhat similar to the ones presented have been developed for the latter case. Many shaly sands of both a laminated and dispersed shale nature have been analyzed using both sets of equations. It was found that the porosities and water saturations obtained independently from the two sets of equations were about the same.[1] Since the equations for sands with laminated shales are more convenient to represent with nomographs, they are used more extensively.

Note that in the case of water saturation excellent agreement was obtained in the values determined by solution of Equation 3 and by use of Fig. 1. In the case of porosity, the agreement was good. Consequently, the nomographs give reliable solutions of the equations and considerably simplify the approach.

This method of determining water saturation and porosity of shaly sands is relatively new and not enough experience has been obtained to fully evaluate its reliability. It depends principally on accurate determination of the electrical parameters involved. Under many borehole and formation conditions various tools fail to give reliable data.

For instance, the determination of the true resistivity of thin formations with the electric log is not always reliable. In the problem under consideration, the sand and adjacent beds have approximately the same resistivity. And since the bulk of sand volume penetrated by the lateral and long normal devices is large compared with the borehole volume, the true resistivity should be approximately that recorded by these devices. Appreciable error could be involved in this assumption.

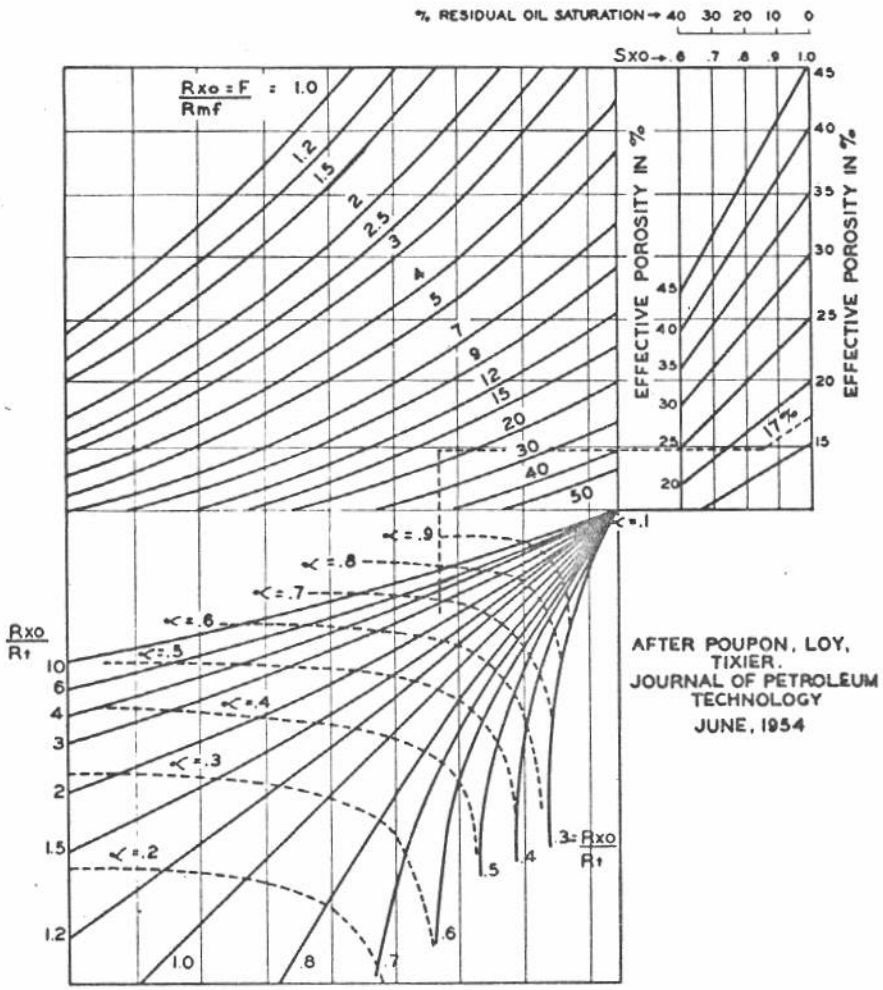

NOMOGRAPH for determination of porosity in shaly sands from log data. Fig. 2.

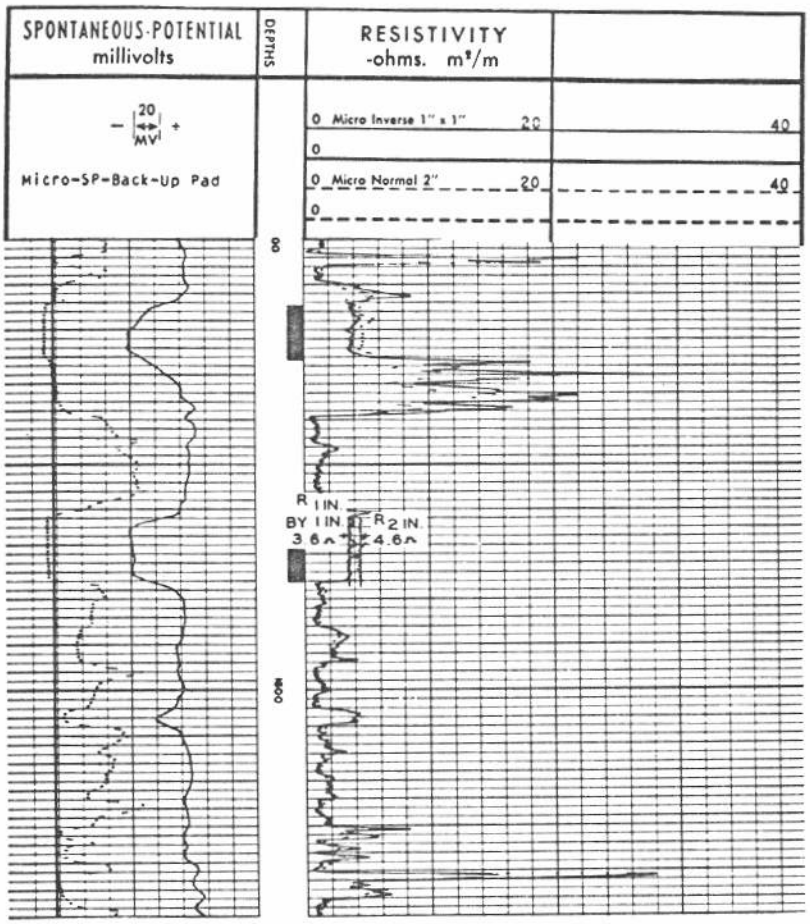

THE MICROLOG, above, and the electric log, below, are of the same shaly sand at a depth of 1,562-76 ft. Figs. 3 and 4.

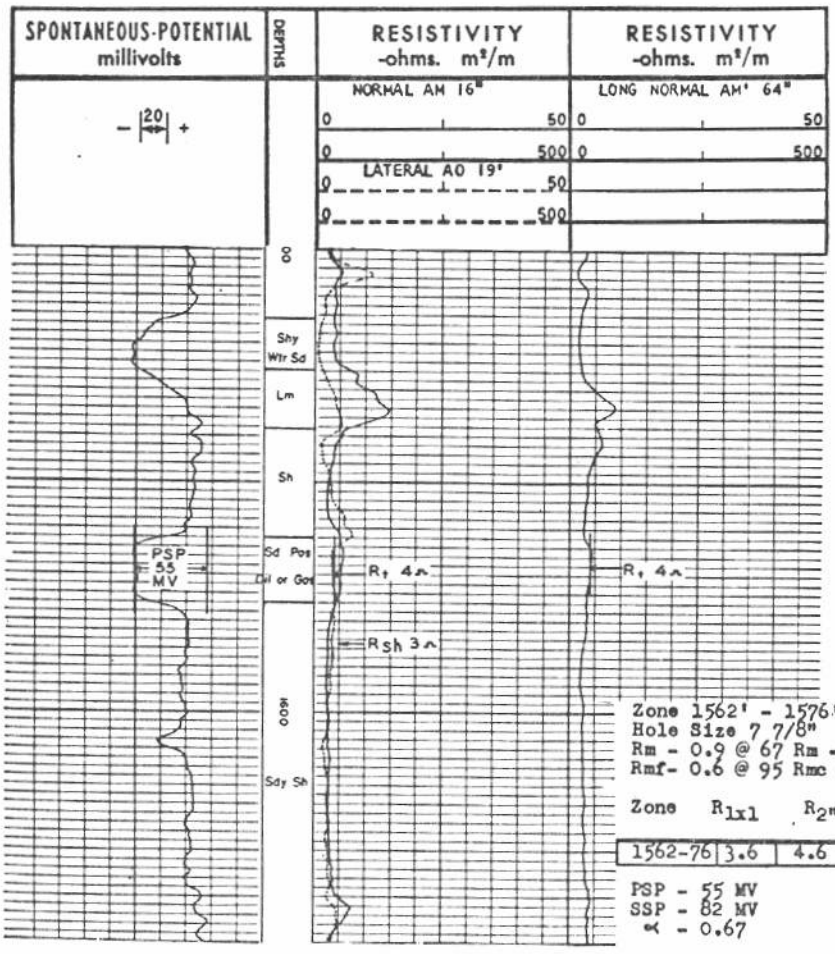

Zone 1562' - 1576' e-14'
Hole Size 7 7/8"
Rm - 0.9 @ 67 Rm - 0.65 @ 95
Rmf- 0.6 @ 95 Rmc - 1.45 @ 95

Zone	R_{1x1}	$R_{2''}$	$\frac{R_{1''x1''}}{Rmc}$	$\frac{R_{2''}}{Rmc}$	$\frac{Rxo}{Rmc}$	Rxo	Rt
1562-76	3.6	4.6	2.5	3.2	7.25	10.5	4

PSP - 55 MV
SSP - 82 MV
α - 0.67

More reliable determination of R_t would have been possible if a focused device (induction log) had been utilized. This device tends to minimize the hole, adjacent bed, and bed-thickness effects on the true-resistivity determination. In the case of low porosities, and often in shaly sands, the MicroLog fails to give reliable values for the resistivity of the invaded zone. Consequently, for each area a careful study should be made to determine the most suitable combination of tools.

It should be noted that S_{xo} is estimated, based on flood-pot tests, and that the SSP (in the absence of known R_w data) must be obtained from a nearby clean sand. Note in Fig. 1 that the ratio R_{mf}/R_w can be used in place of SSP. Where reliable R_w values are available this ratio should be used in place of the SSP from a nearby sand. These and the many other factors that are involved point to the fact that this method should be used with care.

The advantages of this technique are many. It measures the parameters on large samples of the virgin sand from which the shale is eliminated. The results are easily obtained and the cost is low since normally the logs are run for exploration purposes. Although this method has been used sparingly in the past, it is becoming more popular. Better logging tools and techniques will certainly improve its reliability.

Acknowledgments: The authors acknowledge the assistance of W. L. Graham and E. A. Colle, Schlumberger Well Surveying Corp., Tulsa, in the preparation of the paper.

References

1. Poupon, A., Loy, M. E., Tixier, M. P., "A Contribution to Electrical Log Interpretations in Shaly Sands," Journal of Petroleum Technology, June 1954.

2. Doll, H. G., "The SP Log in Shaly Sands," Trans., AIME (1950), 189, 205.

How to measure absolute permeability

(a) Using linear flow and compressible fluid

GIVEN: The following data were obtained during a routine laboratory permeability test:

Run No.	Air flow volume at outlet end, at atm. press., ft.³	Pressure drop across core, in. Hg	Time of flow, sec.
1	0.100	3.90	700
2	0.292	14.96	462
3	0.404	25.64	331
4	0.515	39.91	236

Pressure at outlet end = atmospheric.

Atmospheric pressure = 760 mm. Hg.

Air temperature = 76° F.

Average cross-sectional area of sample = 1.36 sq. cm.

Average length of sample = 1.3 cm.

Viscosity of air at 76° F. = 0.0183 cp.

FIND: Absolute permeability of core.

METHOD OF SOLUTION:

$$Q_m = \frac{A\,k\,(p_1 - p_2)}{\mu\,L} \qquad (1)$$

or

$$Q_a = \frac{A\,k\,(p_1^2 - p_2^2)}{2\,\mu\,p_a\,L} \qquad (2)$$

Where:

Q_m = rate of flow at mean flow conditions of pressure and temperature, cc./sec.

A = core cross-sectional area, sq. cm.

k = absolute permeability, darcies

p_1 = absolute inlet pressure, atm.

p_2 = absolute outlet pressure, atm.

μ = viscosity of flowing fluid at mean conditions, cp.

L = length of core, cm.

p_a = atmospheric pressure

Q_a = rate of flow at atmospheric pressure and flowing temperature, cc./sec.

Solution:

Using Equation 2 and solving for k,

$$k = \frac{2\,\mu\,L\,p_a\,Q_a}{A\,(p_1^2 - p_2^2)} \qquad (3)$$

for run 1

$$k = \frac{(2)\,(0.0183)\,(1.3)\,(1)\,(2{,}831.7)}{(1.36)\,[(1.13)^2 - (1)^2]\,(700)}$$

$$= \frac{134.7}{263.2} = 0.512 \text{ darcies}$$

Where:

$p_a = P_2 = 1$ atm.

$$Q_a = \frac{0.1 \text{ ft.}^3 \times 28{,}317 \text{ cc./ft.}^3}{700 \text{ secs.}}$$

$$= 4.05 \text{ cc./sec.}$$

$$p_v = \frac{3.9 \text{ in. Hg}}{29.92 \text{ in. Hg/atm.}} + 1$$

$$= 1.13 \text{ atm.}$$

$$1/p_m = \frac{1}{\frac{1}{2}\,(1 + 1.13)} = 0.94$$

Similarly for Run 2,

$k = 0.501$ darcies and $1/p_m = 0.80$

for Run 3,

$k = 0.494$ darcies and $1/p_m = 0.70$

for Run 4,

$k = 0.486$ darcies and $1/p_m = 0.60$

DISCUSSION: The characteristic of a porous medium to allow the flow of a fluid or fluids through it is referred to as permeability. When only one fluid is present and flowing through the medium then the measured permeability is defined as the absolute permeability. This is the type usually measured in routine core analysis. Measurements are normally made at room temperature with a pressure drop of less than 1 atm. The calculation of absolute permeability from laboratory measurements is performed by using either Equations 1 or 2. In both equations the following assumptions are made: (1) Single phase flow, (2) laminar or viscous flow, (3) steady-state flow, (4) velocity of flow is equal to Q/A, and (5) no reaction between flowing fluid and porous medium.

It has been found from experimental tests that gases do not strictly follow a laminar flow in porous media. Actually a slippage effect occurs along the walls of the pores resulting in more flow and a higher value of permeability than is true. This effect is a maximum at low mean pressures and for porous media having low permeabilities (less than 20 md.). Note in the graph that the lower the mean pressure, the higher the permeability obtained. At very high mean pressures the slippage phenomenon becomes a minimum and thus (using gases) the true permeability is obtained by extrapolating a curve of the ratio of one to the mean pressure versus permeability to infinite mean pressure as illustrated in the graph.

In routine core analysis no correction is made for the slippage phenomenon and thus a permeability higher than the true absolute permeability is reported. For permeabilities of several hundred millidarcies the error

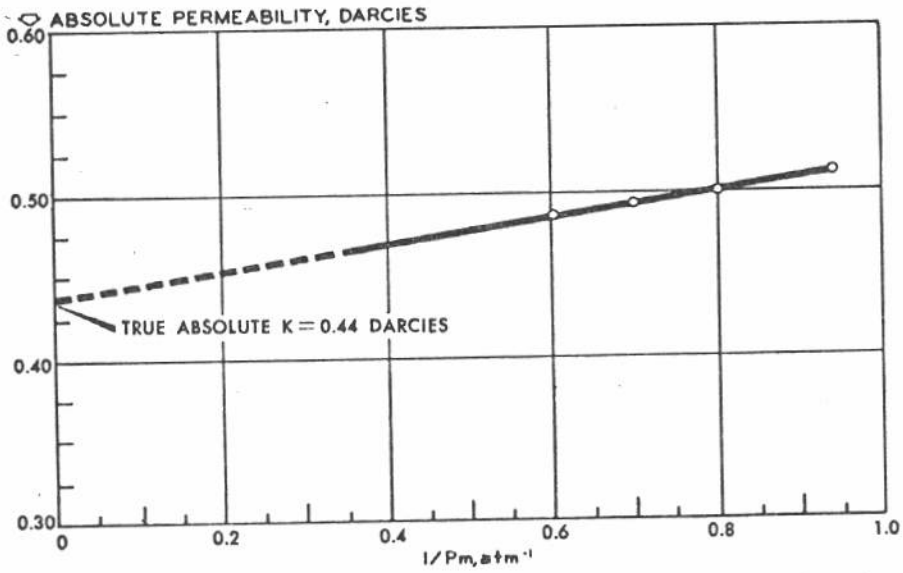

IN LABORATORY ANALYSIS, a low mean pressure yields a value higher than the true permeability of the medium. The true absolute permeability can be found by extrapolating the curve back to an infinite mean pressure.

may be very small (2-5%) while for lower permeabilities (5 to 50 md.), the error may amount to 50% or more. It can safely be said that in most cases permeability is used with other factors that are equally as inexact and thus routine permeability measurements are sufficiently accurate.

Absolute permeabilities are used widely for correlations with (1) interstitial water saturation at a constant capillary pressure, (2) porosity, and (3) injectivity factors. It is also used with relative permeability to calculate effective permeability. Another wide use of absolute permeabilities is for the construction of permeability logs (permeability profiles) so that the formations of interest may be correlated for different wells in a single field. This type of log serves to positively locate tight streaks or shale breaks that may have been missed by other types of well logs. These logs also are indicative of the type and degree of stratification present, this information being useful in completion work and in the selection of wells for injection.

This information is also helpful in determining net sand thickness when used with oil-saturation data. When used for this purpose, any errors in the measurements (resulting from changes in the core due to handling and processing and from the slippage phenomenon, become critical in the low-permeability ranges. Too, it is well to remember that the in-place rock normally contains two or more fluids.

(b) Using linear flow and noncompressible fluid

GIVEN: A permeability test was performed on a sandstone core using water as the flowing fluid and the following data obtained:

Flow rate = 10 cc. water in 500 seconds.

Test temperature = 70° F.

Pressure—upstream = 1.45 atm. abs.; downstream = 1.0 atm. abs.

Viscosity of water at 70° F. = 0.984 cp.

Cross-sectional area of core = 2.0 sq. cm.

Length of core = 2 cm.

FIND: Absolute permeability of core.

METHOD OF SOLUTION:

$$k = \frac{\mu_w Q_w L}{A (p_1 - p_2)} \qquad (4)$$

Where:

μ_w = viscosity of water at test temperature and mean pressure, cp.

Q_w = rate of water flow, cc./second

Other terms as defined in (a).

Solution:

$$Q = \frac{10 \text{ cc.}}{500 \text{ sec.}} = 0.02 \text{ cc./sec.}$$

$$k = \frac{(0.984)\ (0.02)\ (2)}{(2.0)\ (1.45 - 1.0)}$$

$$= 0.044 \text{ darcies}$$

$$= 44 \text{ md.}$$

DISCUSSION: Equation 4 is the steady-state formula for the flow of a noncompressible fluid through a porous medium. When the fluid fully saturates the medium then the measured permeability is the absolute value. If there is no reaction between the flowing fluid and the medium and if viscous flow prevails, it makes no difference what fluid is used (compressible or noncompressible), the absolute permeability obtained will be the same. This means that absolute permeability is independent of the nature of the fluid and is dependent solely upon the structure of the porous medium.

In routine core analysis water is not used to measure absolute permeability because it is difficult to obtain a water compatible with the sample. Most waters will react with the sample to some degree resulting normally in a lower permeability. Also such a test would take considerably more time to perform and be costlier than one utilizing a gas.

References

1. Muskat, M., Physical Principles of Oil Production, McGraw-Hill Publishing Co., pp. 123-124.

2. "Engineering Fundamentals on Petroleum Reservoirs," manual, The Oil and Gas Journal, pp. 34-35.

Part 7

Measurement of absolute permeability

(a) Using radial flow and compressible fluids

GIVEN: The dimensions of a radial core sample are: outside diameter = 6.1 cm.; inside diameter = 1.2 cm.; height = 5.5 cm. At an input pressure of 250 psig. and an outlet pressure of 240 psig. and a temperature of 27° C., the volume of radial air flow through the core is 1.0 cu. ft. (measured at atmospheric pressure) in 1 minute and 10 seconds. The viscosity of air at 27° C. is 0.0178 cp., and atmospheric pressure = 14.6 psi.

FIND: Absolute permeability of core.

METHOD OF SOLUTION: The following equations are used:

$$k = \frac{\mu Q_m \ln (r_e/r_w)}{2\pi h (p_e - p_w)} \qquad (1)$$

$$k = \frac{p_a Z_m \mu Q_a \ln (r_e/r_w)}{\pi h (p_e^2 - p_w^2)} \qquad (2)$$

Where:

k = absolute permeability, darcies.

μ = viscosity of flowing fluid at mean pressure and flowing temperature, cp.

Q_m = rate of gas flow at mean pressure and flowing temperature, cc./sec.

Z_m = compressibility factor at mean pressure and flowing temperature.

Q_a = rate of gas flow at atmospheric pressure and flowing temperature, cc./sec.

r_e = external radius of core, cm.

r_w = internal radius of core, cm.

h = height of core, cm.

p_a = atmospheric pressure, atm.

p_e = absolute pressure at external radius, atm.

p_w = absolute pressure at internal radius, atm.

SOLUTION:

$r_e = 3.05$ cm. $\qquad r_w = 0.6$ cm.

$h = 5.5$ cm. $\qquad p_a = 1$ atm.

$$p_e = \frac{250 + 14.6}{14.6} = 18.1 \text{ atm.}$$

$$p_w = \frac{240 + 14.6}{14.6} = 17.4 \text{ atm.}$$

$Q_a = 404.5$ cc./sec.

$Z_m = 1.0$.

Using Equation 2,

$$k = \frac{(1)\ (1)\ (0.0178)\ (404.5)\ \ln\ (3.05/0.6)}{(3.14)\ (5.5)\ [(18.1)^2 - (17.4)^2]} = 0.0272 \text{ darcies}$$

$$k = 27.2 \text{ md.}$$

(b) Using radial flow and noncompressible fluids

GIVEN: Water is passed through a radial core sample at a rate of 100 cc. per minute. The dimensions of the sample are: outside diameter = 5.6 cm.; inside diameter = 1.0 cm.; and height = 10 cm. The upstream pressure is 15 psig.; the downstream pressure is zero. Room temperature is 80° F. and water viscosity at this temperature is 0.86 cp. Atmospheric pressure = 14.7 psia.

FIND: Absolute permeability of core.

METHOD OF SOLUTION: The equation for radial flow with a noncompressible fluid is:

$$k = \frac{\mu_w\, Q_w \ln (r_e/r_w)}{2\pi h\, (p_e - p_w)} \qquad (3)$$

Where:

μ_w = viscosity of water at mean pressure and flowing temperature, cp.

Q_w = rate of water flow, cc./sec.

and other terms are as defined for Equation 1.

SOLUTION:

$\mu_w = 0.86$ $\quad r_e = 2.8$ cm.

$r_w = 0.5$ cm. $\quad h = 10$ cm.

$Q_w = 100/60 = 1.7$ cc./sec.

$$p_e = \frac{15 + 14.7}{14.7} = 2.02 \text{ atm.}$$

$$p_w = \frac{0 + 14.7}{14.7} = 1.0 \text{ atm.}$$

Therefore:

$$k = \frac{(0.86)\ (1.7)\ \ln\ (2.8/0.5)}{(2)\ (3.14)\ (10)\ (2.02 - 1.0)}$$

$$= 0.039 \text{ darcies or } 39 \text{ md.}$$

DISCUSSION: Equations 1 and 2 are forms of the steady-state formula for radial flow of a compressible fluid which fully saturates the media. Equation 3 is for noncompressible fluid under the same conditions. The same assumptions apply here as were outlined for the linear case.[1] For the same media these equations would give the same value of permeability as would be obtained with the linear equations. The radial flow method of measuring absolute permeability is costlier and less convenient than the linear tests and is not used frequently.

In Part (a) the absolute permeability was not corrected for the slippage affect because the mean pressure used in the measurement was fairly high and thus the error should be a minimum.[1]

Reference

1. Guerrero, E. T., and Stewart, F. M., The Oil and Gas Journal. 3-2-59, p. 119

Part 8

Measurement of effective permeability

(a) Using linear flow and compressible fluid

GIVEN: A core was saturated with brine and then gas-flooded to a constant water saturation of 30%. Under these conditions it was observed that 0.1 cu. ft. of gas (measured at atmospheric pressure) flowed through the core (outside diameter = 2.54 cm., length = 12 cm.) in 2 minutes. The pressure drop across the test interval (8 cm.) of the core was 5 psi., and the viscosity of the air 0.0178 cp. Inlet pressure = 200 psia.; atmospheric pressure = 14.65 psia.

FIND: Effective permeability of the core to gas at 70% gas saturation.

METHOD OF SOLUTION: Equation 3, page 11, applies:

$$k_g = \frac{2\, p_a\, Z_m\, \mu\, Q_a\, L}{A\, (p_1^2 - p_2^2)} \qquad (1)$$

SOLUTION: Q_a, the rate of flow at atmospheric pressure and flowing temperature,

$$= \frac{(0.1 \text{ ft.}^3)\ (28{,}317 \text{ cc./ft.}^3)}{(2)\ (60) \text{ sec.}}$$

$P_1 = 13.65$ atms.
$P_2 = 13.31$ atms.

$$= 23.6 \text{ cc./sec.}$$

$$Z_m = 1.0$$

then:

$$k_g = \frac{(2)\ (1.0)\ (1.0)\ (0.0178)\ (23.6)\ (8)}{(5.06)\ [(13.65)^2 - (13.31)^2]}$$

$$= 0.146 \text{ darcies or } 14\,6 \text{ md.}$$

DISCUSSION: Equation 1 is the same equation as was used in determining the absolute permeability of a linear core using a compressible fluid except that in this case k_g represents the effective permeability of the core to gas for the existing gas saturation.[1]

As implied, this permeability varies with gas saturation. It is not normally obtained in routine core analysis. However, it is measured occasionally in the development of gas-relative permeabilities. It can also be obtained from pressure-buildup tests of gas wells. Effective gas permeabilities are needed in evaluating the steady-state flow behavior of gas wells and with effective oil permeabilities in developing k_g/k_o relationships.

(b) Using linear flow and noncompressible fluid

GIVEN: A linear core having a diameter of 3.0 cm. and a length of 10 cm. was fully saturated with brine and then flooded with crude oil to a constant water saturation of 28%. The oil had a viscosity at test temperature of 3.0 cp. In 10 minutes 25 cc. of oil was flowed through the core

using a pressure drop of 45 psi. across the test interval (7 cm.) of the core, and atmospheric pressure = 14.7 psia.

FIND: Effective permeability of the core to oil at 72% oil saturation.

METHOD OF SOLUTION: Equation 4 of Part 6 of this series applies:

$$k_o = \frac{\mu_o Q_o L}{A (p_1 - p_2)} \qquad (2)$$

Where:

k_o = effective permeability of core to oil, darcies

SOLUTION:

$$Q_o = \frac{25}{10 \times 60} = 0.0417 \text{ cc./sec.}$$

then:

$$k_o = \frac{(3.0)\,(0.0417)\,(7)}{(7.1)\,(3.06)}$$

$= 0.041$ darcies or 41 md.

DISCUSSION: The permeability of a media to a fluid in the presence of one or more other fluids is termed effective permeability. The same equation is used here as was used in the calculation of absolute permeability (incompressible fluid) except that now the effective permeability is obtained. Furthermore, this effective permeability is not only dependent on the nature and structure of the rock but also upon the saturation of the flowing fluid under consideration and the presence of other fluids in the pores of the rock.

Since, in all the reservoirs, two or more fluids exist in the pores of the rock, effective permeability determines their flow behavior. This being the case one could ask why is absolute rather than effective permeability measured in routine core analysis. The reason is that the former is constant and easy to measure whereas the latter is normally a variable and considerably more difficult to measure. The latter is at times determined from production data or pressure-buildup tests.

Effective permeabilities (when available) are used to solve the steady-state equations to determine an estimate of the rate of oil flow for a certain pressure drop or the pressure drop that can be expected for a certain rate of oil flow. The accuracy of the results obtained depend primarily on the ability of the operator to stabilize the well and approach steady-state flow. Other uses of effective permeabilities are (1) to compute productivity index, (2) to develop relative permeabilities, and (3) to determine k_g/k_o and k_w/k_o relationships.

Reference

1. Muskat, M., Physical Principles of Oil Production, McGraw-Hill Publishing Co., pp. 271-274.

Part 9

Measurement of effective permeability

(a) Using radial flow and compressible fluids

GIVEN: Routine steady-state relative-permeability measurements were made on an Edwards limestone core using a multiphase fluid system consisting of brine and gas. The viscosity of the gas at mean pressure and test temperature was 0.0176 cp. The dimensions of the core were: outside diameter = 6.8 cm.; inside diameter = 1.2 cm.; height = 8.2 cm. It was observed that at a constant brine saturation of 50%, 5,000 cc. (measured at test temperature and atmospheric pressure) of gas was flowed through the core in 36 seconds using an inlet pressure of 200 psig. and an outlet pressure of 175 psig. Atmospheric pressure = 14.65 psia. and $Z_m = 0.980$.

FIND: Effective permeability of the core to gas at 50% gas saturation.

METHOD OF SOLUTION: Equations 1 and 2, page 12, apply:

$$k_g = \frac{\mu Q_m \ln (r_e/r_w)}{2\pi h (p_e - p_w)} \qquad (1)$$

$$k_g = \frac{p_a \mu Q_a Z_m \ln (r_e/r_w)}{\pi h (p_e^2 - p_w^2)} \qquad (2)$$

The Z factor should be used when flow rate is reduced tc atmospheric pressure.

In computing permeability from laboratory data, it is more convenient to use the centimeter-gram-second system of units. Equation 1 expressed in field units of standard cubic feet per day, feet, darcies, psi., cp., and °R. is:

$$k_g = \frac{Q_{gs} \mu_g T_f Z_m p_a \ln (r_e/r_w)}{10{,}320\, h (p_e^2 - p_w^2)}$$

Where:

Z_m = gas deviation factor at test temperature and mean pressure.

k_g = effective permeability to gas, darcies.

Q_{gs} = rate of gas flow in standard cubic feet per day.

SOLUTION:

Using Equation 2,

$$k_g = \frac{(0.98)\,(1.0)\,(0.0176)\,(139) \ln (3.4/0.6)}{(3.14)\,(8.2)\,[(14.7)^2 - (12.9)^2]} = 0.0032 \text{ darcies or } 3.2 \text{ md.}$$

DISCUSSION: Equations 1, 2, and 3 are the same as used for determining absolute permeability with a radial system. The one exception is that the permeability obtained in these problems is the effective value which is not only affected by the pore configuration but also by the saturation of the fluid or fluids under consideration.

(b) Using radial flow and noncompressible fluids

GIVEN: A fresh core (outside diameter = 6.3 cm.; inside diameter = 1.3 cm.; height = 5.2 cm.) from the Earlsboro sandstone zone in Oklahoma was placed in a floodpot and flooded with water until the oil saturation remained constant; the resulting oil saturation was 16% (gas saturation = 4.0%). Then 3,000 cc. of brine was flowed radially through the core in 315 minutes (viscosity of water at mean pressure and test temperature = 0.95 cp.) at an inlet pressure of 40 psig. and an outlet pressure of 14.7 psia.

FIND: Effective permeability of the core to brine at 80% brine saturation.

METHOD OF SOLUTION: Equation 3, page 13, applies

$$k_w = \frac{\mu_w\, Q_w\, \ln\,(r_e/r_w)}{2\pi\, h\,(p_e - p_w)} \qquad (3)$$

Where:

k_w = effective permeability to water, darcies.

In solving Equation 1 for permeability using laboratory data, it is convenient to use the centimeter-gram-second system of units. The same equation expressed in "practical oil-field" units of barrels per day, feet, and psi. is:

$$k_w = \frac{\mu_w\, Q_w\, \ln\,(r_e/r_w)}{7.07\, h\,(p_e - p_w)}$$

SOLUTION:

$$Q_w = \frac{3{,}000 \text{ cc.}}{315 \text{ min.} \times 60 \text{ sec./min.}}$$

$$= 0.16 \text{ cc./sec.}$$

then:

$$k_w = \frac{(0.95)\,(0.16)\,\ln\,(3.15/0.65)}{(2)\,(3.14)\,(5.2)\,(3.72 - 1.00)}$$

$$= 0.0027 \text{ darcies or } 2.7 \text{ md.}$$

Effective permeabilities to gas are necessary in the application of the steady-state equations to gas and condensate reservoirs. In spite of this they are not widely measured in routine core analysis by the method implied in this problem. This method is tedious and costly. Furthermore, uncertainties enter regarding the number of tests that should be run to give a reliable statistical average. Normally to obtain the necessary number of tests would be uneconomical.

A convenient manner of expressing effective permeability is as a fraction of the absolute permeability to give the factor known as relative permeability. Although very useful and essential for steady-state calculations effective and relative permeabilities are not often obtained in routine core analysis. Their measurement as a function of saturation is slow, tedious, and costly. Recent development of unsteady-state methods of measuring these parameters show much promise. These will be taken up in subsequent problems.

Part 10

Determination of absolute permeability from well-test data

GIVEN: A water-source well was drilled to a sand lying in the interval 4,200-40 ft. (of which 35 ft. is considered net sand, h). The rate of water flow from the sand was stabilized at 750 bbl. per day, Q_w.

Other data obtained were:

Viscosity of water, $\mu_w = 0.9$ cp., at reservoir conditions.

Formation-volume factor of water, $\beta_w = 1.0$.

External radius of drainage, r_e = 5,000 ft. (estimated).

Radius of well, r_w = 4 in.

Pressure at external radius, p_e = 2,000 psia.

Flowing bottom-hole pressure, p_w = 1,500 psia.

Atmospheric pressure = 14.7 psia.

FIND: Absolute permeability of the sand, k.

METHOD OF SOLUTION: Either of two equations can be used:

$$k = \frac{\mu_w\, \beta_w\, Q_w\, \ln\,(r_e/r_w)}{2\,\pi\, h\,(p_e - p_w)} \qquad (1)$$

or

$$k = \frac{\mu_w\, \beta_w\, Q_w\, \ln\,(r_e/r_w)}{7.07\, h\,(p_e - p_w)} \qquad (2)$$

SOLUTION: Note that the equations are identical except for the units used. Equation 1 is in the centimeter-gram-second system and Equation 2 makes use of practical oil-field units, Table 1. Using Equation 2, the following solution is obtained:

$$k = \frac{(0.9)\,(1.0)\,(750)\,\ln\,(5{,}000/0.333)}{(7.07)\,(35)\,(2{,}000 - 1{,}500)}$$

$$= 0.0525 \text{ darcies}$$

$$= 52.5 \text{ md.}$$

DISCUSSION: This problem is a good example of the determination of absolute permeability with the rock in place. The value of permeability obtained is limited in accuracy by the ability of the operator to stabilize the well and estimate the external radius of drainage and thickness of the sand. The external radius is subject to the most error. However, the significance of the error is reduced by the logrithmic term of the equation.

When care is taken in the measurements, a fair value of permeability should be obtained provided the thickness can be accurately determined. Such a measurement is more realistic since it averages the entire net sand interval and also includes the affects of well bore damage.

Such measurements find application in the estimation of capacity and productivity of water-source wells when only limited actual productivity tests are performed. Thus, once the permeability is known, it is relatively easy to estimate the production to be expected for varying pressure drawdowns and stabilized flow.

TABLE 1—UNITS FOR EQUATIONS 1 AND 2

	Equation 1 CGS units	Equation 2 Oil-field units
k	darcies	darcies
μ_w	cp.	cp.
Q_w	cc. per sec.	bbl. per day
r_e/r_w	cm./cm.	ft./ft.
h	cm.	ft.
p_e, p_w	atm.	psi.

GIVEN: A water-disposal well lies downstructure from oil-producing wells at a depth of 5,260 to 5,300 ft. During initial testing the injection rate was stabilized at 300 bbl. per day, Q_w.

Other data:

Net sand interval, h = 32 ft.

Viscosity of water at reservoir conditions, $\mu_w = 0.9$ cp.

Formation-volume factor of water, $\beta_w = 1.0$.

Radius to farthest point influenced by injected water, r = 500 ft. (estimated).

Radius of well, r_w = 4.0 in.

Reservoir pressure, p = 2,500 psi. at r.

Sand-face injection pressure, p_w = 3,000 psi.

Permeability of reservoir sand in interwell area, k_2 = 61 md. (from pressure-buildup data).

One-half distance between injection well and nearest producer, r_e = 2,000 ft.

FIND: Absolute permeability of sand near well bore and average absolute permeability considering sand near well bore and interwell area sand in series.

METHOD OF SOLUTION: Equation 2 above may be used to find k, the permeability of sand near the well bore. Since this is an injection well, the quantity $(p_e - p_w)$ should be replaced by $(p_w - p_e)$.

Average absolute permeability of sand near well bore and interwell area sand in series can be found from:

$$k_{avg.} = \frac{\ln r_e/r_w}{\frac{1}{k_1}\ln r/r_w + \frac{1}{k_2}\ln r_e/r} \quad (3)$$

SOLUTION: Using Equations 2 and 3, and the given data,

$$k_1 = \frac{(0.9)(1.0)(300)\ln\frac{500}{0.333}}{(7.07)(32)(3{,}000 - 2{,}500)}$$

= 0.0175 darcies or 17.5 md.

and

$$k_{avg.} = \frac{\ln\frac{2{,}000}{0.333}}{\frac{1}{0.0175}\ln\frac{500}{0.333} + \frac{1}{0.061}\ln\frac{2{,}000}{500}}$$

= 0.020 darcies or 20 md.

DISCUSSION: This problem illustrates the use of well-test and injection data in determining the absolute permeability of sand near a well bore. Subsequent problems will show how to determine the interwell area permeability from well pressure-buildup data. In this case a value is given which illustrates typical conditions where the sand near the well bore has a lower permeability than that in the interwell area. The difference is normally caused by drilling and well-completion operations.

Normally the mud filtrate penetrates only a few feet. In this case the assumed radius of influence is 500 ft. which is more practical for the injection rate measured. Changing this value to 20 ft. would result in a permeability for the sand near the well bore of 10 md. However, the average permeability would still be about 20 md. Thus, the logarithm factor in Equation 2 tends to diminish any error that may be involved in the radius.

Equation 3 gives the average permeability for cylindrical sand bodies in series[1] (see drawing). Its development is based on Equation 2. It is interesting to note that although mud and filtrate only penetrate a small distance into the sand, the resulting effect on the average permeability is quite great.

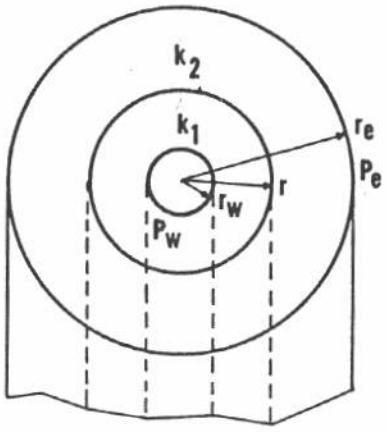

REPRESENTATION of cylindrical sand bodies in series. p_e is the pressure in the unaffected reservoir at a radius r_e, r is the radius of effective well-bore damage, and k_1 and k_2 are the permeabilities of the damaged and undamaged portions respectively of the reservoir. p_w and r_w are as defined in the text.

This type of data is used extensively in determining semiquantitatively the condition of the sand near the well bore. Thus, when the permeability of the sand near the well bore is appreciably lower than that in the interwell area, damage to the sand is indicated. In subsequent problems this will be taken up in more detail.

Reference

1. Calhoun, J. C., "Engineering Fundamentals, Advanced Reservoir Engineering," The Oil and Gas Journal.

Part 11

How to determine effective permeability

(a) From field data. Productivity index and capacity also calculated

GIVEN: The following production and fluid-analysis data were obtained on a well in Lea County, New Mexico. It is believed that the flow from the well was stabilized.

Rate of oil flow, Q_o = 510 stock-tank barrels per day.

Viscosity of oil at reservoir conditions, μ_o = 0.14 cp.

Oil formation-volume factor, β_o = 1.95.

Net oil-sand thickness, h = 15 ft.

External radius of drainage, r_e = 750 ft. (Assumed here as roughly half the distance between wells).

Radius of well, r_w = 4 in.

Static well pressure, P_e = 5,170 psia.

Flowing sand-face pressure, P_w = 4,500 psia.

FIND: The effective permeability to oil (k_o), capacity (k_oh), productivity index (PI), and specific productivity index of this well at the time of the test.

METHOD OF SOLUTION: The general equation for the determination of permeability applies to this problem.

$$k_o = \frac{\mu_o\, Q_o\, \beta_o \ln (r_e/r_w)}{7.07\ h\ (p_e - p_w)} \quad (1)$$

Capacity is defined as the product of permeability and net sand thickness, and is expressed in millidarcy-feet.

$$\text{Capacity} = k_o h \quad (2)$$

Productivity index (PI) is defined as production in stock-tank barrels of oil per day for each pound drop in bottom-hole pressure,

$$PI = \frac{Q_o}{(p_e - p_w)} \quad (3)$$

and is expressed as stock-tank barrels per day per psi. Specific productivity index is found by dividing the PI by the net sand thickness to ob-

tain stock-tank barrels per day per psi. per foot, or PI/h

SOLUTION:

Sand-face injection pressure, p_w = 3,000 psi.

Permeability of reservoir sand in interwell area, k_2 = 61 md. (from pressure-buildup data).

One-half distance between injection well and nearest producer, r_e = 2,000 ft.

FIND: Absolute permeability of sand near well bore and average absolute permeability considering sand near well bore and interwell area sand in series.

METHOD OF SOLUTION: Equation 2 above may be used to find k, the permeability of sand near the well bore. Since this is an injection well, the quantity $(p_e - p_w)$ should be replaced by $(p_w - p_e)$.

Average absolute permeability of sand near well bore and interwell area sand in series can be found from:

$$k_{avg.} = \frac{\ln r_e/r_w}{\frac{1}{k_1}\ln r/r_w + \frac{1}{k_2}\ln r_e/r} \quad (3)$$

SOLUTION: Using Equations 2 and 3, and the given data,

$$k_1 = \frac{(0.9)(1.0)(300)\ln\frac{500}{0.333}}{(7.07)(32)(3{,}000 - 2{,}500)}$$

= 0.0175 darcies or 17.5 md.

and

$$k_{avg.} = \frac{\ln\frac{2{,}000}{0.333}}{\frac{1}{0.0175}\ln\frac{500}{0.333} + \frac{1}{0.061}\ln\frac{2{,}000}{500}}$$

= 0.020 darcies or 20 md.

DISCUSSION: This problem illustrates the use of well-test and injection data in determining the absolute permeability of sand near a well bore. Subsequent problems will show how to determine the interwell area permeability from well pressure-buildup data. In this case a value is given which illustrates typical conditions where the sand near the well bore has a lower permeability than that in the interwell area. The difference is normally caused by drilling and well-completion operations.

Normally the mud filtrate penetrates only a few feet. In this case the assumed radius of influence is 500 ft. which is more practical for the injection rate measured. Changing this value to 20 ft. would result in a permeability for the sand near the well bore of 10 md. However, the average permeability would still be about 20 md. Thus, the logarithm factor in Equation 2 tends to diminish any error that may be involved in the radius.

Equation 3 gives the average permeability for cylindrical sand bodies in series[1] (see drawing). Its development is based on Equation 2. It is interesting to note that although mud and filtrate only penetrate a small distance into the sand, the resulting effect on the average permeability is quite great.

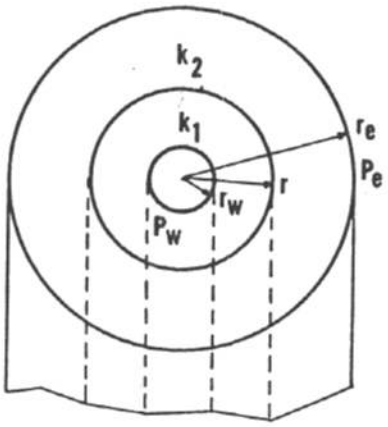

REPRESENTATION of cylindrical sand bodies in series. p_e is the pressure in the unaffected reservoir at a radius r_e, r is the radius of effective well-bore damage, and k_1 and k_2 are the permeabilities of the damaged and undamaged portions respectively of the reservoir. p_w and r_w are as defined in the text.

This type of data is used extensively in determining semiquantitatively the condition of the sand near the well bore. Thus, when the permeability of the sand near the well bore is appreciably lower than that in the interwell area, damage to the sand is indicated. In subsequent problems this will be taken up in more detail.

Reference

1. Calhoun, J. C., "Engineering Fundamentals, Advanced Reservoir Engineering," The Oil and Gas Journal.

Part 11

How to determine effective permeability

(a) From field data. Productivity index and capacity also calculated

GIVEN: The following production and fluid-analysis data were obtained on a well in Lea County, New Mexico. It is believed that the flow from the well was stabilized.

Rate of oil flow, Q_o = 510 stock-tank barrels per day.

Viscosity of oil at reservoir conditions, μ_o = 0.14 cp.

Oil formation-volume factor, β_o = 1.95.

Net oil-sand thickness, h = 15 ft.

External radius of drainage, r_e = 750 ft. (Assumed here as roughly half the distance between wells).

Radius of well, r_w = 4 in.

Static well pressure, P_e = 5,170 psia.

Flowing sand-face pressure, P_w = 4,500 psia.

FIND: The effective permeability to oil (k_o), capacity (k_oh), productivity index (PI), and specific productivity index of this well at the time of the test.

METHOD OF SOLUTION: The general equation for the determination of permeability applies to this problem.

$$k_o = \frac{\mu_o\, Q_o\, \beta_o \ln (r_e/r_w)}{7.07\, h\, (p_e - p_w)} \quad (1)$$

Capacity is defined as the product of permeability and net sand thickness, and is expressed in millidarcy-feet.

$$\text{Capacity} = k_o h \quad (2)$$

Productivity index (PI) is defined as production in stock-tank barrels of oil per day for each pound drop in bottom-hole pressure,

$$PI = \frac{Q_o}{(p_e - p_w)} \quad (3)$$

and is expressed as stock-tank barrels per day per psi. Specific productivity index is found by dividing the PI by the net sand thickness to ob-

behavior. It also includes a modification of the customary use and determination of r_e.

General practice has been to use one-half the distance from the producing well to the adjacent wells as r_e. However, laboratory-model studies, performed by Aronofsky and Jenkins showed that a truer value was about one-half of the assumed distance. Tracy[2] later modified this to 0.472 r_e which is the value shown in Equation 1. Actually r_e is not too critical because the log treatment reduces the magnitude of any error involved. Neglecting the 0.472 factor in the example problem would result in an answer of 8.3 md.

This problem is an example of the measurement of the effective gas permeability of the rock in place. If care is taken to stabilize the flow, the value obtained is indicative of the ability of the rock to flow gas under the existing conditions of saturation and of the sand face.

In this type of test the permeability of the rock near the well bore has a large influence on the over-all value. Consequently if the sand face is badly plugged the resulting over-all permeability will be considerably reduced.

References

1. Aronofsky, J. S., and Jenkins, R., "Nonsteady Radial Flow of Gas Through Porous Media," Proceedings of Fifth Oil-Recovery Conference, TPRC, pp. 125-135.
2. Tracy,. G. W., "Diagnosing Productivity Problems in Gas Wells," presented at Ninth Oil-Recovery Conference, TPRC.

Part 13

How to determine effective permeability

(c) From pressure-buildup data under infinite boundary conditions.

GIVEN: The following data are typical of pressure buildup in a well for an average reservoir where infinite boundary conditions (this prevails early in the life of every reservoir) can be assumed to prevail:

Shut-in time, hours Θ	Sand-face pressure, psi., p_w
2	1,375
3	1,400
4	1,435
5	1,465
7	1,515
8	1,527
10	1,540
12	1,548
19	1,555
24	1,558
36	1,562
60	1,567
94	1,572
150	1,575

Other Data

t, days on production from initial completion = 10.

Q_o, average production rate of stock-tank oil = 125 bbl./day.

μ_o, viscosity of oil at reservoir conditions = 0.8 cp.

h, net sand thickness = 15 ft.

r_w, radius of well = 4 in.

c_o, compressibility of oil at reservoir conditions = 1.5×10^{-5} vol./vol./psi.

ϕ, porosity = 25%.

β_o, oil formation-volume factor = 1.25.

FIND: 1. From a plot of p_w vs. log Θ, the three major portions of the curve: (a) the afterflow period; (b) the proper buildup portion, and (c) near static conditions.

2. Reservoir pressure.

3. Average effective permeability to oil.

METHOD OF SOLUTION: Early in the life of a reservoir the pressure at the sand face (p_w) for Θ time after shut-in is given by the equation

$$p_w = p_o - \frac{162.6\, Q_o \mu_o \beta_o}{k_o h} \log \frac{t+\Theta}{\Theta} \quad (1)$$

$$m = \frac{p_{w2} - p_{w1}}{\log\left(\frac{t+\Theta}{\Theta}\right)_1 - \log\left(\frac{t+\Theta}{\Theta}\right)_2} \quad (1a)$$

Where:

m = slope

p_w = pressure at the sandface for Θ time after shut-in, psi.

p_o = initial reservoir pressure, psi.

k_o = effective permeability to oil, md.

Θ = time well has been shut in, hours

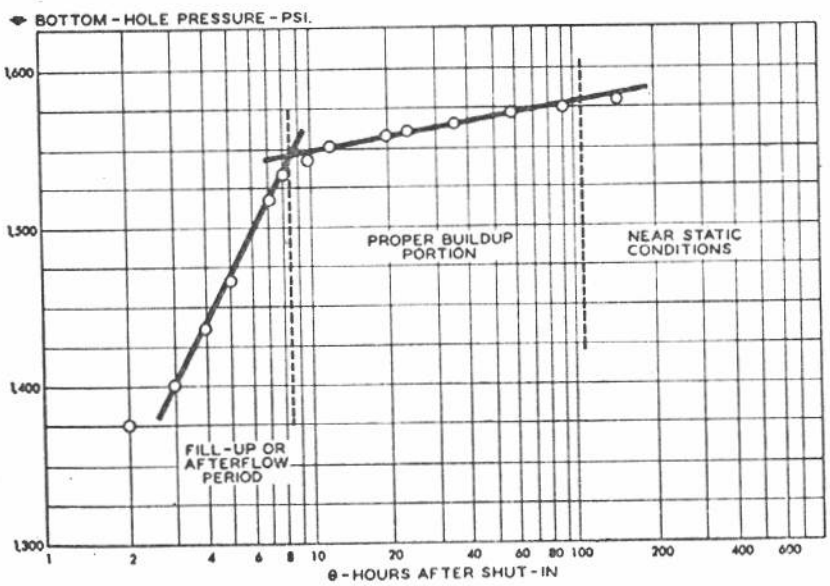

PRESSURE BUILDUP in an average reservoir under infinite boundary conditions. Fig. 1.

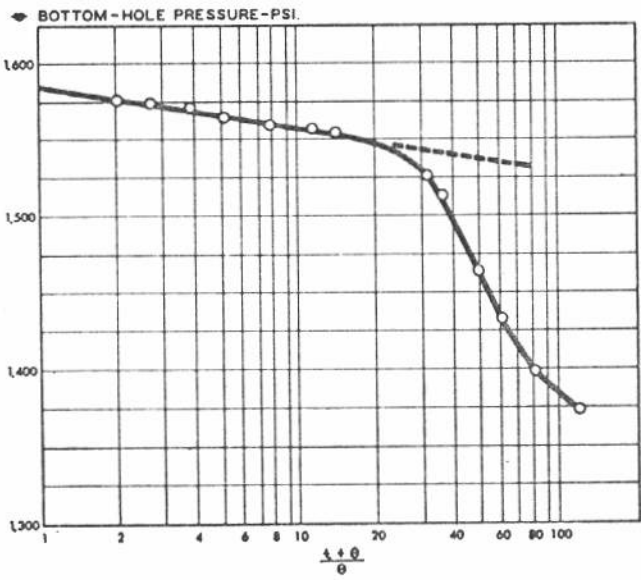

SAME DATA as in Fig. 1, but with pressure plotted vs. $\frac{t+\Theta}{\Theta}$. Fig. 2.

During a pressure-buildup test p_o, Q_o, μ_o, β_o, k_o, h and t of Equation 1 remain essentially constant. Consequently, this is the equation of the straight line obtained by plotting

$$p_w \text{ vs. } \log \frac{t+\theta}{\theta}$$

Furthermore, p_o will be the ordinate intercept and the slope will equal

$$m = \frac{162.6\, Q_o\, \mu_o\, \beta_o}{k_o\, h} \qquad (2)$$

In this equation Q_o, μ_o, β_o, and h are known and m can be determined from the proper buildup portion of the pressure-buildup curve. Thus Equation 2 can be solved for effective permeability.

SOLUTION:

1. Fig. 1 is a plot of θ vs. p_w showing the afterflow period, proper buildup portion, and near-static conditions.
2. An analysis of Equation 1 shows that if θ is allowed to get very large, p_w will equal p_o. Therefore, extrapolation of the proper buildup portion of the pressure-buildup curve to

$$\log \left(\frac{t+\theta}{\theta} \right) = 0$$

(Fig. 2) shows that reservoir pressure, p_o = 1,585 psi.

3. According to Equation 2,

$$k_o = \frac{(162.6)\,(125)\,(0.8)\,(1.25)}{(m)\,(15)}$$

And, from Fig. 2,

$$m = \frac{1{,}585 - 1{,}557}{\log 10 - \log 1} = \frac{28}{1-0} = 28$$

Then

$$k_o = \frac{(162.6)\,(125)\,(0.8)\,(1.25)}{(28)\,(15)} = 48.4 \text{ md.}$$

DISCUSSION:

Equation 1 is obtained from the diffusivity equation using the point-source solution. Assumptions involved in the development are that the reservoir is homogeneous, horizontal, and of uniform thickness; fluid obeys Darcy's law and is present in one phase only; fluid compressibility and viscosity remain essentially constant over the range of temperature and pressure variation encountered; and the fluid density obeys the exponential-type law,

$$\rho = \rho_o\, e^{-c\,(p_o - p)}$$

where ρ is the density at pressure p, ρ_o the density at original reservoir pressure, and c is the fluid compressibility factor.[1] It is further assumed that the system is radial and that disturbances resulting from production will not have reached the outer boundary of drainage. This requires that the tests be run early in the life of a field in a well or wells centrally located. Wells along the edge of a closed (faulted, shaled-out, etc.) reservoir would give erroneous static-pressure values.[2]

There are essentially three periods in the pressure buildup of a well. The first period involves large increases of pressure with time and is known as the fillup or afterflow period as shown in Fig. 1. Equation 1 does not apply in this region. The proper buildup period follows the afterflow period after the casing has filled with oil. After a well has been shut in for a long time (100 to 200 hours or more), the static reservoir pressure is approached.

Fig. 2 shows the pressure-buildup curve plotted in a manner convenient for analysis and interpretation. Thus according to Equation 1 for a value of $\frac{t+\theta}{\theta} = 1.0$, $p_w = p_o$ or the reservoir pressure can easily be obtained from the plot by extrapolating the buildup curve to an abcissa value of 1.0. For the permeability determination care must be taken to use only the proper buildup portion of the curve in obtaining the slope. For the infinite case the proper buildup and near-static portions of the curve have the same slope.

The permeability obtained in this case is the effective value at interstitial-water saturation and maximum oil saturation. Where the rock is wetted by water this permeability value is nearly equal to the absolute permeability. This test is of such a nature (compression of a slightly compressible liquid) that the permeability determined is but slightly affected by the condition of the sand face as long as it will transmit fluids. Consequently, the permeability obtained is representative of the sand away from the well bore and in the interwell area. Furthermore, the measurement involves a very large sample of reservoir rock. This method of permeability determination is believed to be representative and reliable.

Normally a buildup test is not made primarily for permeability determination but also for static reservoir pressure (in tight formations) or for evaluation of well-completion or workover operations. The latter will be covered in a later problem.

References

1. Horner, D. R., "Pressure Buildup in Wells," Proceedings of the Third World Petroleum Congress (II), 1951, 503-531.
2. Matthews, C. S., Brons, F., Hazelbrock, P., "A Method for Determining of Average Pressure in a Bounded Reservoir," AIME Petroleum Transactions, Vol. 201, 1954.

Part 14

How to determine effective permeability

(d.) From pressure-buildup data under finite boundary conditions.

GIVEN: The following data were obtained from a pressure-buildup of a Lea County, New Mexico, well producing from the Pennsylvanian sand.

Shut-in time, hours Θ	$\frac{t+\Theta}{\Theta}$	Sand-face pressure, p_w psig.
0		2,996
0.59	17,000	3,282
0.74	13,500	3,290
1.00	10,000	3,300
1.25	8,000	3,308
1.50	6,670	3,316
2.94	3,400	3,319
5.88	1,700	3,323
9.10	1,100	3,327
25.00	400	3,327
50.00	201	3,327

Assume reservoir to be finite with cumulative oil production from well, N_p = 133,330 stock tank barrels.

Allowable, Q_o = 320 bbl. per day.

Viscosity of oil, μ_o = 0.25 cp. at reservoir conditions.

Oil formation-volume factor, β_o = 1.7.

Composite-compressibility factor, $c_e = 12 \times 10^{-6}$ vol./vol./psi.

Original reservoir pressure, p_o = 3,410 psi. or pressure at last survey.

Porosity, $\phi = 0.05$.

Radius of drainage, r_e = 1,052 ft.

Net sand thickness, h = 26 ft.

Radius of well, r_w = 0.27 ft.

FIND: 1. After flow period, proper buildup portion, and near static conditions from a plot of p_w vs. log Θ.

2. Reservoir pressure and average effective permeability using Horner and Miller, Dyes, and Hutchinson methods.

METHOD OF SOLUTION: The following equations are used in solving the problems by the Horner method.[1]

$$\text{Slope} = m = \frac{p_{w2} - p_{w1}}{\log [(t+\Theta)/\Theta]_1 - \log [(t+\Theta)/\Theta]_2} \quad (1)$$

$$k_o = 162.6\, Q_o\, \mu_o\, \beta_o / m\, h \quad (2)$$

$$p' = p_o - \frac{m}{2.303}\, y(u) \quad (3)$$

$$p_s = p_o - \frac{m}{2.303\, u} \quad (4)$$

By the Miller, Dyes, and Hutchinson method[2] these equations are needed:

$$\text{Slope} = m = \frac{p_{w2} - p_{w1}}{\log \Theta_2 - \log \Theta_1} \quad (5)$$

$$k_o = 162.6\, Q_o\, \mu_o\, \beta_o / m'\, h \quad (6)$$

$$T = 0.000264\, k_o\, \Theta / \phi\, c_e\, \mu_o\, r_e^2 \quad (7)$$

$$p_s = p\Theta + (\Delta p\Theta)\,(m')/1.15 \quad (8)$$

Where:

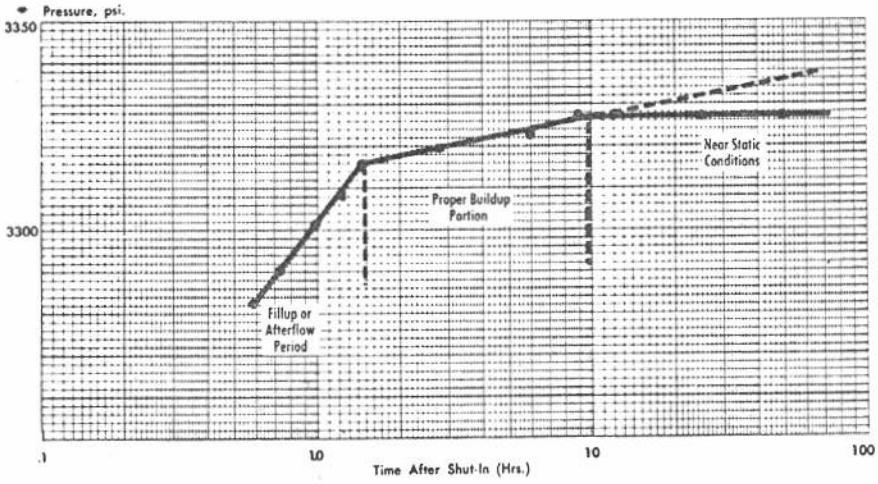

PRESSURE-BUILDUP CURVE, Miller, Dyes, and Hutchinson method. Fig. 2.

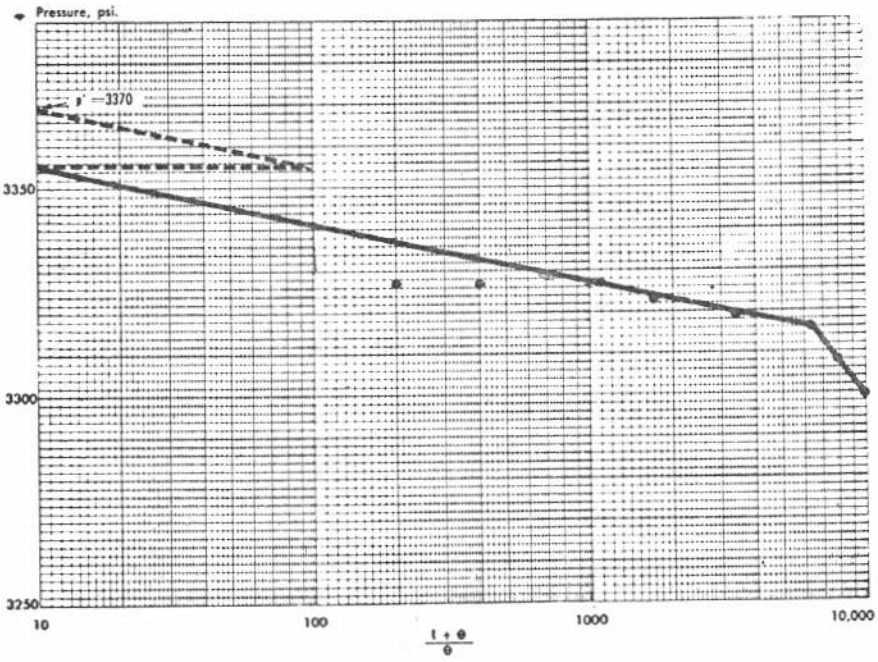

PRESSURE-BUILDUP CURVE, Horner Method. Fig. 1.

Q_o, μ_o, β_o, c_o, p_o, ϕ, r_e, h, r_w are defined with the data and

p' = pressure at log $(t+\Theta)/\Theta$ = 0, psi.

$y(u)$ = independent variable = $(1/u)\, e^{-u} + E_1(-u)$

$u = r_e^2\, \phi\, \mu_o\, c_e / 4\, k_o\, (t+\Theta)$

p_s = current reservoir pressure, psi.

p_θ = pressure at any time Θ after shut-in.

Θ = time after shut-in, hrs.

Δp_θ = dimensionless pressure drop. = .00708 k_o h $(p_s - p_w)/\beta_o\, \mu_o\, q_o$.

t = time from initial completion of well based on N_p and Q_o, or time from last pressure survey, hrs.

k_o = effective permeability, md.

T = dimensionless time.

SOLUTION: Using the Horner method,

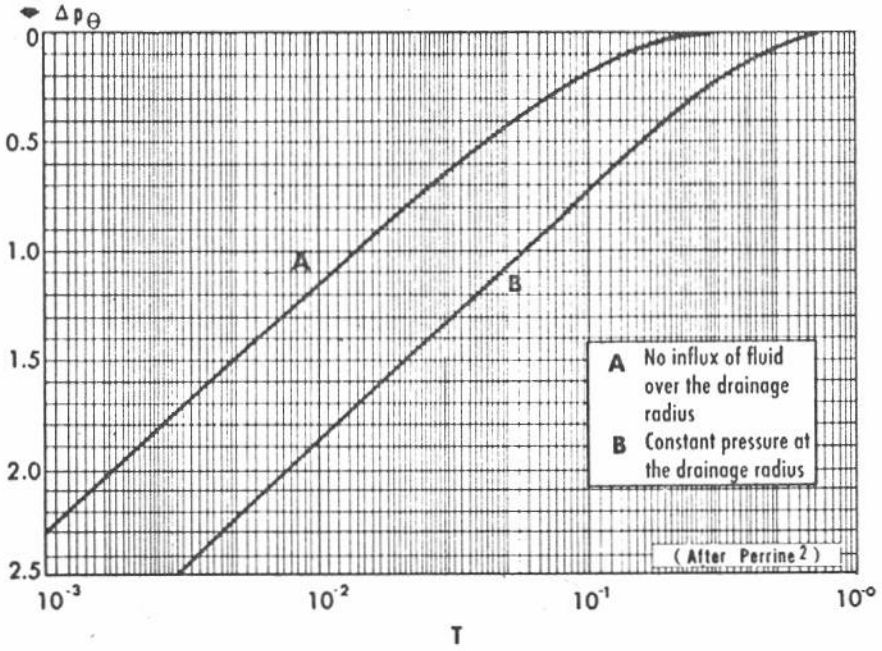

PRESSURE-BUILDUP CURVES for ideal formations. Fig. 3.

$$t = \frac{N_p}{Q_o} = \frac{133{,}330 \text{ bbl.}}{320 \text{ B/D}} \times 24 \frac{\text{hrs.}}{\text{day}} = 10{,}000 \text{ hrs.}$$

The slope m is computed with data obtained from Fig. 1, using abcissa values of 1,000 and 100.

$$m = \frac{3{,}341 - 3{,}327}{-\log 1{,}000 - \log 100} = 14 \qquad \text{(Eq. 1)}$$

$$K_o = \frac{(162.6\,(320)\,(0.25)\,(1.7)}{(14)\,(26)} = 60.7 \text{ md.} \qquad \text{(Eq. 2)}$$

$$3{,}370 = 3{,}410 - (14/2.3)\,y\,(u) \qquad \text{(Eq. 3)}$$

$$y(u) = (3{,}410 - 3{,}370)\ (2.3/14) = 6.56$$

Using Fig. 10 of Ref. 1 or Fig. 6 of Ref. 3

$$u = 0.104$$

$$P_s = 3{,}410 - \frac{14}{(2.3\,(0.104)} = 3{,}351 \text{ psi.} \qquad \text{(Eq. 4)}$$

$$T = 1/4u = 1/(4 \times 0.104) = 2.4$$

From Fig. 7 of Ref. 3 the correction for a slope of 14 and T = 2.4 is about − 5 psi. Therefore, the corrected reservoir pressure is

$$p_s = 3{,}351 - 5 = 3{,}346 \text{ psi.}$$

In the Miller, Dyes, and Hutchinson method, the slope m'is computed with data obtained from Fig. 2. Thus using abcissa values of 1.0 and 10,

$$m' = \frac{3{,}326 - 3{,}313}{\log 10 - \log 1} = 13 \qquad \text{(Eq. 5)}$$

$$K_o = \frac{(162.6)\,(320)\,(0.25)\,(1.7)}{(13)\,(26)} = 65.3 \text{ md.} \qquad \text{(Eq. 6)}$$

For a shut-in time of 2 hours.

$$T_2 = \frac{(0.000264)\,(65.3)\,(2)}{(.05)\,(12\times10^{-6})\,(0.25)\,(1{,}052)^2} = 0.21 \qquad \text{(Eq. 7)}$$

From Fig. 3, and using curve A, $\Delta p_2 \approx 0.1$ and

$$P_s = 3{,}317 + \frac{(0.1)\,(13)}{1.15} = 3{,}318 \text{ psi.} \qquad \text{(Eq. 8)}$$

Fig. 2 shows the afterflow period, proper buildup portion, and near static conditions.

DISCUSSION: This problem is a good example of the use of two methods for computing effective permeability and static reservoir pressure from pressure-buildup data. Both methods involve equations resulting from the solution of the diffusivity equation.

$$\frac{\delta^2 p}{\delta r^2} + \frac{1}{r}\frac{\delta p}{\delta r} = \frac{\phi\, c\, \mu}{k}\frac{\delta p}{\delta t} \qquad (9)$$

Common assumptions involved in the solutions are: (1) an undersaturated, single fluid phase is flowing; (2) the reservoir fluid properties are constant at all reservoir conditions; (3) rate of production is stabilized before shut-in; (4) no fluids are produced into the well bore after shut-in; (5) sand properties are uniform; (6) drainage-area shape is that of a horizontal circular cylinder; (7) well bore is vanishingly small.[2] Obviously all of these assumptions cannot be satisfied by any reservoir. However, experience has shown that all assumptions need not be fulfilled for practical application of the results.[2]

Horner's method involves a solution of Equation 9 which is approximate and applicable for finite boundary conditions (pressure disturbances have been felt at r_e) and no influx of fluid over the drainage radius.[1] This method has been shown to be of practical value in most cases and can be corrected in the rest by utilizing Fig. 7 of Ref. 3. Generally the error involved will be appreciable where the permeability is low and production rate high.

The Miller, Dyes, and Hutchinson method involves more rigorous solutions of Equation 9 for two sets of finite boundary conditions: (1) No influx of fluid over the drainage radius and (2) constant pressure at the drainage radius. The former was used in the solution of this problem.

A careful study of Equations 1 through 8 will show that the two methods are similar in many respects. Both methods require reliable Q_o, μ_o, β_o, and h values. Furthermore, the Horner approach requires a reliable original or previous survey pressure and production data. The other method would require reliable values of r_e and c_o. Where reliable data are available the latter (Miller, et al.) method is easier to apply.

Note that the Horner technique involves a plot using log $(t+\Theta)/\Theta$ as abcissa whereas Miller at al. use log Θ. Actually, for small values of Θ it can be mathematically shown that the slopes obtained should be about equal as was the case in the problem.

It can be observed in both Figs. 1 and 2 that the well was shut in long enough to build up to the approximate reservoir pressure of 3,327 psi. thus providing a good test for the methods. The Horner method resulted in a high value of 3,346 psi. (0.6% error) while the Miller, et al. method resulted in a low value of 3,318 psi. (0.3% error). Both values can be considered of practical value. Because it is based on more rigorous equations, the Miller et al. approach is considered by many to be the better method.[2]

Although relatively new, the meth-

ods used to solve this problem have received wide acceptance in industry and are being used extensively. Involved in the testing are large portions of in-place rock which should give more representative results of effective permeability. At a later time problems will be presented to show further utilization of pressure-buildup data for determination of well-bore damage and success of workover operations.

References

1. Horner, D. R.: "Pressure Buildup in Wells," Proceedings Third World Petroleum Congress, Section 2 (1951), pp. 503-521.

2. Perrine, R. L.: "Analysis of Pressure-Buildup Curves," API Drilling and Production Practice, 1956, pp. 482-495.

3. Hurst, L. L., and Guerrero, E. T.: "Calculating Static Bottom-Hole Pressures," The Oil and Gas Journal, Sept. 29, 1958.

Part 15

How to determine effective permeability

(e.) From multiphase pressure-buildup data under finite boundary conditions

GIVEN: A pressure-buildup test was performed on a well producing oil and free gas into the well bore. The data obtained were as follows:

Time after shut-in, θ hrs.	Sand-face pressure, psig.
.00	1,420
.02	1,500
.03	1,600
.05	1,650
.10	1,695
.20	1,735
.50	1,770
1.00	1,800

Other Data

Estimated average reservoir pressure,

$$p = 1{,}840 \text{ psi.}$$

Reservoir fluid saturations

$$\text{oil, } S_o = 60.1\%$$
$$\text{gas, } S_g = 15.4\%$$
$$\text{water, } S_w = 24.5\%$$

Fluid-production rates,

oil, 900 bbl. per day = Q_o
water, 0 bbl. per day = Q_w
gas, 6,050 s.c.f./bbl.

Viscosity of oil at reservoir conditions,

$$\mu_o = 0.6 \text{ cp.}$$

Net oil sand thickness,

$$h = 21 \text{ ft.}$$

Solution gas-oil ratios, R_s, s.c.f. per stock-tank barrel.

at 2,000 psi. = 480.
at 1,500 psi. = 340.
at 1,840 psi. = 440.

Oil formation-volume factor, β_o

at 2,000 psi. = 1.32.
at 1,500 psi. = 1.25.
at 1,840 psi. = 1.30.

Gas formation volume factor at average reservoir conditions,

$$\beta_g = 1.50 \times 10^{-3} \text{ Res. bbl. s.c.f.}$$

Water compressibility factor at average reservoir conditions,

$$c_w = 3.0 \times 10^{-6} \text{ vol./vol./psi.}$$

Porosity,

$$\phi = 0.16$$

Radius of drainage, $r_e = 400$ ft.

Use finite case of no influx of fluid over the drainage radius.

FIND: Effective permeability to oil and the static reservoir pressure.

Method of Solution

Equations needed for the solution are:

$$\text{Slope} = m = \frac{p_2 - p_1}{\log \theta_2 - \log \theta_1} \quad (1)$$

$$k_o = \frac{162.6\, Q_o\, \mu_o\, \beta_o}{m\, h} \quad (2)$$

$$T = \frac{0.000264\, M_T\, \theta}{\phi\, c_T\, r_e^2} \quad (3)$$

$$p_s = p_w + \frac{(\Delta p_s)\,(m)}{1.15} \quad (4)$$

Where:

$$M_T = M_o + M_g + M_{w/} \quad (5)$$

$$M_o = \frac{162.6\, \beta_o\, Q_o}{m\, h} = \frac{k_o}{\mu_o} \quad (6)$$

$$M_g = \frac{162.6\, (\beta_g)\, (Q_g - Q_o\, R_s)}{m\, h} = k_g/\mu_g \quad (7)$$

$$M_w = \frac{162.6\, \beta_w\, Q_w}{m\, h} = \frac{k_w}{\mu_w} \quad (8)$$

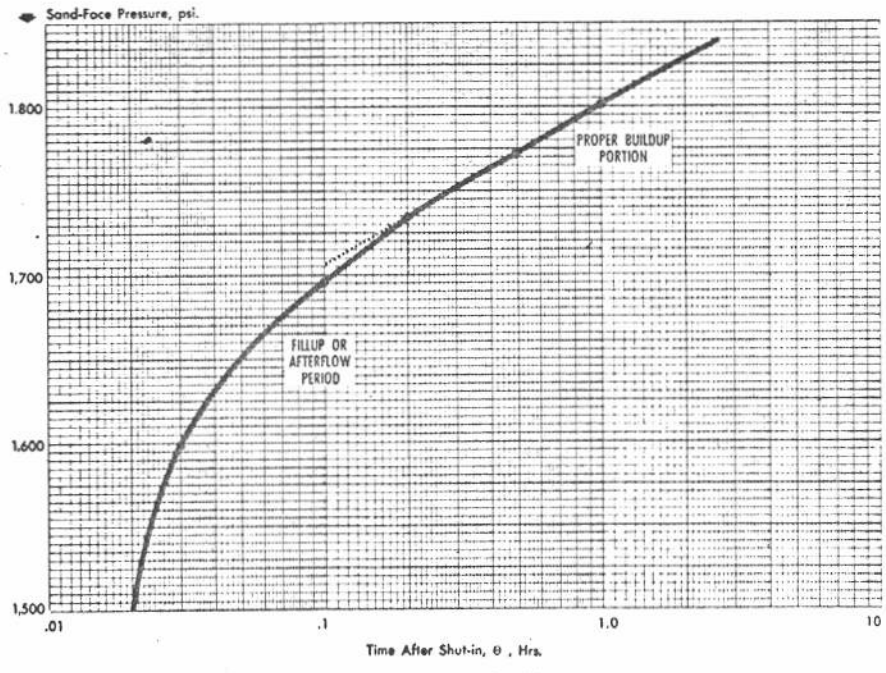

MULTIPHASE pressure-buildup curve.

$$C_T = c_{of} + c_{gf} + c_{wf} \quad (9)$$

$$c_{of} = (S_o/100) \times \left[\frac{\beta_g}{\beta_o}\frac{dR_s}{dp} - \frac{1}{\beta_o}\frac{d\beta_o}{dp}\right] \quad (10)$$

$$c_{gf} = S_g/100\ (1/p) \quad (11)$$

$$c_{wf} = \frac{S_w}{100} c_w \quad (12)$$

θ = time after shut-in, hours.

k_o = effective permeability to oil, md.

$d\beta_o/dp$ = slope of β_o vs. p plot at average reservoir pressure.

dR_s/dp = slope of R_s vs. p plot at average reservoir pressure.

T = dimensionless time.

M_T = total mobility.

M_o, M_g, M_w = mobilities of oil, gas, and water.

p_2, p_1 = pressures at shut-in times Θ_2, Θ_1.

c_T = effective total compressibility factor, vol./vol./psi.

Q_o, Q_w = production rates of oil and water, bbl./day.

Q_g = gas-production rate, standard cu. ft. per day.

β_w = water formation volume factor.

c_{of}, c_{gf}, c_{wf} = oil,* gas, and water fraction compressibilities, vol./vol./psi.

All of the other factors were defined with the data.

SOLUTION: From plots of β_o vs. p and R_s vs. p, these slopes are obtained: $dR_s/dp = 0.28$ and $d\beta_o/dp = 0.00014$. Substituting these and other factors in Equation 10,

$$c_{of} = (60.1/100) \times \left[\frac{(0.0015)}{1.3}(0.28) - \frac{1}{1.3}(0.00014)\right]$$

$$= 1.29 \times 10^{-4} \text{ vol./vol./psi.}$$

$$c_{gf} = (15.4/100)\ (1/1{,}840) = 0.84 \times 10^{-4} \text{ vol./vol./psi.} \quad (11)$$

$$c_{wf} = (24.5/100)\ (3.0 \times 10^{-6}) = 0.007 \times 10^{-4} \approx 0.01 \times 10^{-4} \text{ vol./vol./psi.} \quad (12)$$

$$c_T = (1.29 + 0.84 + 0.01)\ 10^{-4} = 2.14 \times 10^{-4} \text{ vol./vol./psi.} \quad (9)$$

*This use of the term oil compressibility factor is different from the normal usage in that changes in solution-gas content and shrinkage are considered together.

On the graph, extrapolating the proper buildup portion of the curve to $\theta = 0.1$ and using abscissa values of 0.1 and 1.0 gives a slope of:

$$m = \frac{1{,}798 - 1{,}707}{\log 1.0 - \log 0.1} = \frac{91}{1.0} = 91 \quad (1)$$

$$M_o = \frac{(162.6)\ (1.3)\ (900)}{(91)\ (21)} = \frac{k_o}{\mu_o}$$

$$= 100 \text{ md./cp.} \quad (6)$$

$$M_g = \frac{(162.6)\ (0.0015)\ [(900)\ (6{,}050) - (900)\ (440)]}{(91)\ (21)} = \frac{k_g}{\mu_g} \quad (7)$$

$$= 644 \text{ md./cp.}$$

$M_w = 0$ because $Q_w = 0$

$$M_T = 100 + 644 = 744 \text{ md./cp.} \quad (5)$$

$$\text{Effective permeability} = k_o = \frac{(162.6)\ (900)\ (1.3)\ (0.6)}{(91)\ (21)} \quad (2)$$

$$= 60 \text{ md.}$$

For shut-in time of 0.5 hour, dimensionless time becomes:

$$T = \frac{(0.000264)\ (744)\ (0.5)}{(0.16)\ (2.14 \times 10^{-4})\ (400)^2} \quad (3)$$

$$= 1.79 \times 10^{-2}$$

From Fig. 3 of Reference 2,

$$\Delta p_s = 0.90$$

Then static reservoir pressure in drainage area is:

$$p_s = 1{,}770 + \frac{(0.90)\ (91)}{1.15} \quad (4)$$

$$= 1{,}841 \text{ psi.}$$

This problem is an example of the analysis of multiphase pressure-buildup data for the determination of effective permeability and reservoir pressure. The equations used are a modification of the Miller, Dyes, and Hutchinson[2,3] approach as presented by Perrine.[1] Essentially the same equations are used for multiphase flow as for single-phase flow[2] except that effective total mobility (M_T) and compressibility (c_T) are used for equivalent single-phase oil properties. Equations 5 through 12 are Perrine's[1] method of determining these multiphase properties. In them he assumes that the effective total mobility is equal to the sum of the individual fluid mobilities. Furthermore, he defines the total compressibility as the total decrease in reservoir fluid volume per unit volume per psi. pressure increase.[1]

Note that in computing total compressibility an estimate of fluid saturations must be made. Also PVT data (β_o, β_g, R_s, etc.) must be available or be obtained from correlations. Fluid saturations can be determined from a material balance involving initial saturations and production data. All fluid factors in the equations that are a function of pressure are obtained at estimated average reservoir pressure, which can be obtained from an extrapolation of a pressure-vs.-time curve or from recent measurements on nearby wells.

It is of interest to note that the completed static reservoir pressure (1,841 psi.) agrees very well with the estimated average reservoir pressure (1,840 psi.). Also note that in addition to effective oil permeability, effective gas permeability could have been computed from Equation 7 if the gas viscosity at reservoir conditions were known. Thus it is possible by this approach to determine specific values of k_g/k_o and also k_w/k_o. These could serve as a check of specific values determined by laboratory methods.

In spite of the fact that the gas saturation is only one-fourth the oil saturation (liquid plus solution gas) the contribution of the former to the total compressibility is practically equal to that of the latter. It is interesting to note that both are many times that for a liquid alone. The mobility of the gas is more than six times that of the oil. Work performed by R. E. Cook[4] shows that use of single-phase instead of multiphase compressibility, even when producing gas-oil ratios are at or near initial solution values results in static pressures which are low. Cook also found that except for large buildup curve slopes (100+) and/or very low crude gravities (20° API) rather large errors

in gas saturation can be tolerated without appreciable effect on calculated static pressures.

References

1. Perrine, R. L., "Analysis of Pressure Buildup Curves," API Drilling and Production Practice, 1956, pp. 482-495.

2. Guerrero, E. T., and Stewart, F. M., Part 14—"How to Determine Effective Permeability . . .," The Oil and Gas Journal, 10-5-59, p. 167

3. Miller, C. C., Dyes, A. B., and Hutchinson, C. A., Jr., "The Estimation of Permeability and Reservoir Pressure from Bottom-Hole Pressure-Buildup Characteristics," Trans. AIME (1950), 189, 91.

4. Cook, R. E., "Effect of Gas Saturation on Static Pressure Calculations From Two-Phase Pressure-Buildup Curves," SPE-AIME 1958 fall meeting paper 1112-G.

Part 16

How to calculate average permeability of a lease

GIVEN: Core analyses on cores from nine wells of a zone in Sheridan field in Colorado County, Texas, gave the data shown in the first four columns of the table.

FIND: Arithmetic average permeability for the lease, and also the average permeability weighted by thickness, area, and volume.

METHOD OF SOLUTION: These equations define the various averages required:

Arithmetic average permeability

$$= \frac{\Sigma \text{ well average permeabilities}}{\text{Number of wells}} \quad (1)$$

Average permeability, thickness weighted

$$= \frac{\sum_{i=1}^{i=n} k_i h_i}{\sum_{i=1}^{i=n} h_i} \quad (2)$$

Average permeability, area weighted

$$= \frac{\sum_{i=1}^{i=n} k_i A_i}{\sum_{i=1}^{i=n} A_i} \quad (3)$$

Average permeability, volume weighted

$$= \frac{\sum_{i=1}^{i=n} k_i A_i h_i}{\sum_{i=1}^{i=n} A_i h_i} \quad (4)$$

Columns 5 through 8 in the table show the required computations. When the results are substituted into Equations through 4 we get:

Arithmetic average permeability

$$= 21.1/9 = 2.3 \text{ md.}$$

Average permeability, thickness weighted

$$= 466.2/208 = 2.2 \text{ md.}$$

Average permeability, area weighted

$$= 433.4/183 = 2.4 \text{ md.}$$

Average permeability, volume weighted

$$= 9{,}446/4{,}189 = 2.3 \text{ md.}$$

DISCUSSION: For most problems involving permeability, the average for a producing interval, lease, or entire reservoir is desired. This problem shows four methods of averaging permeabilities. Of these the arithmetic average is the most widely used. Note in this case that in spite of the limited data and fair variation in permeability values that the four methods give about the same average. However, such close agreement cannot always be expected, particularly where variations in net sand thickness or area are great.

Before averaging permeability values, it is necessary to analyze the data and exclude all measurements below a minimum value. The measurements below this minimum are not considered representative of the reservoir under consideration. Experience has shown that the minimum permeability below which permeabilities are to be excluded is generally dependent upon the average value. The higher the average the higher the lowest value of permmeability contributing appreciably to the production.

Generally the more involved procedures for averaging permeabilities (volume, thickness, area weighted methods) are not used except in cases where considerable variations occur in permeability, area, and thickness. Of the four methods, the volume weighted is the most accurate.

Computation of Average Permeabilities

(1) Well	(2) Net sand thickness, ft., h	(3) A area, ac.	(4) Average permeability, k, md.	(5) $k_i h_i$ Col. 4 × Col. 2	(6) $k_i A_i$ Col. 4 × Col. 3	(7) $k_i A_i h_i$ Col. 6 × Col. 2	(8) $A_i h_i$ Col. 3 × Col. 2
1	25	20	0.9	22.5	18.0	450	500
2	16	18	1.5	24.0	27.0	432	288
3	19	23	1.1	20.9	25.3	481	437
4	23	19	0.8	18.4	15.2	350	437
5	32	17	2.4	76.8	40.8	1,309	544
6	28	25	2.2	61.6	55.0	1,540	700
7	21	24	3.3	69.3	79.2	1,663	504
8	15	21	6.1	91.5	128.1	1,921	315
9	29	16	2.8	81.2	44.8	1,300	464
Total	208 $= \Sigma h_i$	183 $= \Sigma A_i$	21.1 $= \Sigma k_i$	466.2 $= \Sigma k_i h_i$	433.4 $= \Sigma k_i A_i$	9,446 $= \Sigma k_i A_i h_i$	4,189 $= \Sigma A_i h_i$

Part 17

How to calculate average porosity of a lease

GIVEN: The following data were determined from well logs, lease maps, and core-analysis tests on cores obtained from a Kansas lease:

Well	Net sand thickness, h (ft.)	Area drained by well, A (ac.)	Avg. well porosity, ϕ (%)
1	15	21	28
2	25	20	22
3	28	25	24
4	16	22	28
5	9	28	25
6	24	19	18
7	18	15	27
	135	150	172

FIND:

1. Average porosity for the lease weighing average well porosities by thickness, area, volume, and arithmetically.
2. Average net sand thickness for lease weighing by area.
3. Pore volume for the lease.

METHOD OF SOLUTION: These equations are used to calculate the various averages required.

Arithmetic average porosity

$$= \frac{\Sigma \text{ well average porosities}}{\text{Number of wells}} \quad (1)$$

Average porosity, thickness weighted

$$= \frac{\sum_{i=1}^{i=n} \phi_i h_i}{\sum_{i=1}^{i=n} h_i} \quad (2)$$

Average porosity, area weighted

$$= \frac{\sum_{i=1}^{i=n} \phi_i A_i}{\sum_{i=1}^{i=n} A_i} \quad (3)$$

Average porosity, volume weighted

$$= \frac{\sum_{i=1}^{i=n} \phi_i A_i h_i}{\sum_{i=1}^{i=n} A_i h_i} \quad (4)$$

Average net sand thickness, area weighted

$$= \frac{\sum_{i=1}^{i=n} A_i h_i}{\sum_{i=1}^{i=n} A_i} \quad (5)$$

Pore volume, ac.-ft.

$$= (7{,}758 \text{ bbl./ac.-ft.}) \sum_{i=1}^{i=n} A_i h_i \phi_i \quad (6)$$

SOLUTION:

Arithmetic average porosity $= [28 + 22 + 24 + 28 + 25 + 18 + 27] \div 7$

$= 172 \div 7 = 24.6\%$

Average porosity, thickness weighted

$= [(15)(28) + (25)(22) + (28)(24) + (16)(28) + (9)(25) + (24)(18) + (18)(27)]$

$\div [15 + 25 + 28 + 16 + 9 + 24 + 18] = 3{,}233/135 = 24.0\%$

Average porosity, area weighted

$= [(21)(28) + (20)(22) + (25)(24) + (22)(28) + (28)(25) + (19)(18) + (15)(27)]$

$\div [21 + 20 + 25 + 22 + 28 + 19 + 15] = 3{,}691/150 = 24.6\%$

Average porosity, volume weighted

$= [(15)(21)(28) + (25)(20)(22) + (28)(25)(24) + (16)(22)(28)$

$+ (9)(28)(25) + (24)(29(18) + (18)(15)(27)]$

$\div [(15)(21) + (25)(20) + (28)(25) + (16)(22) + (9)(28)$

$+ (24)(19) + (18)(15)] = 68{,}274/2{,}845 = 24.0\%$

Average net sand thickness, area weighted

$= [(15)(21) + (25)(20) + (28)(25) + (16)(22) + (9)(28) + (24)(19) + (18)(15)]$

$\div [21 + 20 + 25 + 22 + 28 + 19 + 15] = 2{,}845/150 = 19.0\%$

Using $\sum_{i=1}^{i=n} A_i h_i \phi_i = 68{,}274$ determined above.

Pore volume, bbl. $= [(7{,}758)(68{,}274)] \div 100 = 5{,}300{,}000$ bbl.

The factor of 100 converts all per cent porosities to fractions.

DISCUSSION: This problem illustrates many of the commonly used procedures for obtaining the average porosity of a lease, group, of leases, or a reservoir. Note that in this case the average values obtained arithmetically, thickness weighted, area weighted, and volume weighted are all quite similar. This will be true in many reservoirs where coring or logging has been well planned and spaced throughout the lease or field. Normally a sample is analyzed for every foot cored. In the case of logs the porosities determined apply to selected intervals.

Of the methods presented the arithmetic average is perhaps the most used whereas the volume weighted average is considered the most accurate. Normally the increased accuracy given by the latter is not warranted in subsequent applications. A question arises as to the accuracy and representativeness of the porosity determinations. Furthermore, the average porosity is used with such other factors as net sand volume and reservoir oil saturation, the accuracy of which, cannot in most cases, be considered good.

In spite of this, occasions may arise

where the volume weighted average may be justified. This would be particularly true where the porosity and net sand thickness vary considerably over the area under consideration. Another case where accuracy may be sought is unitization work where the most equitable basis for participation is sought.

A volumetric method not illustrated in this problem is one in which a pore-volume map is obtained by plotting well average porosity times net sand thickness on a base map. Contouring results in a map consisting of lines connecting points of equal pore volume per unit area. Planimetering will yield the area between the contours from which an average porosity can be obtained. If desired, porosity alone may be used on the map. Subsequent averaging will require the average net sand thickness for each area between contours.

This method for determining the average net sand thickness is widely used and accepted. The pore volume computed represents the total interconnected pore space available for oil, gas, and water.

Part 18

How to obtain a K_g/K_o curve from laboratory steady-state relative-permeability measurements

GIVEN: The data in Columns 1, 2, and 3 of Table 1 were obtained on a core sample using the conventional laboratory steady-state relative-permeability test.

OTHER DATA: Minimum interstitial-water saturation, S_w, fraction of pore volume = 0.20.

FIND: Relationship between k_g/k_o and the total liquid saturation.

METHOD OF SOLUTION: The following equation applies:

$$k_g/k_o = \frac{k_g/k}{k_o/k} \qquad (1)$$

where:

k_g = effective permeability to gas.
k_o = effective permeability to oil.
k = absolute permeability.
k_g/k = relative permeability to gas.
k_o/k = relative permeability to oil.

SOLUTION: The data in Columns 1, 2, and 3 of Table 1 will be extended for the solution. Total liquid saturations are obtained by adding the minimum interstitial-water saturation value to each oil saturation, Column 4. Division of values in Column 3 by the respective values of Column 2 yields the k_g/k_o ratio, Column 5.

DISCUSSION: Relative permeability is defined as the ratio of the ability of a rock to transmit a fluid when partially saturated by that fluid (effective permeability) to its ability to transmit the same fluid when fully saturated by it (absolute permeability).[2] The ratio of a rock's relative permeability to one fluid to its relative permeability to another fluid at the same liquid saturation is the relative-permeability ratio for that saturation. Equation 1 shows this relationship. Note that this is also equivalent to the ratio of two effective permeabilities.

An example of the use of relative-permeability ratios is in the analytical determination of performance under primary and secondary-recovery conditions. Involved in this type of calculations are the instantaneous gas-oil ratio and fractional-flow equations which require knowledge of the permeability ratios in their solution.

There are essentially three methods for determining relative-permeability ratios: (1) steady-state, (2) unsteady-state, and (3) field data.[1] The first two are considered laboratory methods while the third requires knowledge of production tests. This problem is an example of the steady-state method. Subsequent problems will consider the other methods. In the steady-state method fixed ratios of the fluids of interest are flowed through the sample until equilibrium conditions of saturation and pressure gradient are established. In tests involving gas and oil the sample may contain minimum interstitial-water saturation. Each set of equilibrium conditions results in essentially uniform fluid saturations throughout the test sample and yields a permeability ratio value.

The curve shows the results of this problem in a graph relating gas-oil relative-permeability ratio and total liquid saturation. This graph is characteristically an S-curve becoming asymptotic at both high and low total liquid saturations. At high liquid saturations very little gas flows ($k_g \approx 0$) and the ratio is very small. At low liquid saturations, the oil flow approaches zero and the permeability ratio becomes very large. In between these two extremes is found an almost linear relationship which occurs at total liquid saturations normally encountered in performance calculations.

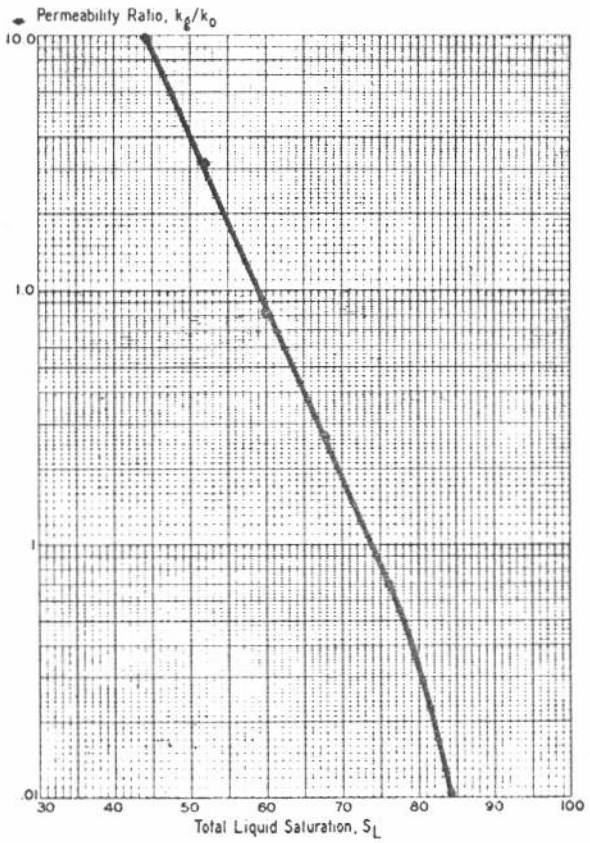

VARIATION of relative permeability ratio (k_g/k_o) with total liquid saturation. Minimum interstitial water saturation = 0.20. Fig. 1.

TABLE 1—DATA AND RESULTS OF PERMEABILITY-RATIO PROBLEM

Run No.	1 Oil saturation S_o % of pore vol.	2 Relative permeability To oil k_o/k	3 Relative permeability To gas k_g/k	4 Total liquid saturation S_L % of pore vol.	5 Permeability ratio k_g/k_o
1	14.4	0	0.90	34.4	∞
2	24.0	0.06	0.60	44.0	10.00
3	32.0	0.10	0.32	52.0	3.20
4	40.0	0.22	0.18	60.0	0.82
5	48.0	0.37	0.10	68.0	0.27
6	56.0	0.55	0.04	76.0	0.07
7	64.0	0.76	0.01	84.0	0.01
8	72.0	0.88	0	92.0	0

The steady-state method of determining permeability ratios was the first developed and used. As noted, the calculations are very simple. But it normally requires several days or weeks to complete the measurements. As a consequence this method is not economically adaptable to routine core analysis. Furthermore, for a lease or pool, many cores must be tested to obtain sufficient data from which to develop a representative average relationship.

It should be emphasized that relative-permeability ratio not only depends on saturation and saturation distribution but also on pore-space geometry and configuration. For this reason it is expected that different rocks and different samples of the same geological zone would have different relative-permeability characteristics. Judgment is essential in the application of relative-permeability tests to actual problems in the same field. Use of such data in computations on fields or formations different from those represented by the samples is hazardous at best.

References

1. Owens, W. W., Parrish, D. R., and Lamoreaux, W. E., "A Comparison of Field k_g/k_o Characteristics and Laboratory k_g/k_o Test Results Measured by a New Simplified Method," Paper 518-G, Trans. AIME, 1956.
2. Calhoun, J. C., "Relative Permeability Ratio," The Oil and Gas Journal manual on Engineering Fundamentals, p. 23.

Part 19

How to obtain a K_g/K_o curve from laboratory unsteady-state flow measurements

GIVEN: Unsteady-state relative-permeability-ratio data were obtained on a core having a pore volume of 1.25 cc. using a pressure differential across the core to 100 psi. (Table 1). Other data measured were downstream pressure = 0 psig., oil viscosity = 31.0 cp., gas viscosity = 0.0185 cp., atmospheric pressure = 14.7 psia., water saturation = 0.25.

FIND: The relationship between the permeability ratio, k_g/k_o, and total liquid saturation using the Welge[2] approach.

METHOD OF SOLUTION: The following equations will be used in the development of the solution in Table 2:

$$S_g = N_p/P.V. \quad (1)$$

$$p = \frac{p_1 + p_d}{2} \quad (2)$$

$$G_{pm} = (G_p/P.V.)\,(p_d/p) \quad (3)$$

$$G_{im} = G_{pm} + S_g \quad (4)$$

$$f_o = \frac{d\,S_g}{d\,G_{im}} \approx \frac{\Delta S_g}{\Delta G_{im}} \quad (5)$$

$$k_g/k_o = \frac{(1 - f_o)\,\mu_g}{f_o\,\mu_o} \quad (6)$$

TABLE 1—UNSTEADY-STATE RELATIVE-PERMEABILITY-RATIO DATA

Run No.	(1) Time, seconds	(2) $N_p + G_p$ cumulative oil plus gas production, cc.	(3) N_p cumulative oil production, cc.
1	0	0	0
2	60	1	0.071
3	80	2	0.090
4	100	5	0.110
5	140	9	0.130
6	180	16	0.148
7	240	31	0.174
8	360	77	0.210
9	510	155	0.245
10	660	260	0.272
11	840	410	0.295
12	1,175	710	0.325
13	1,460	1,060	0.345
14	1,795	1,510	0.361

$$S_{gd} = S_g - f_o\,G_{im} \quad (7)$$

$$S_L = 1 - S_{dg} \quad (8)$$

Where:

S_g = average gas saturation in core, fraction.
N_p = cumulative oil production at outlet pressure and test temperature, cc.
P.V. = pore volume, cc.
p = average pressure, psi.
p_1 = inlet pressure, psi.
p_d = outlet pressure, psi.
G_{pm} = cumulative gas production at mean pressure and test temperature expressed in pore volumes.
G_p = cumulative gas production at outlet pressure and test temperature, cc.
f_o = oil production, fraction of total production.
G_{im} = cumulative injected gas at mean pressure and test temperature expressed in pore volumes.
k_g/k_o = permeability ratio, gas to oil.
μ_g = viscosity of gas at mean pressure and test temperature, cp.

μ_o = viscosity of oil at mean pressure and test temperature, cp.
S_{gd} = gas saturation at outlet end, fraction.
S_L = total liquid saturation, fraction.

EXAMPLE CALCULATION: Run No. 3 will be used to demonstrate the method.

$$S_g = \frac{0.090}{1.25} = 0.0720$$

$$p = \frac{114.7 + 14.7}{2} = 64.7 \text{ psia.}$$

$$G_{pm} = \frac{G_p}{1.25}\,\frac{14.7}{64.7} = 0.1818\ G_p$$

$$= (0.1818)\ (1.910) = 0.347$$

$$G_{im} = 0.347 + 0.0720 = 0.4190$$

$$f_o = \frac{S_{g\,80} - S_{g\,60}}{G_{im\,80} - G_{im\,60}}$$

$$= \frac{0.0720 - 0.0568}{0.4190 - 0.2258} = \frac{0.0152}{0.1932}$$

$$= 0.07867$$

$$k_g/k_o = \frac{(1 - 0.07867)}{0.07867}\,\frac{0.0185}{31.0}$$

$$= 0.00699$$

$$S_{gd} = 0.0720 - (0.0787)\ (0.419)$$

$$= 0.0390$$

$$S_L = 1 - 0.0390 = 0.961,$$

or 96.1%

DISCUSSION

In the laboratory, gas is injected into a core saturated with oil and containing minimum interstitial water saturation. Gas and oil production are measured along with time. During the test the gas saturation varies from a maximum at the inlet end to a minimum at the outlet. This results in a continuously changing gas-oil ratio at each plane in the core. In contrast, fluid saturations in the steady-state method, page 26, are maintained essentially constant throughout the core. Actually, comparable results (to steady-state results) are obtained by the unsteady-state method if the fluid saturations are determined at the outlet end where production occurs.[1]

Equations 1 through 8 are used in computing permeability ratios and compatible fluid saturations from the test measurements, Table 1. The first

Table 2–Calculation Procedure and Results

Run No.	(4) S_g = ($N_p \div$ P.V.)	(5) G_p = (2) − (3)	(6) G_{pm} = (G_p/P.V.) (p_d/p) = 0.1818 G_p	(7) G_{im} = (6) + (4)	(8) ΔS_g = $(4)_1 - (4)_{1-1}$	(9) ΔG_{im} = $(7)_1 - (7)_{1-1}$	(10) $f_o = \Delta S_g/\Delta G_{im}$ = (8) ÷ (9)
1	0	0	0	0	.....	.....	.....
2	0.0568	0.929	0.169	0.2258	.....	.....	.....
3	0.0720	1.910	0.347	0.4190	0.0152	0.1932	0.07867
4	0.0880	4.890	0.889	0.9770	0.0160	0.5580	0.02867
5	0.1040	8.870	1.613	1.7170	0.0160	0.7400	0.02162
6	0.1184	15.852	2.882	3.0004	0.0144	1.2834	0.01122
7	0.1392	30.826	5.604	5.7432	0.0208	2.7428	0.00758
8	0.1680	76.790	13.960	14.1280	0.0288	8.3848	0.00343
9	0.1960	154.755	28.134	28.3300	0.0280	14.2020	0.00197
10	0.2176	259.728	47.219	47.4366	0.0216	19.1066	0.00113
11	0.2360	409.705	74.484	74.7200	0.0184	27.2834	0.00067
12	0.2600	709.675	129.019	129.2790	0.0240	54.5590	0.00044
13	0.2760	1,059.655	192.645	192.9210	0.0160	63.6420	0.00025
14	0.2888	1,509.639	274.452	274.7408	0.0128	81.8198	0.00016

(Table 2 continued)

Run No	(11) k_g/k_o = $[(1 - f_o)/f_o] \times (\mu_g/\mu_o)$	(12) G_{im} avg. = $[(G_{im})_{1-1} + (G_{im})_{1-1}]/2$	(13) G_{im} avg. × f_o = (12) × (10)	(14) S_g avg. = $\frac{(4)_1 + (4)_{1-1}}{2}$	(15) S_{gd} = S_g avg. − $f_o\ G_{im}$ avg. = (14) − (13)	(16) S_L = (1 − S_{gd}) 100%
1	.....	.....	.....	.....	.....	.....
2	.....	.....	.....	.....	.....	.....
3	0.00699	0.3224	0.02536	0.0644	0.0390	96.1
4	0.02023	0.6980	0.02001	0.0800	0.0600	94.0
5	0.02702	1.3470	0.02912	0.0960	0.0669	93.3
6	0.05261	2.3587	0.02646	0.1112	0.0847	91.5
7	0.07816	4.3718	0.03314	0.1288	0.0957	90.4
8	0.17346	9.9356	0.03408	0.1536	0.1195	88.1
9	0.30245	21.2290	0.04182	0.1820	0.1402	86.0
10	0.52772	37.8833	0.04281	0.2068	0.1640	83.6
11	0.89045	61.0783	0.04092	0.2268	0.1859	81.4
12	1.35622	101.9995	0.04488	0.2480	0.2031	79.7
13	2.38740	161.1000	0.04028	0.2680	0.2277	77.2
14	3.73065	233.8309	0.03741	0.2824	0.2450	75.5

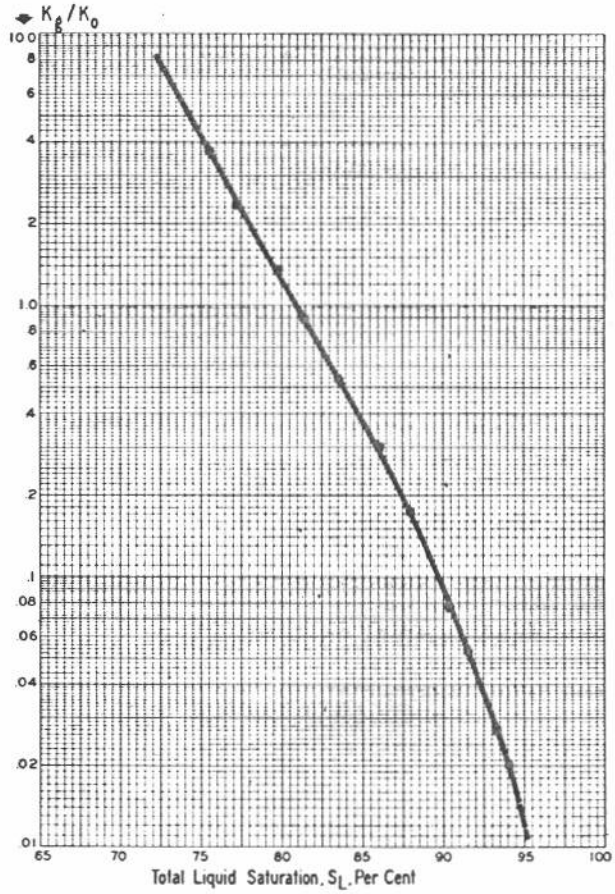

VARIATION of permeability ratio with total liquid saturation. Fig. 1.

five equations are definitions. Equation 6 can readily be derived from the linear Darcy equation. Equation 7 was derived by Welge[2] from the Buckley and Leverett frontal-drive equation using these assumptions: (1) linear and homogeneous system, (2) negligible capillary pressure gradient at outlet end or any other point in the system, (3) gas-oil front (stabilized zone of saturation) has passed through the system, and (4) incompressible fluids.[2] In order to satisfy these requirements it is necessary to select reasonably uniform samples (using visual and X-ray or other techniques), use relatively high flowing pressure gradients (to minimize capillary end effect), and use a 25 to 30-cp. oil (to minimize effect of stabilized zone of saturation). The requirement of incompressible fluids has not been found to be too vital.[1] Computation of the gas volume at mean pressure conditions gives sufficiently accurate results.[2]

Table 2 represents solutions of Equations 1 through 8 at designated times beginning at 60 seconds. Note that this table starts with Column 4 as a continuation of the three columns in Table 1. The differential represented by Equation 5 is approximated by incremental relations and numerically computed. This is sufficiently accurate if enough data are recorded so that the plot of S_g vs. G_{im} is reasonably represented by linear segments between the data points. The value of dS_g/dG_{im} can also be determined from the graph (S_g vs. G_{im}) by drawing a tangent at each data point and evaluating the slope. This latter procedure is tedious and often no more accurate than the former.

Fig. 1 shows the results in a graph typical of k_g/k_o curves, and is representative of a single sample and not necessarily the average for a lease or reservoir. It is necessary to run several samples in an attempt to establish an average curve, and this can become expensive. Often an average laboratory-determined curve based on a few samples is used as a guide in drawing a curve based on limited production data. This latter technique will be covered in a subsequent problem.

Finally, it is well to consider the arguments of those who do not believe that relative-permeability tests adequately represent multiphase flow. The basic equations that utilize permeability ratios are derived assuming a very small unit volume through which the fluids of interest flow uniformly. Work of Chatenever[3] shows that multifluid flow does not often occur in individual pores. That is to say, in certain channels oil alone will be flowing while in others gas alone will flow. The extent to which these deviations affect the results remains to be proven in practical applications. In fact, permeability ratios are now being more widely used and have been found, in many cases, to give reasonable answers.

References

1. Owens, W. W., Parrish, D. R., and Lamoreaux, W. E., "A Comparison of Field k_g/k_o Characteristics and Laboratory k_g/k_o Test Results Measured by a New Simplified Method," Paper 518-G, Trans. AIME, 1956.

2. Welge, H. J., "A Simplified Method for Computing Oil Recovery by Gas or Water Drive," Trans. AIME, (1952), 195, 91.

3. Chatenever, A., A Final Report on API Research Project 47b, "Microscopic Behavior of Fluids in Porous Media."

Part 20

How to obtain and compare k_w/k_o curves from steady-state and laboratory unsteady-state flow measurements

GIVEN: Steady and unsteady-state water and oil relative-permeability data for the same core, Tables 1 and 2, and other data as follows:

Steady-State Test Data

L = length of core = 7.50 cm.
A = cross-sectional area of core = 7.89 cm.^{2}
S_{wm} = minimum interstitial-water saturation = 30.0%.
ϕ = porosity = 23.4%.
μ_w = viscosity of water at mean test conditions = 0.766 cp.
μ_o = viscosity of oil at mean test conditions = 1.20 cp.
W_d = dry weight of core = 178.8830 g.
W_w = water-saturated weight of core = 192.6580 g.
T_t = test temperature = 32° C.
ρ_w = density of water at mean test conditions = 0.9945 g./cc.
ρ_o = density of oil at mean test conditions = 0.7494 g./cc.
PV = pore volume = 13.86 cc.

Unsteady-State Test Data

Average test temperature = 32° C.
Viscosity of oil at mean test conditions = 40.1 cp.
Viscosity of water at mean test conditions = 0.768 cp.

FIND: Variation of water-oil permeability ratios, k_w/k_o, with water saturation by both steady-state and unsteady-state methods.

METHOD OF SOLUTION:
The equations which apply for steady-state conditions are:

$$k_f = \frac{\mu_f Q_f L}{A \Delta p} (1{,}000) \quad (1)$$

$$Q_f = \frac{\text{production of fluid}}{\text{time}} \quad (2)$$

$$S_w = \frac{PV - \dfrac{(W_w - W_d) - (W_e - W_d)}{\rho_w - \rho_o}}{PV}$$

or

$$S_w = \frac{PV - (W_w - W_e)/(\rho_w - \rho_o)}{PV} \quad (3)$$

And for unsteady-state conditions these are used:

$$k_w/k_o = \frac{(1 - f_o)\,\mu_w}{f_o\,\mu_o} \quad (4)$$

TABLE 1—STEADY-STATE LABORATORY DATA

(1) Run No.	(2) Production cc. Water	(3) Production cc. Oil	(4) Time, sec.	(5) Pressure drop, atm. p	(6) Weight of core, g. W_c
1	0.70	9.32	311.6	0.983	190.5363
2	1.93	8.04	331.1	1.020	190.8359
3	3.50	6.53	349.3	1.170	191.0360
4	5.78	4.22	343.2	1.240	191.2567
5	7.90	2.10	336.5	1.340	191.4252

TABLE 2—UNSTEADY-STATE LABORATORY DATA

(1) Measurement No.	(2) Oil prod., cc., ΔN_p	(3) Water prod., cc., ΔW_p
1	1.77	0
2	0.26	0.07
3	0.47	0.43
4	0.50	1.45
5	0.50	3.95
6	0.40	6.20
7	0.30	8.40
8	0.30	13.60
9	0.30	23.10
10	0.30	44.20

TABLE 3—CALCULATION OF WATER-OIL RELATIVE-PERMEABILITY RATIOS FROM STEADY-STATE LABORATORY DATA

Run No.	(7) Q_w = Water prod. ÷ Time (2) ÷ (4) cc./sec.	(8) Q_o = Oil prod. ÷ Time (3) ÷ (4) cc./sec.	(9) $k_w = \frac{\mu_w Q_w L}{A \Delta p}$ × 1,000 md.	(10) $k_o = \frac{\mu_o Q_o L}{A \Delta p}$ × 1,000 md.	(11) k_w/k_o = (9) ÷ (10)	(12) $\frac{W_w - W_e}{\rho_w - \rho_o}$	(13) $S_w = \frac{PV - (12)}{PV}$ fraction	(14) S_w, % (13) × 100
1	0.00225	0.02991	1.67	34.71	0.0481	8.657	0.375	37.5
2	0.00583	0.02428	4.16	27.15	0.1532	7.434	0.464	46.4
3	0.01002	0.01869	6.23	18.22	0.3419	6.618	0.523	52.3
4	0.01684	0.01230	9.89	11.31	0.8744	5.717	0.588	58.8
5	0.02348	0.00624	12.76	5.31	2.4030	5.030	0.637	63.7

$$f_o = \frac{\text{Oil prod.}}{\text{Oil prod.} + \text{water prod.}}$$

$$= \frac{1}{1 + WOR} \quad (5)$$

$$S_{wd} = S_w \text{ avg.} - f_o W_i' \quad (6)$$

$$S_w \text{ avg.} = \frac{N' p}{PV} + S_{wm} \quad (7)$$

$$N_p = N_p - 1/2\ \Delta N_p \quad (8)$$

$$W = \frac{W_p + N_p - 1/2\ [\Delta N_p + \Delta W_p]}{PV} \quad (9)$$

Where:

L, A, S_{wm}, ϕ, μ_w, μ_o, W_d, W_w, T_t, ρ_w, ρ_o, and PV are defined with given data, and

k_f is effective permeability to flowing fluid of interest, md.

μ_f is viscosity of flowing fluid of interest at mean test conditions, cp.

Q_f is rate of flow at mean test conditions, cc./sec.

Δp is pressure drop across core, atm.

S_w is water saturation, fraction of pore volume.

W_c is weight of core containing oil and water, g.

k_w is effective permeability to water, md.

k_o is effective permeability to oil, md.

f_o is oil production, fraction of total production.

WOR is water-oil ratio, no units.

N_p is cumulative oil production, cc.

S_{wd} is water saturation at outlet end, fraction of pore volume.

S_w avg. is average water saturation in core, fraction of pore volume.

W_i' is cumulative water injected to middle of interval, pore volumes.

W_p is cumulative water production, cc.

N_p' is cumulative oil production to middle of interval, cc.

SOLUTION:

The solution is shown for the steady-state data in Table 3. Note that Table 3 contains columns start-

Table 4—Calculation of Water-Oil Relative Permeability Ratios By Unsteady-State Method

Run No.	(4) $\Delta N_p + \Delta W_p$ (2) + (3)	(5) ½ $(\Delta N_p + \Delta W_p)$ = ½ (4)	(6) N_p cc. = Σ (2)	(7) W_p cc. = Σ (3)	(8) WOR = (3) ÷ (2)	(9) 1 + WOR (1) + (8)	(10) f_o = (1) ÷ (9)
1	1.77	0.885	1.77	0	0	1.000	1.000
2	0.33	0.165	2.03	0.07	0.269	1.269	0.7880
3	0.90	0.450	2.50	0.50	0.915	1.915	0.5222
4	1.95	0.975	3.00	1.95	2.90	3.900	0.2564
5	4.45	2.225	3.50	5.90	7.90	8.900	0.1124
6	6.60	3.300	3.90	12.10	15.5	16.50	0.0606
7	8.70	4.350	4.20	20.50	28.0	29.00	0.0345
8	13.90	6.950	4.50	34.10	45.3	46.30	0.0216
9	23.40	11.700	4.80	57.20	77.0	78.00	0.0128
10	44.50	22.250	5.10	101.40	147.3	148.3	0.0067

TABLE 4 (Continued)

Run No.	(11) $[1-f_o] \div f_o$ [1−(10)] ÷ (10)	(12) k_w/k_o = $[(1-f_o)/f_o] \times (\mu_w/\mu_o)$ = (11) × (0.768/40.1)	(13) ½ ΔN_p = ½ (2)	(14) $\frac{N_p - ½\ \Delta N_p}{PV}$ [(6)−(13)] ÷ 13.86	(15) S_w = (14) + S_{wm} (14) + 0.300	(16) $W_p + N_p$ = (7) + (6) W_i
1	0	0	0.885	0.0639	0.364	1.77
2	0.2690	0.00515	0.130	0.137	0.437	2.10
3	0.9150	0.01752	0.235	0.163	0.463	3.00
4	2.900	0.05554	0.250	0.198	0.498	4.95
5	7.897	0.1512	0.250	0.234	0.534	9.40
6	15.50	0.2968	0.200	0.267	0.567	16.00
7	27.99	0.5360	0.150	0.292	0.592	24.70
8	45.30	0.8675	0.150	0.314	0.614	38.60
9	77.13	1.477	0.150	0.335	0.635	62.00
10	148.3	2.840	0.150	0.357	0.657	106.50

TABLE 4 (Continued)

Run No.	(17) (16) − (5)	(18) W_i' (17) ÷ PV	(19) $f_o W_i$ = (10) × (18)	(20) S_{wd} = $S_w - f_o W_i$ = (15) − (19)	(21 S_w, % (20) × 100
1	0.885	0.0639	0.0639	0.300	30.0
2	1.935	0.1396	0.1100	0.327	32.7
3	2.550	0.1840	0.0961	0.367	36.7
4	3.975	0.2868	0.0735	0.424	42.4
5	7.175	0.5177	0.0582	0.476	47.6
6	12.700	0.9163	0.0555	0.511	51.1
7	20.350	1.468	0.0506	0.541	54.1
8	31.650	2.284	0.0493	0.565	56.5
9	50.300	3.629	0.0465	0.588	58.8
10	84.250	6.079	0.0407	0.616	61.6

ing with (7). The first six columns are shown as laboratory data in Table 1. The same procedure was used in the case of the unsteady-state solution in Table 4, where three of its columns are shown as laboratory data in Table 2. The following is a sample calculation for the second row of data in each of Tables 3 and 4.

Steady-state:

$$Q_o = 8.04/331.1 = 0.02428 \text{ cc./sec.}$$

$$Q_w = 1.93/331.1 = 0.00583 \text{ cc./sec.}$$

$$k_o = \frac{(1.20)\,(0.02428)\,(7.50)}{(7.89)\,(1.020)}\,(1{,}000)$$

$$= 27.15 \text{ md.}$$

$$k_w = \frac{(0.766)\,(0.00583)\,(7.50)}{(7.89)\,(1.020)}\,(1{,}000)$$

$$= 4.16 \text{ md.}$$

$$k_w/k_o = 4.16/27.15 = 0.1532$$

$$S_w = \frac{13.86 - \dfrac{(192.6580 - 190.8359)}{(0.9945 - 0.7494)}}{13.86}$$

$$= 0.464 \text{ or } 46.4\%$$

Unsteady-state:

$$WOR = 0.07/0.26 = 0.269$$

$$f_o = 1/(1 + 0.269) = 0.7880$$

$$k_w/k_o = \frac{1 - 0.7880}{0.7880} \times \frac{0.768}{40.1}$$

$$= 0.00515$$

The WOR is calculated using incremental production values occurring over an interval of time. It is necessary that S_w avg. and W_i' be calculated at the middle of the interval of time. Thus:

$$N_p' = N_p - \Delta N_p/2$$

$$= 2.03 - 0.26/2 = 1.90 \text{ cc.}$$

$$S_w \text{ avg.} = 1.90/13.86 + 0.300$$

$$= 0.437$$

$$W_i' = \frac{W_p + N_p - (\Delta W_p + \Delta N_p)/2}{PV}$$

$$= \frac{0.07 + 2.03 - (0.07 + 0.26)/2}{13.86}$$

$$= 0.1396$$

$$S_{wd} = 0.437 - (0.7880)\,(0.1396)$$

$$= 32.7\%$$

DISCUSSION: This problem shows the determination of water-oil relative-permeability ratios on the same core by two methods; steady-state and unsteady-state. The principal difference between the two methods is that the results from unsteady-state data vary with time while those from steady-state data do not. Of the two methods the steady-state has been the most frequently used. Equations 1, 2, and 3 show that the calculations are simple. It is considered reliable by many[1] but has the major disadvantage that several days to weeks may be required to perform the laboratory tests.

The data for the unsteady-state method can be obtained within an hour after the core is prepared. Equations 4 through 9 show that by comparison with the steady-state approach the calculation procedure is more involved.[2] In spite of this the unsteady-state method is more adaptable to routine core-analysis procedures. This is especially true if the calculations can be performed with a small or medium-size electronic computer.

Do the two methods give comparable results? It is well to remember that in the steady-state method, fixed ratios of oil and water are flowed through the core until equilibrium conditions of saturation and pressure gradient are established. Data similar to those shown in Table 1 are then recorded.

In the unsteady-state method a core saturated with oil and interstitial (minimum) water is subjected to a water drive, and data similar to those shown in Table 2 are recorded. Both of these tests involve the same assumptions that were discussed for gas-oil relative-permeability determinations. Parts 18 and 19 of this series. Work performed by Lee[1] shows that the agreement between the two methods is not too good.

The results of this problem are in fair agreement over a large water-saturation range. Another thing to consider is that at least several curves would be required in order to obtain an average relationship for a lease or reservoir. Lee's[1] results show that the unsteady-state data may be both higher or lower than the steady-state data. Thus in the averaging of several curves compensation may occur and better agreement obtained. Furthermore, these data are used in the prediction of water-drive performance with other data, the reliability of which, may also be subject to limitations.

References

1. Lee, George C., "A Water-Oil Relative Permeability Ratio" unpublished thesis, University of Tulsa, 1957.

2. Welge, H. J., "Simplified Method for Computing Oil Recovery by Gas or Water Drive," Trans, AIME, 1952, 195.

THIS CURVE shows that the agreement in the results by the steady-state and the unsteady-state methods is fair, and probably within the limits of accuracy of some of the data used. It is believed that the accuracy justifies the use of the more approximate unsteady-state method to obtdin results faster and cheaper.

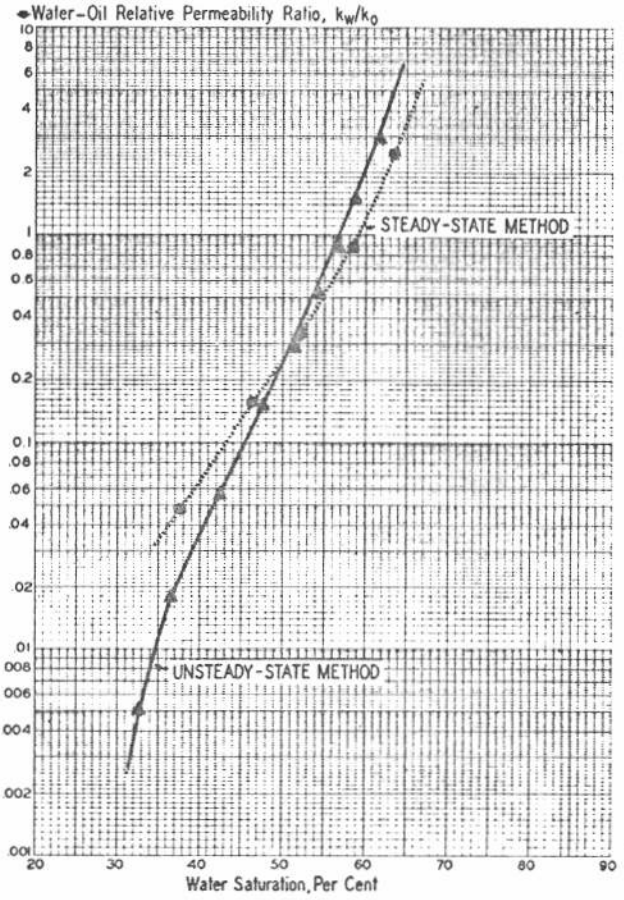

Part 21

How to obtain relative permeabilities and relative permeability ratios

. . . from laboratory unsteady-state displacement data. A sandstone core is used and the results are compared with steady-state data

GIVEN: A sandstone core saturated with water (minimum interstitial) and oil was used in a water-displacement experiment. The same core was later cleaned and used to obtain water and oil relative permeabilities by steady-state method. Basic data for the unsteady-state displacement test data are given in Columns 1, 2, and 3 of Table 2.

Other known data are as follows:

Absolute permeability, k = 2.68 darcies.

Cross-sectional area of core, A = 5.03 sq. cm.

Constant rate of water injection, Q_t = 8.10 cc./min.

Permeability to water at end of flood = 670 md.

Water saturation at outlet end at end of flood = 69.0%.

Permeability to oil at minimum interstitial - water saturation = 2.68 darcies.

Minimum interstitial - water saturation = 12.6%.

Viscosity of oil at mean test conditions, μ_o = 45.7 cp.

Viscosity of water at mean test conditions, μ_w = 0.90 cp.

Length of core, L = 15.7 cm.

Steady-state test data are given in Columns 1, 2, and 3 of Table 1.

FIND: Variation of relative permeability to oil, relative permeability to water, and water-oil relative-permeability ratios with water saturation by both steady and unsteady-state methods.

METHOD OF SOLUTION: Actual calculation of effective permeabilities from steady-state data is not included in this problem because this was shown in a previous problem.[2] (Page 13.) Equations defining relative permeabilities are:

$$k_{ro} = k_o/k \quad (1)$$

$$k_{rw} = k_w/k \quad (2)$$

For unsteady-state conditions:

$$f_{o2} = \frac{d_{sw}}{d_{w1}} \approx \frac{\Delta S_w}{\Delta W_i} \quad (3)$$

(Columns 4 through 6, Table 2)

$$k_{ro} = \frac{f_o}{d\,(1/W_i I_r)/d\,(1/W_i)} \approx f_o \frac{\Delta(1/W_i)}{\Delta(1/W_i I_r)} \quad (4)$$

(Columns 7 through 13, Table 2)

$$\frac{1}{I_r} = \frac{v_s/\Delta p_s}{v_t/\Delta p} = \frac{k/L\,\mu_o}{14.7 Q_t/60A\,\Delta p} = \frac{k\,A\,\Delta p}{Q_t L\,\mu_o}\,\frac{60}{14.7} \quad (5)$$

$$v_s/\Delta p_s = \frac{k}{L\,\mu_o} \quad (6)$$

$$v_t/\Delta p = \frac{14.7\,Q_t}{60A\,\Delta p} \quad (7)$$

$$S_{w2} = S_w \text{ avg.} - W_i \text{ avg. } f_{o2} \quad (8)$$

(Columns 14 through 17, Table 2)

$$k_{rw} = k_{ro}\left(\frac{1-f_o}{f_o}\right)\frac{\mu_w}{\mu_o} \quad (9)$$

(Columns 18 through 21, Table 2)

$$k_{rw}/k_{ro} = k_w/k_o \quad (10)$$

(Columns 22 through 24, Table 2)

Where:

Q_t was defined with the data.

f_o and f_{o2} are fractions of oil in total flow at any point and at the outlet end, respectively.

S_w, S_{w2}, S_w avg. are water saturations at any point, at the outlet end, and in an interval of interest, respectively.

I_r is the relative injectivity or the ratio of the intake capacity at any point in a flood to the intake capacity of the system at the initiation of the flood.

v_t and v_s are average velocities in the pores, cm./second, at any point and at the initiation of the flood, respectively.

p and p_s are pressure drops across the core, psi., at any time and at the initiation of the flood, respectively.

All others are standard AIME symbols (Journal of Petroleum Technology, October 1956).

SOLUTION:

The results of the steady-state method are shown in Table 1, Columns 4, 5, and 6. As an example calculation take a water saturation of 20.0% where k_o = 2,360 md. and k_w = 21.4 md.

$$k_{ro} = \frac{(2{,}360)}{(2.68)\,(1{,}000)} = 0.881$$

TABLE 1—RELATIVE-PERMEABILITY RATIOS FROM STEADY-STATE DATA

Run No.	(1) k_o, md.	(2) k_w, md.	(3) S_w, %	(4) k_{ro}	(5) k_{rw}	(6) k_w/k_o
1	2,680	0	12.6	1.00	0	0
2	2,360	21.4	20.0	0.881	0.008	0.00908
3	2,140	34.8	24.0	0.799	0.013	0.0163
4	1,770	48.2	30.0	0.660	0.018	0.0273
5	1,610	53.6	32.5	0.601	0.020	0.0333
6	1,110	75.0	40.0	0.414	0.028	0.0676
7	697	142	50.0	0.260	0.053	0.204
8	536	214	54.5	0.200	0.080	0.400
9	375	335	60.0	0.140	0.125	0.893
10	255	536	66.0	0.095	0.200	2.11
11	0	844	74.0	0	0.315	∞

Absolute permeability, k = 2.68 darcies.

TABLE 2—BASIC DATA AND CALCULATION OF RELATIVE PERMEABILITIES AND RELATIVE-PERMEABILITY RATIOS FROM THE UNSTEADY-STATE WATER-DISPLACEMENT TESTS

Run No.	(1) W_i PV	(2) S_w fraction	(3) Δp psi.	(4) ΔS_w $(2)_n - (2)_{n-1}$	(5) ΔW_i $(1)_n - (1)_{n-1}$	(6) $\Delta S_w/\Delta W_i = f_{o2}$ (4) ÷ (5)	(7) $1/I_r$ $\Delta p \div 105.63$	(8) $1/W_i$ $1 \div (1)$
1	0.2	0.325	61.5				0.5822	5.0000
2	0.3	0.398	50.0	0.073	0.1	0.730	0.4734	3.3333
3	0.4	0.466	41.3	0.068	0.1	0.680	0.3910	2.5000
4	0.5	0.504	34.3	0.038	0.1	0.380	0.3247	2.0000
5	0.6	0.530	29.3	0.026	0.1	0.260	0.2774	1.6667
6	0.7	0.552	25.2	0.022	0.1	0.220	0.2386	1.4286
7	0.8	0.569	22.2	0.017	0.1	0.170	0.2102	1.2500
8	0.9	0.581	20.0	0.012	0.1	0.120	0.1893	1.1111
9	1.0	0.590	18.7	0.009	0.1	0.090	0.1770	1.0000
10	1.2	0.602	16.7	0.012	0.2	0.060	0.1581	0.8333
11	1.4	0.614	15.2	0.012	0.2	0.060	0.1439	0.7143
12	1.6	0.624	14.5	0.010	0.2	0.050	0.1373	0.6250
13	1.8	0.633	13.8	0.009	0.2	0.045	0.1306	0.5556
14	2.0	0.642	13.1	0.009	0.2	0.045	0.1240	0.5000
15	2.2	0.648	12.5	0.006	0.2	0.030	0.1183	0.4545
16	2.4	0.655	12.1	0.007	0.2	0.035	0.1146	0.4167
17	2.6	0.661	11.4	0.006	0.2	0.030	0.1079	0.3846
18	2.8	0.666	11.0	0.005	0.2	0.025	0.1041	0.3571
19	3.0	0.671	10.6	0.005	0.2	0.025	0.1004	0.3333
20	3.4	0.678	10.0	0.007	0.4	0.018	0.0947	0.2941
21	3.8	0.685	9.5	0.007	0.4	0.018	0.0899	0.2632
22	4.2	0.692	8.8	0.007	0.4	0.018	0.0833	0.2381

TABLE 2 (Continued)

Run No.	(9) $1/W_i I_r$ (7) × (8)	(10) $\Delta(1/W_i)$ $(8)_n - (8)_{n-1}$	(11) $\Delta(1/W_i I_r)$ $(9)_n - (9)_{n-1}$	(12) $\frac{\Delta(1/W_i)}{\Delta(1/W_i I_r)}$ (10) ÷ (11)	(13) k_{ro} (6) × (12)	(14) S_w avg. $\frac{(2)_n + (2)_{n-1}}{2}$	(15) W_i avg. $\frac{(1)_n + (1)_{n-1}}{2}$	(16) $f_o W_i$ avg. (6) × (15)
1	2.9110	.....	.....	.....	.....	.....	....	.....
2	1.5780	1.6667	1.3330	1.2503	0.9127	0.3615	0.25	0.1825
3	0.9775	0.8333	0.6005	1.3877	0.9436	0.4320	0.35	0.2380
4	0.6494	0.5000	0.3281	1.5239	0.5791	0.4850	0.45	0.1710
21	0.0237	0.0309	0.0042	7.3571	0.1324	0.6815	3.60	0.0648
22	0.0198	0.0251	0.0039	6.4359	0.1158	0.6885	4.00	0.0720

TABLE 2 (Continued)

Run No.	(17) S_{w2} (14) − (16)	(18) $f_w = \frac{(1 - f_o)}{1 - (6)}$	(19) f_w/f_o (18) ÷ (6)	(20) $(f_w/f_o) \times k_{ro}$ (19) × (13)	(21) $k_{rw} = f_w/f_o \times k_{ro} \times \mu_w/\mu_o$ (20) × μ_w/μ_o	(22) $k_{rw}/k_{ro} = k_w/k_o$ (21) ÷ (13)	(23) k_o, md.	(24) k_w, md.
1	.....	.....	.....	.....	.....	.....	....	....
2	0.1790	0.270	0.3699	0.3376	0.0066	0.0072	2,446	17.7
3	0.1940	0.320	0.4706	0.4441	0.0087	0.0092	2,529	23.3
4	0.3140	0.620	1.6316	0.9449	0.0186	0.0321	1,552	49.8
21	0.6167	0.982	54.5556	7.2232	0.1422	1.0740	355	381
22	0.6165	0.982	54.5556	6.3175	0.1244	1.0743	310	333

Note: Columns 9 to 24 abridged.

$$k_{rw} = \frac{21.4}{(2.68)\,(1{,}000)} = 0.008$$

$$\frac{k_w}{k_o} = \frac{k_{rw}}{k_{ro}} = \frac{0.008}{0.881} = 0.00908$$

The calculating steps and results by the unsteady-state method are shown in Columns 4 through 24 of Table 2. As an example calculation take the data for a water saturation of 39.8%

where $W_i = 0.3$ and $\Delta p = 50$ psi.

$$f_o = \frac{0.398 - 0.325}{0.3 - 0.2} = 0.73$$

$$\frac{I}{I_r} = \frac{(2.68)\,(5.03)\,(\Delta p)\,(60)}{(8.10)\,(15.7)\,(45.7)\,(14.7)}$$

$$= \frac{\Delta p}{105.63} = \frac{50.0}{105.63} = 0.4734$$

$$k_{ro} = (0.73)\frac{(5.0000 - 3.3333)}{(2.9110 - 1.5780)}$$

$$= 0.9127$$

Note that numerical differentiation has been used in the solution of this problem. Columns 14 and 15 show average values of S_w and W_i corresponding to the midpoint of the interval involved.

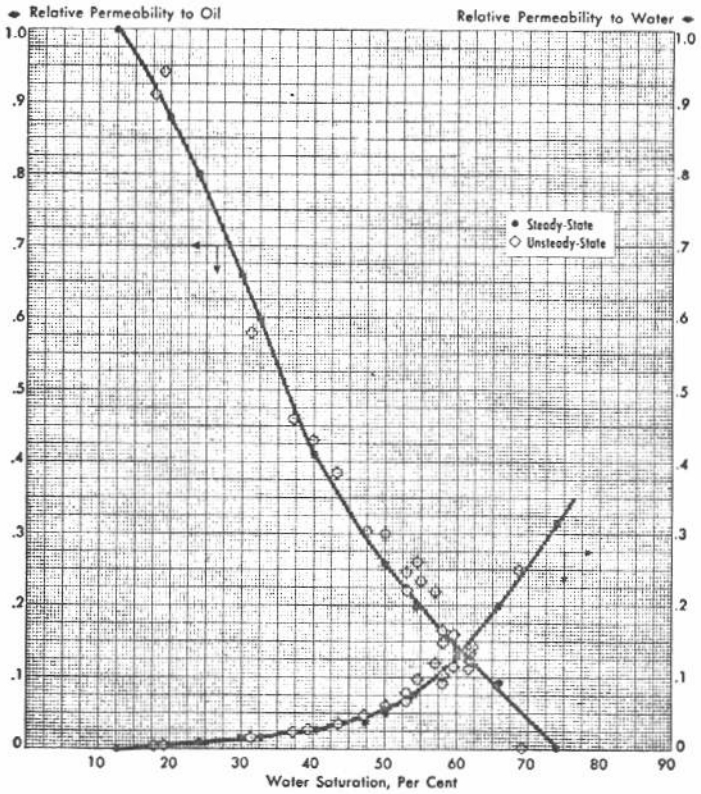

OIL-AND-WATER relative-permeability curves. These show the fairly close agreement btween the two methods of calculation. Fig. 1.

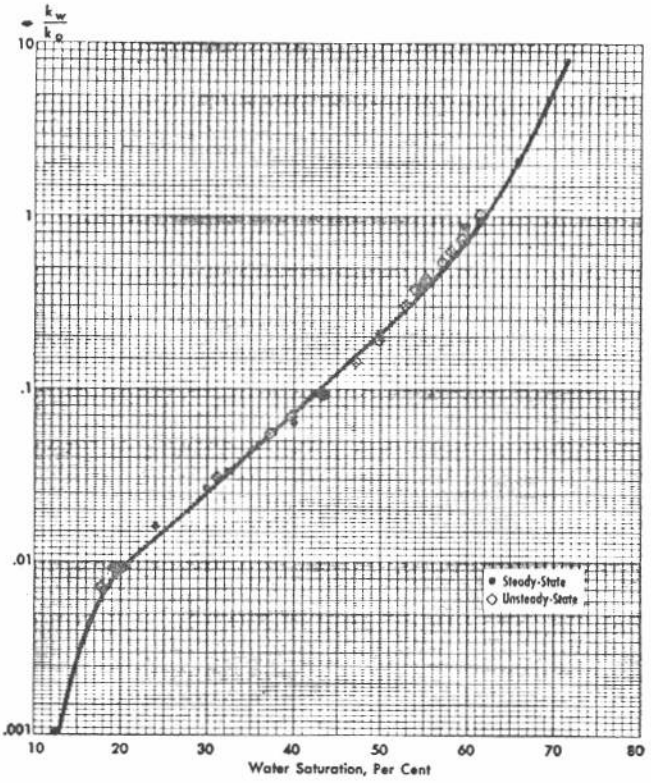

PERMEABILITY RATIO CURVE for the same data as shown in Fig. 1. This curve emphasizes the small differences in the two calculation methods. Fig. 2.

Thus:

$$W_i \text{ avg.} = \frac{0.2 + 0.3}{2} = 0.25$$

$$S_w \text{ avg.} = \frac{0.325 + 0.398}{2} = 0.3615$$

and

$$S_{w2} = 0.3615 - (0.25)\,(0.73) = 0.1790$$

$$k_{rw} = 0.9127 \times \frac{1 - 0.73}{0.73} \times \frac{0.90}{45.7} = 0.0066$$

$$\frac{k_{rw}}{k_{ro}} = \frac{k_w}{k_o} = \frac{0.0066}{0.9127} = 0.0072$$

$$k_w = (0.0066)\,(2.68) = 0.0177 \text{ darcies} = 177 \text{ md.}$$

$$k_o = (0.9127)\,(2.68) = 2.446 \text{ darcies} = 2{,}446 \text{ md.}$$

DISCUSSION: This problem illustrates the use of one of the latest extended applications of the original Buckley and Leverett Frontal Advance theory.[5] For a long time this theory was used as extended by Welge (examples of which are Part 19[6] and Part 20[7] of this series). Welge's extension[3] made it possible to use this theory in the laboratory determination of permeability ratios, k_g/k_o and k_w/k_o. Johnson et al.[1] added to Welge's work in order to make possible the determination of relative and effective permeabilities (in addition to permeability ratios) from laboratory displacement tests. Although their method is applied in this problem to water-displacement test data, it can be used to calculate equivalent values from gas displacement tests. The assumptions necessary for the validity of the theory were discussed in Part 19.[6]

Equations 3, 8, and 9 were previously discussed and used.[6 7] Equations 4 and 5 were developed by Johnson et al.[1] using the frontal-advance equation and Rapaport's[4] relative-injectivity function. The obtainment of values for the derivative terms in Equations 3 and 4 can be accomplished by either graphical or numerical methods. The numerical method used in this case is simple, sufficiently accurate, and easy to perform. It assumes that a graph of the factors involved (S_w vs. W_i and $1/W_i$ vs. $1/W_i I_r$) is a straight line between any two successive data points.

By comparison, the calculations involved in the unsteady-state method are considerably more involved than for the steady-state approach. However, the basic data for the former method can be obtained in a matter of a few hours where the latter may require days or even weeks. The disadvantage of complex calculations becomes minor when the use of an electronic computer is available.

Fig. 1 shows oil and water relative permeabilities as determined from steady and unsteady-state tests. Note that the two methods give comparable results. Fig. 2 shows the same data plotted in ratio form. Here a typical relative-permeability ratio graph is obtained with the data from the two methods again agreeing quite well. The graph has been extended to form the typical S-curve based on knowledge of the fluid saturations at which each of the fluids begins and stops to flow.

The unsteady-state method of obtaining flow data illustrated by this problem is more practical than the Welge technique[3 6 7] since it gives effective permeabilities in addition to permeability ratios. This is true despite the fact that the two methods use similar displacement data.

References

1. Johnson, E. F., Bossler, D. P., and Nanmann, V. O., "Calculation of Relative Permeability From Displacement Experiments," Third Biennial Secondary-Recovery Symposium, 1958, AIME paper 1023-G.

2. Guerrero, E. T., and Stewart, F. M., "Measurement of Effective Permeability," The Oil and Gas Journal, April 20, 1959, p. 120

3. Welge, H. J., "Simplified Method for Computing Oil Recovery by Gas or Water Drive," Trans. AIME (1952), 195, 91.

4. Rapaport, L. A., and Lies, W. J., "Properties of Linear Water Floods," Trans. AIME (1953), 198, 139.

5. Buckley, S. E., and Leverett, M. C., "Mechanism of Fluid Displacement in Sands," AIME Tech. Pub. 1337.

6. Guerrero, E. T., and Stewart, F. M., Part 19, The Oil and Gas Journal, Feb. 1, 1960, p. 96

7. Guerrero, E. T., and Stewart, F. M., Part 20, The Oil and Gas Journal, Feb. 22, 1960, p. 104

Part 22

How to determine the k_g/k_o ratio from production and fluid-analysis data

GIVEN: The following production and fluid-analysis data were obtained from a sand reservoir in Arkansas:

Run No.	(1) Pressure, p, (psig.)	(2) Inst. GOR, R_I, std. cu. ft. per stock-tank bbl.	(3) Oil FVF, β_o, res. bbl. per stock-tank bbl.	(4) Gas FVF, β_g res. bbl. per std. cu. ft.	(5) Sol. GOR, R_s, std. cu. ft. per stock-tank bbl.	(6) Cum. oil prod., N_p M.M. bbl.	(7) Viscosity ratio, μ_o/μ_g
1	3,548	770	1.450	0.000815	770	0	....
2	3,448	850	1.443	0.000840	752	0.476	30.4
3	3,303	920	1.432	0.000875	725	1.743	32.1
4	3,153	990	1.420	0.000910	695	2.818	34.0
5	2,938	1,000	1.403	0.000970	657	4.632	36.8
6	2,813	1,020	1.393	0.001010	632	6.030	38.4
7	2,678	1,180	1.382	0.001062	608	7.360	40.5
8	2,533	1,420	1.371	0.001122	580	8.751	42.4
9	2,453	1,510	1.364	0.001162	565	9.873	43.6
10	2,318	1,660	1.354	0.001230	540	11.259	45.5
11	2,153	1,920	1.340	0.001330	509	12.619	48.0
12	1,978	2,220	1.326	0.001453	476	13.998	50.8
13	1,818	2,480	1.313	0.001590	446	15.321	53.8
14	1,658	2,710	1.301	0.001758	416	16.552	57.4
15	1,625	2,800	1.298	0.001795	410	16.929	58.2

OTHER DATA: Original stock-tank oil in place, from geological and volumetric analysis, 116.5 million barrels; interstitial-water saturation, 28.5%; bubble-point pressure, 3,548 psig.

FIND: Relationship between permeability ratio (gas to oil) and total liquid saturation.

METHOD OF SOLUTION: The determination of the k_g/k_o ratio from production and fluid-analysis data involves the use of the instantaneous gas-oil-ratio equation.

$$R_I = R_s + \frac{\mu_o}{\mu_g}\frac{k_g}{k_o}\frac{\beta_o}{\beta_g} \qquad (1)$$

or

$$\frac{k_g}{k_o} = (R_I - R_s)\frac{1}{\mu_o/\mu_g}\frac{\beta_g}{\beta_o} \qquad (2)$$

Where:

R_I is instantaneous GOR, std. cu. ft. per stock-tank bbl.

R_s is solution GOR, std. cu. ft. per stock-tank bbl.

μ_o is viscosity of oil at reservoir conditions, cp.

μ_g is viscosity of gas at reservoir conditions, cp.

k_g/k_o is permeability ratio, gas to oil.

β_o is formation volume factor of oil, res. bbl. per stock-tank bbl.

β_g is formation volume factor of gas, res. bbl. per std. cu. ft.

The total liquid saturation corresponding to each respective k_g/k_o is given by the equation:

$$S_L = S_w + (1 - S_w) \times \frac{N - N_p}{N} \times \frac{\beta_{oi}}{\beta_o} \qquad (3)$$

Table 1—Calculations of Permeability Ratios

Run No.	(8) β_g/β_o (4) ÷ (3)	(9) $(\mu_g/\mu_o)\times(\beta_g/\beta_o)$ (8) ÷ (7)	(10) $R_I - R_s$ (2) − (5)	(11) k_g/k_o (10) × (9)	(12) $N - N_p$ 116.5 − (6) M.M. bbl.
1	0.000562	0	0	0	116.500
2	0.000582	0.0000191	98	0.00187	116.024
3	0.000611	0.0000190	195	0.00371	114.757
4	0.000641	0.0000189	295	0.00558	113.682
5	0.000691	0.0000188	343	0.00645	111.868
6	0.000725	0.0000189	388	0.00733	110.470
7	0.000768	0.0000190	572	0.01087	109.140
8	0.000818	0.0000193	840	0.01621	107.749
9	0.000852	0.0000195	945	0.01843	106.627
10	0.000908	0.0000200	1,120	0.02240	105.241
11	0.000993	0.0000207	1,411	0.02921	103.881
12	0.001096	0.0000216	1,744	0.03767	102.502
13	0.001211	0.0000225	2,034	0.04577	101.179
14	0.001351	0.0000235	2,294	0.05391	99.948
15	0.001383	0.0000238	2,390	0.05688	99.571

Where:

S_L is total liquid saturation, fraction of pore volume.

S_w is interstitial water saturation, fraction of pore volume.

N is initial oil in place, stock-tank bbl.

β_{oi} is initial oil formation volume factor.

SOLUTION: For a problem of this type it is best to set up the solution in tabular form. The table of basic data here as Columns 1 through 7 will be continued in the solution.

The data for a pressure of 1,625 psi. will be used with Equations 2 and 3 to illustrate the method of calculation.

$$k_g/k_o = (2{,}800 - 410) \times \frac{1}{58.2} \times \frac{0.001795}{1.298}$$

$$= 0.05688 \approx 0.057$$

$$S_L = 0.285 + (1 - 0.285) \times \frac{116.500 - 16.929}{116.500} \times \frac{1.298}{1.450}$$

$$= 0.832 \text{ or } 83.2\% \text{ of pore volume}$$

DISCUSSION: Equation 1 is normally used to compute the instantaneous gas-oil ratio, R_I, when the necessary fluid and rock properties are known.

In this problem it is used to solve for the average gas-oil permeability ratio of a sand reservoir. The assumptions made in this application are: (1) the pressure drawdown in the vicinity of the wells is negligible, (2) the gas and oil are uniformly distributed throughout the porous media and are flowing according to the equilibrium relative permeability concept, (3) the pressure gradients are the same in the oil and gas phases, and (4) gravity and capillary pressure effects are negligible.[1,2]

Data for the solution of Equation 2 are obtained from laboratory tests on reservoir fluid samples and from well tests. Twenty-four-production tests are usually used to evaluate R_I, the instantaneous gas-oil ratio.

For each permeability ratio computed it is necessary to determine a corresponding total liquid saturation. Equation 3 defines this parameter with the assumptions that (1) the reservoir pore volume remains constant during the production history (no water or gas influx) and (2) oil and gas remaining within the reservoir are distributed evenly throughout the pore space.[1] For conditions where the reservoir is not of constant volume, the equation must be modified for the amount of water or gas encroachment and the resulting expression becomes considerably more complex. Note that in Equation 3 the initial oil in place (N) and cumulative oil production (N_p) must be known.

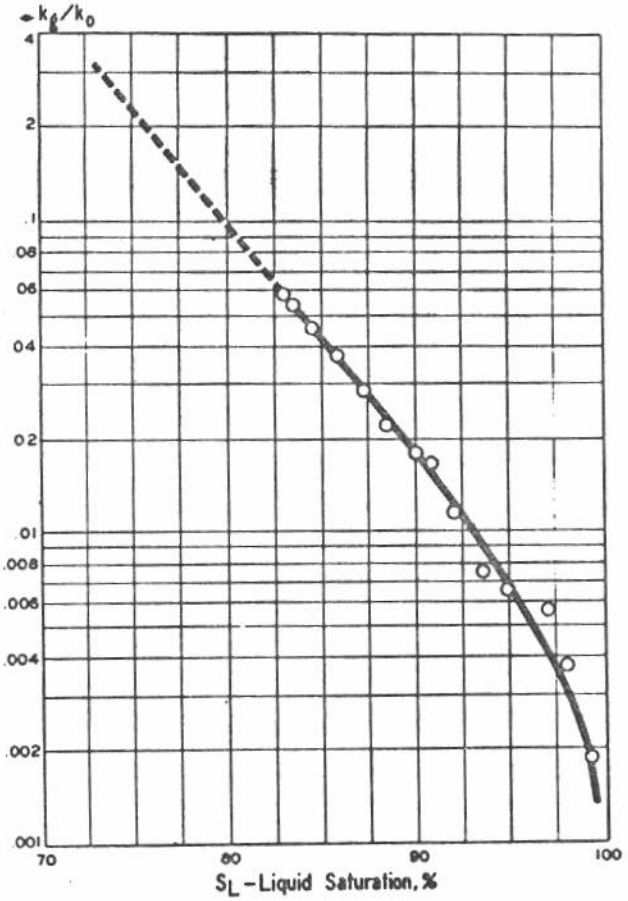

PERMEABILITY RATIO for sand reservoir in Arkansas. Fig. 1.

It is difficult to conceive that any reservoir could satisfy the assumptions made in the equations used because: (1) in most cases pressure drawdown occurs at the well bore, (2) free gas distribution will not be uniform, either vertically or horizontally, (3) gas will often come from a primary or secondary gas cap into the producing wells. These factors frequently tend to make the apparent R_I and k_g/k_o higher than they actually may be at the existing liquid saturation. The opposite effects may also be observed.

In spite of the many limitations imposed by field conditions, permeability ratios determined by this method are perhaps more representative of the reservoir than the average of data determined on a few small cores. Frequently the amount of field data is limited. In such a case laboratory data could be used (follow same slope or trend) to extrapolate the field data. Where no field data are available, an average laboratory determined relationship can be used and later checked with field data.

and corresponding total liquid saturations

Run No.	(13) $(N - N_p)/N$ (12) ÷ 116.5	(14) β_o/β_{oi} (3) ÷ 1.450	(15) $[(N - N_p)/N]$ (β_o/β_{oi}) (13) × (14)	(16) $(1-S_w)(N-N_p)$ $\times (\beta_o/\beta_{oi})$ $(1/N)$ 0.715 × (15)	(17) S_L 0.285 + (16)
1	1.000	1.000	1.000	0.715	1.000
2	0.996	0.995	0.991	0.709	0.994
3	0.985	0.988	0.973	0.696	0.981
4	0.976	0.979	0.956	0.684	0.969
5	0.960	0.968	0.929	0.664	0.949
6	0.948	0.961	0.911	0.651	0.936
7	0.937	0.953	0.893	0.638	0.923
8	0.925	0.946	0.875	0.626	0.911
9	0.915	0.941	0.861	0.616	0.901
10	0.903	0.934	0.843	0.603	0.888
11	0.892	0.924	0.824	0.589	0.874
12	0.880	0.914	0.804	0.575	0.860
13	0.868	0.906	0.786	0.562	0.847
14	0.858	0.897	0.770	0.551	0.836
15	0.855	0.895	0.765	0.547	0.832

References

1. Calhoun, J. C., Engineering Fundamentals, booklet published by The Oil and Gas Journal, pp. 40-43.

2. Pirson, S. J., Oil Reservoir Engineering, 2nd Edition, McGraw-Hill Book Co., Inc., pp. 402-404.

Part 23

How to compute an average-permeability-ratio curve

. . . for a lease or a reservoir, using individual sample curves

GIVEN: Laboratory permeability-ratio data for five curves within a permeability range and average curves for four additional ranges as shown in Tables 2 and 3, columns 1 through 6. The respective ranges represent the formation according to the percentage thickness factors given in Table 1.

TABLE 1—WEIGHTING FACTORS FOR DIFFERENT RANGES

Ranges		% of formation thickness
Number	Permeability range, md.	
1	Less than 10	15.1
2	10-50	38.5
3	50-100	32.7
4	100-300	11.3
5	300-500	2.4

FIND: 1. Average permeability-ratio curve for the five curves of range 1 by visual approximation and by the least-squares method.

2. Average reservoir (or lease) permeability-ratio curve by (a) visual approximation, (b) least-squares method, and (c) weighting according to the sand represented by each range.

METHOD OF SOLUTION: For solution by the method of least squares, this equation applies:

$$\log (k_g/k_o)' = \left[\frac{n \Sigma (S_L \log k_g/k_o) - \Sigma S_L \Sigma \log k_g/k_o}{n \Sigma S_L^2 - (\Sigma S_L)^2}\right] S_L' + \left[\frac{\Sigma S_L^2 \Sigma \log k_g/k_o - \Sigma S_L \Sigma (S_L)(\log k_g/k_o)}{n \Sigma S_L^2 - (\Sigma S_L)^2}\right] \quad (1)$$

And for the weighted average solution, this equation is used:

$$S_{Lav.} = \sum_{1=1}^{1=5} S_{Li} H_i \quad (2)$$

Where:

$(k_g/k_o)'$ is average permeability-ratio for a given saturation.

S_L' is average saturation corresponding to $(k_g/k_o)'$.

S_L is total liquid saturation.

k_g/k_o is permeability ratio.

H_i is fraction of formation thickness represented by a permeability range.

S_{Li} is range average total liquid saturation corresponding to a selected k_g/k_o.

$S_{Lav.}$ is average reservoir (or lease) total liquid saturation corresponding to a selected k_g/k_o.

SOLUTION: Table 2, columns 7 through 15, show the basic least-squares calculations for the equation of the average curve for the five graphs of range 1. With these data, Equation 1 can be solved:

$$\log (k_g/k_o)' = \left[\frac{(35)(134.7) - (2,640)(4.628)}{(35)(202,220) - (2,640)^2}\right] S_L + \frac{(202,220)(4.628) - (2,640)(134.7)}{(35)(202,220) - (2,640)^2} = -0.06941\, S_L' + 5.368 \quad (3)$$

For $S_L' = 90\%$

$$\log (k_g/k_o)' = -(0.06941)(90) + 5.368$$

$$= 9.121 - 10$$

$$(k_g/k_o)' = 0.132$$

Table 3, columns 7 through 15, shows the basic least-squares calculations for the equation of the average curve for the graphs of the five ranges. Again solving Equation 1:

$$\log (k_g/k_o)' = \left[\frac{(30)(-329.2) - (2,190)(-2.677)}{(30)(161,720) - (2,190)^2}\right] S_L' + \left[\frac{(161,720)(-2.677) - (2,190)(-329.2)}{(30)(161,720) - (2,190)^2}\right] = -0.0723\, S_L' + 5.190 \quad (4)$$

For $S_L' = 80\%$

$$\log (k_g/k_o)' = (-0.0723)(80) + 5.190$$

$$= 9.406 - 10$$

$$(k_g/k_o)' = 0.255$$

Using the data for $k_g/k_o = 0.04$ in Table 4, and the weighting factors from Table 1,

$$S_{Lav.} = (93.1)(0.151) + (93.9)(0.385) + (90.6)(0.327) + (86.7)(0.113) + (83.6)(0.024)$$

$$= 91.6\%$$

DISCUSSION: This problem essentially illustrates three methods of averaging relative-permeability-ratio curves. The approximate and least-squares methods are similar in that they give each curve equal weight. The former is performed by visual inspection and approximation; the latter method involves the solution of Equation 1. It is the equation of the straight line best fitting the data points. The slope and ordinate intercept constants

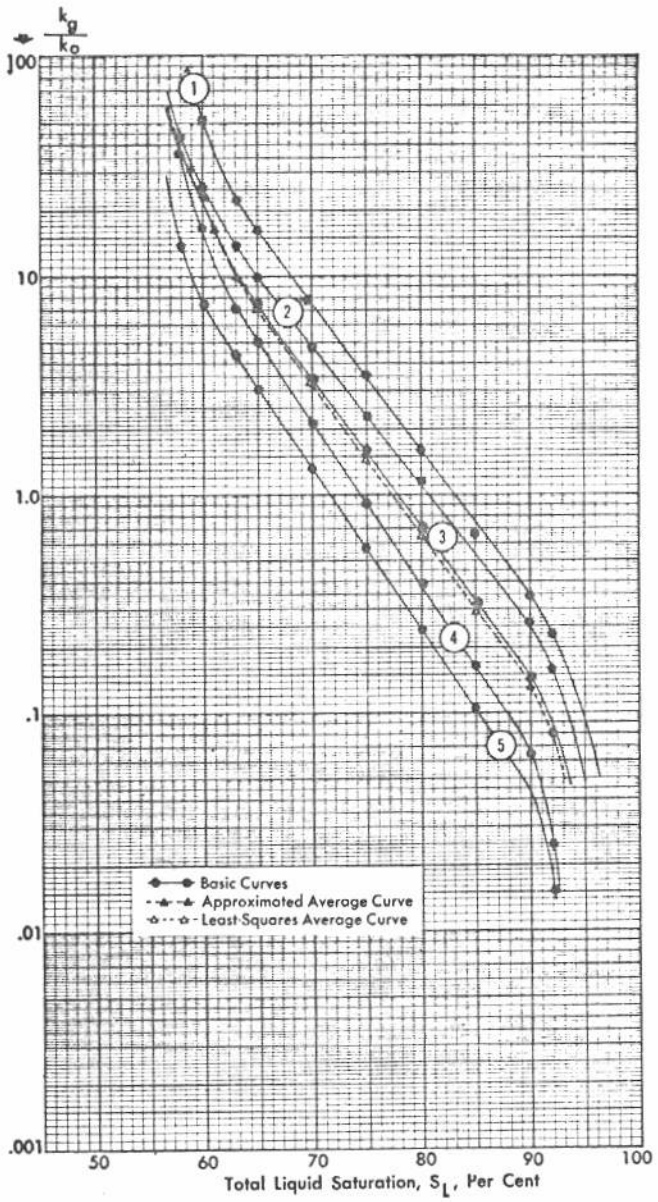

INDIVIDUAL CURVES for range 1 data and the average curves by visual inspection and least-squares approach. Difference between the last two is apparent only at high values of k_g/k_o. Fig. 1.

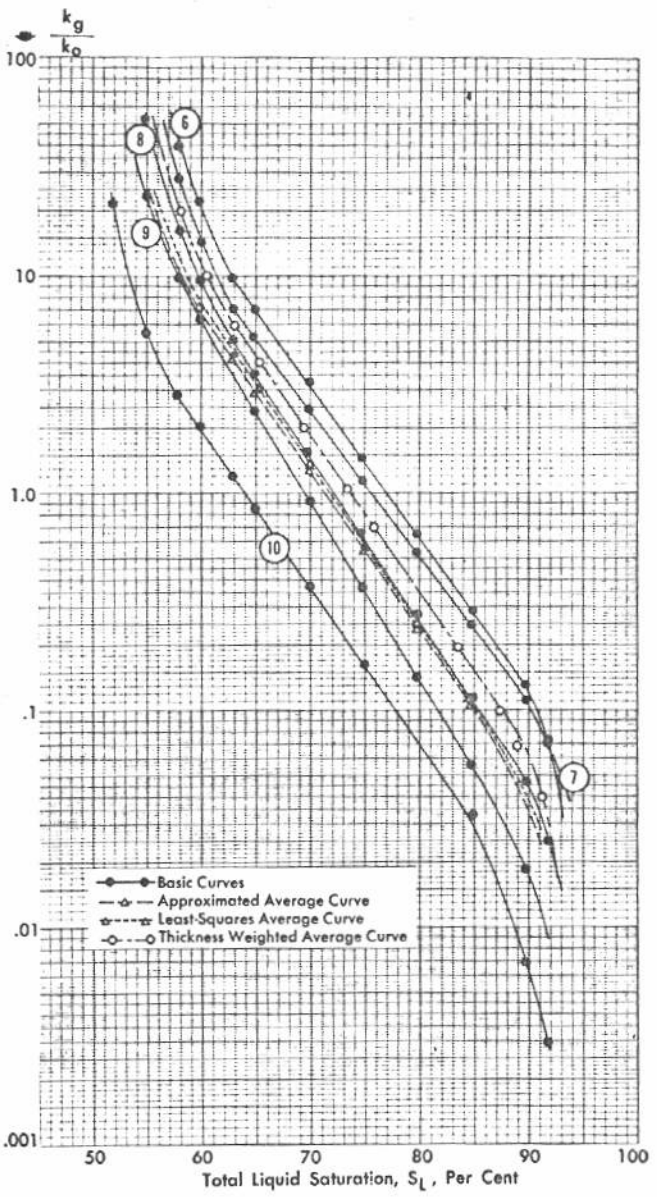

INDIVIDUAL AVERAGE RANGE CURVES, and the average of these determined by three different methods. The thickness weighted average curve is considered the most reliable in this case. Fig. 2.

are so determined that they make the sum of the squares of the residuals a minimum.[1] In cases similar to this problem where the ordinate variable is considered dependent on the abscissa variable the residual is defined as the difference between the ordinate of a given point and the ordinate of the corresponding point on the least-squares line.[1] In its simplest form Equation 1 can be written as

$$y = m\,x + b$$

where

$$y = \log (k_g/k_o)'$$

$$m = \frac{n \Sigma (S_L \log k_g/k_o) - \Sigma S_L \Sigma \log k_g/k_o}{n \Sigma S_L^2 - (\Sigma S_L)^2}$$

$$b = \frac{\Sigma S_L^2 \Sigma \log k_g/k_o - \Sigma S_L \Sigma (S_L \log k_g/k_o)}{n \Sigma S_L^2 - (\Sigma S_L)^2}$$

$$x = S_L'$$

Finding m and b involves writing an ordinate residual for each data point. These are squared, summed, and arranged to give quadratic equations in b and m which can be partially differentiated (with respect to m and b) and solved for b and m.

The third method used involves weighing the saturations of the various curves at a given k_g/k_o according to the fraction of sand represented by each respective curve.

There are many possible methods of averaging k_g/k_o data. It can be assumed that each section of a reservoir is in capillary equilibrium with surrounding sections. Thus capillary-pressure data can then be used to develop average saturation values from which corresponding average k_g/k_o values can be obtained. Tests conducted by Owens et al.[2] show that this method gives average curves that lie well above corresponding field average curves. The deviation was appreciable and thus this method is not recommended.[2]

Another method involves the assumption that all sections of a reservoir were depleted evenly and thus contained essentially equal saturation. This is difficult to justify because the higher-permeability sections would deplete faster than the lower-permeabil-

Table 2–Relative-Permeability Data and Least-Squares Calculations for Range 1

(1)	(2)	(3)	(4)	(5)	(6)	(7)	(8)	(9)	(10)	(11)	(12)	(13)	(14)	(15)
	Basic data													
Tot. liquid satn. % S_L	k_g/k_{ro} for less than 10 md. range curves										$\log k_g/k_{ro} =$ (7) + (8) + (9) + (10) + (11)	$S_L \log k_g/k_o =$ (1) × (12)	S_L^2	$(k_g/k_o)'$ Eq. (3)
	1	2	3	4	5	$\log (k_g/k_{ro})_1$	$\log (k_g/k_{ro})_2$	$\log (k_g/k_{ro})_3$	$\log (k_g/k_{ro})_4$	$\log (k_g/k_o)_5$				
92	0.230	0.160	0.078	0.025	0.017	9.362 − 10	9.204 − 10	8.893 − 10	8.398 − 10	8.231 − 10				
90	0.345	0.260	0.150	0.065	0.045	9.538 − 10	9.415 − 10	9.176 − 10	8.813 − 10	8.654 − 10	− 4.404	− 396.4	8,100	0.132
85	0.650	0.550	0.330	0.168	0.108	9.814 − 10	9.740 − 10	9.519 − 10	9.226 − 10	9.034 − 10	− 2.667	− 226.7	7,225	0.293
80	1.60	1.12	0.720	0.390	0.248	0.205	0.050	9.858 − 10	9.592 − 10	9.395 − 10	− 0.900	− 72.0	5,400	0.654
65	16.3	9.70	7.40	5.00	3.00	1.213	0.987	0.870	0.700	0.478	4.248	276.1	4,225	7.160
63	22.0	14.0	10.5	7.20	4.30	1.344	1.147	1.022	0.858	0.634	5.005	315.3	3,969	9.870
											4.628	134.7	40,444	

n = (7) (5)* = 35. $\Sigma \log k_g k_{ro} = 4.628$. $\Sigma (S_L \log k_g k_{ro}) = 134.7$. $\Sigma S_L = (5^*)(90 + 85 + 80 + 75 + 70 + 65 + 63) = 2,640$. $\Sigma S_L^2 = (40,444)(5)^* = 202,220$. *Five data points exist at each saturation.

Table 3–Relative-Permeability-Ratio Data and Least-Squares Calculations for All Ranges

(1)	(2)	(3)	(4)	(5)	(6)	(7)	(8)	(9)	(10)	(11)	(12)	(13)	(14)	(15)
	Average k_g/k_{ro} for ranges													
Tot. liquid satn. %	0-10 md.	10-50 md.	50-100 md.	100-300 md.	300-500 md.						$\log (k_g/k_o) =$ (7) + (8) + (9) + (10) + (11)	$S_L \log k_g/k_{ro} =$ (1) × (12)	S_L^2	$(k_g/k_o)'$ Eq. (4)
	6	7	8	9	10	$\log (k_g/k_{ro})_6$	$\log (k_g/k_o)_7$	$\log (k_g/k_o)_8$	$\log (k_g/k_o)_9$	$\log (k_g/k_o)_{10}$				
92	†0.075	0.073	0.025	0.010	0.003									
90	0.132	0.115	0.046	0.019	0.007	9.121 − 10	9.062 − 10	8.663 − 10	8.279 − 10	7.845 − 10				
85	0.293	0.250	0.118	0.057	0.034	9.467 − 10	9.398 − 10	9.072 − 10	8.756 − 10	8.532 − 10	− 4.775	− 405.9	7,225	0.111
80	0.654	0.530	0.280	0.145	0.073	9.816 − 10	9.724 − 10	9.448 − 10	9.162 − 10	8.864 − 10	− 2.986	− 238.9	6,400	0.255
65	7.160	5.20	3.60	2.40	0.870	0.855	0.716	0.556	0.380	9.940 − 10	2.447	159.1	4,225	3.085
63	9.870	7.10	5.10	3.50	1.20	0.995	0.852	0.708	0.544	0.080	3.179	200.3	3,969	4.315
											− 2.677	− 329.2	32,344	

n = (6) (5)* = 30. $\Sigma \log k_g k_{ro} = -2.677$. $\Sigma (S_L \log k_g/k_o) = -329.2$. $\Sigma S_L^2 = (32,344)(5)^* = 161,720$. $\Sigma S_L = 5^*(85 + 80 + 75 + 70 + 65 + 63) = 2,190$. *Five data points exist at each saturation.
†From extrapolated average curve.

TABLE 4—WEIGHTED AVERAGE PERMEABILITY-RATIO DATA

k_g/k_o from Fig. 2	Total liquid saturation, per cent — From Fig. 2					Thickness weighted avg.
	S_{L6}	S_{L7}	S_{L8}	S_{L9}	S_{L10}	
0.04	93.1	93.9	90.6	86.7	83.6	91.6
0.07	92.0	92.0	87.8	83.8	80.3	89.4
0.10	91.0	90.5	85.7	81.9	78.0	87.7
0.20	87.3	86.3	81.7	78.2	73.9	83.7
0.40	83.0	81.8	77.7	74.5	69.7	79.5
0.70	79.4	78.1	74.4	71.5	66.3	76.1
1.00	77.2	75.8	72.3	69.6	64.1	73.9
2.00	72.9	71.2	68.3	65.9	60.0	69.6
4.00	68.5	66.7	64.3	62.2	56.3	65.4
6.00	66.0	64.1	62.1	60.2	54.9	63.1
10.00	62.9	61.5	59.9	57.9	53.6	60.6
20.00	60.3	59.0	57.4	55.6	52.1	58.1

ity sections. In spite of this, some success has come with this method.[2]

It can be visualized that in the depletion process the tighter sections would tend to produce into the more permeable strata. This migration would continue until all the sections were producing at the same k_g/k_o but having different saturations. Or this is the same as assuming that all sections will produce at equal gas-oil ratios.[2] This principle was used in averaging the permeability range k_g/k_o curves of Fig. 2.

Note in Tables 2 and 3 that only part of the data were used in the least-squares calculations. A check of the basic curves in Figs. 1 and 2 will show that the data selected essentially represent the linear portion of the plots. This was necessary because the linear least-squares approach was used. Such an approach is sufficiently accurate since the linear portion of the graphs represents the major part of the history of a depletion-type reservoir.

Fig. 1 shows the individual curves for range 1 and the average curves determined by visual inspection and the least-squares approach. The former was drawn first in order that the latter would not influence the approximation. In this particular case the approximate curve is about the same as the least-squares curve. It is well to note that the position of the approximate curve will depend to some degree on the engineer whereas the least-squares curve will be the same regardless of who computes it.

Fig. 2 shows the individual average range curves and the average of these determined by three methods. In this case a slight difference is noted between the approximate and the least-squares average curves. Still a greater difference is found between these and the thickness weighted average curve. The latter is considered the most applicable because it gives more weight to those ranges which represent the bulk of the formation. The least-squares average curve was extrapolated by visual inspection.

In comparing the approximate and least-squares methods of averaging k_g/k_o curves, it might be said that for most cases the error involved in using the former method does not justify use of the more tedious least-squares approach. However, where an electronic computer is used the least-squares method is considered practical. Of more importance than the averaging method utilized is the question of determining just how well the curves used actually represent the formation under consideration.

References

1. Richardson, C. H., "An Introduction to Statistical Analysis," Revised Edition, 1943, Harcourt, Brace & Co., pp. 210-219.

2. Owens, W. W., Parrish, D. R., and Lamoreaux, W. E., "A Comparison of Field k_g/k_o Characteristics and Laboratory k_g/k_o Test Results Measured by a Simplified Method," Transactions AIME, 1956.

Part 24

How to analyze capillary-pressure data

GIVEN: Capillary-pressure curves measured on 75 cores taken at random from cored intervals of a sandstone reservoir. Five of these curves are shown in Fig. 1. Other data obtained were as follows:

σ_{ow}, interfacial tension, oil-water at reservoir conditions = 33 dynes/cm.

σ_w, surface tension, water-air at test conditions = 71 dynes/cm.

ρ_w, density of brine at reservoir conditions = 0.45 psi./ft.

ρ_o, density of the reservoir oil at reservoir conditions = 0.31 psi./ft.

k_{av}, average absolute permeability for reservoir obtained from some 1,000 samples analyzed = 155 md.

FIND:

1. Correlations between permeability and water saturation.
2. Average capillary-pressure curve for reservoir.
3. Conversion factor for relating capillary-pressure scale with subsurface elevation from free water level.
4. Minimum interstitial-water saturation.

TABLE 1—FERMEABILITY VS. WATER SATURATION AT CONSTANT CAPILLARY PRESSURE

Permeability	Water saturations for constant capillary pressure, %				
	75 psi.	50 psi.	25 psi.	10 psi.	5 psi.
950	14.0	16.5	22.0	30.0	39.0
300	22.5	25.5	34.0	45.5	56.0
50	30.0	36.0	47.0	61.5	78.0
25	44.5	47.5	59.0	71.5	83.0
10	50.5	53.0	63.5	81.0	92.0

METHOD OF SOLUTION:

1. Fig. 1 shows 5 typical capillary-pressure curves of the 75 involved in this problem. Each curve was obtained from an individual core, the permeability of which is noted on the curve. Using a constant capillary pressure of 75 psi., the water saturation for each curve was read and plotted on Fig. 2 versus permeability. Table 1 shows the values read from Fig. 1 for constant capillary pressures of 75, 50, 25, 10, and 5 psi.

An average linear line is drawn through the data to give the relation between permeability and water saturation at constant capillary pressure. (This was done for the 75-psi. capillary pressure in Fig. 2.) Curves for five capillary pressures are shown in

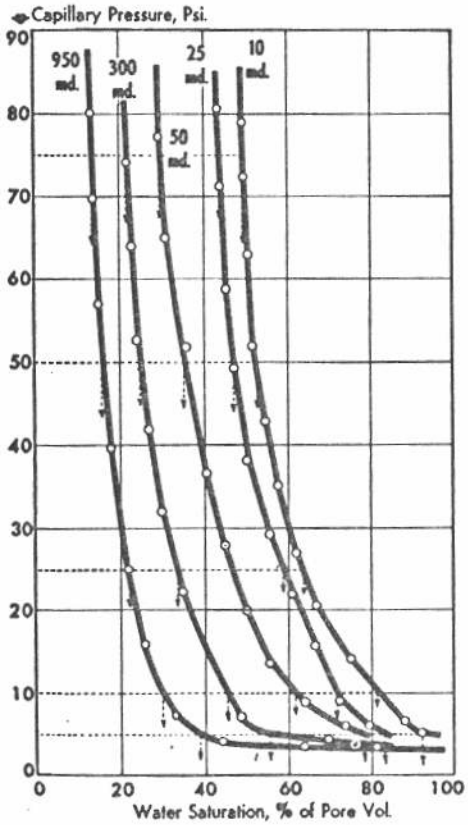

TYPICAL capillary-pressure curves for a sandstone reservoir (air-water). Fig. 1.

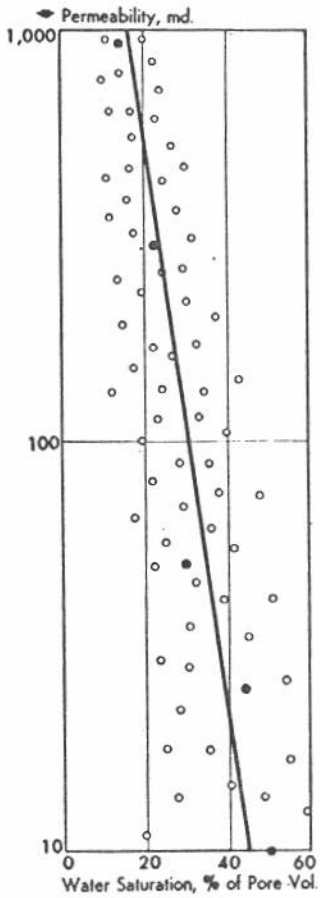

VARIATION of water saturation with permeability at a constant capillary pressure of 75 psi. Fig. 2.

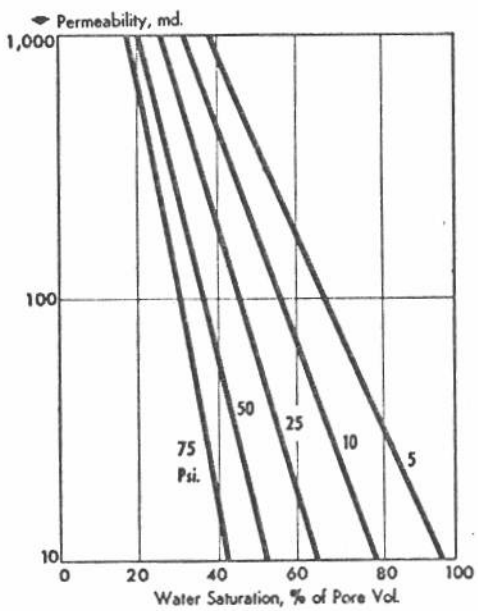

VARIATION of water saturation with permeability at selected capillary pressures. These were obtained in the manner of the single curve in Fig. 2. Fig. 3.

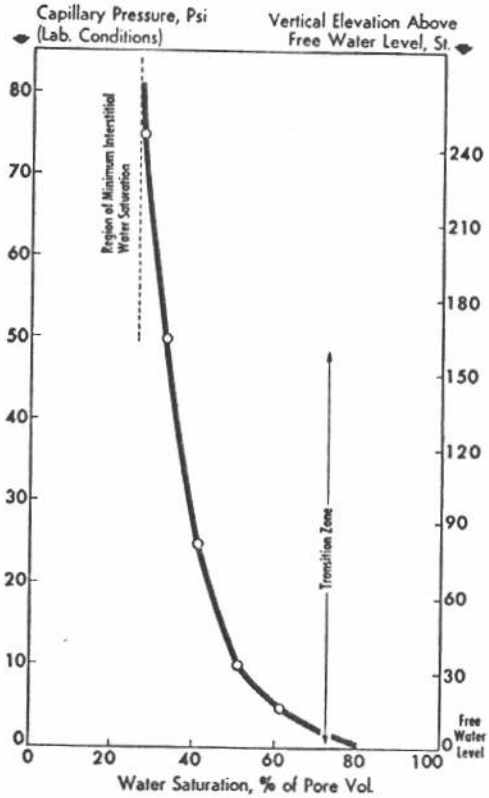

DATA from Fig. 3 were read at an average permeability of 155 md. and used to plot this average reservoir capillary-pressure curve. Fig. 4.

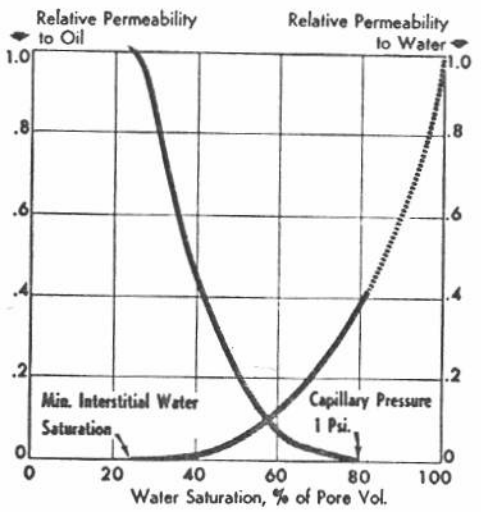

TYPICAL oil - water relative-permeability curves for average rock properties of the reservoir under study. Fig. 5.

Fig. 3; these were derived individually in the same manner as for the 75-psi. curve.

2. Figs. 1, 2, and 3 show an acceptable method for averaging capillary - pressure data. From all the core-analysis data an average reservoir permeability is found and used to obtain the reservoir average capillary-pressure curve from the average data of Fig. 3. The data of Table 2 were read from Fig. 3 for an average reservoir permeability of 155 md. and are plotted in Fig. 4. The average conditions of Fig. 4 are shown by the comparable and typical oil and water relative-permeability curves of Fig. 5. The latter were drawn to show the relation between capillary pressure and relative-permeability curves.

TABLE 2—AVERAGE RESERVOIR CAPILLARY-PRESSURE DATA

(k_{av} = 155 md.)

Capillary pressure (psi.)	Water saturation (%)
75	27.0
50	33.0
25	41.0
10	51.0
5	61.5

3. Correlation between capillary pressure and distance from free water level can be found from the given data and the equation:

$$P_{cL} = \frac{\sigma_w}{\sigma_{ow}} (\rho_w - \rho_o)\, h \qquad (1)$$

$$P_{cL} = (71/33)\ (0.45 - 0.31)\ h$$

$$P_{cL} = (2.15)\ (0.14)\ h = 0.301\ h$$

$$\text{or} \quad h = 3.3\ P_{cL}$$

In this case 3.3 is the factor for relating mean laboratory capillary pressure data with corresponding subsurface vertical distance from the free water level (lower end of transition zone or highest elevation at which 100% water saturation is encountered).

4. From Fig. 4 it is seen that the minimum interstitial-water saturation is about 26.0%.

DISCUSSION: Capillary pressure is defined as the pressure difference across an interface between two fluid phases.[1,2] It is given by the equation:

$$P_c = \sigma\ (1/R_1 + 1/R_2) \qquad (2)$$

and also by the equation:

$$P_c = \Delta\rho g h \qquad (3)$$

Considering Equation 2 at laboratory and reservoir conditions and Equation 3 at reservoir conditions, it is easy to develop Equation 1 which relates laboratory and reservoir conditions.

In using these relations the following assumptions are made: (1) Laboratory cleaning and other processing does not change the matrix surface characteristics of the rock; (2) rock is 100% water wet; (3) radii of curvature in reservoir and at laboratory conditions are identical; (4) reservoir was initially fully saturated with water which was subsequently displaced by hydrocarbons; the water displacement was not complete but enough water was retained to satisfy the capillary forces; (5) at discovery the reservoir contained amounts of water and hydrocarbons equivalent to those required for equilibrium between gravitational and capillary forces.[3]

Obviously the first three assumptions are very difficult to satisfy fully. Laboratory restored-state procedures are believed to alter the wetting and other grain surface properties of the rock. The degree of alteration and its final effect on the results are not too well known. Most reservoir rocks are believed to be preferentially wet with water; but there are many which are apparently oil wet, including some of the larger important fields.

Capillary-pressure data have long been used in finding reservoir interstitial-water saturation. It is necessary to analyze enough cores for a lease or reservoir to assure average statistical results. In this case (large reservoir) 75 samples were analyzed. Fig. 1 shows the capillary-pressure curve for five of the samples. Note that the capillary pressure increases as the water saturation decreases. A point is reached where large changes in pressure do not change the saturation appreciably. This region of the curve gives the so-called minimum interstitial-water saturation. Another characteristic of some of these curves is that a considerable amount of desaturation may take place with a comparatively small increase in capillary pressure. This is true of the curve for the 950-md. sample. Such behavior indicates a fairly uniform sample. The capillary pressure at which

the nonwetting phase (oil in a water-wet system) can first be forced into the pores (i.e., the lowest capillary pressure at which there is some oil saturation) is called the displacement pressure. In the 950-md. sample of Fig. 1 this pressure is 3 psi.

Theoretical concepts indicate that permeability and capillary pressures are related.[3] That is, for a particular reservoir rock and a given water saturation, the capillary pressure should be increasingly greater for samples arranged in decreasing order of permeability. This phenomenon is noted in Fig. 1. However, the scattering of data in Fig. 2 show that other factors are also influential. The scattering of points for the other graphs of Fig. 3 was similar to that of Fig. 2.

Fig. 4 shows the average reservoir capillary-pressure curve obtained from Fig. 3, using the average reservoir absolute permeability. Note that this graph has two capillary-pressure scales, one at laboratory conditions and the other at reservoir conditions. With this graph it is possible to obtain a value of the water saturation (for the average permeability rock) at any point above the free water level. For instance, at 90 ft. the water saturation is 40%.

If desired, the curves of Fig. 3 can be used to determine the mean capillary-pressure curves of segments of the reservoir. From core data for each respective segment, average permeabilities are computed and used with Fig. 3. A problem that will be treated later will illustrate the reservoir segment approach.

Many engineers and geologists define the oil-water contact as the lowest elevation at which water-free oil production can be obtained.

The maximum water saturation below which only free oil will be produced is of course defined by the oil-water relative-permeability characteristics of the reservoir rock with its reservoir fluids.[4] Fig. 5 shows that even at a water saturation of 40% very little water is flowing and essentially only oil is flowing. Where applicable relative-permeability data are not available, it is usually assumed that water saturation in the free oil productive zone is represented by that corresponding to 45 to 75 psi. capillary pressure.

For clean sands (of good to high porosity and permeability) this is a reasonable assumption because the transition zone is only a few feet in height, and the minimum interstitial water value may be approached on the order of 10 ft. or so above the free water level. Furthermore, there is little difference in the water saturation at that level and at higher levels with their correspondingly higher capillary pressures.

In dirty or tight sands, the minimum interstitial-water saturation may be reached only at comparatively high capillary pressures.

In such cases, there is a considerable variation in water saturation with height within the free-oil productive zone. Here the broad assumption of 45 or 75 psi. for capillary pressure may lead to sizable error.

The transition zone is defined as that interval in which the saturations are such that both oil and water flow. Here again this interval is defined by the oil-water relative-permeability data for the reservoir rock and its fluids. Where oil reserves are believed to exist in this zone, the determination of average reservoir water saturation becomes more complex. An illustration involving such a case will be covered in a later problem.

The capillary method of interstitial-water-saturation determination has been found to be good (in many fields) for points above the transition zone.[1] For such conditions, laboratory measurements can be restricted to a data point per sample taken at a pressure sufficiently high to assure minimum water saturation. If enough points are obtained to define the capillary-pressure curve, the testing becomes tedious, time consuming, and expensive.

Comparisons[1] have been made between water saturations determined by analysis of oil-base mud cores and the capillary-pressure method. Agreement was usually found to ge good. Cases have been found, however, where large differences existed, generally when the actual reservoir interstitial-water saturation was rather low, 15% or less. Such low water saturations indicate possible oil-wetting conditions. Laboratory restoration of oil-wet cores may well result in changing wetting characteristics and thus explain the discrepancies encountered.

Nomenclature

h = subsurface vertical elevation from free water level, ft. R_1 and R_2 are radii of curvature of fluid interfaces. All others are standard AIME symbols (Journal of Petroleum Technology, October 1956).

References

1. Thornton, O. F., and Marshall, D. L., "Estimating Interstitial Water by the Capillary Method": Trans. AIME, 170, 69 (1947).
2. Leverett, M. C., "Capillary Behavior in Porous Solids": Trans. AIME, 142, 152 (1941).
3. Muskat, M., "Physical Principles of Oil Production": first edition, McGraw-Hill Pub. Co., pp. 304-311.
4. Calhoun, J. C., "Effective and Relative Permeability": Engineering Fundamentals—Advanced Reservoir Engineering, Part 1, The Oil and Gas Journal, p. 20.

Part 25

How to make use of capillary-pressure data

GIVEN: A reservoir divided into five segments. Using the top and base of the net-sand maps, the areas shown in Columns 2 and 3 of Table 1 were planimetered. The free-water level was determined to be at a subsea depth of 5,130 ft. The net-to-gross ratio of sand volumes for segment 1 was determined to be 0.7 and the net sand volumes and average water saturations for the other segments were found to be as follows:

Segment	Net sand volume, ac.-ft.	Avg. Interstitial water saturation % pore vol.
2	3,050	33.0
3	950	35.0
4	1,580	34.5
5	4,100	30.5

FIND:

1. Gross sand volume distribution for segment 1.
2. Average water saturation for segment 1 assuming that the data given and average capillary pressure curve (Fig. 4) developed in No. 24 of this series (OGJ, July 4, 1960) apply to this segment.
3. Average interstitial water saturation for the reservoir.

METHOD OF SOLUTION: These equations will be used in the solution of the problems:

$$A_x = A_{Ti} - A_{Bi} \qquad (1)$$

$$A_{xavg} = \frac{A_{x1} + A_{x2}}{2} \qquad (2)$$

$$\Delta V_{Gi} = A_{xavg} \times h' \qquad (3)$$

$$h = H + H' \qquad (4)$$

$$V_G = \sum_{i=1}^{i=n} \Delta V_{Gi} \qquad (5)$$

$$V_N = \sum_{i=1}^{i=n} (V' \times \Delta V_{Gi}) \qquad (6)$$

$$S'_w = \frac{\sum_{i=1}^{i=m} S_{wi} \Delta V_{Gi}}{V_G} \qquad (7)$$

$$S_{wav} = \frac{\sum_{j=1}^{j=m} S'_{wj} V_{Nj}}{\sum_{j=1}^{j=m} V_{Nj}} \qquad (8)$$

Where:

A_x = Gross sand horizontal cross-sectional area at a contour, acres.

A_{Ti} = Area enclosed by a contour on the top of the sand, acres.

H' = Elevation in feet between oil-water contact and free-water level.

V' = Factor representing net sand as a fraction of gross sand.

n = Total number of areas contained between contours.

m = Total number of segments.

A_{Bi} = Area enclosed by a contour on the base of the sand, acres.

A_{xavg} = Average cross-sectional area between two successive contours, acres.

ΔV_{Gi} = Gross sand volume contained between two successive contours, acre-ft.

h' = Contour interval, ft.

V_G = Gross sand volume for segment, acre-ft.

V_{Nj} = Net sand volume for segment, j acre-ft.

S_{wi} = Avg. interstitial water saturation in sand volume contained between two successive contours, % pore volume.

S'_{wj} = Average interstitial water saturation for segment, j %.

S_{wav} = Average interstitial water saturation for reservoir, %.

H = Distance from oil-water contact to middle of sand volume, ΔV_{Gi}, ft.

h = Distance from free-water level to middle of sand volume, ΔV_{Gi}, ft.

SOLUTION:

Columns 4, 5, 6, and 7 of Table 1 show the computation of gross and net sand volumes. Note that column 4 is a solution of Equation 1, column 5 of Equation 2, column 6 of Equation 3, the total of column 6 of Equation 5, and the total of column 7 of Equation 6.

Columns 8 through 11 show calculations for average water saturation.

TABLE 1—AREAS MEASURED AND COMPUTATIONS FOR SAND VOLUMES AND WATER SATURATION IN SEGMENT 1

Measured data			Gross and net sand volume computation				Average water-saturation calculations			
(1)	(2)	(3)	(4)	(5)	(6)	(7)	(8)	(9)	(10)	(11)
Subsea depth, ft.	Area enclosed, acres: Top of sand	Area enclosed, acres: Base of sand	Cross-sectional area, acres: At each contour (2) − (3)	Cross-sectional area, acres: Average for two contours	Sand volume, acre-ft.: Gross (5) × h' h'=10.0 ft.	Sand volume, acre-ft.: Net (6)×0.7	Dist. from o/w to middle of sd. vol. increment, ft.	Dist. from free-water level to middle of sd. vol. increment, ft. (8)+100	Avg. water saturation at middle of sd. vol. increment, %	Gross sd. vol. times water saturation (6)×(10)
4,950 (G/O)	50	0	50	...	...	...	...	...	...	...
4,960	55	2	53	51.5	515	360.5	75	175	32.5	16,738
4,970	65	12	53	53.0	530	371.0	65	165	33.3	17,649
4,980	80	22	58	55.5	555	388.5	55	155	34.2	18,981
4,990	90	32	58	58.0	580	406.0	45	145	35.0	20,300
5,000	105	44	61	59.5	595	416.5	35	135	35.8	21,301
5,010	125	59	66	63.5	635	444.5	25	125	36.8	23,368
5,020	135	74	61	63.5	635	444.5	15	115	37.8	24,003
5,030 (o/w)	145	94	51	56.0	560	392.0	5	105	38.9	21,784
					4,605	3,223.5				164,124

Column 9 is a solution of Equation 4 and the total of column 11 of the numerator of Equation 7. The values shown in column 10 were obtained from Fig. 4 of No. 24 in this series at the respective elevations shown in column 9. The average water saturation for the segment is obtained from Equation 7.

$$S'_w = \frac{164124}{4605} = 35.6\%$$

$$S_{wa} = [(0.356)\ (3{,}224) + (0.330)\ (3{,}050) + (0.350)\ (950) + (0.345)\ (1{,}580) + (0.305)\ (4{,}100)] \div [3{,}224 + 3{,}050 + 950 + 1{,}580 + 4{,}100] = [4{,}282.3] \div [12{,}904] = 0.332 \text{ or } 33.2\%$$

DISCUSSION:

This problem illustrates a method for determining water saturation in those reservoirs which are believed to contain reserves in the transition zone. In such cases an appreciable part of the recoverable oil may initially be situated in a zone from which both oil and water would be produced; i.e., at a subsurface elevation below the lowest point at which water-free oil will be produced. Consequently, an appreciable variation in water saturation may be involved going from the lowest elevation which would contribute recoverable oil to the higher areas of the reservoir. For instance, in segment 1 of the reservoir considered, the water saturation varied from 39.5% at the oil-water contact to 32.0% at the highest elevation. This segment lies in the interval between 100 and 180-ft. vertical elevation above the free-water level. It was necessary to develop the variation of gross sand-volume distribution in order to conform with the curvature of the average capillary-pressure curve (Fig. 4, No. 24 in this series). In this case volume increments over a vertical distance of 10 ft. were used. Thus it can be seen that for such a distance the curve can be represented by straight-line increments.

This method of interstitial-water saturation determination is theoretically sound. However, difficulty is often encountered in obtaining sufficient data and in satisfying the assumptions made. Best results are obtained for a media of uniform permeability. Variations of permeability along the bedding plane will cause deviations. It is also believed that wettability may vary from point to point within a porous media.

Perhaps the most difficult thing to establish is the location of the free-water level. This is not normally a thing obtained in routine measurements and thus generally may not be readily available. The elevation of the free-water level may be estimated by correlating the capillary-pressure water-saturation profile with the profile of water saturations determined from core analyses or electric-log computations, or both. Also the interfacial tension at reservoir conditions is normally not available. The latter can, however, be estimated from limited published data.[2]

References

1. Guerrero, E. T., and Stewart, F. M., The Oil and Gas Journal, July 4, 1960, p. 106 (p. 42, this manual).
2. Hocott, C. R., "Interfacial Tension Between Water and Oil Under Reservoir Conditions," Trans. AIME, 1939, 132, 184.

Part 26

How to find interstitial-water saturation from analysis of oil-base-mud cores

GIVEN: The pay sand in a development well was cored with oil-base mud. Samples from the core were analyzed for water content, using a retort-type[1] apparatus. The following data pertain to one of the samples:

Volume of water extracted = V_w = 1.11 cc.

Pore volume of core = PV = 4.10 cc.

Sand thickness represented by sample = 1 ft.

FIND: Reservoir water and initial oil saturations at the well and in the interval of sand represented.

METHOD OF SOLUTION: The observed data are used with the following equations to find the needed saturations:

$$S_w = V_w/PV \qquad (1)$$

$$S_{oi} = 1 - S_w \qquad (2)$$

Where:

V_w and PV are defined with the data and

S_w = water saturation at reservoir conditions, fraction

S_{oi} = initial oil saturation at reservoir conditions, fraction

SOLUTION:

$$S_w = 1.11/4.10 = 0.271 \text{ or } 27.1\%$$

$$S_o = 1 - 0.271 = 0.729 \text{ or } 72.9\%$$

DISCUSSION: This problem illustrates what is considered to be the best method for finding interstitial-water saturation. The assumption is made that none of the interstitial water is flushed by the coring process using oil-base mud. The invading oil filtrate will merely displace formation oil. Furthermore, while the core is removed from the well, it is assumed that the evolvement of solution gas does not cause a change in water saturation. These assumptions should be valid for any core in which the water content is equal to or less than the minimum interstitial value. It will be recalled that the minimum interstitial is the maximum water saturation that a porous media can contain and still virtually have zero effective permeability to water. In cases where the water saturation is much higher than the minimum interstitial, the oil filterate may flush water and thus make the results misleading.

Although considered reliable, this method of interstitial-water-saturation determination is not used very much. Because of high cost, oil-base muds are not frequently used. It is not even considered economical to convert to oil-base mud for coring and well completion except in special cases to prevent the caving of certain shales and to drill into formations susceptible to damage by water.[2] The method is recommended, however, on special occasions where it is desired to check the applicability of the capillary or electric-log approaches.

At discovery, the oil column of a pool generally contains two fluids, oil and water. Thus if the fraction of either can be obtained, the saturation of the other can easily be computed with a relationship such as given by Equation 2.

References

1. Pirson, S. J., Oil Reservoir Engineering: McGraw-Hill Publishing Co., Inc., second edition, 1958, pp. 47-51.
2. McGray, A. W., and Cole, F. W., Oil Well Drilling Technology: University of Oklahoma Press, first edition, 1958, p. 79.

Part 27

How to find interstitial-water saturation

. . . from electric-log data

GIVEN: Electric log showing the SP, normal, and lateral curves for a clean sandstone formation.

FIND: Interstitial-water saturation in the interval 7,185-7,200 ft.

METHOD OF SOLUTION: In his paper "The Electrical Resistivity Log as an aid in Determining Some Reservoir Characteristics," Archie[7] suggests this empirical relationship:

$$S_w = (R_o/R_t)^{1/2}$$

Where:

S_w = interstitial-water saturation, fraction of pore volume

R_o = resistivity of formation when 100% saturated with connate water

R_t = true resistivity of formation, ohm m^2/m

SOLUTION: Fig. 1 shows the SP and resistivity curves for the formation under study. The log shows the characteristic resistivities of a thick sandstone having an oil pay underlain by a water zone. Note that the resistivity for the long normal, $R_{64''}$, has been read as 7.4 in the pay and 0.2 in the water sand. Both of these values are apparent resistivity values. Other data recorded on the log are as follows:

H = gross pay thickness for the oil zone, = 14 ft.

R_m = resistivity of mud at formation temperature, 124° F. = 1.3 (often not given at formation temperature but can easily be converted to same by referring to Chart A-6 of Reference 5).

R_s = resistivity of surrounding shale beds ≈ 0.3

Invasion estimated small.

Gross bed thickness for water zone is greater than 20 ft.

TABLE 1[1]—ESTIMATION OF TRUE RESISTIVITY FROM 64 IN. NORMAL IN RESISTIVITY BEDS

($R_{16''}/R_m \leqq 10$, Invasion $\leqq 2$ dia.)

Gross bed thickness	Necessary conditions	Estimated R_t
$H > 20$ ft.		$R_t = R_{64''}$
$H \approx 15$ ft.	$R_m \approx R_s$, $R_{64''}/R_s \geqq 2.5$	$R_t = 1.5\ R_{64''}$
$H \approx 15$ ft.	$R_m \approx R_s$, $R_{64''}/R_s \leqq 1.5$	$R_t = R_{64''}$
$H \approx 10$ ft.	$R_m \approx R_s$, $R_{64''}/R_s \geqq 2.5$	$R_t = 2\ R_{64''}$
$H \approx 10$ ft.	$R_m \approx R_s$, $R_{64''}/R_s = 1.5$	$R_t = 1.5\ R_{64''}$

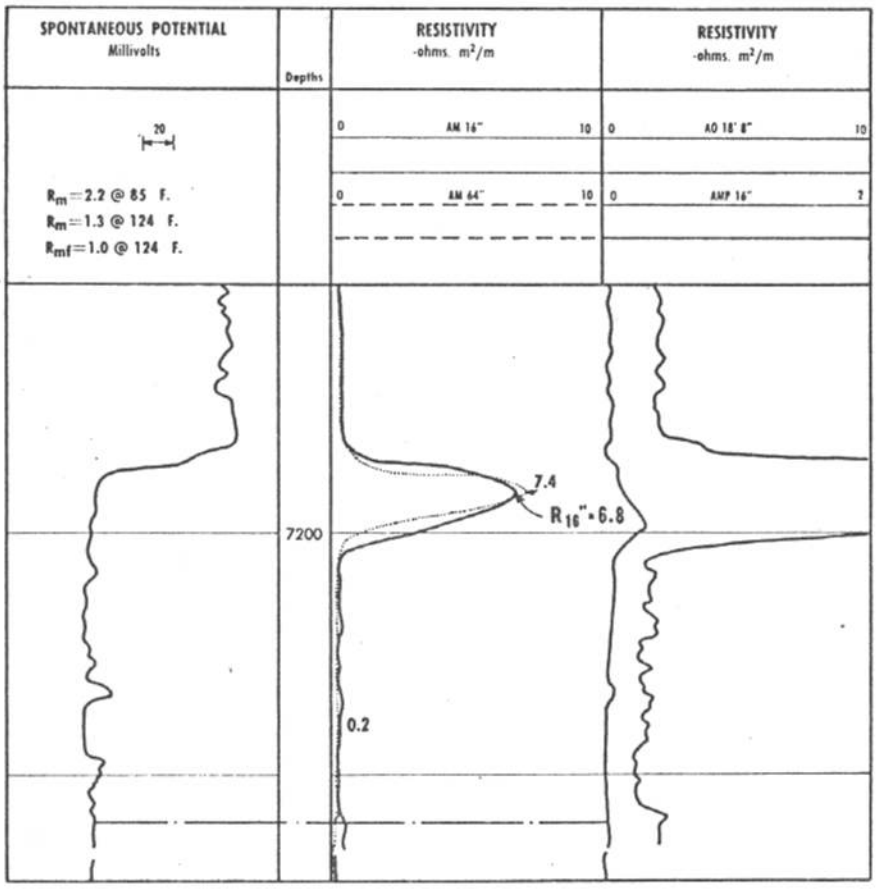

ELECTRIC LOG showing responses in a sandstone reservoir. Fig. 1.

Thus in the oil pay

$$R_{64''}/R_s = 7.4/0.3 = 25$$
$$R_{16''}/R_m = 6.8/1.3 = 5.2$$

From Table 1, estimated values of the true resistivities in the oil sand can be found to be:

$R_t \approx (3/2)\ R_{64''} = (3/2)\ (7.4) = 11.1$

and in the water sand

$$R_t \approx R_o = R_{64''} = 0.2$$

Therefore

$$S_w = (0.2/11.1)^{1/2} = (0.018)^{1/2} = 0.134$$

or 13.4%

DISCUSSION: Data needed to find reserves and reservoir performance can be obtained by direct or indirect methods. The former involves measurement of the desired property on samples of the rock, fluid, or combined rock-fluid system. In the indirect method a relationship between the desired property and a measurable secondary property is established[2].

This problem is a good example of the indirect method in that interstitial-water saturation is related to the resistivities of the in-place rock. The latter are measured and used to com-

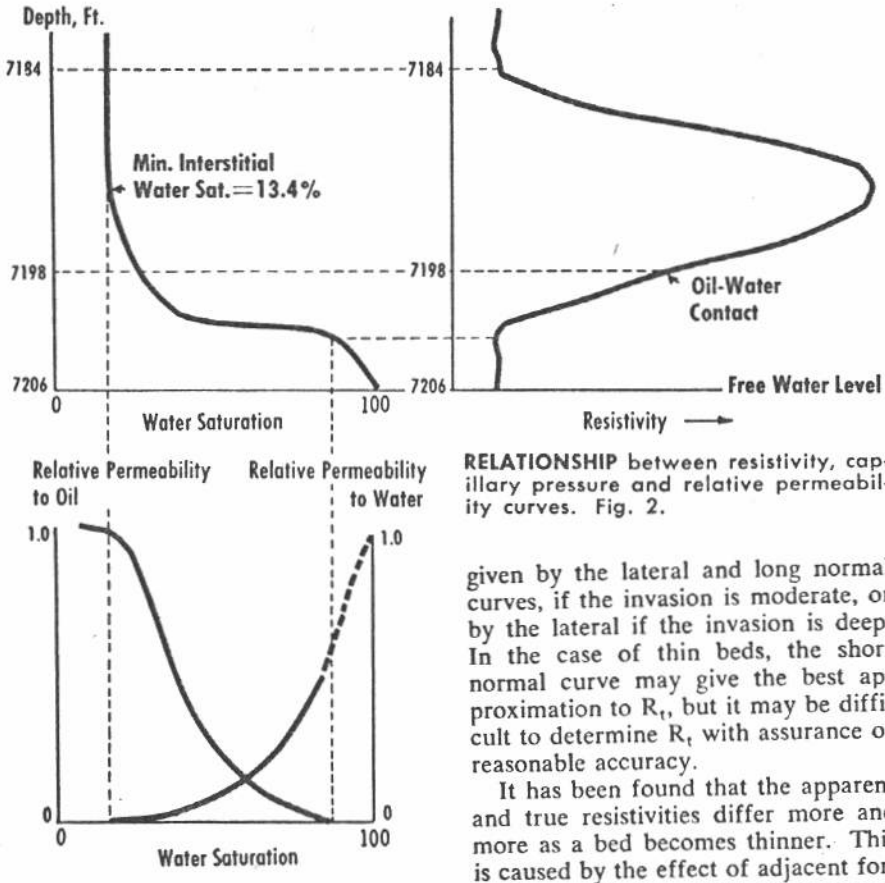

RELATIONSHIP between resistivity, capillary pressure and relative permeability curves. Fig. 2.

pute the per cent of water saturation.

Required in the solution are the true resistivity (R_t) of the rock and the resistivity of the same media when 100% saturated with formation water (R_o). True resistivity is an intrinsic property of a rock and is absolutely independent of the manner used to make the electrical measurements.[3] The instruments used do not measure true resistivity but an apparent resistivity which is affected by several factors in addition to the true resistivity.[3] These factors are mud resistivity, hole diameter, type and spacing of electrode assembly used, bed thickness, filtrate invasion, and resistance of adjacent beds. The presence of a normal drilling fluid may cause current to escape up and down the hole, tending to reduce the indicated resistivity of a bed. The effect is greatest for small electrode spacing, a minimum for large spacings.

Type and spacing of electrode assembly is important because for any set of conditions (hole size, resistivity of mud, filtrate invasion, etc.) one electrode arrangement may measure much closer to the true resistivity than another.[4] Table 1 shows combinations of conditions where the long normal curve may be used. Other sets of conditions where the short normal and lateral curves may be used to estimate true resistivity are presented in the literature.[5]

When the bed under study is reasonably homogeneous and thick. R_t is given by the lateral and long normal curves, if the invasion is moderate, or by the lateral if the invasion is deep. In the case of thin beds, the short normal curve may give the best approximation to R_t, but it may be difficult to determine R_t with assurance of reasonable accuracy.

It has been found that the apparent and true resistivities differ more and more as a bed becomes thinner. This is caused by the effect of adjacent formation resistivities. Still other factors are the size and resistivity of the filtrate invaded zone and lithologic or formation changes.

This brief discussion shows the trouble met in finding true resistivities from apparent-resistivity measurements. Theoretical and laboratory research, along with mathematical work on ideal systems, has led to new methods for estimating true resistivity from apparent resistivity measurements. The two principal approaches are the one used in this problem[5] and one using departure curves (examples of which are Charts B-2 and B-4 of Reference 5). Both methods are applicable under specific conditions and occasionally conditions are such that both can be used. Although some progress has been made on this problem, the methods still only give an estimate of the true resistivity. Both are based to some degree on the assumptions of uniform and horizontal beds which are seldom, if ever, encountered.

Furthermore, some of the factors involved (such as degree of invasion) are often difficult to determine. This limitation is minimized to some extent by the experience that an interpreter may have in the area under study.

Fig. 1 shows that the well penetrates an apparently thick uniform bed. Drill-stem tests showed that the same formation becomes a water sand at a depth of about 7,200 ft.

It is quite rare to encounter an electric log that clearly defines the oil-water contact. Also, such conditions simplify the determination of R_o which normally has to be determined from self-potential and resistivity measurements made with contact logging devices (MicroLog, contact log, micropetrograph). A subsequent problem will illustrate such an application.

Where data for the determination of R_o are not available in the well of interest the data from a nearby well may be used or R_o read from the log of an edge well drilled through the water sand. Sometimes R_o can be read from a water sand lying above or below the formation of interest if the sand characteristics and water composition (and salinity) are believed to be about the same.

In Fig. 2 the resistivity curve of Fig. 1 is drawn using a large scale and related with comparable capillary pressure and relative permeability curves. This points out the possibility of developing capillary-pressure curves from electrical-survey data and should clarify, to some extent, the relationships among the respective types of data.

Determination of interstitial-water saturation from electrical-survey data has been widely accepted. In many wells electrical surveys are made as a routine exploration practice and thus are available for use in water saturation determination. Furthermore, this method has the advantage that a fairly large sample of in-place rock is involved. Other methods (Part 25 and Part 26 of this series) involve tests on many small samples of the formation. Of course the use of cores cut with oil-base mud is considered the most reliable method of determining interstitial-water saturation. However, it is often not economically practical, but may be used on a limited scale to determine the proper selection of electrical surveys and/or their reliability.

Acknowledgment

The authors acknowledge assistance of E. A. Finklea, Schlumberger Well Surveying Corp., in the preparation of this paper.

References

1. Hamilton, R. G., and Charrin, P., "How to Interpret Electric Logs—Quantitative Log Analysis": Booklet published by The Oil and Gas Journal.
2. Calhoun, J. C., "Advanced Reservoir Engineering," Part 3, Manual published by The Oil and Gas Journal, p. 17.
3. Guyod, H., "True Resistivity": Oil Weekly, Vol. 120, No. 3, December 17, 1945.
4. Document No. 2, Schlumberger Well Surveying Corp.
5. Log Interpretation Charts, Chart B-8, Schlumberger Well Surveying Corp. Chart B-8.
6. Guyod, H., "Estimation of Petroleum Saturation": Oil Weekly, Vol. 120, No. 4, December 24, 1945.
7. Archie, G. E., "The Electrical Resistivity Log as an Aid in Determining Some Reservoir Characteristics": Pet. Tech., Vol. 5, 1942.

Part 28

How to find interstitial-water saturation

. . . in a clean sand from electric and contact log data

GIVEN: Electric and contact logs showing the Gibson sand (Fig. 1) for a well in Oklahoma. Resistivity of interstitial water = R_w = 0.088 (measured on samples of formation water at formation temperature = 115° F. Residual-oil saturation in flushed zone = ROS = 20.0% of pore space. All other data shown on the logs.

FIND: Interstitial-water saturation in the interval 203-223 ft.

METHOD OF SOLUTION: Relationships needed in the solution of this problem are:

$$F = R_o/R_w \qquad (1)$$

$$S_w = (R_o/R_t)^{1/2}$$

$$= (FR_w/R_t)^{1/2} \qquad (2)$$

$$F_a = R_{xo}/R_{mf} \qquad (3)$$

Where:

F = formation-resistivity factor

R_o = resistivity of a formation 100% saturated with water of resistivity R_w

R_w = resistivity of interstitial water

R_t = true formation resistivity

S_w = interstitial-water saturation, fraction of pore volume

F_a = apparent formation-resistivity factor

R_{xo} = resistivity of flushed zone (close to borehole)

R_{mf} = resistivity of mud filtrate. (Normally not given at formation temperature but can easily be converted to same by use of Chart A-6 of Reference 2.)

SOLUTION: Fig. 1 shows the electric and contact logs for the Gibson sand in an Oklahoma well. The SP and resistivity readings for the curves are indicated as:

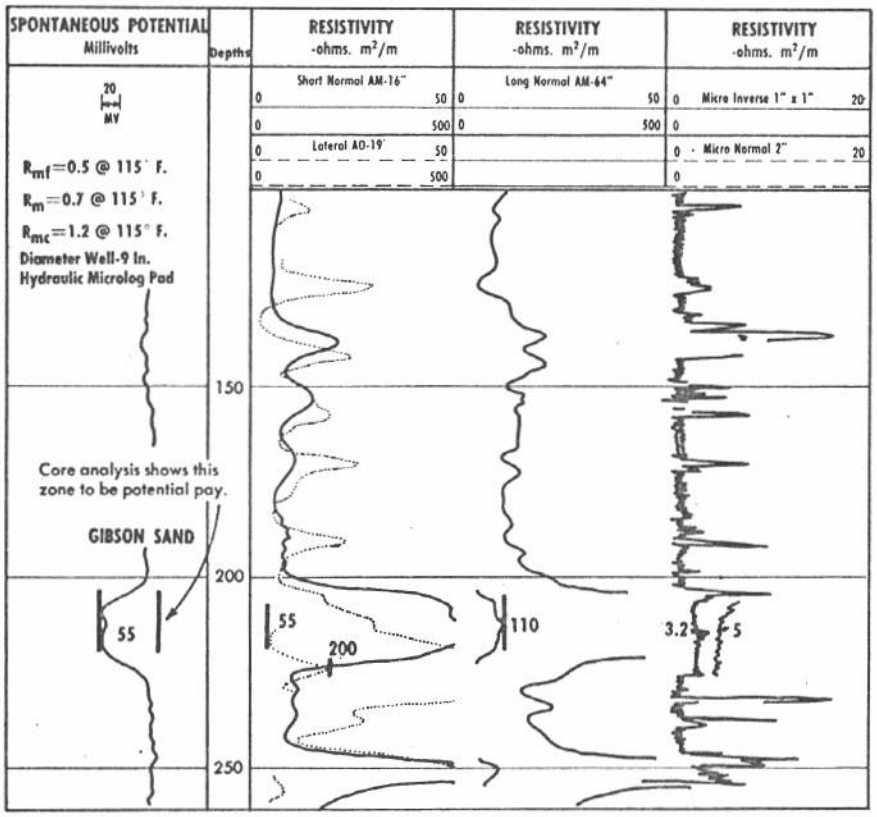

ELECTRIC AND CONTACT LOGS for a well showing responses in Gibson sand. Fig. 1.

$R_{1"\times 1"}$ = resistivity of microinverse

= 3.2

$R_{2"}$ = resistivity of micronormal

= 5.0

R_{mc} = resistivity of mud cake

= 1.2 (measured at formation temperature, 115° F.)

R_{mf} = 0.5 at 115° F.

$$\frac{R_{1"\times 1"}}{R_{mc}} = \frac{3.2}{1.2} = 2.67$$

$$\frac{R_{2"}}{R_{mc}} = \frac{5.0}{1.2} = 4.17$$

On page 4[1] of this manual a chart was presented which related the above ratios with R_{xo}/R_{mc}. This chart was applicable for an 8-in. hole. The same chart can be used for a 9-in. hole if the $R_{1"\times 1"}/R_{mc}$ ratio is multiplied by 0.96 (Chart C-3 of Reference 2). Thus:

$$(R_{1"\times 1"}/R_{mc})_{corr.} = 2.67 \times 0.96$$

$$= 2.56$$

and

R_{xo}/R_{mc} = 27 (From Fig. 2, Part 3[1])

$$R_{xo} = (27)(1.2) = 32.4$$

$$F_a = R_{xo}/R_{mf} = 32.4/0.5 = 65$$

Using this value for the apparent-formation factor, a given residual-oil saturation of 20.0%, and Fig. 2:

$$F = 41$$

$$\phi = 14.3\%$$

Thus F and R_w are now known for the solution of Equation 2. For estimating R_t, the long normal, $R_{64"}$ and/or the lateral, $R_{18'8"}$ is usually used. The long normal can be used if $(R_{16"}/R_m) < 10$ (Chart B-8 of Reference 2). In this case $R_{16"}/R_m$ = 55/0.7 = 79 which exceeds 10 and therefore the long normal cannot be

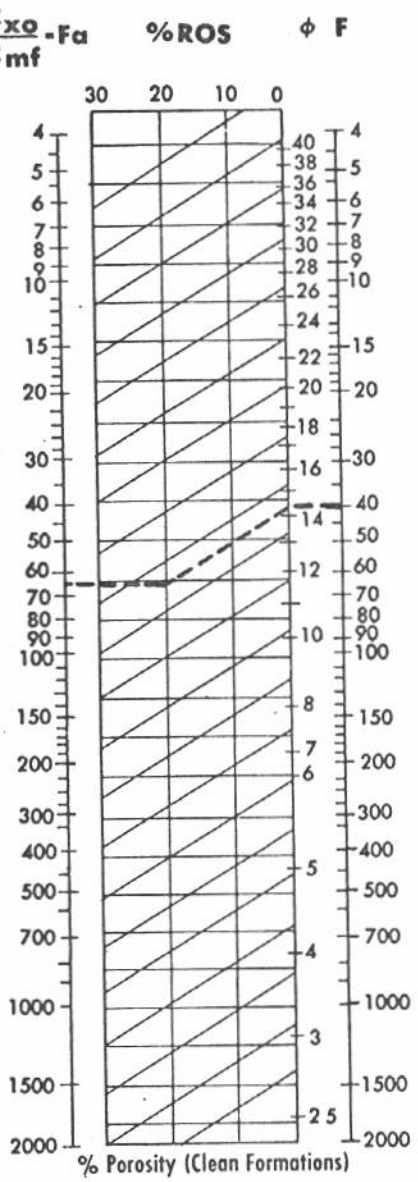

NOMOGRAPH for finding formation factor and porosity. Courtesy Schlumberger Well Surveying Corp. Fig. 2.

used. The selection of the appropriate rule concerning the use of the lateral curve depends principally on the gross thickness of the formation. In this case the gross thickness is about 20 ft. and for such a thickness the maximum reading is a good estimation of R_t if $R_{16''}/R_m < 50$ (Chart B-8 of Reference 2).

$$R_{18'8''} = 200$$

Since $R_{16''}/R_m = 79$ this value must be corrected for drilling fluid and hole effect in order to obtain a value of R_t. This is performed with the aid of Fig. 3.

$$R_{18'8''}/R_m = 200/0.7 = 286$$

and

$$R_t/R_m = 170 \text{ (Fig. 3)}$$

$$R_t = (170)\ (0.7) = 119$$

Therefore

$$S_w = [(41 \times 0.088)/119]^{1/2}$$

$$= (3.61/119)^{1/2} = (0.0303)^{1/2}$$

$$= 0.174 \text{ or } 17.4\%$$

DISCUSSION: This problem shows some of the complexities involved in finding interstitial - water saturation from electrical-survey data. In this case R_w was given as a measured value. Often such a value is not available and has to be found from mud resistivity and SP data and the use of this relationship:

$$SP = -K \log (R_{mf}/R_{we}) \quad (4)$$

Where:

S.P. = spontaneous potential
K = coefficient
R_{we} = resistivity of water containing mixture of electrolytes

Often the SP read on the log is an apparent value and must be corrected. SP is caused by the movement of ions from the interstitial water in a porous rock into the borehole in an effort to equalize the activities of the water and the mud fluid.[4] The magnitude of the SP is affected by the salt concentrations of the water and drilling fluid, bed thickness, borehole diameter, shale in bed, and invasion. The true SP is a result principally of the differences in salt concentration between the interstitial water and drilling fluid.

As a result of the method used to measure it the SP decreases as a bed becomes thinner, as amount of shale in a bed increases, and as hole diameter and invasion increase.[4] Methods to correct for these various effects have been developed.[2]

In Equation 4, K is a factor dependent on formation temperature[2] and R_{mf} has been related to R_m by laboratory studies.[2] Having determined values for SP, K, and R_{mf}, R_{we} can be computed. R_{we} is often nearly equal to R_w but when the formation waters are either fresh ($R_w > 0.2$) or very saline ($R_w < 0.05$) some deviations occur.[4] In both cases R_w is actually greater than R_{we}. Based on theoretical and experimental work, Gondouin et al.[4] developed a chart relating R_{we} and R_w.[2,4]

It is not always possible to measure R_o and it must be computed from a knowledge of F and R_w (Equation 1). As pointed out above, R_w is determined using the SP reading. F is best gotten from the ratio of the resistivity of the invaded zone to the mud filtrate resistivity corrected for residual-oil saturation (Equation 3 and Fig. 2). As noted in this problem,

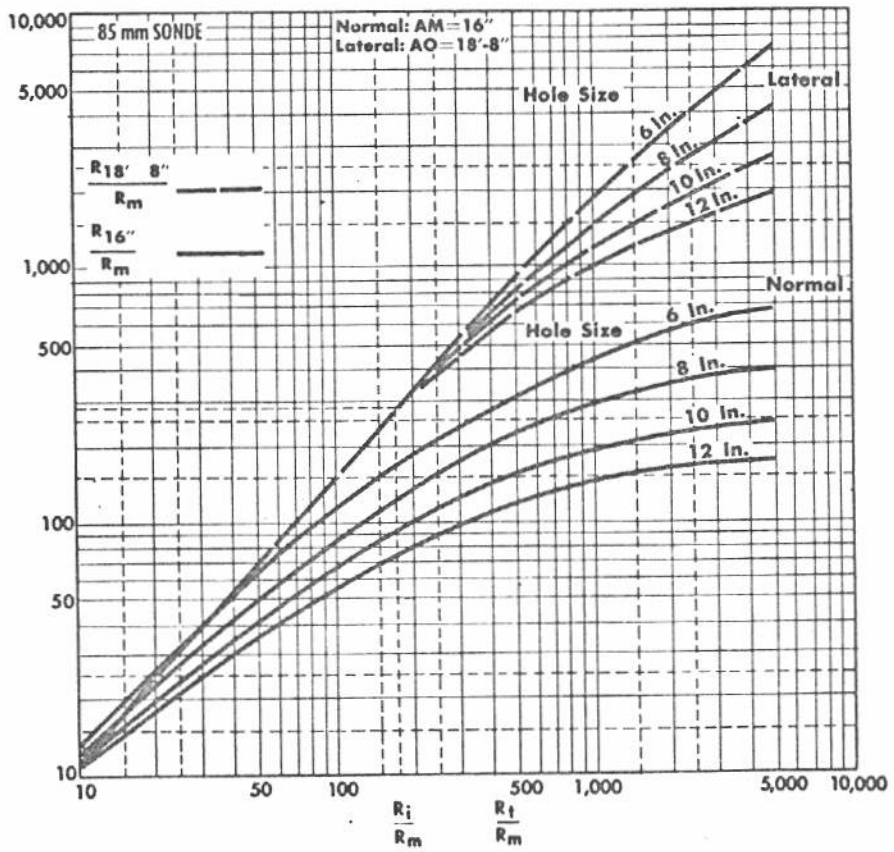

SIMPLIFIED RESISTIVITY departure curves. Courtesy Schlumberger Well Surveying Corp. Fig. 3.

a good method for obtaining F involves the use of contact log data. Generally the measured resistivities are functions of the resistivity of the flushed zone (R_{xo}), residual hydrocarbon saturation (ROS), hole diameter, resistivity of mud cake, and thickness of mud cake.[5] As pointed out in the solution of the problem, graphs have been developed based on laboratory measurements relating the contact log readings with R_{xo} and taking these factors into consideration.[2]

Note on Fig. 1 that the formation of interest has been found to contain hydrocarbons by core analysis. A formation containing hydrocarbons normally shows a higher resistance than one containing only brine. However, the absence or presence of resistance is not always an assurance that hydrocarbons are not or are present. The true resistivity of a bed is a function of hydrocarbon saturation, interstitial water salinity, porosity, and cementation.[6]

Decreasing salinity and porosity and increasing cementation cause the resistivity of a rock to increase. Hence the use of Equation 2 in the determination of hydrocarbon saturation ($1 - S_w$) assumes that the resistivity measured is caused principally by the hydrocarbon saturation. This assumption is not bad when it is remembered that many clean formations have porosities between 20.0 to 30.0%, contain brines with salinities of 30,000 to 60,000 p.p.m., and are not too well consolidated. Under such conditions porosity, cementation, and salinity have a small effect on the true resistivity compared to hydrocarbon saturation.

Use of contact logs, as outlined here, in estimating S_w (and ϕ and F) becomes unreliable generally for tight, highly cemented formations. As a guide, the values of S_w, ϕ, and F, so obtained, should not be trusted without checking by other methods when the porosity so determined is less than 15% and F_a greater than 100.

Thus far problems have been presented on the determination of water saturation from log data involving an electrical survey (Part 27), electrical survey and contact log (this problem), and shaly-sand interpretation (Part 5, The Oil and Gas Journal, February 9, 1959). Other applications of this type of data involve the use of (1) SP, normal, and induction log[2] for use with very resistive muds, (2) Rocky Mountain method,[2] (3) Laterolog and Microlaterolog[2] for use with salt muds, and (4) porosity balance[7] used for verification of water saturation determined from log data.

Acknowledgments

The authors acknowledge the assistance of E. A. Finklea, Schlumberger Well Surveying Corp., Tulsa, in the preparation of this paper.

References

1. Guerrero, E. T., and Stewart, F. M., "Effective Porosity from MicroLog and Microlaterolog Data": Part 3 of Series, The Oil and Gas Journal, 12-22-58, p. 81 (p. 4, this manual).

2. Log Interpretation Charts, Schlumberger Well Surveying Corp.

3. Gondouin, M., Tixier, M. P., and Simard, G. L., "An Experimental Study on the Influence of the Chemical Composition of Electrolytes on the SP Curve," AIME Trans. 1957.

4. Wyllie, M. R. J., "The Fundamentals of Electric Log Interpretation": Academic Press, second edition, 1957.

5. Roberts, I. L., "Fundamental Theory and Instrumentation of Electrical Logging": A Symposium on Formation Evaluation, AIME paper 583-G.

6. Guyod, H., "Estimation of Petroleum Saturation": Oil Weekly, Vol. 120, No. 4, Dec. 24, 1945.

7. Tixier, M. P., "Porosity Balance Verifies Water Saturation Determined from Logs": Trans, AIME, Vol. 213, 1958.

Part 29

How to find initial reservoir pressure from various data

GIVEN: Pressure and production data for a drill-stem test taken from the first well drilled in a pool.

Time after shut in, minutes θ	Bottom-hole pressure, p, psia.	$\frac{t_o + \theta}{\theta}$
1.0	2,735	46.0
2.0	2,746	23.5
3.0	2,750	16.0
7.0	2,757	7.4
12	2,762	4.8
20	2,766	3.3
32	2,769	2.4

t_o = time drill-stem tool was open = 45 minutes

p_{ws} = static bottom-hole pressure or reservoir pressure = 2,775 psi.

D = depth to middle of formation tested = 6,110 ft.

ρ_w = average density of brine or gradient for area in which well is located = 0.450 psi. per ft.

FIND: Initial reservoir pressure obtained by measurement, pressure buildup data, and from hydrostatic gradient.

METHOD OF SOLUTION: Horner's[1] basic buildup equation for a single well in an infinite reservoir applies in this case.

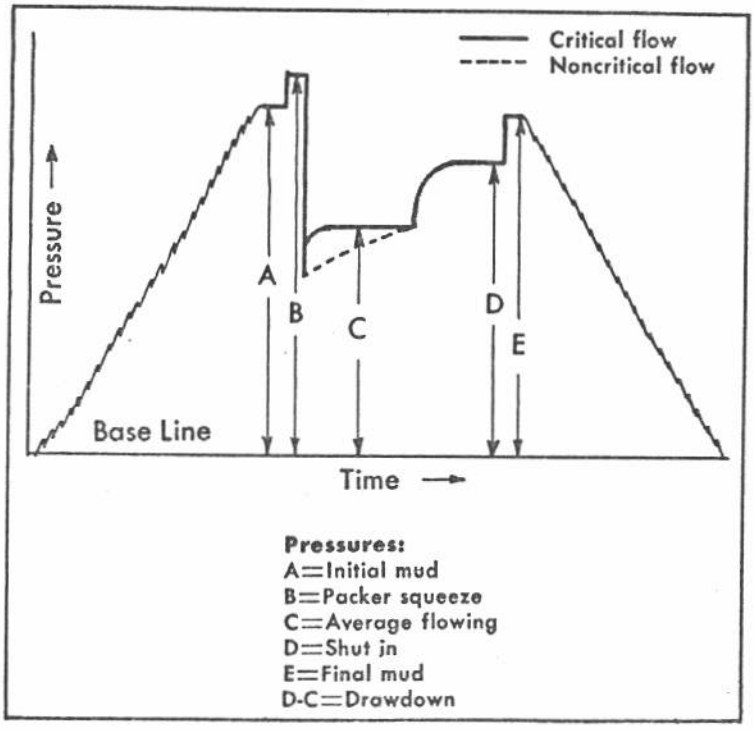

TYPICAL CHART for a satisfactory pressure test. Fig. 1.

$$p_w = p_i - \frac{162.6\, Q_o\, \mu_o\, B_o}{k_o\, h} \log \frac{t_o + \Theta}{\Theta} \quad (1)$$

When using the hydrostatic gradient method:

$$p_{ws} = D\, \rho_w \quad (2)$$

Where: Θ, p_{ws}, t_o, D, and ρ_w were defined with the data, and

p_w = sand face or bottom-hole pressure at Θ time after shut-in, psi.

p_i = initial reservoir pressure, psi.

Q_o = constant production rate at mean reservoir conditions before shut-in, stock-tank barrels per day.

μ_o = viscosity of oil at mean reservoir conditions, cp.

B_o = oil formation volume at mean reservoir conditions.

k_o = effective permeability to oil, md.

h = net sand thickness, ft.

SOLUTION: Since Q_o, μ_o, B_o, k_o, and h are assumed constant during the test, Equation 1 can be written as

$$p_w = p_i - m \log \frac{t_o + \Theta}{\Theta}$$

Where:

$$m = \frac{162.6\, Q_o\, \mu_o\, B_o}{k_o h}$$

This relation is the equation of a straight line resulting from plotting $(t_o + \Theta)/\Theta$ vs p_w on semilogarithmic paper with $(t_o + \Theta)/\Theta$ on the log scale. Since this is true, m is the slope of the straight line and p_i the ordinate intercept. The factor $(t_o + \Theta)/\Theta$ is shown with the given data. In Fig. 2 it has been plotted against the bottom-hole pressure (p_w). Thus the ordinate intercept in Fig. 2 is

$$p_i = 2{,}777 \text{ psi.}$$

Fig. 1 shows a typical pressure-time chart for a satisfactory drill-stem test. The D value shows that the tool was allowed to remain shut in long enough for the pressure to build up to static conditions. Under such conditions the original reservoir pressure is measured directly and in this case was

$$p_i = p_{ws} = 2{,}775 \text{ psi.}$$

Equation 2 gives the pressure exerted by a column of fluid of height D and having an average density of ρ_w. Therefore

$$p = p_{ws} = (6110)\,(0.450) = 2{,}750 \text{ psi.}$$

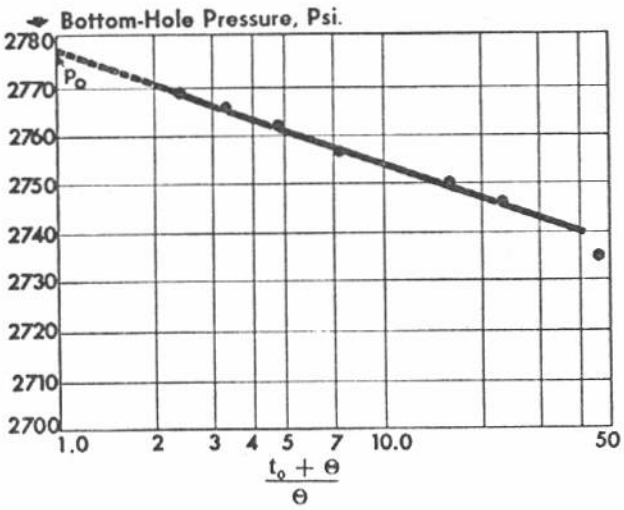

PRESSURE-BUILDUP CURVE from drill-stem test data. Fig. 2.

DISCUSSION:

Of the many factors that are involved in reservoir-engineering problems, perhaps none is as important or as much used as reservoir pressure. It is indicative of reservoir energy and is needed in finding and correlating fluid properties such as solution gas-oil ratio, formation-volume factors, viscosity, and compressibility. Good pressure histories are vital, beginning with the initial reservoir pressure. This problem shows three ways to find this factor. The most accurate, and the most used, is direct measurement with a subsurface pressure gage. However, such an approach requires that the measurement be made on discovery of a pool, as production will cause the pressure to decline.

Here the assumption is made that sufficient shut-in time was allowed for the pressure at the sand face to build up to initial reservoir conditions. If there has been any appreciable production from the well, and to insure against error, it is recommended that at least two measurements be made on the well with an intervening time of several hours to a day until identical maximum readings are obtained. Also, it is advisable that more than one of the original wells be tested.

Occasionally the pressure in a well is not given enough time to build up to static conditions. The permeability of the formation or zone being tested may be so low that, as a practical matter, the time required for complete buildup is too long for continuous or spot measurements until actual buildup is achieved. Under such conditions a pressure-buildup test can be used to determine the initial reservoir pressure. The application and theory of this method were covered in Part 13[2] of this series. This problem uses the same concepts but obtains the necessary data from a drill-stem test.

Pressure buildup is shown in Fig. 1 between pressures C and D. It is from this interval that data such as those given and used in Fig. 2 are obtained.[3,4] Recommended procedures in drill-stem testing necessary for obtaining good presssure-buildup data have been presented by Black[4] and Dolan, et al.[3] Such data are not only useful in determining initial reservoir pressure but also for evaluation of formation damage[3] at the well bore.

Use of a hydrostatic gradient to determine initial reservoir pressure results in a reasonable estimate when experience in the area has made possible the development of an average hydrostatic gradient. In a large number of areas the hydrostatic gradient will lie between 0.433 to 0.470 psi. per ft.[5] The range is caused by a variation of dissolved salts content. Gradients lower and higher than these are generally considered abnormal and may be caused by hydrodynamic conditions, compaction of loosely consolidated rock, and precipitation of crystalline minerals in a closed system.[5] As a result of all these factors, this method of determining initial reservoir pressure is the least reliable of the three used in this problem. However, it is valuable as a means of rough-checking results from the other methods or for those cases where actual or reliable pressure measurements are not available.

References

1. Horner, D. R. "Pressure Build-up in Wells," Proc. 3rd World Petroleum Congress Section III, 1951.
2. Guerrero, E. T., and Stewart, F. M., "How to Determine Effective Permeability," The Oil and Gas Journal, Aug. 10, 1959, p. 119
3. Dolan, J. P., Einarsen, C. A., and Hill, G. A., "Special Applications of Drill-Stem Test Pressure Data," Journal of Petroleum Technology, Nov., 1957.
4. Black, W. M., "A Review of Drill-Stem Testing Techniques and Analyses," AIME Paper 589-G published in A Symposium on Formation Evaluation.
5. Landes, K. K., "Petroleum Geology, John Wiley and Sons, 2nd Edition, 1959, pp. 211-213.

Part 30

How to find average reservoir pressure

- by arithmetic weighting
- by thickness weighting
- by area weighting
- by volume weighting

GIVEN: Pressure survey results for a reservoir having 27 producing wells. Columns 2 and 3 of Table 1 show the net sand thickness at each well and pressures measured. Columns 4 and 5 of the same table show the estimated drainage area of each well and the average net sand thickness in each drainage area.

REQUIRED: Draw an isobaric map with the measured pressures and compute the average reservoir pressure by weighting arithmetically, by thickness, by area, and volumetrically.

METHOD OF SOLUTION: The summation equations below may be used for the method shown.

Arithmetic weighting—

$$p_{avg} = \sum_{i=1}^{i=n} p'_i/n \qquad (1)$$

Thickness weighting—

$$p_{avg} = \sum_{i=1}^{i=n} h_i p_i / \sum_{i=1}^{i=n} h_i \qquad (2)$$

Area weighting—

$$p_{avg} = \sum_{i=1}^{i=n} A_i p_i / \sum_{i=1}^{i=n} A_i \qquad (3)$$

Volume weighting—

$$p_{avg} = \sum_{i=1}^{i=n} A_i h_i p_i / \sum_{i=1}^{i=n} A_i h_i \qquad (4)$$

Where:

p_{avg} = average reservoir pressure, psi.

p'_i = measured pressure for well i, psi.

p_i = average pressure in drainage area of well i, psi.

n = number of pressures involved.

h_i = net sand thickness at well i, ft.

A_i = drainage area of well i, acres.

SOLUTION:

Arithmetic weighted—

Using the summation of column 3 in Table 1:

$p_{avg} = 22{,}961/15 = 1{,}531$ psi.

Thickness weighted—

Using the summation of columns 8 and 5 of Table 1:

$p_{avg} = 687{,}265/450 = 1{,}527$ psi.

Area weighted—

Using the summations of columns 10 and 4 of Table 1:

$p_{avg} = 1{,}771{,}410/1{,}147 = 1{,}544$ psi.

Using the summation of column 5 of Table 2 and a total area of 1,140 acres:

$p_{avg} = 1{,}763{,}755/1{,}140 = 1{,}547$ psi.

Volume weighted—

Using the summations of columns 9 and 7 of Table 1:

$p_{avg} = 29{,}259{,}390/19{,}078$

$= 1{,}534$ psi.

DISCUSSION: There is possibly no factor used more in reservoir engi-

TABLE 2—AVERAGE PRESSURE FROM ISOBARIC MAP DATA

(1) Isobar	(2) Area inclosed by isobar, acres	(3) Area between isobars, acres	(4) Avg. pressure in area, psi.	(5) (Area)×(Pressure) (3)×(4)
1,380	0	0	....	.....
1,400	67	67	1,390	93,130
1,450	230	163	1,425	232,275
1,500	422	192	1,475	283,200
1,550	608	186	1,525	283,650
1,600	764	156	1,575	245,700
1,650	868	104	1,625	169,000
1,700	1,100	232	1,675	388,600
1,710	1,140	40	1,705	68,200
				1,763,755

TABLE 1—BASIC DATA AND CALCULATIONS FOR AVERAGE PRESSURE

(1) Well	(2) Net sand thickness at well, ft.	(3) Static press. measured, corrected to datum, psi.	(4) Estimated area drained by well, acres	(5) Avg. net sand thickness in drainage area, ft.	(6) Avg. pressure in drainage area, psi.	(7) (Thickness)×(Area) (5)×(4)	(8) (Thickness)×(Pressure) (5)×(6)	(9) (Volume)×(Pressure) (7)×(6)	(10) (Area)×(Pressure) (4)×(6)
1	4	1,600	40	5	1,590	200	7,950	318,000	63,600
2	11	....	40	10	1,530	400	15,300	612,000	61,200
3	9	1,520	40	10	1,520	400	15,200	608,000	60,800
4	9	....	40	7	1,540	280	10,780	431,200	61,600
5	8	1,621	54	8	1,640	432	13,120	708,480	88,560
24	12	....	52	14	1,650	728	23,100	1,201,200	85,800
25	14	1,650	46	15	1,645	690	24,675	1,135,050	75,670
26	12	....	47	12	1,640	564	19,680	924,960	77,080
27	12	1,660	51	14	1,650	714	23,100	1,178,100	84,150
		22,961	1,147	450		19,078	687,265	29,259,390	1,771,410

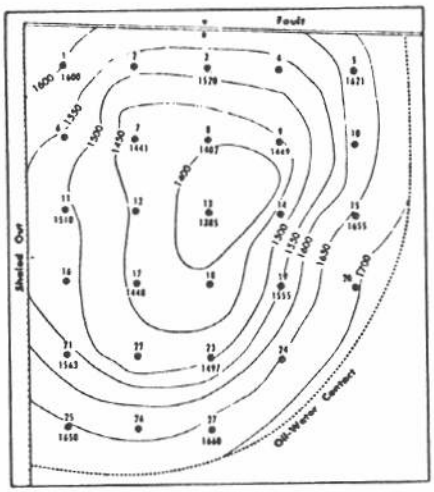

ISOBARIC MAP of a sandstone reservoir. Fig. 1.

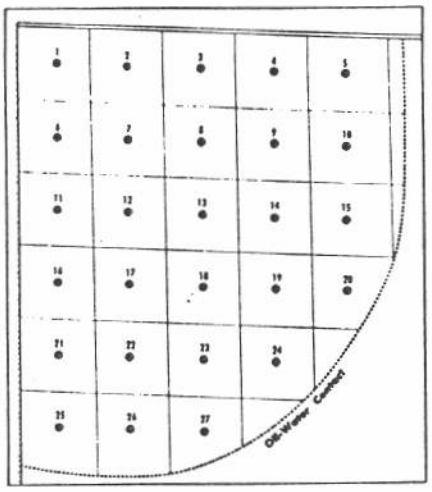

ASSUMED DRAINAGE AREA has been assigned to each well in the field. Fig. 2.

neering than reservoir pressure. It is needed to analyze reservoir performance, calculate productivity indexes, evaluate reserves, institute repressuring, and define the physical characteristics of the reservoir fluid at any time.[1]

Normally pressure surveys are conducted for a lease or pool every 6 to 12 months. The practice is to survey about one-third to one-half of the wells each time. Some alteration (when possible) of the wells selected may be done to maintain pressure histories on as many wells as possible. Or, rather than alternating, the same wells (called "key wells") may be surveyed each time in order to have a continuous, more consistent history.

The wells selected are shut in for 24 hours (sometimes 48 to 72 hours, or even more, may be required) to allow the bottom-hole pressures to build up to or equalize with static reservoir conditions. The pressure in each well in the survey is then measured with a bottom-hole-pressure bomb.[2] For those cases where too much time is required for the bottom-hole pressure to reach static conditions, pressure-buildup tests may be used.[3,4]

Measurements made with properly calibrated subsurface-pressure gages may be read to an accuracy of 3 to 5 psi. in every 1,000 psi. The pressures measured represent the average reservoir pressure within the drainage radius of each respective well. Due to variations in permeability, structural elevation, sand thickness, well allowables, edge-water encroachment, gas-cap encroachment, or other causes, the reservoir pressures measured may vary appreciably from well to well over a lease or reservoir.

Usually the deviation caused by differences in structural elevation is eliminated by referring the measured pressures to a common datum. The datum is a horizontal plane normally selected about in the middle of the producing section. Good practice involves computation of the reservoir pressure at the middle of the sand in each well, using the pressures measured at the last stop and the gradients (psi./ft.) existing at the bottom of the wells. From the middle of the sand the reservoir pressures are computed at the datum, using the existing hydrocarbon gradient since it is desired to know the pressure in the hydrocarbon phase.

In the application of the material-balance equation, as in other reservoir problems, average reservoir pressures are required. This problem shows four ways of averaging pressure measurements. The simplest and possibly most used is the arithmetic average. In all averaging procedures nonrepresentative pressures are excluded. These may result from insufficient buildup, tubing leaks, or instrument failure.

Since the pressure measured at the center of each producing well represents the volume from which that well drains, the volumetric averaging procedure should give the most suitable results for material balance or calculations treating the reservoir as a whole. There are many different ways of determining the area and sand volume drained by a well. Fig. 2 shows the areas assigned in this case. Except for the edge wells, the spacing was taken as the drainage area of each well. Average sand thickness over this area was obtained by laying Fig. 2 over the sand isopach map of the pool. Table 1 shows the area, average net sand thickness, and net sand volume of each drainage area. Note that an average pressure was estimated from Fig. 1 for each drainage area. The isobaric map, Fig. 1, is useful in averaging pressures and for graphically presenting pressure gradients, highs, and sinks over a pool. In this case the higher pressure along the oil-water contact probably indicates some edge-water encroachment. Such maps drawn over intervals of time provide a good visual history of reservoir-energy variations.

Note in this problem that two different procedures have been used in weighing by area, use of drainage areas, and areas between isobars, Table 2. Area weighing should give a good average where the net sand thickness does not vary appreciably over the pool. Where enough measurements are made over a pool to account for variations in net sand thickness, area of drainage, allowables, and rock properties, the arithmetic average also gives reliable averages. It is the simplest to develop and should be used where possible.

Where a gas cap exists above the oil column, it is usually advisable, for material-balance purposes, to obtain an average pressure for the gas cap as well as for the oil portion of the reservoir. In this case, bottom-hole pressures in the gas cap zone should be adjusted to a datum representative of the average elevation in the gas cap. As before, oil-zone pressures should be adjusted to the oil-column datum representing the average elevation of the oil portion of the reservoir. Correction to the datums will be by reservoir free gas or oil gradients, depending on whether the adjustment is through the gas cap or oil column, i.e., above the gas-oil contact or below. This, incidentally, leads to a good way of determining the elevation of the gas-oil contact:

On a coordinate graph of pressure versus elevation, draw a reservoir-oil gradient up from the elevation of the pressure measurement from a well in the oil column, and draw a gas gradient down from the elevation of the pressure measurement from a nearby well in the gas cap. The elevation where the two gradient lines intersect should be the gas-oil contact.

References

1. Calhoun, J. C., "Averaging Reservoir Pressures": Engineering Fundamentals—Advanced Reservoir Engineering, Part 2, Manual published by The Oil and Gas Journal, p. 3.

2. "Engineering Fundamentals on Petroleum Reservoirs": Manual published by The Oil and Gas Journal, pp. 7-15.

3. Guerrero, E. T., and Stewart, F. M., "How to Determine Effective Permeability": The Oil and Gas Journal, 10-5-59, p. 167

4. Perrine, R. L., "Analysis of Pressure-Buildup Curves": API Drilling and Production Practice, 1956, pp. 482-495.

Part 31

How to find reservoir-oil properties from laboratory fluid-analysis data

GIVEN: Laboratory fluid-analysis data on a subsurface oil sample from the discovery well of a pool. The middle of the producing formation was at 6,700 ft. and the initial reservoir pressure was measured as 3,000 psi. From the pressure chart an initial gradient of 0.300 psi. per ft. was found. The basic fluid-analysis data are in Table 2 and the first six columns of Table 1.

FIND: Using the fluid-analysis and bottom-hole-pressure data given determine:

1. Initial saturation conditions of pool.
2. Expansibility factor for the oil at 3,000 psi. and 150° F.
3. Variation with pressure at reservoir temperature of the following:
   (a) Relative-volume factor.
   (b) Two-phase formation-volume factor.
   (c) Single-phase oil formation-volume factor.
   (d) Solution gas-oil ratio.
   (e) Viscosity.
   (f) Y factor.
4. Single-phase oil formation-volume factors at bubble-point pressure for flash and differential liberations.
5. Single-phase formation-volume factor at initial reservoir conditions using subsurface-pressure data, specific gravity of gas, and °API gravity of oil.

METHOD OF SOLUTION: These equations will be used in the solution of the problem.

$$C_o = \frac{1}{V}\frac{dV}{dp} \approx \frac{V_2 - V_1}{V_1(p_1 - p_2)} \quad (1)$$

$$B_t = (V_{og}/V_{sat})\, B_{ob} \quad (2)$$

$$Y = \left(\frac{p_b - p}{p\left(\frac{V_{og}}{V_{sat}} - 1\right)}\right) \quad (3)$$

TABLE 2—FLUID-SEPARATOR TESTS

(1) Separator pressure, psig.	(2) Gas-oil ratios, std. cu. ft. per st.-tk. bbl. Separator	(3) Gas-oil ratios, std. cu. ft. per st.-tk. bbl. Total	(4) St. tk. gravity, °API	(5) Bubble point formation vol. factor V_{sat}/V_s	(6) Sp. gr. of flashed gas	(7) Separator temp., °F.
0	463	463	42.2	1.339	1.162	68
37	368	413	43.8	1.239	0.963	68
72	315	406	44.0	1.235	0.891	68
115	290	413	44.4	1.241	0.847	68
Differential	...	524	43.8	1.386	....	..

TABLE 1—SUBSURFACE FLUID-ANALYSIS DATA AND CALCULATIONS

(1)	Measured data: (2) Flash liberation	(3) Flash liberation	(4) Differential liberation at 150° F.	(5) Differential liberation at 150° F.	(6) Differential liberation at 150° F.	Calculations: (7)	(8)	(9)	(10)	(11)
Press., psia.	Relative vol. factor at 150° F., V_{og}/V_{sat}	Viscosity of oil at 150° F. Cp.	Gas liberated, std. ft.³/s.t. bbl.	Gas in solution, std. ft.³/s.t. bbl.	Formation vol. factor, V_o/V_s	Two-phase formation vol. factor	$p_b - p =$ 1,155 − (1)	$\frac{V_{og}}{V_{sat}} - 1$ (2) − 1	$p\left(\frac{V_{og}}{V_{sat}} - 1\right)$ (1)×(9)	Y (8)÷(10)
5,015	0.9635	0.94	...	...	.....	1.3357	....	.....	.....	....
4,165	0.9700	0.88	...	...	1.3447	1.3447	....	.....	.....	....
4,015	0.9712	0.87	...	...	.....	1.3464	....	.....	.....	....
3,015	0.9798	0.79	...	...	.....	1.3583	....	.....	.....	....
2,515	0.9847	....	...	...	.....	1.3651	....	.....	.....	....
2,015	0.9897	0.74	...	...	.....	1.3720	....	.....	.....	....
1,515	0.9953	....	...	...	.....	1.3798	....	.....	.....	....
1,415	0.9965	....	...	...	.....	1.3814	....	.....	.....	....
1,315	0.9978	....	...	...	.....	1.3833	....	.....	.....	....
1,215	0.9992	0.70	...	...	.....	1.3852	....	.....	.....	....
1,155	1.0000	0.70	0	524	1.3863=B_{ob}	1.3863	0	0	0	....
1,145	1.0025	....	...	...	.....	1.3898	10	0.0025	2.8625	3.493
1,135	1.0051	....	...	...	.....	1.3934	20	0.0051	5.7885	3.455
1,115	1.0111	....	...	...	.....	1.4017	40	0.0111	12.3765	3.232
1,105	1.0142	....	...	...	.....	1.4060	50	0.0142	15.6910	3.187
1,085	1.0213	....	...	...	.....	1.4158	70	0.0213	23.1105	3.029
1,045	.....	0.71	28	496	1.3712	.....	110	.....	.....	.....
935	1.0858	0.72	56	468	1.3549	1.5052	220	0.0858	80.2230	2.742
785	1.1879	0.74	90	434	1.3359	1.6468	370	0.1879	147.502	2.508
635	1.3536	0.79	131	393	1.3148	1.8765	520	0.3536	224.536	2.316
485	1.6527	0.85	175	349	1.2957	2.2911	670	0.6527	316.560	2.117
335	2.2418	0.98	226	298	1.2726	3.1078	820	1.2418	416.003	1.971
215	3.4100	1.08	275	249	1.2490	4.7273	940	2.4100	518.150	1.814
15	.....	1.38	524	0	1.0458	.....	1,140	.....	.....	....

V_{sat} = volume reservoir oil at 1,155 psia. and 150° F.
V_s = Stock-tank-oil volume at 14.7 psia. and 60° F.
V_{og} = volume at given pressure and 150° F. of oil plus liberated gas.
V_o = volume at given pressure and 150° F. of oil only.

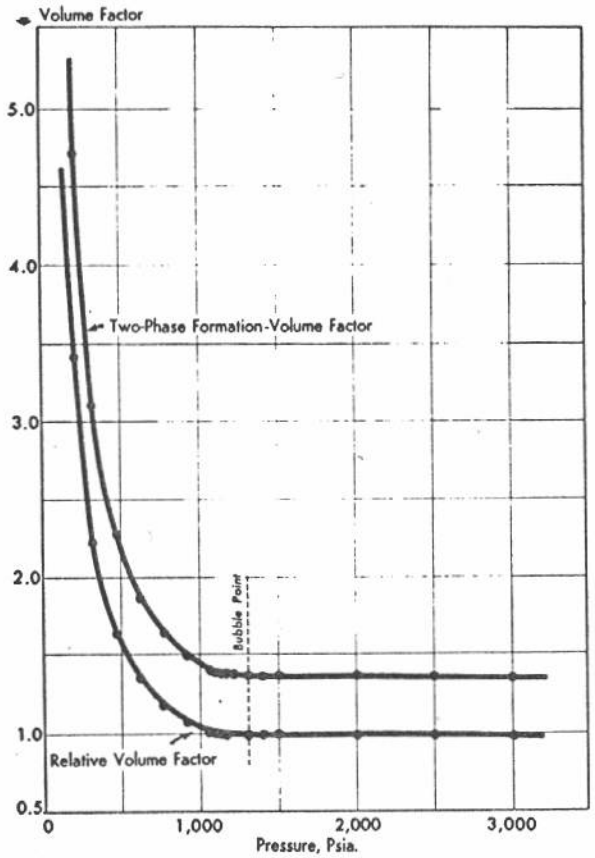

PRESSURE-VOLUME relations at reservoir temperature. Fig. 1.

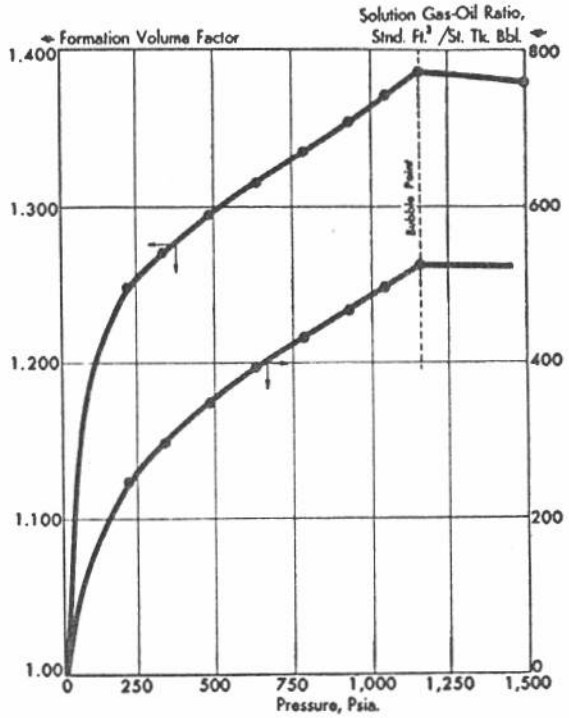

VARIATION of formation volume factor and solution gas-oil ratio with pressure at reservoir temperature. Fig. 2.

$$\text{Sp. gr.}_{60/60} = \frac{141.5}{131.5 + {}^\circ\text{API}} \quad (4)$$

$$\text{Mole. wt.}_{(gas)} \approx \text{Mole wt.}_{(air)} \times \text{sp. gr.}_{(gas)} \approx 28.8 \times \text{sp. gr.}_{(gas)} \quad (5)$$

$$B_o = \frac{\rho_o\, 350 + R_{sb}\,(M_g/379)}{(5.615)\,(144)\,(dp/dh)} \quad (6)$$

Where:

c_o = expansibility factor of oil, vol./vol./psi.

V = volume at given pressure and reservoir temperature, bbl.

V_{og} = volume at given pressure and reservoir temperature of oil and liberated gas, bbl.

p = pressure, psi.

B_t = two-phase formation-volume factor, reservoir pore space occupied by 1 bbl. stock-tank oil and its initially dissolved gas at reservoir conditions.

V_{sat} = volume of reservoir oil at bubble-point conditions, bbl.

V_s = stock-tank-oil volume at 14.7 psia. and 60° F., bbl.

B_{ob} = single-phase oil formation-volume factor at bubble-point pressure and reservoir temperature.

Y = factor defined by Equation 3.

p_b = bubble-point pressure, psia.

B_o = single-phase oil formation-volume factor at pressure p and reservoir temperature.

ρ_o = density of oil at 14.7 psia. and 60° F., g./cc. = sp. gr.

R_{sb} = solution gas-oil ratio at bubble-point conditions, std. cu. ft./st. tk. bbl.

M_g = molecular weight of liberated gas.

dp/dh = gradient at reservoir conditions, psi./ft.

350 = density of water at 4° C. and atmospheric pressure, lb./bbl.

379 = std. cu. ft. of gas per lb. mole at 60° F. and 14.7 psia.

5.615 = cu. ft. in 1 bbl.

144 = sq. in. per sq. ft.

SOLUTION:

1. Relative volumes are normally listed such that the bubble-point volume is unity. Note in Table 1, column 2, that in this case the bubble point occurs at 1,155 psia. Since the initial reservoir pressure was measured as 3,000 psi. then the pool was undersaturated at initial pressure.

2. Using the relative volume factors (Table 1, column 2) at 4,015 psia. (V_1) and 2,015 psia. (V_2) the oil expansibility factor at 3,000 psi. and 150° F. is given by

$$C_o = \left(\frac{1}{0.9712}\right)\left(\frac{0.9897 - 0.9712}{4,015 - 2,015}\right)$$

$$= \frac{0.0185}{(0.9712)\,(2{,}000)} = \frac{0.0185}{1{,}942.4}$$

$$= 9.524 \times 10^{-6}\ \frac{\text{bbl.}}{\text{bbl. psi.}}$$

or vol./vol./psi.

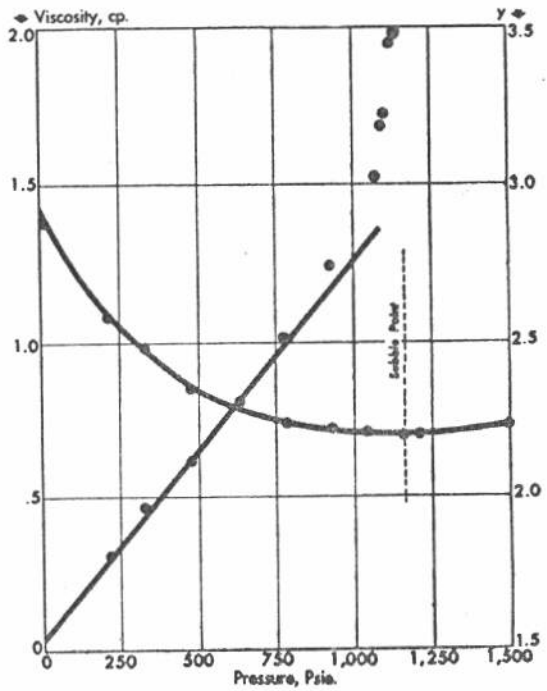

VARIATION of viscosity and Y factor with pressure at reservoir temperature. Fig. 3.

"... formation-volume factor decreases and the oil gravity increases as the separator pressure increases."

A similar calculation for the expansibility from initial pressure of 3,015 psia. down to the bubble point, 1,155 psia., gives $C_o = 11.08 \times 10^{-6}$ vol./vol./psi. The different result is to be expected as expansibility of oil above the bubble point is not exactly a straight line function with pressure.

3. See Figs. 1, 2, and 3.

4. Single-phase oil formation - volume factors at the bubble-point pressure are obtained for differential and flash liberations from Tables 1 and 2.

Type liberation	Formation vol. factor
Differential	1.386
Flash	1.339

5. Using a gas specific gravity of 1.162 and oil gravity of 42.2 (Table 2)—

$$\text{Sp. gr. oil}_{(60/60)} = \frac{141.5}{131.5 + 42.2}$$

$$= 0.8146$$

This is the specific gravity of the oil at 60° F. and atmospheric pressure compared to water at 60° F. and the same pressure. It can be related to water at 4° C. (39° F.) by multiplying by 0.999 or atmospheric pressure.

$$\rho_o = \text{sp. gr.}_{(\text{oil})} = 0.8146 \times 0.999$$
$$= 0.814$$

$$M_g = 28.8 \times 1.162$$
$$= 33.5$$

$$B_o = \frac{(0.814)(350)+[(524)(33.5)\div 379]}{(5.615)(144)(0.30)}$$

$$= 1.36$$

DISCUSSION: In the solution of the material balance, volumetric and frontal-advance equations, and most reservoir engineering problems, fluid properties are required. This problem illustrates the most widely used method of obtaining oil properties. Procedure involves securing representative subsurface samples of the oil early in the life of a pool.[1] This will make possible the definition of the properties from initial reservoir conditions. Normally it is advisable to obtain several samples at different structural positions in the reservoir. These are analyzed in the laboratory for the variation with pressure (at constant temperature) of oil volume, viscosity, gas in solution, and formation-volume factor. Columns 1 through 6 of Table 1 and Table 2 show the measured data.

In columns 2 and 3 of Table 1 flash liberation was involved, whereas in columns 4, 5, and 6 differential liberation was used. The two liberation processes differ in that in the former the gas evolved from solution is kept in contact with the oil during the entire liberation process. In the differential process gas evolved from solution is removed from contact with the oil after each pressure decrement. Actually the two processes give different results. For most nonvolatile crudes flash liberation gives higher oil viscosity, formation - volume factor, solution gas-oil ratio, and lower API gravity. But, in most instances this difference is not appreciable and can be neglected.

It is well to remember that the liberation that occurs between the reservoir rock and stock tank is a combination of flash and differential. Also, the resulting fluid properties are used with other data (rock properties and sand volumes) that are apt to be less accurate.

Note from Equation 2 and Fig. 1 that the relative volume factor for oil plus gas (V_{og}/V_{sat}) and the two-phase formation volume factor B_{ob} (V_{og}/V_{sat}) differ only by a constant multiplier. Above the bubble point only undersaturated liquid is present and these factors increase slightly as the liquid expands with decreasing pressure. Below the bubble point both liquid and free gas occur. As the pressure decreases the liquid portion shrinks while the free-gas portion increases and expands.[2]

The increase of the latter is much larger than the shrinkage of the former and this accounts for the growth of the oil and gas volume factor below the bubble-point pressure. In contrast, the single-phase oil formation-volume factor (V_o/V_a) decreases below the bubble point as shown in Fig. 2. Above the bubble point it becomes similar to the two-phase curve since both represent only liquid in this region.

Increasing pressures cause gas to go into solution with oil. This process continues as long as free gas is available. At the bubble point all the free gas is in solution and the solution gas-oil ratio remains constant for pressures above this point, Fig. 2. Note in Figs. 2 and 3 that increasing amounts of gas in solution have a net effect of increasing the single-phase formation volume factor and decreasing the oil viscosity. As pressure is increased above the bubble point the liquid is compressed and viscosity increases.

Equation 3 defines the Y factor which is computed for pressures below the bubble point and plotted in Fig. 3. It is an empirical factor which gives a linear graph when plotted against pressure for systems composed almost entirely of hydrocarbons. It is very sensitive at pressures near the bubble point. And it is useful for smoothing and averaging pressure-volume data.

All of the measured data of Table 1 were obtained at reservoir temperature. Table 2 shows data obtained at separator temperature. Note that the zero separator pressure formation-volume factor and solution gas-oil ratio of Table 2 are not too different from the comparable bubble-point data of Table 1. This is typical for comparatively nonvolatile crudes. However, large differences may be noted in more volatile crudes.

The principal purpose of the data in Table 2 is to assist engineers in the selection of separator pressures. Note that the formation-volume factor decreases and the oil gravity increases as the separator pressure increases. The large change occurs between 0 and 50 to 75 psi. separator pressures. Decreasing the formation-volume factor increases stock-tank-oil recovery; and increasing the oil gravity (below 40° API) increases the value of the oil.

The properties of oil and gas mixtures are primarily functions of pressure, temperature, composition of gas, and composition of oil. No satisfactory analytical relations have been found to define these properties.[2] They must be determined by laboratory measurement. For those cases where samples of the reservoir fluid were not obtained early in the life of a pool, fair estimates of the fluid properties can be obbtained from empirical correlations and a knowledge of reservoir pressure, temperature, gas gravity, and oil gravity.[3,4]

Acknowledgment

The authors acknowledge the assistance of C. C. Wilson, Wright Laboratories, Tulsa, and T. W. Brinkley, Sunray Mid-Continent Oil Co., Tulsa, in the preparation of this article.

References

1. Standing, M. B., "Volumetric and Phase Behavior of Oil Field Hydrocarbon Systems": Reinhold Publishing Corp., 1952.

2. Calhoun, J. C., "Engineering Fundamentals—Advanced Reservoir Engineering": Manual published by The Oil and Gas Journal, Vol. 1, Articles No. 300-345.

3. Standing, M. B., "A General Pressure-Volume-Temperature Correlation for Mixtures of California Oils and Gases": The Oil and Gas Journal, May 17, 1947, p. 95.

4. Beal, C., "The Viscosity of Air, Water, Natural Gas, Crude Oil, and Its Associated Gases at Oil-Field Temperatures and Pressures": Trans. AIME, 165, 94 (1946).

Part 32

How to find original oil in place by the volumetric method

GIVEN: Electric and MicroLog data on lower Strawn sand from wells drilled in Northwest Trimue field, Tillman County, Oklahoma, Table 1. Other data are as follows:

ϕ = average porosity, thickness weighted = 15.9%.

S_w = average interstitial water saturation from electric and contact logs = 23.0% of pore volume.

B_{oi} = initial formation volume factor = 1.56.

K = planimeter constant = 1.0.

REQUIRED:

1. Draw an isopach map and find net sand volume by trapezoidal rule and square pick methods.

2. Draw an isovol map and find pore volume by trapezoidal rule method.

3. Compute initial oil in place using the results of (1) and (2).

METHOD OF SOLUTION: These equations will be used in the solution of the problem.

Trapezoidal rule:

$$V_s = K\{I[(A_o/2) + A_1 + A_2 + \cdots + A_{n-1} + (A_n/2)] + h_n A_n\} \quad (1)$$

Square pick method:

$$V_s = \sum_{i=1}^{i=n} A_{si}\, h_{si} \quad (2)$$

Initial oil in place:

$$N = \frac{7{,}758\, V_s \phi (1 - S_w)}{B_{oi}} \quad (3)$$

$$N = \frac{7{,}758\,(P.V.)(1 - S_w)}{B_{oi}} \quad (4)$$

Where:

V_s = net sand volume, acre-ft.

I = Isopach interval, ft., or isovol interval, porosity-ft.

A_o = area enclosed by zero contour line, acres.

$A_{1,2,etc.}$ = area enclosed by each successive contour line above the zero line, acres.

h_n = average net sand thickness above maximum contour line, ft.

A_n = area enclosed by maximum thickness contour line, acres.

A_{si} = net sand area covered by square i, acres,

h_{si} = average net sand thickness in sand area covered by square i, ft.

N = initial oil in place, stock-tank bbl.

ϕ, S_w, B_{oi}, and K were defined with data.

P.V. = pore volume, acre-ft.

TABLE 1—LEASE, ELECTRIC AND CONTACT LOG DATA, LOWER STRAWN SAND, NORTHWEST TRIMUE FIELD, TILLMAN COUNTY, OKLA.

Operator and Lease	(1) Well No.	(2) Subsea elev., ft. Top	(3) Subsea elev., ft. Base	(4) Gross thickness, ft.	(5) h, ft.*	(6) Porosity fraction†	(7) h × φ (6) × (7)
Sunray Mid-Continent							
B. J. Alexander	1	−3,762	....	....	0	....	....
	2	−3,783	−3,793	10	2	0.170	0.34
D. D. Alexander	1	−3,770	−3,778	8	6	0.180	1.08
	2	−3,814	−3,842	28	28	0.185	5.18
	3	−3,750	−3,764	14	13	0.140	1.82
	4	−3,793	−3,822	29	29	0.185	5.37
Copeland-Ray	1	−3,722	....	....	0	....	....
	2	−3,838	−3,865	27	27	0.172	4.64
	3	−3,866	....	....	0	....	....
	4	−3,833	−3,843	10	0	....	....
Kadane & Sons							
Parris "B"	1	−3,807	−3,825	18	18	0.165	2.97
	2	−3,890	−3,911	21	20	0.220	4.40
	3	−3,830	−3,861	31	31	0.160	4.96
	4	−3,949	−3,957	8	0	....	....
Ray	1	−3,743	−3,765	20	20	0.085	1.70
	2	−3,828	−3,851	23	23	0.160	3.68
	3	−3,853	−3,875	22	22	0.135	2.97
	4	−3,956	....	....	0	....	....
C. P. Burton							
Amyx	1	−3,804	−3,810	6	6	0.120	0.72
S. D. Johnson							
Watson	1	−3,818	−3,826	8	0	....	....

*Net oil-sand thickness from contact logs. †From log data.

SOLUTION:

Net sand thickness values, Column 5, Table 1, were recorded on wells within respective leases of a property map. Isopach lines connecting points of equal net thickness were drawn (interval = 5 ft.) to get Fig. 1. This map was then planimetered, by leases, to give the data in Columns 1 through 10, Table 2. Column 13 is a solution of Equation 1 for each lease. For example, using the data for the D. D. Alexander lease

$$V_s = 1.0\{5[(80.8/2) + 72.0 + 58.3 + 43.4 + 28.8 + 16.5 + (4.9/2)] + 1 \times 4.9\}$$

$$= (5)(261.9) + 4.9$$

$$= 1{,}314 \text{ acre-ft.}$$

Summation of the individual lease volumes gave a pool net sand volume of 4,641 acre-ft.

Leases involved in this pool are bounded by north-south and east-west lines. The middle portion is Sec. 3, 3-3s-19w, Tillman County, Oklahoma. On transparent paper Sec. 3, which contains 640 acres, was divided into sixty-four 10-acre squares and the eastern part of Sec. 2 (east of Sec. 3) and eastern part of Sec. 4 were also divided into 10-acre squares. This overlay was placed over the isopach map, Fig. 1, and net sand and average thickness recorded for each square that covered a portion of the pool.

Only area covering productive sand volume was recorded. The product of

TABLE 2—PLANIMETER DATA FOR LEASE AND POOL NET SAND VOLUME DETERMINATIONS, NORTHWEST TRIMUE FIELD, TILLMAN COUNTY, OKLAHOMA

Operator and Lease	(1) 0 ft.	(2) ½×(1)	(3) 5 ft.	(4) 10 ft.	(5) 15 ft.	(6) 20 ft.	(7) 25 ft.	(8) 30 ft.	(9) ½ × Last area	(10) Total	(11) Avg. thickness above max. isopach, ft.	(12) Volume above max. isopach, ac.-ft.	(13) Net sand volume, ac. ft. (10)×5+(12)
	Areas Enclosed by respective isopach lines, acres												
Sunray Mid-Continent													
B. J. Alexander ..	17.3	8.7	9.2	3.9	1.0	0.1	...	...	0.1	22.9	...	...	115
D. D. Alexander..	80.8	40.4	72.0	58.3	43.4	28.8	16.5	4.9	2.5	261.9	1	4.9	1,314
Copeland-Ray	52.5	26.3	41.0	29.5	16.9	8.3	2.3	...	1.2	123.2	1	2.3	618
Kadane & Sons													
Parris "B"	79.1	39.6	67.1	55.3	44.4	30.2	10.2	2.6	1.3	248.1	1	2.6	1,243
Ray	70.4	35.2	63.5	57.5	48.0	36.1	14.3	...	7.2	247.5	1	14:3	1,252
McGuire	8.3	4.2	2.8	...	...	...	...	...	1.4	5.6	2	5.6	34
C. P. Burton													
Amyx	9.4	4.7	2.6	...	...	...	...	...	1.3	6.0	2	5.2	35
S. D. Johnson													
Watson	8.8	4.4	2.3	...	...	...	...	...	1.2	5.6	1	2.3	30
Field total	....	....	....	....	....	....	....	....	....	....	....	....	4,641

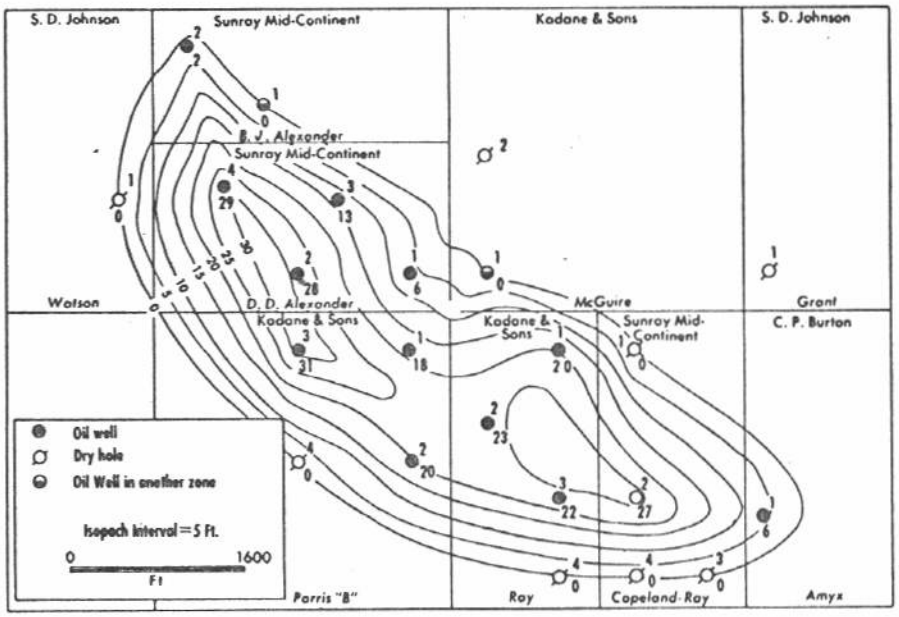

NET SAND-THICKNESS VALUES from Table 1 were used in preparing this isopachous map of the lower Strawn sand, Northwest Trimue field, Oklahoma. Fig. 1.

net sand area and average thickness recorded for a square gives net sand volume covered by the square. Summation of all such products for squares in a lease gives the lease net sand volume (Equation 2). For example, in the D. D. Alexander lease:

$$V_s = (2)(15) + (2)(13) + (1)(3) + (10)(18) + (10)(24) + (10)(12) + (5)(4) + (10)(13) + (10)(27) + (10)(20) + (10)(7)$$

$$= 30 + 26 + 3 + 180 + 240 + 120 + 20 + 130 + 270 + 200 + 70$$

$$= 1{,}289 \text{ acre-ft.}$$

Table 3 shows net sand volumes for all leases and a field total of 4,590 acre-ft.

Column 6 of Table 1 shows the average porosities found for respective wells using core data, electrical survey and contact log data. The value for a well was multiplied by the well's net sand thickness to give the data of Column 7, Table 1. This gives net sand thickness in porosity-feet. These values were recorded on a base map and isovol lines (lines connecting points of equal porosity-feet) drawn. The resulting isovol map is Fig. 3. Areas enclosed by contours on this map were planimetered and recorded in Table 4. Pore volume was computed using these data and Equation 1:

$$P.V. = 1.0\{1.0[(325/2) + 247 + 176 + 113 + 45 + (9/2)] + 0.2 \times 9\}$$

$$= 162.5 + 247 + 176 + 113 + 45 + 4.5 + 1.8$$

$$= 750 \text{ acre-ft}$$

Using Equation 3 and the pool net sand volume from Table 2

$$N = \frac{(7{,}758)(4{,}641)(0.159)(1.00-0.23)}{1.56}$$

$$= 2{,}825{,}700 \text{ st. tk. bbl.}$$

Or using Equation 4

$$N = \frac{(7{,}758)(750)(1.00-0.23)}{1.56}$$

$$= 2{,}871{,}950 \text{ st. tk. bbl.}$$

DISCUSSION: This problem is an example of one of the oldest and most-used methods of finding initial oil in place. It is normally referred to as the volumetric or pore-volume method. Included in its solution are rock and fluid properties and net sand volume data. The final solution of volumetric-type formulas (Equations 3 and 4) is simple. But a lot of work and engineering judgment are needed in arriving at values of porosity, oil saturation, initial formation-volume factor, and net sand volume. Determination of average porosity, initial oil saturation ($1-S_w$), and initial formation-volume factor for a lease or reservoir have been covered in previous articles.[1 2 3]

In finding net sand volume of a lease or pool we must first define the limits. This is done with log and core-analysis information. We can find depth to the top and base of net sand, and amount of gross productive interval.

From such data cross-sections and maps can be drawn to define structure. From logs, drill-stem tests, core analyses, and well-completion data, the outer limits (pinchout or oil-water contact) can be defined. When a gas

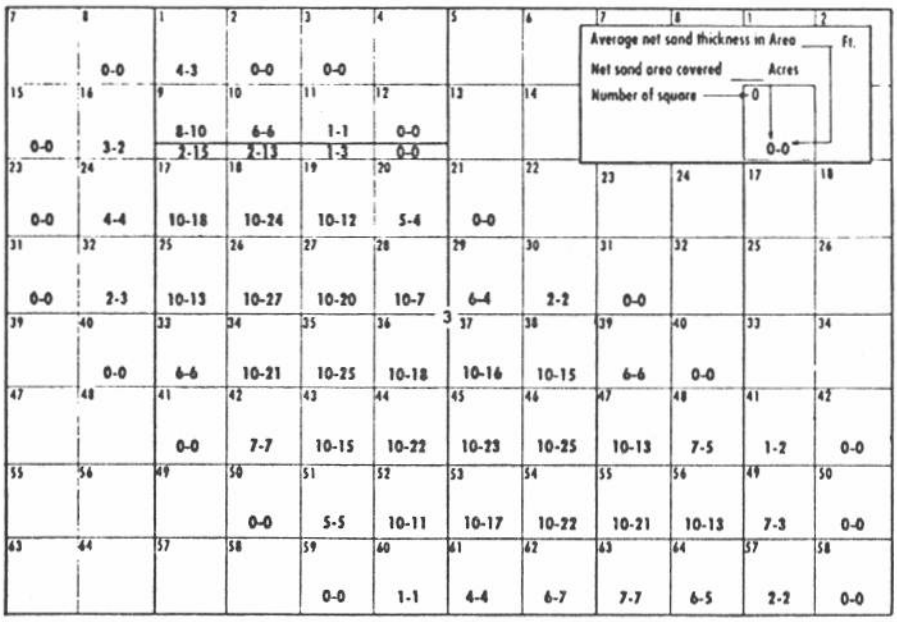

AN OVERLAY OF THIS TYPE, on transparent paper, is used to record the net sand and average thickness of each 10-acre tract in the field. Fig. 2.

cap exists initially, we must establish the gas-oil contact using core analyses or drill-stem and production test data. Objective is to find the area and vertical limits within which lies oil-productive net sand.

Once this is done maps such as those in Figs. 1 and 3 can be drawn and sand volume found by one or more of the procedures shown in this problem.

In the volumetric formula, net sand volume is perhaps the least reliable factor. Thus considerable care should be used in its determination. Best results are obtained when use is made of all information available.

It should be possible to establish a net sand thickness for every well. The portion of gross interval which is productive is usually best obtained from core analyses data but fairly reliable values may also be obtained from contact, self potential, and other types of log data. Where more than one type of data are available, all types should be used and the results compared.

Several methods can be used to find net volume from isopach maps.[4] Two of the most common were used in this problem and results show they give comparable values. Planimetering is preferred by many, but the use of square picks is faster when we want to know individual lease volumes in addition to pool volume. It is also more adaptable for machine data processing. In those portions of the country where the range-township-section system of surveying is used, it is possible to develop clear-film or other transparent overlays containing known area squares covering one or more sections for use on isopach maps of a given scale.

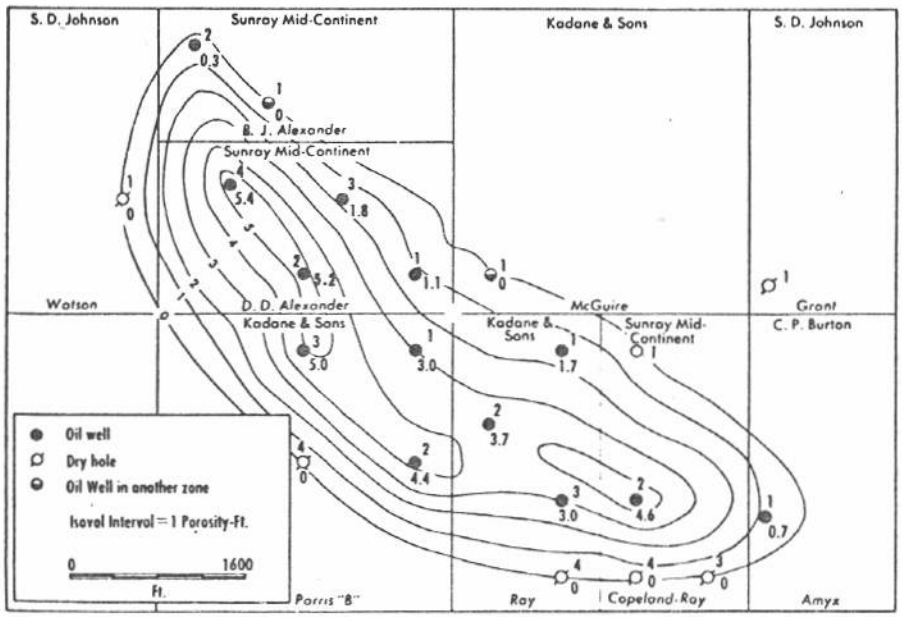

PRODUCT OF POROSITY and net sand thickness (Column 7, Table 1) were used in preparing this isovol map. Lines are drawn through points of equal porosity-feet. Fig. 3.

Table 3—Lease and Field Net Sand Volumes (Square Pick Method) Northwest Trimue Field, Tillman County, Oklahoma

Operation and Lease	Net sand, ac.-ft.*
Sunray Mid-Continent	
B. J. Alexander	129
D. D. Alexander	1,289
Copeland-Ray	620
Kadane & Sons	
Parris "B"	1,231
Ray	1,238
McGuire	28
C. P. Burton	
Amyx	27
S. D. Johnson	
Watson	28
Field total	4,590

*Summation net sand volumes of squares in lease.

Table 4—Data from Isovol Map for P.V. Determination, NW Trimue Field, Tillman County, Oklahoma

Contour	Area enclosed by isovol, acres
0	325
1	247
2	176
3	113
4	45
5	9

h_n = 0.20 porosity ft.

Fig. 3 shows another type of map that can be used for getting initial oil in place, the isovol map. It consists of isovol lines connecting points of equal porosity-feet. The volume from it is the pore volume of the pool (or lease) or the product of $V_s\phi$ in Equation 3. It has the advantage that average well porosities are volumetrically weighed in the process of pore-volume determination.

A further step is the development of a map giving the product of $V_s\phi(1-S_w)$ in Equation 3. By connecting points of equal hydrocarbon pore space the result is an isohydrocarbon or "isocarb" map.

References

1. Guerrero, E. T., and Stewart, F. M., The Oil and Gas Journal, 11-23-59, p. 101

2. Guerrero, E. T., and Stewart, F. M., The Oil and Gas Journal, 7-4-60, p. 106

3. Guerrero, E. T., and Stewart, F. M., The Oil and Gas Journal, 1-2-61, p. 92

4. Vance, Harold, Petroleum Subsurface Engineering, Educational Publishers, Inc., 1950, Chapter 8.

Part 33

How to find original oil in place by material balance above the bubble point

GIVEN: Production, rock, and fluid data for an undersaturated oil reservoir are as follows:

p_i = initial reservoir pressure = 2,400 psia.

N_p = cumulative oil production = 148,400 st.-tk. bbl.

P_{ws} = average reservoir pressure = 1,832 psia.

p_b = bubble-point pressure = 1,500 psia.

R_{sb} = solution gas-oil ratio for pressures at and above bubble-point pressure = 490 s.c.f./st.-tk. bbl.

S_w = interstitial water saturation = 20.0% of pore vol.

B_w = water formation-vol. factor = 1.0.

B_{oi} = initial oil-formation volume factor = 1.234.

B_o = oil-formation volume factor at p_{ws} = 1.241.

B_f = rock-formation vol. factor = 1.0.

Compressibility factors at average reservoir conditions above 1,832 psig. are:

for oil, $C_o = 8 \times 10^{-6}$ vol./vol./psi.

for water, $C_w = 3 \times 10^{-6}$ vol./vol./psi.

for rock formation, $C_f = 4 \times 10^{-6}$ vol./vol./psi.

No water has been produced and no water influx is believed to have taken place. Thus $W_p = O$ and $W_e = O$.

FIND: Original oil in place.

METHOD OF SOLUTION:

Equations:

$$N = \frac{N_p B_o + (W_p - W_e)}{B_{oi} C_e (p_i - p_{ws})} \quad (1)$$

$$C_e = C_o + \frac{S_w}{1 - S_w} C_w + \frac{C_f}{1 - S_w} \quad (2)$$

Where B_f, B_w, N_p, B_o, B_{oi}, p_i, S_w, and p_{ws} have been defined with the given data and

N= original oil in place, st.-tk. bbl.

C_e = composite compressibility, vol./vol./psi.

W_p = cumulative water production, bbl.

W_e = cumulative water influx, bbl.

SOLUTION:

$$C_e = \left[8 + \left(\frac{0.20}{1.00 - 0.20} \right) (3) + \frac{(4)}{1.00 - 0.20} \right] 10^{-6}$$

$$= \left[8 + \frac{0.60}{0.80} + \frac{4}{0.80} \right] 10^{-6}$$

$$= 13.75 \times 10^{-6}$$

$$N = \frac{(148{,}400)\,(1.241)}{(1.234)\,(13.75 \times 10^{-6})\,(2{,}400 - 1{,}832)}$$

$$= 19.1 \times 10^{6} \text{ st. tk. bbl.}$$

DISCUSSION. Application of the material-balance equation in the form used here assumes: (1) pressure equilibrium within the reservoir at any time, (2) applicability of laboratory PVT data, and (3) reliable production data. There is little doubt that with proper care and procedures assumptions (2) and (3) can be well satisfied. The same is not true of assumption (1).

For undersaturated conditions, the magnitude of the pressure at any point in a pool is sensitive to the amount of oil production. Furthermore, variations in porosity, water saturation, and sand volume would cause appreciable pressure variations between wells producing at the same production rate. Normal development practices might conceivably cause a part of the field to be producing at a pressure slightly below the bubble point and the rest of the field at undersaturated conditions.

Also, large pressure gradients near the well bores are caused by production. This may mean that well pressures are below the bubble point. Thus the definition of reservoir conditions in an apparently undersaturated pool can be difficult. The sensitivity of pressure to fluid withdrawals makes the assumption of pressure equilibrium hard to satisfy.

Equation 1 defines the undersaturated conditions and shows that if no water production and influx are taking place, oil recovery is a direct function of pressure drop and effective compressibility. The com-

pressibility is given by Equation 2 and includes oil, interstitial water, and rock compressibilities. A drop in pressure within a reservoir rock results in an expansion of oil, interstitial water, and solid rock material and a reduction of rock pore volume. Importance of including the water and rock compressibilities can be readily shown and has been a practice in the past. If 8.00×10^{-6} (compressibility of oil) had been used in the solution instead of 13.75×10^{-6} then an answer of 32.8×10^{6} st.-tk. bbl. would have been obtained. This, and Equation 2, show the necessity of including results of interstitial water and rock expansion for undersaturated reservoir conditions.

A reliable figure of the initial oil in place for this reservoir was calculated to be 23.5×10^{6} st.-tk. bbl. This was obtained from material-balance calculations performed using pressure data below the bubble point and from volumetric calculations. Thus the value of 19.1×10^{6} bbl. computed in the problem is low by 19%.

Use of the material balance to determine initial oil in place from data obtained at undersaturated conditions is recommended only if a pool is initially highly undersaturated (say 2,000 psi. above bubble point), or has high permeability, and was completely developed over a short interval of time.

References

1. Craft, B. C., and Hawkins, M. F., "Applied Petroleum Reservoir Engineering," Prentice-Hall, Inc. (1959), pp. 132-138.

2. Pirson, S. J., "Oil Reservoir Engineering," McGraw-Hill Book Co., Inc., 2nd edition, (1958), p. 480.

Part 34

How to estimate oil in place

in a solution gas drive by material balance below bubble point

GIVEN: Pressure, production, and fluid-analysis data for Reservoir A as shown in Table 1.

Reservoir data were taken after a decline to the bubble-point pressure of 1,800 psia. There has been negligible water production. Reservoir temperature is 98° F.

FIND: Original oil in place in the reservoir using the material-balance equation and the data at times 1, 2, and 3 (Table 1).

METHOD OF SOLUTION:

The basic material-balance equation states that the cumulative fluid withdrawals from a reservoir to any time equal the change in volume of the fluids initially present plus the inflow of any fluids into the reservoir.

Solving this for the initial oil in place, N, the complete form applicable to all types of reservoirs is:

$$N = \frac{N_p B_o + N_p B_g (R_p - R_s) + W_p - W_e}{(B_o - B_{oi}) + (R_{si} - R_s) B_g + m B_{oi} [(B_g/B_{gi}) - 1]} \qquad (1)$$

Where:

Z, p_b, p_i, N_{pb}, p, N_p, R_p, W_p, B_o, R_s, p_a were defined with the data and

N = initial oil in place, st.-tk. bbl.

B_g = gas formation-volume factor, res. bbl./s.c.f.

W_e = cumulative water influx, bbl.

B_{oi} = oil formation-volume factor at initial reservoir conditions.

R_{si} = solution gas-oil ratio at initial reservoir conditions, s.c.f./st.-tk. bbl.

B_{gi} = gas formation-volume factor at initial reservoir conditions, res. bbl./s.c.f.

m = ratio of initial reservoir pore volume occupied by free gas to that occupied by oil.

i = subscript referring to initial reservoir conditions.

b = subscript referring to bubble-point reservoir conditions.

T_f = reservoir temperature in °R.

If there is no initial gas cap, the last term in the denominator is zero and may be dropped. Since there is uncertainty as to whether fluid influx into the reservoir exists, let it be assumed that the water influx is zero for the time being.

With these simplifications, the material balance for a closed reservoir, using the bubble point for initial conditions becomes:

$$N' = \frac{N_p [B_o + B_g (R_p - R_s)] + W_p}{(B_o - B_{ob}) + (R_{sb} - R_s) B_g}$$

= st.-tk. bbl. oil in place at bubble point reservoir conditions (2)

and

$$N = N' + N_{pb} \qquad (3)$$

To solve the problem given, substitute the applicable data for time "1" in the above equation and solve for N'. Similarly, solve for N' using the data for time 2, and then for time 3. If the data are reasonably accurate, and the reservoir is truly closed, the three values of N' should be in fairly close agreement.

Sample calculations of N' from data at time "1"

1. First compute B_g at time "1"

$$B_g = \frac{p_a}{p} \times \frac{T_f}{520} \times \frac{Z}{5.615}$$

$$B_g = \frac{14.7}{1,482} \times \frac{558}{520} \times \frac{0.625}{5.615}$$

$$= 0.00119$$

2. Substitute in the material balance. Because it is desired to have the answer in barrels, it will be necessary to express all volumes in barrels.

TABLE 1—PRESSURE, PRODUCTION, AND FLUID-ANALYSIS DATA FOR RESERVOIR "A"

(1) Time	(2) $\bar{p}$ Weighed avg. res. pres., psia.	(3) N_p Cum. oil prod. thous. st.-tk. bbl.	(4) R_p Cum. GOR s.c.f. per st.-tk. bbl.	(5) W_p Cum. water prod. bbl.	(6) B_o Oil res. vol. factor, bbl. res. oil/ bbl. st.-tk. oil	(7) R_s Gas in solution s.c.f. per st.-tk. bbl.	(8) Z Gas compressibility factor	(9) B_g Computed gas formation vol. factor, res. bbl./s.c.f.
0	$1,800 = p_b$	0	....	...	1.268	577	0.621	0.00097
1	1,482	2,223	634	0	1.233	491	0.625	0.00119
2	1,367	2,981	707	0	1.220	460	0.631	0.00130
3	1,053	5,787	1,034	0	1.186	375	0.656	0.00175

p_i = initial reservoir pressure = 2,500 psia.
N_{pb} = st.-tk. bbl. oil produced above bubble point = 440,000.
p_b = bubble-point pressure = 1,800 psia.
p_a = atmospheric pressure = 14.7 psia.

$$N' = \frac{2{,}223{,}000\,[1.233 + 0.00119\,(634 - 491)] + 0}{(1.233 - 1.268) + (577 - 491)\,0.00119}$$

N' = 46.3 million barrels, stock-tank oil in place at the bubble point.

SOLUTION: From data for times 1, 2, and 3, the stock-tank oil in place at the bubble point is computed as 46.3, 44.1, and 49.9 million barrels respectively. The average for N' is thus 46.8 × 10^6 bbl. and

$$N = 46{,}800{,}000 + 440{,}000$$
$$= 47{,}240{,}000 \text{ bbl.}$$

DISCUSSION: The material-balance equation as used assumes that the following conditions hold:[1,2]

1. Reservoir volume is constant. This assumption is justified if the reservoir pressure is below the bubble point since the expansibility of the rock and water is negligible compared to that of gas evolved from solution. However, above the bubble point the equation must be modified to take into account rock and connate-water compressibility or serious error may occur in the results.

2. Pressure is uniform throughout the reservoir at any time. This is necessary to apply average fluid properties. If gas is at different pressures in various portions of the reservoir, serious error can result.

3. Laboratory PVT data obtained from analysis of bottom-hole samples are applicable. Actually the method of running the analysis does not exactly simulate reservoir pressure and volume behavior. Errors introduced here are generally minor.

4. There is no geostatic compression. This condition is satisfied by all consolidated formations.

5. The reservoir is continuous and uniform and the fluid withdrawals are uniformly distributed throughout. Although few reservoirs are uniform, reasonable results are obtained using average conditions for a pool.

6. Production data are reliable. Usually reported oil production is satisfactory. But gas-production data may be in error. Particularly this may be true where high gas-oil ratios cause penalized oil allowables. Where gas is metered and sold the data are more reliable. But even in these cases some of the gas produced is vented, flared, or used on the lease. In addition, a large fraction of the solution gas is usually separated (flash-type separation) at some pressure and temperature other than standard conditions. Thus corrections for separator conditions are important in determining the cumulative free gas produced, $N_p\,(R_p - R_s)$, particularly in the early life of the reservoir when solution gas is a sizable fraction of the gas produced.

Water production data are usually not accurate either. But this error may be unimportant if the water produced is only a few per cent of the total production. However, in a new field, it is not always safe to disregard water production as is frequently done in supposedly volumetric reservoirs.

In Equation 3 N' is a constant. For a reservoir that is closed (no migration in or out) that satisfies the assumptions for use of the material balance equation and for which reliable data are available, the solution for N' using data for different times should agree within a few per cent and tend to be constant, as in this problem.

If there is fluid migration into the reservoir area, then the solutions for N' with time should give increasing values, none of which is the true figure for oil in place at the bubble point. This incoming fluid may be water from an adjoining aquifer, gas from an adjoining gas cap, or even oil from an unknown undeveloped area.

In most cases it is advisable to check the value of N found by material balance. This may be done by the pore-volume method.

In low-permeability reservoirs, it is usually difficult to determine a representative weighted average pressure for it is possible to have substantial pressure variations even in a closed reservoir. Another difficult case is a reservoir which is developed slowly such that the productive area is progressively larger during the critical first few years when drilling is performed and when the value of oil in place is most needed.

Once the ultimate productive area is determined, we must correct each previous pressure survey using an isobaric map of the entire reservoir to get volumetrically weighted average pressures for revision of previous estimates of original oil in place. Here again this is more important in the less-permeable reservoirs.

References

1. Pirson, S. J., "Oil Reservoir Engineering": McGraw-Hill Book Co., second edition, 1958, p. 477.
2. Muskat, M., "Physical Principles of Oil Production": McGraw-Hill Book Co., first edition, 1949, pp. 378-381.
3. Guerrero, E. T., Part 33, The Oil and Gas Journal, Feb. 27, 1961, p. 104.

Part 35

How to estimate oil in place

by material balance for reservoir with initial gas cap

GIVEN: Pressure, production, and fluid data for a reservoir as shown in columns 1 through 6 of Table 1. Other data on this pool are as follows:

p_i = initial reservoir pressure = 2,920 psia.

N = initial oil in place, st.-tk. bbl. = 223×10^6 (from volumetric calculations).

V_g = original reservoir pore vol. occupied by gas = 46.4×10^6 bbl.

T_r = reservoir temperature, °F. = 211.

B_{oi} = initial oil formation vol. factor = 1.454.

W_e = cumulative water influx assumed negligible.

FIND: Original oil in place by material balance.

METHOD OF SOLUTION: This equation, representing all changes in reservoir fluid content will be used:

$$N = \frac{N_p\,[B_t + B_g\,(R_p - R_{si})] + W_p}{\{B_t - B_{oi} + M_i\,B_{oi}\,[(B_g/B_{gi}) - 1]\}} \qquad (1)$$

Where:

p_i, N, B_{oi} are defined above.

N_p = cum. oil production, st.-tk. bbl.

B_t = two-phase formation vol. factor, res. bbl. per st.-tk. bbl.

B_g = gas formation-vol. factor, res. bbl. per s.c.f.

R_p = cum. gas-oil ratio, s.c.f. per st.-tk. bbl.

R_{si} = initial solution gas-oil ratio, s.c.f. per st.-tk. bbl.

R_I = producing or instantaneous gas-oil ratio, s.c.f. per st.-tk. bbl.

W_p = cum. water production, bbl.

B_{oi} = initial oil formation - vol. factor, res. bbl. per st.-tk. bbl.

M_i = ratio of initial pore space occupied by free gas to pore space occupied by oil.

B_{gi} = initial gas formation - vol. factor, res. bbl. per s.c.f.

G_p = cum. gas production, s.c.f.

ΔN_p = oil produced in a pressure interval, st.-tk. bbl.

ΔW_p = water produced in a pressure interval, bbl.

f_w = water cut, fraction of total liquid production.

SOLUTION: Columns 7-11 of Table 1 show the solution of the cumulative gas-oil ratio, R_p, or:

$$R_p = \frac{G_p}{N_p} = \frac{\Sigma\,\Delta N_p\,R_{I(av)}}{N_p}$$

$$= \frac{\sum_{i=1}^{i=j} (\Delta N_p)_i\,[(R_{I(n)} + R_{I(n-1)})/2]_i}{N_p} \qquad (2)$$

Thus for a pressure of 2,300 psia.:

$$R_p = \frac{\frac{770 + 1{,}150}{2}(4.1) + \frac{1{,}150 + 1{,}885}{2}(4.2) + \frac{1{,}885 + 2{,}670}{2}(4.4)}{12.7}$$

$$= [(960)\,(4.1) + (1{,}518)\,(4.2) + (2{,}278)\,(4.4)] \div 12.7 = 1{,}601$$

Cumulative gas production has been found from oil production and average gas-oil ratios. This can also be obtained by direct measurement of separator and stock-tank gas.

Columns 12-15 show the solution for cumulative water production, W_p, based on average water cut, f_w, values:

$$W_p = \Sigma\,\Delta W_p$$

$$= \sum_{i=1}^{i=n} \left[\frac{f_{wav} \times \Delta N_p}{1 - f_{wav}}\right]_i \qquad (3)$$

for a pressure of 2,300 psia.:

(Turn to Page 103.)

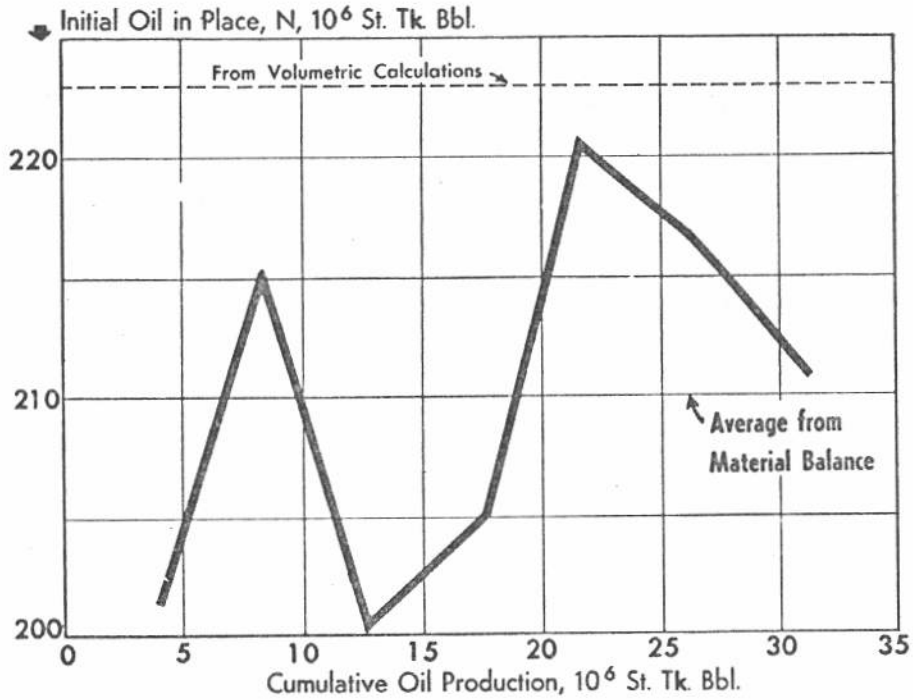

OIL-IN-PLACE VALUES found by material balance show some variation at different periods in the productive life of the reservoir. Fig. 1.

Table 1—Basic Data and Solution of Material-Balance Equation for Initial Oil in Place

(1) Pressure, p, psia.	(2) Producing gas-oil ratio, s.c.f. per st.-tk. bbl.	(3) Cum. oil prod., N_p M.M. st.-tk. bbl.	(4) Two-phase FVF, B_t	(5) Water cut, per cent f_w	(6) Gas FVF, $B_g \times 10^3$ reservoir bbl. per s.c.f.	(7) Oil produced in pres. interval, $\Delta N_p = (3)_n - (3)_{n-1}$ M.M. st.-tk. bbl.
2,920	780	0	1.454	0	0.954	...
2,740	1,150	4.1	1.477	0.6	1.004	4.1
2,560	1,885	8.3	1.506	4.7	1.072	4.2
2,300	2,670	12.7	1.565	7.3	1.194	4.4
2,050	3,713	17.1	1.648	8.0	1.347	4.4
1,800	4,480	21.7	1.757	6.7	1.550	4.6
1,500	4,320	26.3	1.956	7.2	1.905	4.6
1,220	4,020	31.2	2.276	11.0	2.390	4.9

(8) Avg. prod. gas-oil ratio, s.c.f. per st.-tk. bbl. $\frac{(2)_n + (2)_{n-1}}{2}$	(9) Gas prod. in pres. interval, M.M.s.c.f. (7) × (8)	(10) Cum. gas prod., M.M.s.c.f. Σ (9)	(11) Cum. gas-oil ratio, R_p s.c.f./st.-tk. bbl. (10)/(3)	(12) Average water cut fraction, f_{wav}	(13) (7) × (12) 10^6 bbl.	(14) Water prod. in pres. interval, 10^6 bbl. $\frac{(13)}{1 - (12)}$
....	.....	.....	....	.....	....	....
960	3,936	3,936	960	0.0030	0.0123	0.0123
1,518	6,376	10,312	1,242	0.0265	0.1113	0.1143
2,278	10,023	20,335	1,601	0.0600	0.2640	0.2809
3,192	14,045	34,380	2,011	0.0765	0.3366	0.3645
4,097	18,846	53,226	2,453	0.0735	0.3381	0.3649
4,400	20,240	73,466	2,793	0.0695	0.3197	0.3436
4,170	20,433	93,899	3,010	0.0910	0.4459	0.4905

(15) Cum. water prod., 10^6 bbl.	(16) $R_p - R_{si}$ (11) − 780 s.c.f./st.-tk. bbl.	(17) $B_g \times$ (16), res. bbl. per st.-tk. bbl.	(18) $B_t +$ (17), res. bbl. per st.-tk. bbl.	(19) $N_p \times$ (18), 10^6 res. bbl.	(20) (19) + W_p, (19) + (15), 10^6 res. bbl.	(21) $B_t - B_{oi}$ (14) − 1.454
....	....	....	....	.....	.....	....
0.0123	180	0.181	1.658	6.798	6.810	0.023
0.1266	462	0.495	2.001	16.608	16.735	0.052
0.4075	821	0.980	2.545	32.322	32.730	0.111
0.7720	1,231	1.658	3.306	56.533	57.305	0.194
1.1369	1,673	2.593	4.350	94.395	95.532	0.303
1.4805	2,013	3.835	5.791	152.303	153.784	0.502
1.9710	2,230	5.330	7.606	237.307	239.278	0.822

(22) $B_g \div B_{gi}$ (6) ÷ 0.954	(23) $\frac{B_g}{B_{gi}} - 1$	(24) (23) $B_{oi} M_i$ (23) (0.208)	(25) (21) + (24)	(26) Initial oil in place, N, 10^6 st.-tk. bbl. (20) ÷ (25)
1.000	....	.....	.....	....
1.052	0.052	0.01082	0.03382	201.4
1.124	0.124	0.02579	0.07779	215.1
1.252	0.252	0.05242	0.16342	200.3
1.412	0.412	0.08570	0.27970	204.9
1.625	0.625	0.13000	0.43300	220.6
1.997	0.997	0.20738	0.70938	216.8
2.505	1.505	0.31304	1.13504	210.8
			Average	210.0

$$W_p = \left[\frac{\frac{0 + 0.006}{2}\ (4.1)}{1.0 - (0 + 0.006)/2} + \frac{\frac{0.006 + 0.047}{2}\ (4.2)}{1.0 - (0.006 + 0.047)/2} + \frac{\frac{0.047 + 0.073}{2}\ (4.4)}{1.0 - (0.047 + 0.073)/2} \right] 10^6 = 407{,}500 \text{ bbl.}$$

Columns 16-26 represent solutions of Equation 1. For a pressure of 2,300 psia.

$$N = \frac{(12.7)\ (10^6)\ [1.565 + 0.001194\ (1{,}601 - 780)] + 407{,}500}{\{(1.565 - 1.454) + (0.143)\ (1.454)\ [(0.001194/0.000954) - 1]\}}$$

$$= 200.3 \times 10^6 \text{ st.-tk. bbl.}$$

$$\text{Where } M_i = \frac{V_g}{NB_{oi}} = \frac{46.4 \times 10^6}{(223 \times 10^6)\ (1.454)} = 0.143$$

DISCUSSION: This problem shows how material-balance calculations are used to find initial oil in place for a reservoir with an initial gas cap. Since a volumetric estimate of the initial oil in place is known, the results serve as a check.

A question arises as to which estimate is more reliable, the volumetric (pore volume) estimate or that found by material balance. The former is better known and is more widely used. But the latter is now accepted and often used when needed data are available.

The assumptions involved in each method have been mentioned before.[1,2] For depletion-type reservoirs, it is felt that both methods can give reliable results. The accuracy of the answers obtained will, of course, depend on the reliability and sufficiency of the data. A careful review of the assumptions involved shows that even under favorable conditions, errors of 15 to 20% in the final results are possible by either method.

For a reservoir initially containing a gas cap the volumetric estimate of original oil in place is usually more reliable than that obtained by material balance. To apply the latter approach the size of the gas cap must be known.[3] It is normally obtained by the volumetric method. Such a reservoir will produce under a combined drive of solution gas and gas-cap expansion assuming gravity effects and water influx are negligible as in the case used for this problem. Where the amount of pore volume occupied initially by gas is about one-half of more of that occupied by oil (M_i), the energy contribution by the gas cap becomes significant compared to that of the solution gas (Columns 21 and 24 of Table 1). This statement does not hold true in this problem because $M_i = 0.143$. However, when M_i is about 0.5 or greater, errors in average reservoir pressure of 25 to 50 psi. (which are quite possible) can cause appreciable error in N due to over or underexpansion of the gas cap. This expansion is directly proportional to pressure and thus largely affected by error in this factor.

Note that in the solution of the problem, water production is included but water influx neglected. The latter was assumed negligible. If this assumption is wrong, then the computed values for initial oil in place are high. Fig. 1 shows the variation of computed initial oil in place values with cumulative oil production. The values vary between 200 and 220 million with the average being 210 million. This compares fairly well with the known volumetric estimate of 223 million stock-tank barrels.

References

1. Guerrero, E. T., and Stewart, F. M.: Problem 32, The Oil and Gas Journal, Feb. 13, 1961, p. 89.

2. Guerrero, E. T., Problem 34, The Oil and Gas Journal, Mar. 27, 1961, p. 92.

3. Muskat, M.: "Physical Principles of Oil Production": McGraw-Hill Publishing Co., first edition (1949), p. 385.

Part 36

How to find original oil in place

by material balance for reservoir with partial water drive

GIVEN: Production, rock, and fluid data for an initially undersaturated Wilcox reservoir as shown below and in Columns 1 through 10 of Table 1. The extent of the aquifer surrounding the pool is considered infinite.

ϕ = porosity, fraction = 0.209.

B_{ob} = oil-formation volume factor at bubble-point conditions = 1.53846.

k_w = permeability, md. = 275.

μ_w = viscosity of water at bubble-point conditions, cp = 0.25.

c_w = compressibility of water at bubble-point conditions, vol./vol./psi. = 6.8×10^{-6}.

r_w = radius of oil-bearing portion of reservoir, ft. = 7,100.

N = initial oil in place from volumetric estimate, st.-tk. bbl. = 24×10^6.

N_{pb} = cumulative oil recovery to bubble-point pressure, stk.-tk. bbl. = 171,884 (see Fig. 1).

W_{pb} = cumulative water recovery to bubble-point pressure, bbl. = 1,750.

p_b = bubble-point pressure, psia. = 3,699.

R_{si} = initial solution gas-oil ratio, std. cu. ft. per st.-tk. bbl. = 900.

Δt = time increment, days = $91.25 \approx 91$.

FIND: Original oil in place.

METHOD OF SOLUTION: These equations will be used in solving this problem.

$$T = 6.33 \times 10^{-3} \times \frac{n k_w \Delta t}{\phi \mu_w c_w r_w^2} \quad (1)$$

$$N' = Y - BX \quad (2)$$

Where:

$$Y = \frac{N_p'[B_t + B_g(R_p - R_{si})] + W_p'}{B_t - B_{ob}}$$

$$X = \frac{\sum_{i=1}^{i=a} \Delta p_i Q_{T(n+1-i)} - \sum_{i=1}^{i=b} \Delta p_i Q_{T(n+1-i)}}{B_t - B_{ob}}$$

$$Y = N' + BX \quad (2a)$$

$$N_p' = N_p - N_{pb} \quad (3)$$

$$W_p' = W_p - W_{pb} \quad (4)$$

$$N' = N - N_{pb} \quad (5)$$

$$N' = \frac{\Sigma X^2 \Sigma Y - \Sigma X \Sigma XY}{n \Sigma X^2 - (\Sigma X)^2} \quad (6)$$

$$B = \frac{\Sigma Y - nN'}{\Sigma X} \quad (7)$$

Where:

Δt, R_{si}, k_w, ϕ, μ_w, c_w, r_w, B_{ob}, N, N_{pb}, W_{pb}, and p_b have been defined with the data.

T = dimensionless time.

ΔT = change in dimensionless time.

n = number of time increments.

N′ = oil in place at bubble point conditions, st.-tk. bbl.

N_p' = cumulative oil production, from bubble point, st.-tk. bbl.

B_t = two-phase formation-volume factor, res. bbl. per stk.-tk. bbl.

B_g = gas-formation volume factor, res. bbl. per std. cu. ft.

R_p = cumulative gas-oil ratio, s.c.f. per st.-tk. bbl.

W_p' = cumulative water production from bubble point, bbl.

B = proportionality factor to convert reduced units into bbl.[1 2]

Δp_i = pressure drops occurring

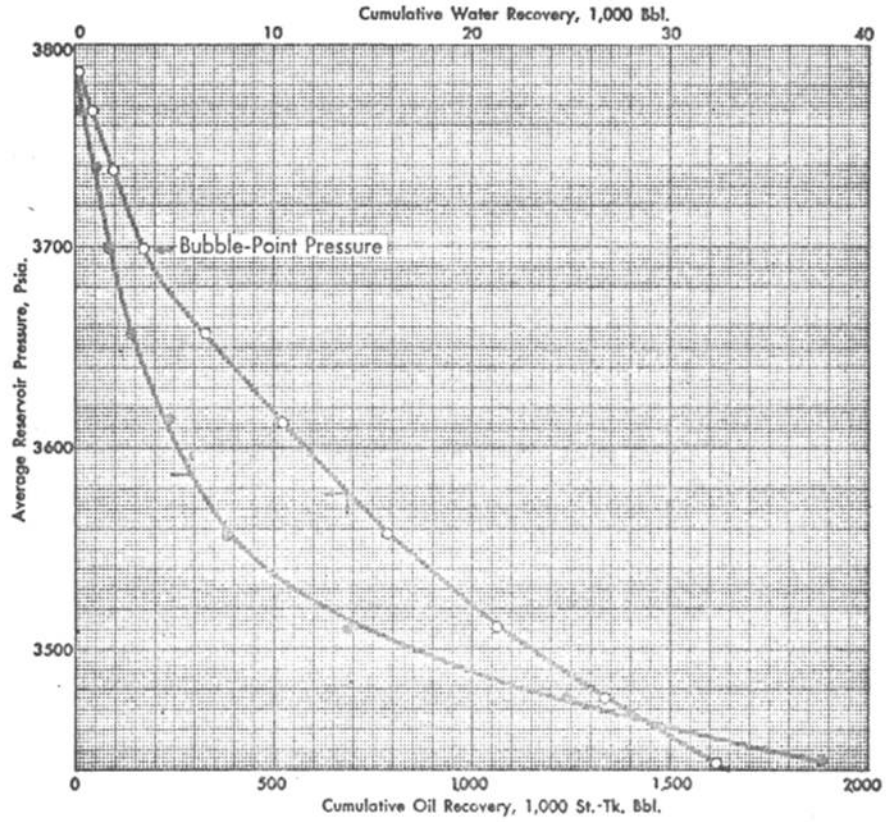

OIL AND WATER PRODUCTION HISTORY for an initially undersaturated Wilcox reservoir, Fig. 1.

TABLE 1—BASIC DATA AND MATERIAL-BALANCE CALCULATIONS FOR INITIAL OIL IN PLACE — INFINITE AQUIFER AND ASSUMING $\Delta T = 15$

(1) Time, days, t	(2) Avg. reservoir pressure at datum, p, psia.	(3) Cum. oil prod., st.-tk. bbl. Total, N_p	(4) From bubble pt., N_p'	(5) Two-phase FVF, B_t	(6) Cum. gas-oil ratio, R_p, cu. ft./bbl.	(7) Gas FVF $\times 10^3$, B_g, res. bbl. per std. cu. ft.	(8) Cum. water prod., bbl. Total, W_p	(9) From bubble pt., W_p'	(10) Pres. at oil-water contact, psia.
0	3,793	.....	.....	.....	900	.....	0	.....	3,793
91	3,786	13,549	.....	1.5357862	900	0.8366066	0	.....	3,788
182	3,768	49,005	.....	1.5362877	900	0.8404456	370	.....	3,774
273	3,739	99,774	.....	1.5370954	900	0.8456424	1,030	.....	3,748
365	3,699	171,884	0	1.5384600	900	0.8532299	1,750	0	3,709
456	3,657	324,843	152,959	1.5426846	900	0.8614110	2,834	1,084	3,680
547	3,613	528,068	356,184	1.5484923	919	0.8702281	4,840	3,090	3,643
638	3,558	788,009	616,125	1.5560508	914	0.8816134	7,749	5,999	3,595
730	3,511	1,066,911	895,027	1.5627831	910	0.8916796	13,895	12,145	3,547
821	3,476	1,339,902	1,168,018	1.5679692	911	0.8993873	24,808	23,058	3,518
912	3,444	1,615,461	1,443,577	1.5728430	917	0.9065961	37,653	35,903	3,485
1,003	3,408	1,890,560	1,718,676	1.5784815	937	0.9149005	58,449	56,699	3,437
1,095	3,375	2,171,963	2,000,079	1.5838030	952	0.9226956	111,863	110,113	3,416
1,186	3,333	2,441,226	2,269,342	1.5907907	970	0.9328846	163,250	161,500	3,379
1,277	3,309	2,713,986	2,542,102	1.5948969	987	0.9388428	219,848	218,098	3,358
1,368	3,293	2,970,088	2,798,204	1.5976815	1,006	0.9428714	301,256	299,506	3,338
1,460	3,277	3,175,948	3,004,064	1.6005046	1,016	0.9469482	381,548	379,798	3,329

(11) (R_p-R_{si}), (6)−900	(12) $B_g(R_p-R_{si})$, (7)×(11)	(13) $B_t+B_g(R_p-R_{si})$ (5)+(12)	(14) $N_p'\times(13)$ (4)×(13) (millions)	(15) (14) + (9) (millions)	(16) Δp_i psi.	(17) Avg. Δp for Q_T, psi.	(18) Dimensionless time, T	(19) Q_T, from Ref. 4 for infinite case	(20) $\sum_{i=n}^{i=n} \Delta p_i Q_{T(n+1-i)}$	(21) (20)−947.4315
0	0	.....	.....	.....	..	....	0	.....	.....	.....
0	0	1.5357862	.....	.....	5	2.5	15	9.949	24.8725	.....
0	0	1.5362877	.....	.....	14	9.5	30	16.742	136.3705	.....
0	0	1.5370954	.....	.....	26	20.0	45	22.897	415.2715	.....
0	0	1.5384600	0	0	39	32.5	60	28.691	947.4315	0
0	0	1.5426846	0.235967	0.237051	29	34.0	75	34.247	1,698.5030	751.0715
19	0.0165343	1.5650266	0.557437	0.560527	37	33.0	90	39.626	2,639.9290	1,692.4975
14	0.0123426	1.5683934	0.966326	0.972325	48	42.5	105	44.858	3,859.8060	2,912.3745
10	0.0089168	1.5716999	1.406714	1.418859	48	48.0	120	49.968	5,376.8005	4,429.3690
11	0.0098933	1.5778625	1.842972	1.866030	29	38.5	135	54.976	7,068.1170	6,120.6855
17	0.0154121	1.5882551	2.292769	2.328672	33	31.0	150	59.895	8,878.0990	7,930.6675
37	0.0338513	1.6123328	2.771078	2.827777	48	40.5	165	64.737	10,923.2915	9,975.8600
52	0.0479802	1.6317832	3.263695	3.373808	21	34.5	180	69.512	13,116.2905	12,168.8590
70	0.0653019	1.6560926	3.758240	3.919740	37	29.0	195	74.226	15,415.2765	14,467.8450
87	0.0816793	1.6765762	4.262028	4.480126	21	29.0	210	78.886	17,837.2455	16,889.8140
106	0.0999444	1.6976259	4.750304	5.049810	20	20.5	225	83.497	20,300.1240	19,352.6925
116	0.1098460	1.7103506	5.138003	5.517801	9	14.5	240	88.062	22,771.8200	21,824.3885

(22) B_T-B_{ob}	(23) Y = (15) ÷ (22) (millions)	(24) ΣY Σ (23)	(25) X = (21) ÷ (22) (millions)	(26) ΣX = Σ (25)	(27) XY (millions)	(28) ΣXY (millions)	(29) X^2 (millions)	(30) ΣX^2 (millions)	(31) $(\Sigma X)^2$ (millions)
0	0	0	0	0	0	0	0	0	0
0.0042246	56.112058	56.112058	0.177785	0.177785	9.975882	9.975882	0.031608	0.031608	0.031608
0.0100323	55.872233	111.984291	0.168705	0.346490	9.425925	19.401807	0.028461	0.060069	0.120055
0.0175908	55.274632	167.258923	0.165562	0.512052	9.151379	28.553186	0.027411	0.087480	0.262197
0.0243231	58.333806	225.592729	0.182105	0.694157	10.622878	39.176064	0.033162	0.120642	0.481854
0.0295092	63.235533	288.828262	0.207416	0.901573	13.116061	52.292125	0.043021	0.163663	0.812834
0.0343830	67.727423	356.555685	0.230657	1.132230	15.621804	67.913929	0.053203	0.216866	1.281945
0.0400215	70.656447	427.212132	0.249263	1.381493	17.612038	85.525967	0.062132	0.278998	1.908523
0.0453430	74.406369	501.618501	0.268373	1.649866	19.968660	105.494627	0.072024	0.351022	2.722058
0.0523307	74.903259	576.521760	0.276470	1.926336	20.708504	126.203131	0.076436	0.427458	3.710770
0.0564369	79.382921	655.904681	0.299269	2.225605	23.756847	149.959978	0.089562	0.517020	4.953318
0.0592215	85.269877	741.174558	0.326785	2.552390	27.864917	177.824895	0.106788	0.623808	6.514695
0.0620446	88.932816	830.107374	0.351753	2.904143	31.282385	209.107280	0.123730	0.747538	8.434047

(32) $\Sigma X^2 \Sigma Y$ (millions)	(33) $\Sigma X \Sigma XY$ (millions)	(34) (32)−(33) (millions)	(35) n	(36) $n\Sigma X^2$ (millions) (35)×(30)	(37) $n\Sigma X^2-(\Sigma X)^2$ (millions) (36)−(31)	(38) N' = (34)÷(37) MM st.-tk. bbl.	(39) nN	(40) $\Sigma Y - nN$ (24)−(39)	(41) B = (40)÷(26)
0	0	0	0	0	0	.....	.....	.....	....
1.773590	1.773562	0.000028	1	0.031608	0	.....	.....	.....	....
6.726784	6.722532	0.004252	2	0.120138	0.000083	51.228916	102.457832	9.526459	27.5
14.631811	14.620716	0.011095	3	0.262440	0.000243	45.658436	136.975308	30.283615	59.1
27.215958	27.194339	0.021619	4	0.482568	0.000714	30.278711	121.114844	104.477885	150.5
47.270500	47.145168	0.125332	5	0.818315	0.005481	22.866630	114.333150	174.495112	193.5
77.324805	76.894188	0.430617	6	1.301196	0.019251	22.368552	134.211312	222.344373	196.4
119.191330	118.153525	1.037805	7	1.952986	0.044463	23.340868	163.386076	263.826056	191.0
176.079129	174.051998	2.027131	8	2.808176	0.086118	23.538993	188.311944	313.306557	189.9
246.438838	243.109635	3.329203	9	3.847122	0.136352	24.416239	219.746151	356.775609	185.2
339.115838	333.751677	5.364161	10	5.170200	0.216882	24.733085	247.330850	408.573831	183.6
462.350619	453.878484	8.472135	11	6.861888	0.347193	24.401802	268.419822	472.754736	185.2
620.536806	607.277443	13.259363	12	8.970456	0.536409	24.718756	296.625072	533.482302	183.7

NOTE: Columns 1-10 are basic data. Remaining columns are solution to the problem.

during successive time intervals of equal duration, psi.

Q_{Ti} = dimensionless function obtained from solution of diffusivity equation for desired boundary conditions and production time in reduced units, T. Values of this function for an infinite aquifer are given by Van Everdingen and Hurst[2] as a function of T.

b = bubble point.

N_p = total cumulative oil production, st.-tk. bbl.

W_p = total cumulative water production, bbl.

SOLUTION: Equation 2 gives the oil in place at the bubble-point pressure. Knowing this, Equation 5 can be solved for initial oil in place. Note that there are three unknowns in Equation 2: N′, B, and Q_{Ti}. Also this relationship can be reduced to Equation 2a which is the equation for a straight line with N′ the ordinate intercept and B equal to the slope. Thus if Q_{Ti} can be found by some independent means, Equation 2 can be used to get N′ and B. Q_{Ti} is a function of dimensionless time, T_i, defined by Equation 1. If k_w, ϕ, μ_w, c_w and A were accurately known for the aquifer, Equation 1 could readily be solved for T since n and Δt are known. Usually little is known about the aquifer extent, rock and fluid properties and this is not possible. Consequently, a trial-and-error procedure must be used.

If equal time increments are used to define the history then

$$T = n\,\Delta T$$

with ΔT a constant and n an integer variable. The first estimate for ΔT can be obtained from Equation 1 using the best values obtainable and n = 1.0. Thus

$$\Delta T = \frac{(6.33 \times 10^{-3})\,(275)\,(91)}{(0.209)\,(0.25)\,(6.8 \times 10^{-6})\,(7{,}100)^2} = 8.8 \approx 9.0$$

Equation 2 should now be solved for values of ΔT = 5, 10, 15, and 20. Since N′ and B are constants, the correct value of ΔT will give fairly constant values of these factors. If more than one of the estimates results in nearly constant values for N′ and B then the standard deviation can be found to get the best selection of ΔT:

$$\text{Standard deviation} = \left(\sum_{i=1}^{i=n} \frac{(\text{Y observed} - \text{Y computed})_i^2}{n} \right)^{1/2} \quad (8)$$

Y observed is given by Column 23 in Table 1 and Y computed is obtained with Equation 2a using the best values for N′ and B and the X values of Column 25. The ΔT that results in the lowest value for the standard deviation is considered representative. Since the estimated ΔT's may not yield a minimum value, a plot of standard deviation versus ΔT for a late history point (say t = 1,460 days in this problem) can be used to interpolate for the best value.[1]

If all the computations involved in this problem were shown, they would include four tables similar to Table 1 and standard deviations computed for each ΔT. Space does not permit the presentation of all the computations. The best ΔT was found to be 15 and Table 1 shows the computations for this value. Columns 1 through 10 show basic data while Columns 11 through 23 and Column 25 solve major portions of Equation 2. Columns 24 and 26 through 41 show the solution of Equations 6 and 7 for N′ and B. The Q_T values shown in Column 19 were obtained from Table 2 of Reference 3 for the respective T values. Similar but slightly different values can be obtained from Table 1 of Reference 2. The former represent slightly more accurate solutions of the unsteady-state equation involved and were used in this problem.

Column 20 of Table 1 involves the use of the superposition theorem.[4] In the summation for any particular time the various average Δp's are multiplied by Q_T's obtained for the time, T, that each respective average Δp has been in effect. Thus the value of Q_T associated with an average Δp, changes for each time step and increases as time increases.

As an illustration, the computation of values in Column 20 for times of 365 days (T = 60) and 456 days (T = 75) will be shown.

When T = 60, n = 4

$$\sum_{i=1}^{i=4} \Delta p_i\, Q_{5-i} = (2.5)\,(28.691) + (9.5)\,(22.897) + (20.0)\,(16.742) + (32.5)\,(9.949) = 947.4315$$

When T = 75, n = 5

$$\sum_{i=1}^{i=5} \Delta p_i\, Q_{T\,6-i} = (2.5)\,(34.247) + (9.5)\,(28.691) + (20.0)\,(22.897) + (32.5)\,(16.742) + (34.0)\,(9.949) = 1{,}698.5030$$

The first average Δp value is always associated with the largest Q_T term and the last average Δp is associated with the smallest Q_T at each history point. Note in Columns 38 and 41 that the last four values for N′ and B remain fairly constant. Although all values after the first three seem good, the last four were chosen to obtain the best values of

$$N' = 24{,}567{,}500 \text{ and}$$

$$B = 184$$

since the data are generally better later in the pressure history.

The original oil in place is found by Equation 5

$$N = 24{,}567{,}500 + 171{,}884$$

$$= 24{,}739{,}384$$

or 24,700,000 st.-tk. bbl.

Instead of using Equations 6 and 7, N′ and B could have been found graphically. Fig. 2 shows a plot of the Y and X values of Columns 23 and 25, Table 1. In this case the values give a good correlation and it is easy to draw a straight line through the data and obtain N′ = 25,300,000 st.-tk. bbl. (ordinate in-

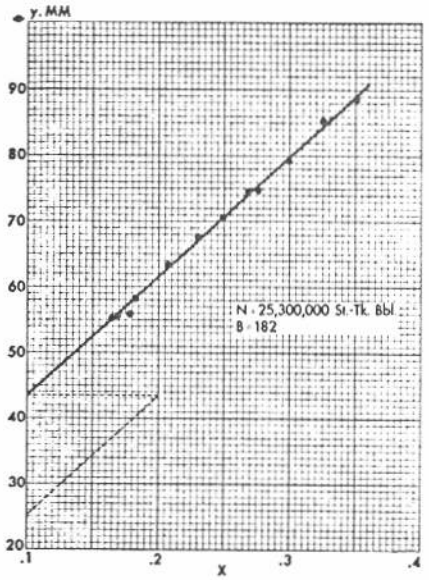

GRAPHICAL SOLUTION of material-balance equation for original oil in place, Fig. 2.

tercept) and B = 182 (slope). These results are comparable to those obtained by the more accurate least squares procedure. Such is not normally the case as material-balance data do not often correlate as well as they did in Fig. 2.

DISCUSSION: This problem illustrates the solution of the material-balance equation with two unknowns—original oil in place and cumulative water influx. Equation 2 is the general material-balance equation for a reservoir without an original gas cap and with the cumulative water influx term replaced by the Hurst-Van Everdingen "Unsteady-State Terms" for the same.[2] These authors solved the diffusivity equation for various boundary conditions and combined the results with Darcy's law to develop an analytical unsteady-state expression for cumulative water influx. In their developments they assumed (1) a homogeneous formation, (2) the initial datum pressure at all points in the reservoir was the same, (3) effects of gravity on flow were negligible, (4) all flow in reservoir systems is macroscopically laminar, (5) radial symmetry, and (6) only one slightly compressible fluid flowing. In spite of the restrictions imposed by these assumptions, their equations have been found useful in determining the cumulative water influx.

The data for this problem are from a Wilcox reservoir which was initially undersaturated.[1] Bubble-point pressure was estimated as 3,699 psia. In order to verify the validity of this value, cumulative oil recovery and cumulative water recovery were plotted versus average reservoir pressure, Fig. 1. Recovery normally varies linearly with pressure above the bubble point. Fig. 1 verifies that 3,699 psia. is the bubble-point pressure.

Note in Table 1 that material-balance calculations were made for pressures below the bubble point only. Actually it is possible to start these calculations at pressures above the bubble point. However, considerable care must be taken in using such a procedure because equivalent values of the oil-formation volume factor are obtained for pressures slightly above and below the bubble point. Furthermore, for pressures above and slightly below the bubble point the material-balance equation is very sensitive to errors in pressure and fluid properties and good results are hard to get.

Thus in this case the material-balance equation was used to compute oil in place at the bubble-point pressure. For such an application, production of oil, gas, and water are measured from the bubble point. Consequently fluids produced up to the bubble point must be subtracted from the cumulative figures, Column 4, Table 1.

Since the bubble-point pressure is taken as the beginning point, the cumulative water influx must be zero at this point also, Column 21, Table 1. (The small amount of water produced above the bubble point, 1,750 bbl., may represent water influx also but was neglected in this application.) Thus Equation 2 is a slightly modified form of the generalized material-balance equation to make it applicable for pressures at and below the bubble point of an originally undersaturated reservoir.

The data and computations of Table 1 show six and seven-decimal accuracy. The use of such accuracy may be questionable, but was felt justified due to the sensitivity of the formation-volume factors,[1] and the fact that Columns 23 and 25 involve the difference in two formation-volume factors as the divisor.

Of course the accuracy shown in the formation-volume factors of Column 5 is not obtained in laboratory measurements. The relationship between formation-volume factor and pressure is expressed with an equation which in turn is solved to obtain the assumed accuracy desired for the computations. It is not intended to imply that the measured data warrant such accuracy. The assumption is made that measured values can be expressed to the accuracy shown in Column 5. The same arguments apply to gas formation-volume factors in Column 7.

Column 38 shows oil in place at the bubble-point pressure for each time point below the bubble point. Note that the first three values seem to be high and then become fairly constant. Since the oil in place at the bubble point is a constant value, all of the computed results should be equivalent. However, as was mentioned above, the material-balance equation is sensitive to small errors for pressures near the bubble point. As the reservoir pressure falls below the bubble point, the accuracy of the initial oil in place by the material-balance method improves. The last four entries were averaged to give the oil in place at the bubble point. To this was added 171,884 bbl. of oil produced above the bubble point to give initial oil in place of 24,700,000 st.-tk. bbl.

This value agrees very well with that obtained by the volumetric method of 24,000,000 st.-tk. bbl. In view of the many assumptions and limitations involved in the two methods, it cannot be expected that such an excellent agreement would be obtained too often.

The success that can be expected from the material-balance equation depends principally on two things: (1) reliable fluid, rock, and production data, and (2) satisfaction of the assumptions involved in the material-balance equation and unsteady-state water-influx terms.

References

1. A. F. Van Everdingen, E. H. Timmerman, and J. J. McMahon, "Application of the Material Balance Equation to a Partial Water Drive Reservoir": Trans. AIME (1953), 198, 51.

2. A. F. Van Everdingen and W. Hurst, "The Application of the Laplace Transformation to Flow Problems in Reservoirs": Trans. AIME (1949), 186, 305.

3. A. T. Chatas, "A Practical Treatment of Nonsteady-State Problems in Reservoir Systems": Part 3, Petroleum Engineer (Aug. 1953), B-44.

4. I. S. Sokolnikoff and R. M. Redheffer "Mathematics of Physics and Modern Engineering": McGraw-Hill Book Co., Inc., (1958), p. 51

Part 37

How to determine performance and ultimate recovery by exponential decline-curve analysis

GIVEN: The production data shown in columns 1, 2, and 3 of Table 1 through 1953 are for a Kansas sandstone pool. It is estimated that the economic limit for this pool will be 25 bbl. per day.
FIND: Using analytical and graphical approaches, determine reserves and performance of this pool.
METHOD OF SOLUTION: These equations involving production rate and decline rate will be used in the solution of this problem:

$$D = -\frac{dq_o/dt}{q_o} = -\frac{2.3\log(q_{oi}/q_o)}{t} \approx \frac{-\Delta q_o/\Delta t}{q_{o\,av.}} \qquad (1)$$

$$q_o = q_{oi}\,e^{-Dt} \qquad (2)$$

$$\text{Reserves} = \frac{q_o - q_{oi}}{D} \qquad (3)$$

SOLUTION: Using the data for 1948:

$$D = \frac{99{,}200 - 88{,}210}{(1-0)(99{,}200+88{,}210)/2}$$

$$= 0.117\ \text{yr.}^{-1}$$

Equation 2 can be used to compute the remaining life to abandonment.

q_{oi} = 38,770 bbl./yr. (rate at beginning of eighth year).

$q_{o\,(abnd)}$ = 25 × 365 = 9,125 bbl./yr.

Thus $9{,}125 = 38{,}770\ e^{-.145\,t}$

$$0.145\,t = \ln(38{,}770/9{,}125) = \ln 4.25$$

$$t = 1.447/0.145 = 10.0\ \text{yrs.}$$

$$\text{Remaining Reserves} = \frac{38{,}770 - 9{,}125}{0.145} = \frac{29{,}645}{0.145}$$

= 204,448 st.-tk. bbl.

DISCUSSION: Decline-curve analysis is the most commonly used method of determining reservoir performance and reserves. Data needed to correlate production rate, time, and cumulative recovery are readily available and are generally accurately recorded.

But some assumptions must be made:

1. Reservoir is produced at capacity.

2. Future performance of a reservoir will be similar to its past performance.

Although the word reservoir has been used, the technique can be applied to a well or lease.

The first assumption implies that the method cannot be used where the rate of oil production is constant or nearly constant with time. This would be true under proration or where the reservoir had a large gas cap or an active water drive. A change in production rate with time is implied and the method should be used on depletion-type reservoirs producing at capacity. Under proration conditions the method will work as soon as the wells are not

TABLE 1—PRODUCTION DATA AND COMPUTATION OF YEARLY DECLINE FOR KANSAS SANDSTONE POOL

(1)	(2)	(3)	(4)	(5)	(6)	(7)	(8)	(9)
						$D = \frac{\Delta q_o/\Delta t}{q_{o\,av.}}$		$N_p - \frac{\Delta N_p}{2}$
	Time, years		q_o = Oil prod. rate,	Δq_o	$q_{o\,av.} = \frac{(4)_{n-1} + (4)_n}{2}$		N_p = Cum. oil recovery,	$(8) - \frac{(4)}{2}$
Year	Total	Avg.	bbl./yr.	$(4)_{n-1} - (4)_n$		(5) ÷ (6)	bbl.	
1947	1	0.5	99,200	.....	.....	....	99,200	49,600
1948	2	1.5	88,210	10,990	93,705	0.117	187,410	143,305
1949	3	2.5	73,240	14,970	80,725	0.185	260,650	224,030
1950	4	3.5	63,990	9,250	68,615	0.135	324,640	292,645
1951	5	4.5	54,910	9,080	59,450	0.153	379,550	352,095
1952	6	5.5	47,400	7,510	51,155	0.147	426,950	403,250
1953	7	6.5	41,580	5,820	44,490	0.131	468,530	447,740
						0.868		
Future Performance					$D_{av.} = 0.868 \div 6 = 0.145$			
1954	8	...	35,960	5,620	38,770	0.145	504,490	.....
1955	9	...	31,099	4,861	33,530	0.145	535,589	.....
1956	10	...	26,895	4,204	28,997	0.145	562,484	.....
1957	11	...	23,260	3,635	25,078	0.145	585,744	.....
1958	12	...	20,116	3,144	21,688	0.145	605,860	.....
1959	13	...	17,397	2,719	18,757	0.145	623,257	.....
1960	14	...	15,045	2,352	16,221	0.145	638,302	.....
1961	15	...	13,011	2,034	14,028	0.145	651,313	.....
1962	16	...	11,252	1,759	12,132	0.145	662,565	.....
1963	17	...	9,731	1,521	10,492	0.145	672,296	.....
1964	18	...	8,416	1,315	9,074	0.145	680,712	.....

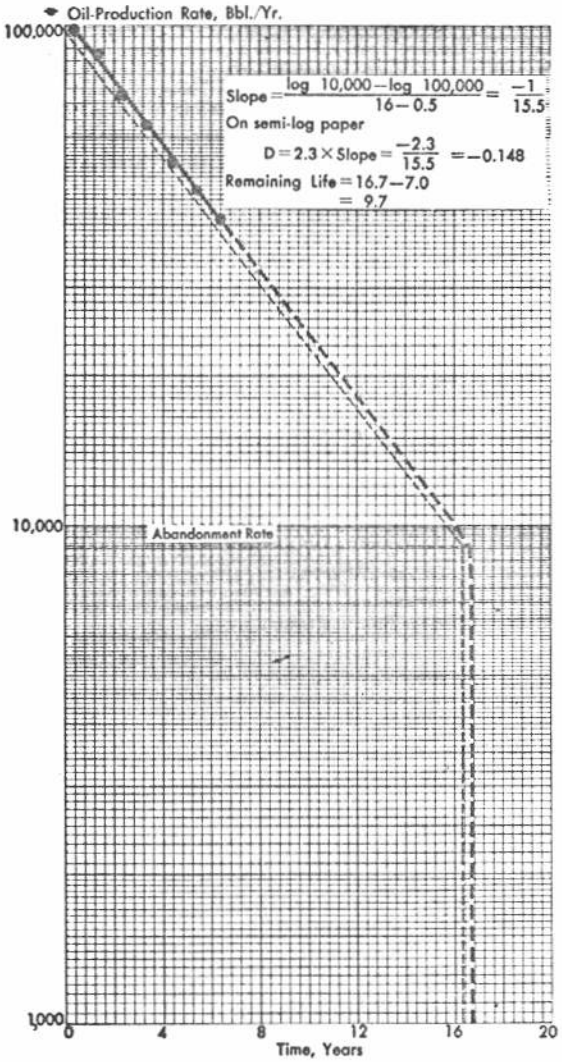

VARIATION of oil-production rate with time. Fig. 1.

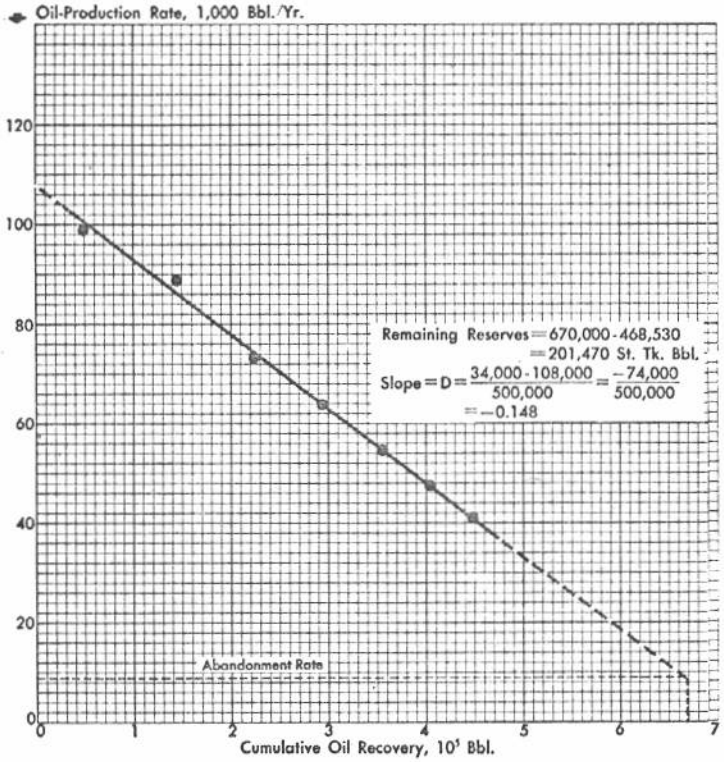

RELATION of oil-production rate and cumulative oil recovery. Fig. 2.

able to produce their allowable.

The second assumption implies that past performance is used to predict future performance. In other words, the production rate will decline in the future in a manner similar to that of the past. Any workover or cleanout operations may likely result in higher production rates than predicted by the analysis. Thus it must also be assumed that the conditions of the hole and sand face will remain unchanged.

The most commonly used types of decline are the constant-percentage or exponential decline and the hyperbolic decline.[1,2,3,4,5] This problem illustrates the exponential decline-curve analysis. Year-by-year performance has been computed analytically in Table 1 and is shown graphically in Figs. 1 and 2. Future performance computations of Table 1 are obtained using Equations 2 and 3. Use of these equations to determine remaining life and reserves is shown in the example calculations.

The same values can be obtained from Figs. 1 and 2. Note that the rate of decline from the graphs is slightly larger than that computed in Table 1. The graphical value is actually better since the rate of decline is an instantaneous value and thus theoretically can be applied to only a very short time interval. In Table 1 intervals of 1 year were used in its computation. Note that the computation of D from Equation 1 involves a slope at a certain rate q_o. However, in Table 1 it has been computed using an approximation of increments in rate and time and an average rate in the time increment.

In the graphs the rates were plotted at the mid-point of the time-cumulative recovery intervals. This provides a correction for the fact that the time interval used may be larger than permissible. This correction is an added precaution which in most practical cases is not necessary as the resulting error is small.

In this example the results obtained by the two methods are in satisfactory agreement. In practice the graphical approach is used most. The analytical method is useful in determining the type of decline. Note in column 7 of Table 1 that the rate of decline remains fairly constant at about 0.145. This indicates an exponential type of decline. If the rate decline in column 7 were increasing, a hyperbolic type of decline would have been indicated. Its recognition and analysis will be considered in the next problem.

NOMENCLATURE

q_o = oil-production rate.
q_{oi} = initial oil-production rate.
D = rate of decline (inverse of loss ratio).
t = time.

References

1. Arps, J. J., "Analysis of Decline Curves": Trans. AIME, (1945), 160, 228.
2. Arps, J. J., "Estimation of Primary Oil Reserves": Trans. AIME, (1956), 207, 182.
3. Pirson, S. J., "Mathematical Methods of Decline Curve Extrapolation and Reserve Calculation": Oil Weekly, Sept. 9, 1946, 45-59.
4. Menzie, D. E., "How to Select the Best Decline Curve": World Oil, Dec. 1953, 180-196.
5. Clark, R. W., "How to Estimate Crude Oil Reserves by Decline Trend Method": Petroleum Engineer, Sept. 1951, B 7-35.

Part 38

How to determine

Performance and ultimate recovery of a reservoir declining hyperbolically

GIVEN: Data shown in columns 1, 2, and 3 of Table 1 obtained from a lease producing from the Arbuckle lime in Kansas.

FIND: Reserves and remaining economic life to an abandonment rate of 2,400 bbl. per half year using analytical and graphical methods.

METHOD OF SOLUTION: The equations on the next page relate production, time, and cumulative recovery:

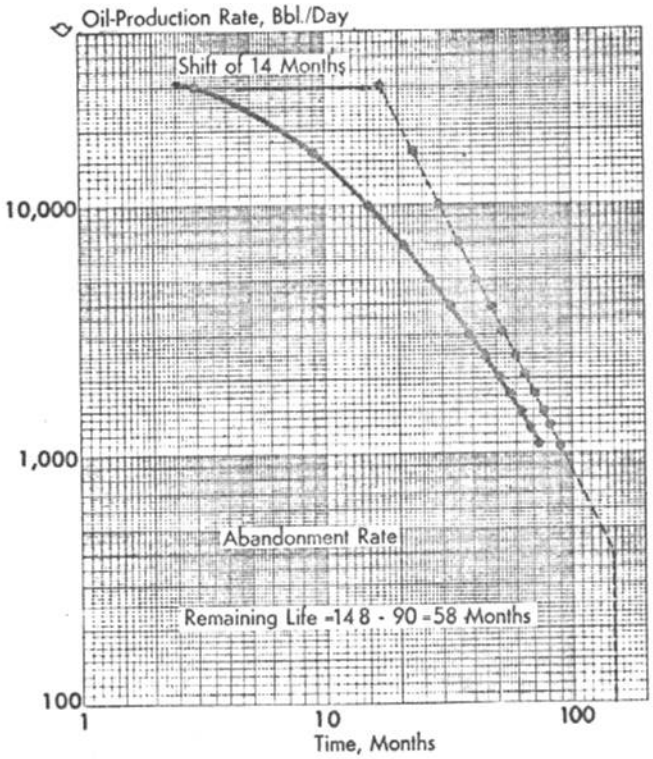

VARIATION of oil-production rate with time for Arbuckle limestone lease. Fig. 1.

TABLE 1—PRODUCTION DATA AND COMPUTATION OF DEC

(1) Date	(2) Time, Total	(3) months, Average	(4) Oil prod. rate, q_o bbl./mo.	(5) Δq_o $(4)_{n-1} - (4)_n$ bbl./mo.	(6) $q_{o(av)}$ $\frac{(4)_n + (4)_{n-1}}{2}$ bbl./mo.	(7) Monthly ratio $-a = \frac{\Delta q_o}{\Delta t = 6}$
1/52	6	3	29,500			
7/52	12	9	16,100	13,400	22,800	10.21
1/53	18	15	9,910	6,190	13,005	12.61
7/53	24	21	6,820	3,090	8,365	16.24
1/54	30	27	5,015	1,805	5,918	19.67
7/54	36	33	3,855	1,160	4,435	22.94
1/55	42	39	3,050	805	3,453	25.74
7/55	48	45	2,475	575	2,763	28.83
1/56	54	51	2,050	425	2,263	31.95
7/56	60	57	1,720	330	1,885	34.27
1/57	66	63	1,465	255	1,593	37.48
7/57	72	69	1,263	202	1,364	40.51
1/58	78	75	1,099	164	1,181	43.21
Future Performance						
7/58	6	3	965	134	1,032	46.27
1/59	12	9	854	111	910	49.27
7/59	18	15	761	93	808	52.27
1/60	24	21	683	78	722	55.27
7/60	30	27	616	67	650	58.27
1/61	36	33	558	58	587	61.27
7/61	42	39	508	50	533	64.27
1/62	48	45	465	43	487	67.27
7/62	54	51	427	38	446	70.27
1/63	60	57	393	34	410	73.27

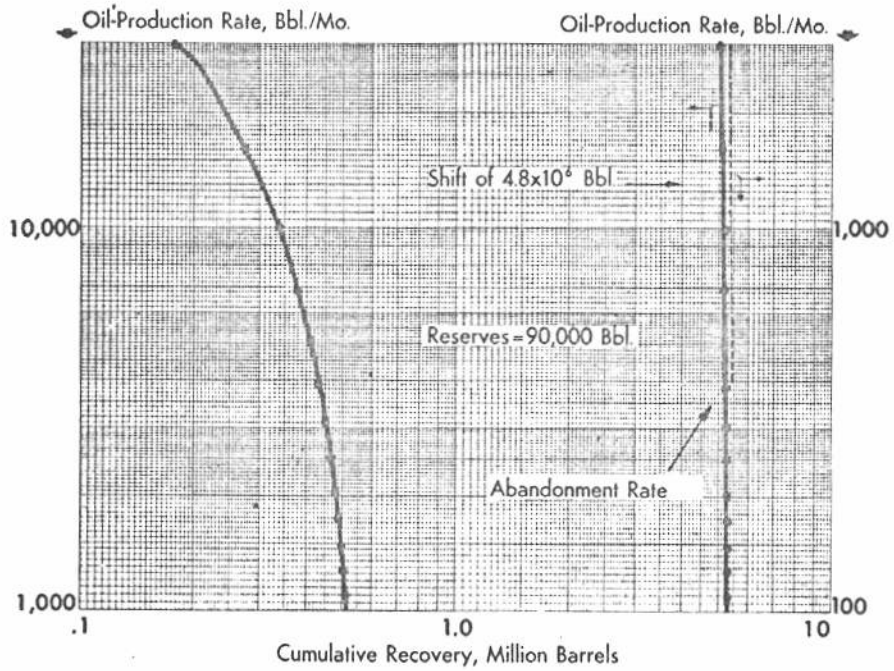

VARIATION of oil-production rate with cumulative recovery for Arbuckle limestone lease. Fig. 2.

$$a = -\frac{q_o}{dq_o/dt} \approx \frac{-q_{o(av)}}{\Delta q_o/\Delta t} \quad (1)$$

$$b = da/dt \approx \Delta a/\Delta t \quad (2)$$

$$q_o = q_{oi}\,(1 + bt/a_o)^{-1/b} \quad (3)$$

$$\text{at } t = o \quad a = a_o \quad (4)$$

$$N_p = \frac{(q_{oi})^b\, a_o}{1 - b} \times [(q_{oi})^{1-b} - (q_o)^{1-b}] \quad (5)$$

Where:

a = loss ratio.

q_o = oil-production rate at some time t.

t = time.

b = first derivative with respect to time of loss ratio.

q_{oi} = oil-production rate at zero time.

a_o = loss ratio at zero time.

N_p = cumulative oil recovery from zero time.

NSAS ARBUCKLE LIMESTONE LEASE

(8) Δa	(9) First derivative of loss ratio, $b \approx \Delta a/\Delta t$ $\Delta t = 6$ mo.	(10) Incremental recovery, bbl., (4) × 6	(11) Cumulative oil recovery, bbl.
...	....	177,000	177,000
...	....	96,600	273,600
2.40	0.400	59,460	333,060
3.63	0.605	40,920	373,980
3.43	0.572	30,090	404,070
3.27	0.545	23,130	427,200
2.80	0.467	18,300	445,500
3.09	0.515	14,850	460,350
3.12	0.520	12,300	472,650
2.32	0.387	10,320	482,970
3.21	0.535	8,790	491,760
3.03	0.505	7,578	499,338
2.70	0.450	6,594	505,932
	5.501		

$b = 5.501 \div 11 = 0.500$

erformance

3.00	0.500	5,790	511,722
3.00	0.500	5,124	516,846
3.00	0.500	4,566	521,412
3.00	0.500	4,098	525,510
3.00	0.500	3,696	529,206
3.00	0.500	3,348	532,554
3.00	0.500	3,048	535,602
3.00	0.500	2,790	538,392
3.00	0.500	2,562	540,954
3.00	0.500	2,358	543,312

SOLUTION: The solution to this problem is shown in Table 1. For July 1955:

$$a = \frac{2{,}763}{(3{,}050 - 2{,}475)/6} = 28.83$$

$$b = \frac{28.83 - 25.74}{6} = 0.515$$

For the future performance, factor b is constant at 0.500 and Δa is constant at 3.00. From these factors and Equation 1 the future performance data are determined. For example the rate for July 1961, is:

$$64.21 = \frac{(558 + q_o)/2}{(558 - q_o)/6}$$

from which:

$$q_o = 508$$

Equation 3 could also be used to obtain the future rates. Letting:

q_{oi} = 1,099 bbl./mo.
$q_{o\,(abnd)}$ = 400 bbl./mo.
b = 0.500.
a_o = 43.21.

and solving Equation 3 the remaining life is obtained:

$$400 = 1{,}099 \times \left[1 + \frac{(0.500)\,(t)}{43.21}\right]^{-1/0.5}$$

and $t \approx 57$ months.

This compares well with the 58 months found graphically in Fig. 1 and slightly less than 60 months computed in Table 1.

Remaining reserves are found using Equation 5:

$$N_p = \frac{(1.099)^{0.500}\ 43.21}{1.000 - 0.500} \times [(1{,}099)^{0.500} - (400)^{0.500}]$$

$$N_p = 37{,}871 \text{ bbl.}$$

From Table 1 the reserves are 543,312 − 505,932, or 37,380 bbl. These two compare well but deviate considerably from the value of about 90,000 bbl. in Fig. 2. Note that

the curve had to be shifted considerably before it became straight. In so doing it developed a very steep slope and moved to a region of high cumulative recovery values. Thus it became very insensitive to error and interpretation.

DISCUSSION: The hyperbolic or log-log type of decline is claimed by Arps[1 2] to occur most frequently. In this type both the rate-time and rate-cumulative recovery relationships are nonlinear on log-log plots, Figs. 1 and 2. An easier method of recognition is afforded by the loss ratio "a" defined by Equation 1. In column 7 of Table 1 it was computed with the approximate form of Equation 1.

Note that the loss ratio increases uniformly with time. This is an indication that the production may be declining hyperbolically. If the loss ratio remains essentially constant, the decline is exponential.[3]

Factor b is defined by Equation 2 and represents the first derivative of the loss ratio with respect to time, column 9, Table 1. Notice that it remains essentially constant around 0.500. This tendency of the b factor to remain constant shows that the decline is hyperbolic. When this factor is equal to 1, the decline is referred to as harmonic.

The analysis of hyperbolic decline-type curves is based on these assumptions: (1) the lease must have been producing at capacity, and (2) future trends will be the same as past trends.

In this problem 6-month production intervals were used to eliminate monthly fluctuations by using the general trend of the decline. The problem has been solved both analytically and graphically to show and compare the two approaches. Calculated future performance is shown in Table 1, remaining life and reserves have been found using Equations 3 and 5, and graphical solutions are shown in Figs. 1 and 2. Note in the figures that both curves had to be shifted in order to straighten them out. Values for remaining life found by the two methods agree quite well. However, this is not true in the case of reserves.

Analytical solution showed that some 38,000 bbl. of oil remain to be produced while graphically a value of more than 90,000 bbl. was obtained. In this case the graphical value is not reliable because of the steepness of the curve and its insensitivity to error.

Of the two methods used in solving this type problem, the graphical is more convenient and generally used. Except for special conditions, as in this problem, the graphical method is as accurate as the analytical approach. The latter method is useful in showing the type of decline through the computation of the loss ratio. It would also be preferred in machine computations. When time permits, both methods should be used in order to use one as a check on the other.

References

1. Arps, J. J., "Analysis of Decline Curves": Trans. AIME (1945), 160, 228.
2. Arps, J. J., "Estimation of Primary Oil Reserves": Trans. AIME (1956), 207, 182.
3. Guerrero, E. T., Part 37, The Oil and Gas Journal, May 22, 1961, p. 86.

Part 39

How to find ultimate recovery and performance of oil reservoirs

GIVEN: (1) Range of ultimate oil recoveries by type of drive, Table 1; (2) cumulative gas production vs. cumulative oil production for Bankline-Owen field in Texas, Fig. 1; (3) percentage of oil in total fluid produced vs. cumulative oil production for Calvin field in Illinois, Fig. 2; and (4) oil-water contact vs. cumulative oil production for lease in East Texas field, Fig. 3.

FIND: Use given data to estimate ultimate oil recovery by four empirical approaches.

SOLUTION: Table 1 shows ultimate recoveries by type of drive. The ranges and average values apply to most pools and are based on observed performances.[1 2 3] However, exceptions to these values can be found. Figs. 1, 2, and 3 show three correlations which can be used to find remaining reserves and ultimate recovery. Fig. 1 relates cumulative oil and gas recoveries on a log-log plot. Extrapolation of the general trend to total gas available gives an ultimate oil recovery of 172,000 bbl. in this example.

Fig. 2 shows a correlation of cumulative oil recovery with percentage of oil in total fluid produced on a semilog plot. Extrapolation of the trend to the abandonment water cut gives an estimated ultimate oil recovery of 342,000 bbl. for this field. Such a correlation is applicable to water drive or water-flood pools.

For an edge or bottom-water drive a correlation such as shown in Fig. 3 can often be used. Here cumulative oil recovery is related to elevation of oil-water contact. Extrapolation of the trend to the average top of the sand gives the ultimate oil recovery which, for the lease shown, is 216,000 bbl.

TABLE 1—RANGE OF ULTIMATE OIL RECOVERIES BY TYPE OF DRIVE

Type of drive—	Ultimate oil recoveries, per cent of initial in place: Range	Average
Liquid and rock expansion	2- 5	3
Solution gas	12-25	18
Gas cap	20-40	30
Edge water	35-60	45
Bottom water	20-40	30
Gravity	50-70	60

DISCUSSION:

Two previous problems (Pages 11 and 13) showed the use of decline curves, which are empirical methods. This problem illustrates four additional empirical methods.

If the initial oil in place and principal type of drive for a pool are known, then the data of Table 1 can be used as a guide to estimate ultimate oil recovery. They are based on observed and recorded performances.[1 2 3] Exceptions can be found, and the ranges and averages shown may change in future applications.

For example, the recovery by liquid and rock expansion depends largely on the amount of undersaturation involved. This is tending to

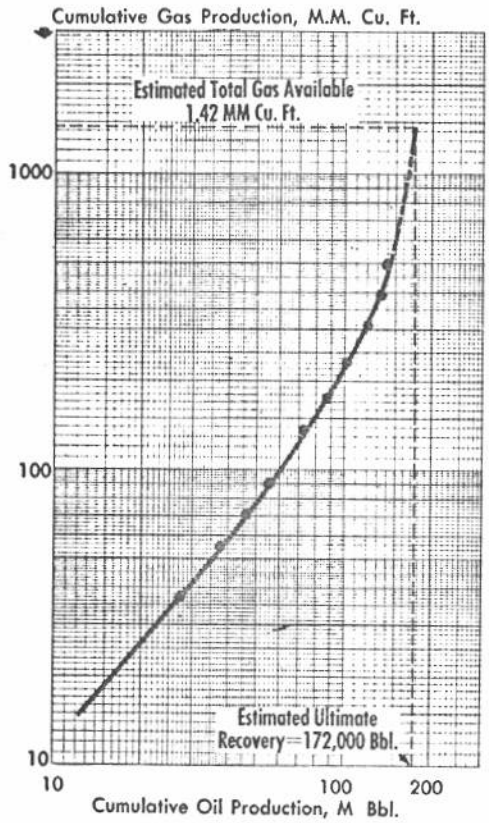

CUMULATIVE PRODUCTION DATA, both oil and gas, can be extrapolated to total available gas to estimate ultimate oil recovery. (After Arps[1].) Courtesy AIME. Fig. 1.

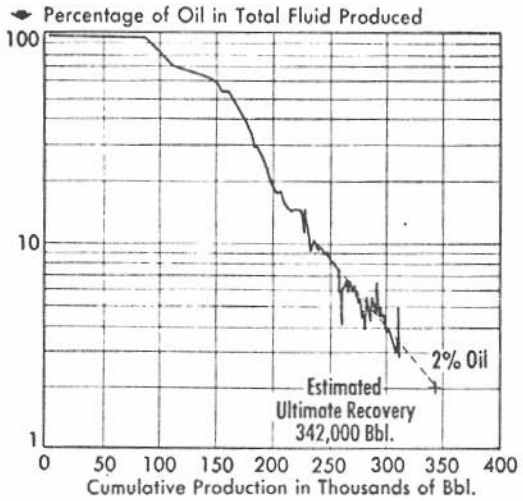

VARIATION of cumulative recovery with fraction of oil in total fluid, Tar Springs sand, Calvin field, Illinois. (After Arps[1].) Courtesy AIME. Fig. 2.

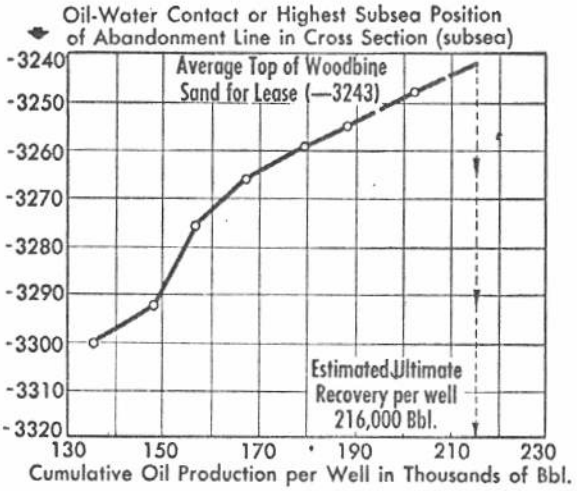

VARIATION of cumulative recovery with advancement of oil-water contact, East Texas field (After Arps[1].) Courtesy AIME. Fig. 3.

increase as deeper and deeper pools are discovered.

A notable exception to the values shown for liquid and rock expansion is that reported by E. V. Watts[6] for the D-7 zone in Ventura Avenue field where 40% of the initial oil in place was recovered. It may be possible in this case that gravity drainage assisted the liquid and rock expansion process.

Normally the driving mechanism in a pool involves several types of drive. Certainly fluid separation or gravity drainage is present in every case to a varying degree. Gas-cap and/or water drives may also augment solution-gas drives. Although all pools have combination drives, it is not uncommon to observe that one of the types of drives will be predominant. Under such conditions pools are referred to as having a single type of drive. This assumption is valid since the contribution from the other types is insignificant by comparison. Also, some of the ranges shown in Table 1 are influenced by combination drives. This is particularly true of the solution-gas and gas-cap drive ranges. The upper end of each of these ranges is believed to include some assistance from gravity drainage. The lower end of the ranges for these two types of drives may be due to poor sand conditions, thin oil sands, improper production practices, and other causes.

Efficiency obtained from an edgewater drive depends to a large extent on the uniformity of the formation and the size of the pool. Excessive nonuniformity leads to fingering of the water, bypassing of oil, and the production of large quantities of water along with the oil. In the larger pools a better sweep efficiency is obtained. Gravity is less of a factor here than in the case of the gas drive. This is due to the fact that oil and water do not differ appreciably in density.

A bottom-water drive is often less efficient in oil displacement than the edgewater drive. Bottom-water drive needs adequate vertical permeability. This permits the water to rise vertically and displace the oil to the producing wells. Involved in this process is the problem of water coning. This is more severe in thin formations than in the thicker formations, and explains to some degree the range in recoveries obtained. For a thin oil column of 10 to 15-ft. thickness the 20% value might even be high. In this case production rate would also have an effect on the recovery obtained. A low production rate would tend to minimize the coning problem and would afford time for gravity to as-

sist the recovery process.

Gravity drainage shows the highest ultimate oil recovery. This type of drive requires a dip of 10° or more and a permeability of 50 md. or greater. Recovery from this type of reservoir is rate sensitive. Therefore, the rate of production must be controlled to minimize pressure gradients in order to permit the differences in densities between the oil and gas to create a condition where the oil flows down and the gas flows up.

Pressure gradients created in the upper portions of the structure tend to eliminate the gravity effects. This type of drive seems to work best after the pressure in a pool has been depleted. It tends to be very slow and the higher recoveries are obtained from the larger pools where enough drainage occurs to make the operation economical.

It is well to point out again that the ranges and averages shown in Table 1 are based on past observations. They will probably decrease to some extent in the future because the fracturing well completion and workover technique has made possible the economical recovery of oil from poor-quality reservoirs. Many pools which could not be produced before because of very low permeabilities can now be exploited.

Figs. 1, 2, and 3 are examples of possible empirical correlations that can be used to estimate remaining reserves. Fig. 1 is based on the assumption that the amount of producible gas to abandonment conditions can be computed. Since gas moves freely through a reservoir it can generally be assumed that at abandonment residual gas will consist of that in solution plus free gas at abandonment pressure. This determination can be made with fair accuracy using volumetric and fluid-property data. Thus the end point to a curve such as that shown in Fig. 1 can be found.[1]

For water-drive fields correlations such as shown in Figs. 2 and 3 are popular. The end point in Fig. 2 is represented by the lowest oil percentage which, combined with a fluid-producing capacity of a lease, will just cover operating expenses. This plot shows a history correlation which can easily be extrapolated to an abandonment water cut of 98%.

In Fig. 3 the depth of the oil-water contact or abandonment contour is selected as the dependent variable and plotted against the cumulative oil recovery as the independent variable. Here the end point is the average depth of the top of the sand. The method of extrapolation is based on the simple assumption that when the abandonment contour progresses to the top of the sand, the lease must be abandoned. In this case also, history gave a correlation that could easily be extrapolated to the end point.[1]

This article presents examples of empirical methods for determining reserves and ultimate oil recovery. When careful judgment is used in their application reliable results can be obtained.

The use of the average values in Table 1 assumes that the type of drive for the pool in question can be defined and that its recovery will be equal to the average of many similar types of pools. The use of correlations such as shown in Figs. 1, 2, and 3 assumes that future performance will be similar to past performance.

References

1. Arps, J. J., "Estimation of Primary Oil Reserves": Trans. AIME (1956), 207, 182.
2. Craze, R. C., and Buckley, S. E., "A Factual Analysis of the Effect of Well Spacing on Oil Recovery": API Drilling and Prod. Pract. (1945), 144.
3. Guthrie, R. K., and Greenberger, M. H., "The Use of Multiple Correlation Analyses for Interpreting Petroleum-Engineering Data": API Drill. and Prod. Pract. (1955).
4. Güerrero, E. T., Part 37, The Oil and Gas Journal, May 22, 1961, p. 86.
5. Guerrero, E. T., Part 38, The Oil and Gas Journal, July 17, 1961, p. 94.
6. Watts, E. V., "Some Aspects of High Pressures in the D-7 Zone of the Ventura Avenue Field": Trans. AIME (1948), 174, 191.

Acknowledgment

The author acknowledges the assistance of T. W. Brinkley, Sunray Mid-Continent Oil Co., Tulsa, and P. Essley, of Skelly Oil Co., Tulsa, in the preparation of this article.

Part 40

Performance and ultimate oil recovery of a depletion-type pool

. . . by the Schilthuis material-balance approach

GIVEN: Production tests and history data show that a reservoir is of constant-volume type (no gas cap or water encroachment). It is also known that it was saturated at initial reservoir pressure of 2,500 psia. and temperature of 180° F.

Using the volumetric approach the initial oil in place was found to be 56 × 10^6 st. tk. bbl. The average water saturation for the pool was 20% and the relationship between the average permeability ratio and total liquid saturation is shown by Fig. 1. Other basic fluid-property data are shown in the first seven columns of Table 1.

FIND: Performance and ultimate oil recovery for this reservoir.

METHOD OF SOLUTION:

Schilthuis form of the material balance equation for a depletion-type pool is as follows:[1]

$$N = \frac{N_p [B_t + B_g (R_p - R_{sb})]}{B_t - B_{ob}} \quad (1)$$

In addition to this equation two others are required;[3] the instantaneous gas-oil-ratio equation:

$$R_i = R_s + \frac{k_g}{k_o} \frac{\mu_o}{\mu_g} \frac{B_o}{B_g} \quad (2)$$

and the total liquid-saturation equation:

$$S_L = S_w + (1.00 - S_w) \times [(N - N_p)/N] (B_o/B_{ob}) \quad (3)$$

where N, N_p, B_t, B_g, R_p, R_s, B_o, k_g, k_o, μ_o, μ_g, and S_w are AIME symbols,[2] and

R_i = instantaneous gas-oil ratio, s.c.f. per st. tk. bbl.

S_L = total liquid saturation, fraction of pore volume.

b = subscript indicating bubble point.

SOLUTION: Finding performance and ultimate oil recovery with Equations 1, 2, and 3 involves a trial-and-error procedure. In these computations it is convenient to use Equation 1 in a modified form obtained by dividing each side by N or:

$$1.000 = \frac{(N_p/N) [B_t + B_g (R_p - R_{sb})]}{B_t - B_{ob}} \quad (4)$$

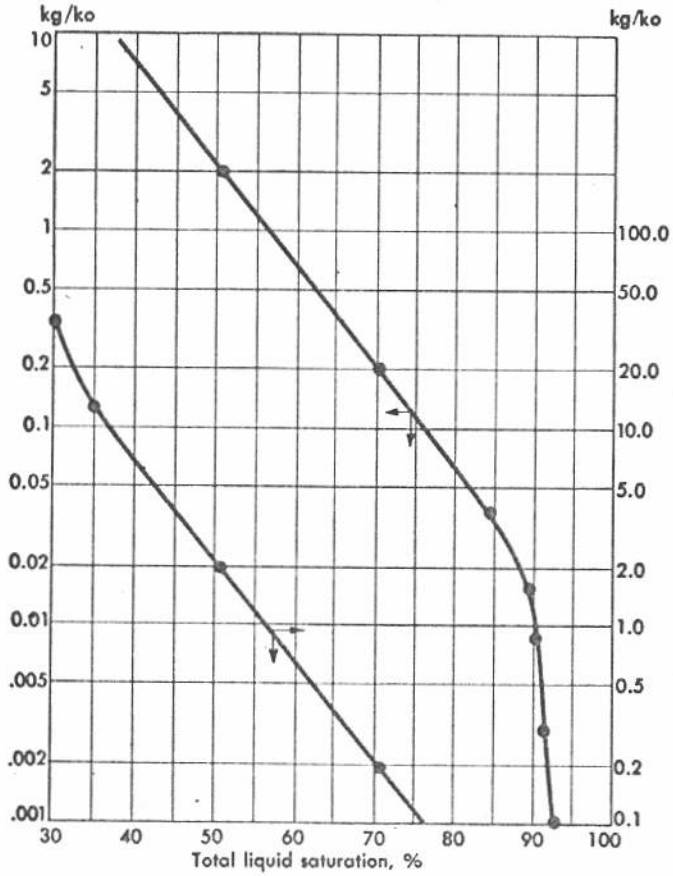

PERMEABILITY-RATIO RELATIONSHIP for depletion-type reservoir. Fig. 1.

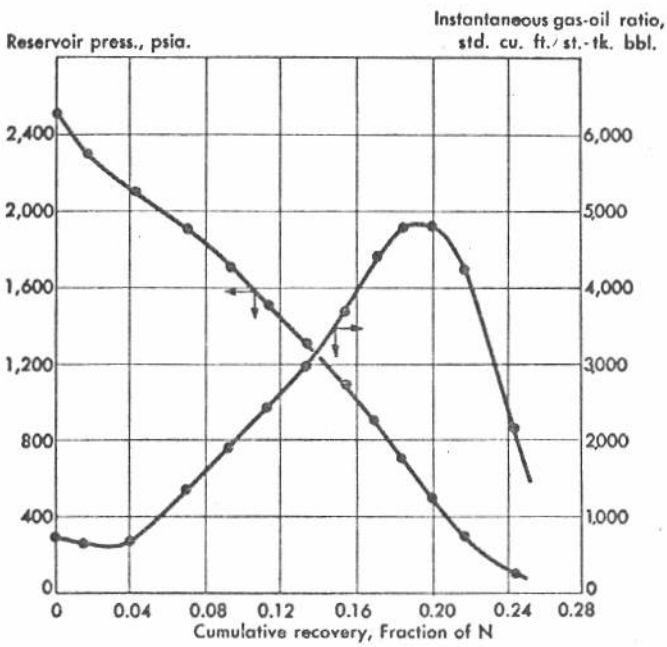

RESERVOIR pressure and gas-oil ratio vs. cumulative recovery in depletion-drive performance.

Equation 3 can also be modified to a more convenient form:

$$S_L = S_w + (1.00 - S_w) \times \frac{(N - N_p)/N}{N/N} \times \frac{B_o}{B_{ob}}$$

or

$$S_L = S_w + (1.00 - S_w) \times \frac{1.000 - (N_p/N)}{B_{ob}} \times B_o \quad (5)$$

Calculations involve the solution of Equation 4 at each reservoir pressure of interest. When correct data are used in Equation 4 for a certain pressure, the right-hand side will compute to be 1.0. Actually, in this equation all the data are known for a particular pressure except N_p/N and R_p.

An accepted computation procedure is as follows:

1. Estimate the incremental oil production ($\Delta N_p/N$) for a small drop in pressure (Δp = 200 psi. in this problem).

2. Compute the cumulative oil production to pressure $p_n = p_{n-1} - \Delta p$ by summing all incremental oil productions, or:

$$N_p/N = (1/N) \sum_{i=1}^{i=n} (\Delta N_p)_i \quad (6)$$

3. Solve Equation 5 for S_L at the reservoir pressure p_n of interest.

4. Obtain k_g/k_o corresponding to S_L using the permeability-ratio plot, Fig. 1, and solve Equation 2 for R_{in} at pressure p_n.

5. Compute the incremental gas production (ΔG_p) from:

$$\frac{\Delta G_p}{N} = \frac{\Delta N_p}{N} R_{iav} \quad (8)$$

where

$$R_{iav} = \frac{R_{i(n-1)} + R_{in}}{2} \quad (9)$$

6. Find cumulative gas production to pressure p_n using:

Table 1-Basic data and calculation of performance and reserv

$N = 56 \times 10^6$ STOB, $S_w = 0.20$, $W_p = 0$, $W_e = 0$

BASIC DATA						
(1) p, psia.	(2) B_o	(3) R_s s.c.f./st. tk. bbl.	(4) $B_g \times 10^3$ bbl./s.c.f.	(5) μ_o cp.	(6) μ_g cp.	(
2,500	1.498	721	1.048	0.488	0.0170	1.
2,300	1.463	669	1.155	0.539	0.0166	1.
2,100	1.429	617	1.280	0.595	0.0162	1.
1,900	1.395	565	1.440	0.658	0.0158	1.
1,700	1.361	513	1.634	0.726	0.0154	1.
1,500	1.327	461	1.884	0.802	0.0150	1.
1,300	1.292	409	2.206	0.887	0.0146	1.
1,100	1.258	357	2.654	0.981	0.0142	2.
900	1.224	305	3.300	1.085	0.0138	2.
700	1.190	253	4.315	1.199	0.0134	3.
500	1.156	201	6.163	1.324	0.0130	4.
300	1.121	149	10.469	1.464	0.0126	7.
100	1.087	97	32.032	1.617	0.0122	21.

$R_i = R_s + (k_g/k_o)(\mu_o/\mu_g)(B_o/B_g)$					(21)		
(16) k_g/k_o from Fig. 1	(17) B_o/B_g (2)/(4)	(18) μ_o/μ_g (5)/(6)	(19) $(\mu_o/\mu_g)(B_o/B_g)(k_g/k_o)$ (18)×(17)×(16)	(20) R_i R_s + (19) s.c.f./st. tk bbl.	$\frac{R_{in} + R_{i(n-1)}}{2}$ s.c.f./st. tk bbl.	(22) Gas production ΔG_p (8) × (21)	(23 ÷ N G Σ (2
0	1,429.4	28.706	0	721	....	.....	...
0	1,266.7	32.470	0	669	695	11.676	11.6
0.001	1,116.4	36.728	41	658	664	17.198	28.8
0.020	968.8	41.646	807	1,372	1,015	27.913	56.7
0.035	832.9	47.143	1,374	1,887	1,630	37.653	94.4
0.051	704.4	53.467	1,921	2,382	2,135	45.903	140.3
0.072	585.7	60.753	2,562	2,971	2,677	49.525	189.8
0.102	474.0	69.085	3,340	3,697	3,334	73.348	263.2
0.140	370.9	78.623	4,083	4,388	4,043	59.836	323.0
0.183	275.8	89.478	4,516	4,769	4,579	68.685	391.7
0.240	187.6	101.846	4,585	4,786	4,778	74.059	465.7
0.327	107.1	116.190	4,069	4,218	4,502	79.235	545.0
0.456	33.9	132.541	2,049	2,146	3,182	81.141	626.1

$$G_p/N = (1/N) \sum_{i=1}^{i=n} (\Delta G_p)_i \quad (10)$$

7. Solve for R_p at p_n with the equation that defines this variable:

$$R_p = \frac{G_p/N}{N_p/N} \quad (11)$$

8. Using the N_p/N of step 2 and R_p of step 7 solve Equation 4. If the right-hand side does not equal 1.0, estimate another value for ΔN_p and repeat the entire procedure. The trial - and - error procedure is continued until the solution of Equation 4 yields 1.0.

For example, if p_n = 1,700 psia., assume $\Delta N_p/N = 0.0231$ for Δp = 200 psi. between 1,900 and 1,700 psia.

Thus, $N_p/N = 0.0168 + 0.0259 + 0.0275 + 0.0231 = 0.0933$.

$$S_L = 0.20 + (1.00 - 0.20) \times \frac{1.0000 - 0.0933}{1.498} \times 1.361$$

$$S_L = 0.20 + 0.80 \times \frac{0.9067}{1.498} \times 1.361 = 0.200 + 0.659 = 0.859$$

From Fig. 1, $k_g/k_o = 0.035$ and:

$$R_i = 513 + (0.035) \times \frac{1.361}{0.001634} \times \frac{0.726}{0.0154} = 1,887 \text{ s.c.f./st. tk. bbl.}$$

$$R_{iav} = \frac{1,372 + 1,887}{2} = 1,630 \text{ s.c.f./st. tk. bbl.}$$

$$\Delta G_p/N = (0.0231)\ (1,630) = 37.653$$

$$G_p/N = 11.675 + 17.198 + 27.913 + 37.653 = 94.440$$

a depletion-type pool using Schilthuis material-balance approach

$$S_L = S_w + (1.00 - S_w)\ [1.00 - (N_p/N)]\ (B_o/B_{ob})$$

(8) ...very, fraction of initial in place, ΔN_p	(9) N_p	(10) $\frac{N - N_p}{1.00 - (9)}$	(11) $\frac{N - N_p}{N}$ $\frac{1.00 - (9)}{1.00}$	(12) B_o/B_{ob} $(2)/B_{ob}$	(13) $\frac{N-N_p}{N} \times \frac{B_o}{B_{ob}}$ (11) × (12)	(14) $\frac{N-N_p}{N} \times \frac{B_o}{B_{ob}}$ × (1.00 − S_w) (13) (0.80)	(15) S_L 0.20 + (14)
0	0	1.0000	1.0000	1.000	1.000	0.800	1.000
168	0.0168	0.9832	0.9832	0.977	0.961	0.769	0.969
259	0.0427	0.9573	0.9573	0.954	0.913	0.730	0.930
275	0.0702	0.9298	0.9298	0.931	0.866	0.693	0.893
231	0.0933	0.9067	0.9067	0.909	0.824	0.659	0.859
215	0.1148	0.8852	0.8852	0.886	0.784	0.627	0.827
185	0.1333	0.8667	0.8667	0.862	0.747	0.598	0.798
220	0.1553	0.8447	0.8447	0.840	0.710	0.568	0.768
148	0.1701	0.8299	0.8299	0.817	0.678	0.542	0.742
150	0.1851	0.8149	0.8149	0.794	0.647	0.518	0.718
155	0.2006	0.7994	0.7994	0.772	0.617	0.494	0.694
176	0.2182	0.7818	0.7818	0.748	0.585	0.468	0.668
255	0.2437	0.7563	0.7563	0.726	0.549	0.439	0.639

$$1.000 = \frac{(N_p/N)\ [B_t + B_g\ (R_p - R_{sb})]}{B_t - B_{ob}}$$

(24) R_p G_p/N_p st. tk bbl.	(25) $R_p - R_{sb}$ (24) − 721 s.c.f./st. tk bbl.	(26) $B_g\ (R_p - R_{sb})$ (4) × (25)	(27) $B_t + B_g$ × $(R_p - R_{sb})$	(28) $N_p \times (27)$	(29) $B_t - B_{ob}$ $B_t - 1.498$ (7) − 1.498	(30) N (28) ÷ (29) = 1.000	(31) Cumulative recovery N_p bbl. (9) × 56 × 10^6
...	...	...	...	...	...	...	...
695	−26	−0.030	1.493	0.02508	0.025	1.003	940,800
676	−45	−0.058	1.504	0.06422	0.064	1.003	2,391,200
809	88	0.127	1.747	0.12264	0.122	1.005	3,931,200
,012	291	0.475	2.176	0.20302	0.203	1.000	5,224,800
,223	502	0.946	2.763	0.31719	0.319	0.994	6,428,800
,424	703	1.551	3.518	0.46895	0.469	1.000	7,464,300
,695	974	2.585	4.836	0.75103	0.753	0.997	8,696,800
,899	1,178	3.887	6.484	1.10293	1.099	1.004	9,525,600
,116	1,395	6.019	9.228	1.70810	1.711	0.998	10,365,600
,322	1,601	9.867	14.228	2.85414	2.863	0.997	11,233,600
,498	1,777	18.603	25.712	5.61036	5.611	1.000	12,219,200
,569	1,848	59.195	80.270	19.56180	19.577	0.999	13,647,200

$$R_p = \frac{94.440}{0.0933} = 1{,}012 \text{ s.c.f./st. tk. bbl.}$$

$$1.000 = \frac{0.0933\ [1.701 + 0.001634\ (1{,}012 - 721)]}{1.701 - 1.498}$$

$$= \frac{(0.0933)\ (2.176)}{0.203} = 1.000$$

DISCUSSION: Performance of oil-producing reservoirs is determined mostly by the nature of the energy available for moving the oil to the well bores. It is influenced also by the way existing energy is used during the production history. These controlling factors in turn depend on several variables such as reservoir structural conditions, nature of the oil, gas in solution, flow capacity of the rock, mobility of contiguous aquifers, if present, and rates of oil, gas, and water withdrawal.[4]

Principal natural energies are (1) expansion of oil, water, and rock, (2) force of gravity, (3) expansion of gas coming out of solution, (4) expansion of initially free gas, and (5) expansion of waters in reservoirs that are in communication with the oil column. In actual practice conditions are never such that an oil reservoir can be described throughout its life by any single type of producing mechanism. Very often, however, one of the natural types of energy will predominate and control the performance of a pool.

Energy for a depletion-type drive comes from gas dissolved in the oil. It is made available as this gas comes out of solution and expands in place, or flows to low-pressure regions surrounding the producing wells.[4] As pressure declines, more gas comes from solution and expands with previously evolved gas. Then an equivalent volume of oil and gas is expelled from the rock into the well bores.

The solution of this problem involves the material-balance equation for a depletion-type reservoir, (Equation 1) the instantaneous gas-oil-ratio equation, (Equation 2) and the liquid saturation equation, (Equation 3). While the basic principles involved in these equations are well understood, we need to introduce simplifications in their application. These include the assumptions of (1) reservoir uniformity, (2) neglect of the localization of actual fluid withdrawals through well bores, and (3) neglect of the effect of gravity in inducing fluid segregation and downstructure gravity drainage of the oil.[4] In addition, it is assumed that the pool in question is one deriving its energy principally from expansion of gas initially in solution. This can best be established with production tests, and pressure and production history.

Table 1 shows the basic data and calculated results for performance and reserves of the pool in question. Note that the first seven columns give the necessary pressure and fluid property data. In addition to this, the permeability-ratio relationship for this pool is given in Fig. 1.

A major portion of the work involved in solving problems of this nature is consumed in the collection, analysis, and evaluation of the basic data. It should be obvious that the results depend, to a large degree, on the use of average rock and fluid-property data as well as reservoir-pressure data. Note that columns 8 through 15 are a solution of Equation 5; columns 16 through 20, a solution of Equation 2; and columns 25 through 30, a solution of Equation 4.

Note that Equation 9 adds an assumption to those listed above. Here it is assumed that the producing gas-oil ratio varies linearly throughout a pressure increment. This assumption simplifies the computation of produced gas and cumulative gas-oil ratio. Note in column 30 that the trial-and-error procedure is continued until the incremental recovery, ΔN_p, satisfies Equation 4 to an accuracy of $\pm 1\%$.[3] Only the best-fitting values are shown in Table 1. Normally it takes from three to four estimates of the incremental production to satisfy Equation 4 to the accuracy desired.

Columns 8 and 9 of Table 1 show the incremental and cumulative recoveries expressed as fractions of initial oil in place. Values in column 9 have been converted to cumulative recovery in stock-tank barrels in column 31. Note in column 9 that the cumulative oil recovery to a pressure of 300 psi. is about 22% of the initial oil in place. Such a cumulative recovery is representative of recoveries obtained in depletion-type pools.

This problem has shown that the Schilthuis form of the material-balance equation can conveniently be used for a trial-and-error solution of depletion-drive problems. The method is flexible and can be easily modified for special applications. The same cannot be as readily done with the Tarner approach[5] and the Muskat method,[4] particularly when gravity segregation occurs simultaneously with the depletion process, and when considering the effect of gas injection and cycling under the assumption that only part of the reservoir rock is contacted by the injected gas.[3]

The final results of the problem are plotted in Fig. 2. Shown are reservoir pressure and gas-oil ratio vs. cumulative recovery. In spite of the drastic assumptions made in the solution of the equations, these graphs show typical depletion-drive behavior. The reservoir pressure declines rather rapidly while the gas-oil ratio remains fairly constant in the initial stages and then rises rapidly to a peak. When most of the gas has been produced the gas-oil ratio declines rapidly.

Reservoir performance here has been related to reservoir pressure. In a subsequent problem it will be related to the more desirable parameter of time. Generally the computations involved in the solution of this problem are rather tedious, but this type of problem can easily be adapted to an electronic computer.

References

1. Schilthuis, R. D., "Active Oil and Reservoir Energy": Trans. AIME, (1936) 118, 33.
2. "Standard Letter Symbols for Petroleum Reservoir Engineering and Electric Logging": Journal of Petroleum Technology, (Oct. 1956).
3. Pirson, S. J., "Oil Reservoir Engineering": McGraw-Hill Book Co., second edition, 1958.
4. Muskat, M., "Physical Principles of Oil Production": McGraw-Hill Book Co., first edition, 1949.
5. Tarner, J., "How Different Size Gas Caps and Pressure-Maintenance Programs Affect Amount of Recoverable Oil": Oil Weekly, June 12, 1944.

Part 41

How to find performance and ultimate oil recovery of a depletion-type pool

. . . using the Muskat material-balance approach

GIVEN: Production tests and history data show that a reservoir is of constant volume (no gas cap or water encroachment). It was found also that this pool was saturated at initial reservoir pressure of 2,500 psia. and reservoir temperature of 180° F. Using the volumetric approach, the initial oil in place was found to be 56×16^6 stock-tank barrels. Average water saturation for the pool was 20.0% and the average permeability ratio-total liquid saturation relationship that shown by Fig. 1 on Page 18. All of the conditions and data for this problem are identical to that of the problem starting on Page 18. Consequently, other basic data required for the solution are given in the first six columns of Table 1, Page 18.

FIND: Performance and ultimate oil recovery for the reservoir using the Muskat material-balance approach.[2]

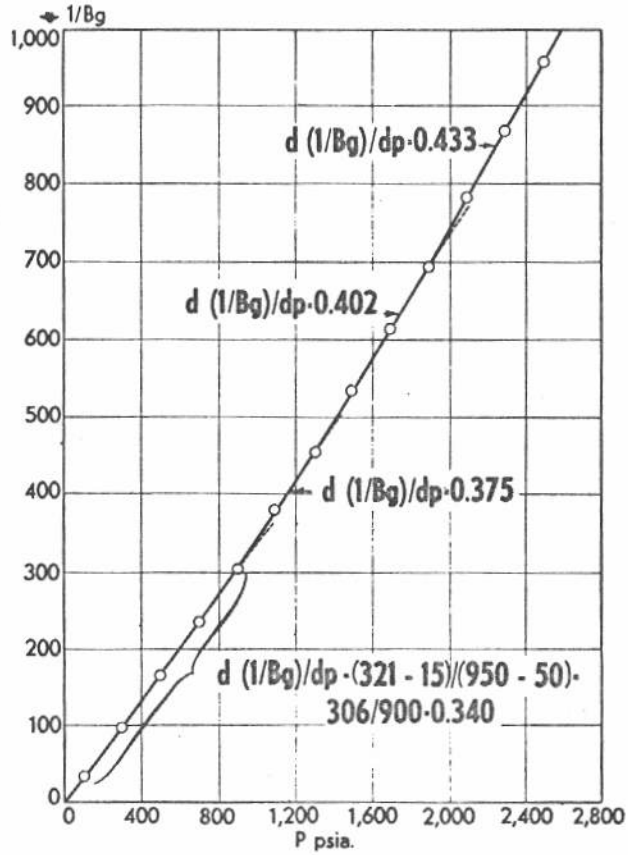

SLIGHT CURVE results when $1/B_g$ is plotted against p, but it can be approximated by four straight-line portions, Fig. 1.

METHOD OF SOLUTION: Muskat's form of the material-balance equation for a depletion type pool is as follows:[2]

$$\frac{dS_o}{dp} \approx \frac{\Delta S_o}{\Delta p} \approx \frac{S_o\lambda(p) + S_o(k_g/k_o)\eta(p) + (1.00 - S_o - S_w)\epsilon(p)}{1 + (\mu_o/\mu_g)(k_g/k_o)} \quad (1)$$

Where:

$$\lambda(p) = \frac{B_g}{B_o}\frac{dR_s}{dp} \quad (2)$$

$$\eta(p) = \frac{1}{B_o}\frac{\mu_o}{\mu_g}\frac{dB_o}{dp} \quad (3)$$

$$\epsilon(p) = B_g\frac{d(1/B_g)}{dp} \quad (4)$$

and S_o, p, k_g, k_o, S_w, μ_o, μ_g, B_g, B_o and R_s are standard AIME symbols.[3]

SOLUTION: Finding performance and ultimate oil recovery with Equation 1 involves the following procedure:

1. Plot R_s vs. p and develop $\frac{dR_s}{dp}$ vs. p.

In this problem the plot R_s vs. p yielded a straight line between the pressures of 2,500 and 100 psia. The slope of the line was $\frac{dR_s}{dp} = 0.260$ and the equation of the straight line was

$$R_s = 0.260\,p + 71 \quad (5)$$

2. Plot B_o vs. p and develop $\frac{dB_o}{dp}$ vs. p.

Table 1—Basic data and computation of performance for

(1) p, psia.	(2) B_o	(3) $B_g \times 10^3$ bbl./s.c.f.	(4) $B_g/B_o \times 10^3$	(5) R_s s.c.f./STB	(6) $\lambda(p) = (B_g/B_o)(dR_s/dp) = (4) \times 0.26 \times 10^3$	(7) μ_o, cp.	(8) μ_g, cp.	(9) μ_o/μ_g
2,500	1.498	1.048	0.700	721	0.182	0.488	0.0170	28.71
2,300	1.463	1.155	0.789	669	0.205	0.539	0.0166	32.47
2,100	1.429	1.280	0.896	617	0.233	0.595	0.0162	36.73
1,900	1.395	1.440	1.032	565	0.268	0.658	0.0158	41.65
1,700	1.361	1.634	1.201	513	0.312	0.726	0.0154	47.14
1,500	1.327	1.884	1.420	461	0.369	0.802	0.0150	53.47
1,300	1.292	2.206	1.707	409	0.444	0.887	0.0146	60.75
1,100	1.258	2.654	2.110	357	0.549	0.981	0.0142	69.08
900	1.224	3.300	2.696	305	0.701	1.085	0.0138	78.62
700	1.190	4.315	3.626	253	0.943	1.199	0.0134	89.48
500	1.156	6.163	5.331	201	1.386	1.324	0.0130	101.85
300	1.121	10.469	9.339	149	2.428	1.464	0.0126	116.19
100	1.087	32.032	29.468	97	7.662	1.617	0.0122	132.54

(18) $S_o(k_g/k_o) =$ (14)×(15)	(19) $S_o \frac{k_g}{k_o} \eta(p)$ (18)×(11)×10^3	(20) $1.0000-S_w-S_o$ $=1.0000-0.2000$ $-(14)$	(21) $(20 \times \epsilon(p))$	(22) $1+\frac{\mu_o}{\mu_g}\frac{k_g}{k_o}$ $=1+(16)$	(23) [(17)+(19)+(21)] $\times 10^3$	(24) $\Delta S_o/\Delta p =$ [(23) ÷ (22)] $\times 10^3$	(25) $\frac{(\Delta S_o/\Delta p)_{n-1}+(24)_n}{2}$
0.0000	0.0000	0.0000	0.0000	1.0000	0.1456	0.1456	0.1456
0.0000	0.0000	0.0291	0.0146	1.0000	0.1726	0.1726	0.1591
0.0000	0.0000	0.0663	0.0367	1.0000	0.2077	0.2077	0.1902
0.0145	0.0740	0.1113	0.0695	1.8747	0.3281	0.1750	0.1914
0.0236	0.1398	0.1431	0.0940	2.6970	0.4388	0.1627	0.1689
0.0327	0.2253	0.1744	0.1320	3.7911	0.5881	0.1551	0.1589
0.0446	0.3586	0.2047	0.1816	5.5563	0.8045	0.1448	0.1500
0.0590	0.5540	0.2327	0.2315	8.1843	1.0969	0.1340	0.1394
0.0758	0.8325	0.2584	0.2899	12.0068	1.5021	0.1251	0.1296
0.0952	1.2240	0.2825	0.4144	17.4643	2.1264	0.1218	0.1235
0.1199	1.8065	0.3066	0.6423	25.7496	3.1327	0.1217	0.1218
0.1515	2.6852	0.3309	1.1777	38.5294	5.0019	0.1298	0.1258
0.1977	4.1220	0.3578	3.8968	60.2454	11.4069	0.1893	0.1596

In this problem the plot of B_o vs. p gave a straight line between the pressures of 2,500 and 100 psia. This is normally true in most cases.

The slope and equation of the line were $\frac{dB_o}{dp} = 0.000171$ and

$$B_o = 1.71 \times 10^{-4}p + 1.07 \quad (6)$$

3. Plot $1/B_g$ vs. p and develop $\frac{d(1/Bg)}{dp}$ vs. p.

In this problem the plot of $\frac{1}{B_g}$ vs. p gave a slightly curving line that could be approximated with four straight-line portions, Fig. 1. In most field cases similar divisions can be used.

Thus slopes were developed for pressure intervals as follows:

Pressure Interval, psi.	Slope, $\frac{d(1/B_g)}{dp}$
2,500-1,850	0.433
1,850-1,250	0.402
1,250- 950	0.375
950- 50	0.340

4. Solve Equation 1 for initial pressure and oil-saturation conditions

$$S_{oi} = 1.0000 - 0.2000 = 0.8000$$

5. Estimate the oil saturation at the next pressure point (2,300 psi.).

$$S_{on} = S'_{o(n-1)} - (p_{n-1}-p_n)(\Delta S_o/\Delta p)_{(n-1)} \quad (7)$$

$$= 0.8000 - (2,500 - 2,300) \times (0.0001456)$$

$$= 0.8000 - 0.0291 = 0.7709$$

Where $S'_{o(n-1)}$ is computed (see step 9).

letion-type pool using Muskat's material balance method

(10) μ_o/μ_g B_o ÷ (2)	(11) $\eta(p) = \frac{\mu_o}{\mu_g}\frac{1}{B_o}\frac{dB_o}{dp}$ (10) × 0.000171 × 10^3	(12) $\frac{d(1/B_g)}{dp} \times 10^3$ From Fig. 1	(13) $\epsilon(p) = B_g \times \frac{d(1/B_g)}{dp}$ (3)×(12)×10^3	(14) Est. S_o $= (28)_{n-1} - (\Delta S_o/\Delta p)_{n-1}\Delta p$	(15) k_g/k_o for $S_L = S_o + 0.20$	(16) $(\mu_o/\mu_g)(k_g/k_o)$ (9) × (15)	(17) $S_o \lambda(p) =$ (14)×(6)×10^3
19.17	3.278	0.433	0.454	0.8000	0.0000	0.0000	0.1456
22.19	3.794	0.433	0.500	0.7709	0.0000	0.0000	0.1580
25.70	4.395	0.433	0.554	0.7337	0.0000	0.0000	0.1710
29.86	5.106	0.433	0.624	0.6887	0.0210	0.8747	0.1846
34.64	5.923	0.402	0.657	0.6569	0.0360	1.6970	0.2050
40.29	6.890	0.402	0.757	0.6256	0.0522	2.7911	0.2308
47.02	8.040	0.402	0.887	0.5953	0.0750	4.5563	0.2643
54.91	9.390	0.375	0.995	0.5673	0.1040	7.1843	0.3114
64.23	10.983	0.340	1.122	0.5416	0.1400	11.0068	0.3797
75.19	12.857	0.340	1.467	0.5175	0.1840	16.4643	0.4880
88.11	15.067	0.340	2.095	0.4934	0.2430	24.7496	0.6839
03.65	17.724	0.340	3.559	0.4691	0.3230	37.5294	1.1390
21.93	20.850	0.340	10.891	0.4422	0.4470	59.2454	3.3881

(26) $\Delta S_o =$ 25) × Δp = 200 psi.	(27) $\Sigma \Delta S_o =$ Σ (26)	(28) Computed S_o' 0.8000 − (27)	(29) $S_o \div (1 - S_w)$ (28) ÷ 0.8000	(30) B_{oi}/B_o 1.498 ÷ (2)	(31) (29) × (30)	(32) $N_p/N =$ 1 − (31)	(33) N_p (32)×56×10^6 st.-tk. bbl.
0.0000	0.0000	0.8000	.....	...	.....	.....	.....
0.0318	0.0318	0.7682	0.9603	1.024	0.9833	0.0167	935,200
0.0380	0.0698	0.7302	0.9128	1.048	0.9566	0.0434	2,430,400
0.0383	0.1081	0.6919	0.8649	1.074	0.9289	0.0711	3,981,600
0.0338	0.1419	0.6581	0.8226	1.101	0.9057	0.0943	5,280,800
0.0318	0.1737	0.6263	0.7829	1.129	0.8839	0.1161	6,501,600
0.0300	0.2037	0.5963	0.7454	1.159	0.8639	0.1361	7,621,600
0.0279	0.2316	0.5684	0.7105	1.191	0.8462	0.1538	8,612,800
0.0259	0.2575	0.5425	0.6781	1.224	0.8300	0.1700	9,520,000
0.0247	0.2822	0.5178	0.6473	1.259	0.8150	0.1850	10,360,000
0.0244	0.3066	0.4934	0.6168	1.296	0.7994	0.2006	11,233,600
0.0252	0.3318	0.4682	0.5853	1.336	0.7820	0.2180	12,208,000
0.0319	0.3637	0.4363	0.5454	1.378	0.7516	0.2484	13,910,400

$$\frac{\Delta S_o}{\Delta p} = \frac{(0.8000)\times\frac{0.001048}{1.498}\times(0.26)+(0.8000)(0)\times\frac{0.488}{0.0170}\times\frac{1}{1.498}(0.000171)}{1+\frac{0.488}{0.0170}(0)}$$

$$+\frac{(1.0000-0.8000-0.2000)(0.001048)(0.433)}{1+\frac{0.488}{0.0170}(0)}$$

$$= [(0.8000)(0.000182) + (0.8000)(0)(0.003278)$$

$$+ (1.000 - 0.8000 - 0.2000)(0.000454)]/1.0$$

$$= 0.0001456$$

6. Solve Equation 1 for the oil saturation obtained in step 5. This gives $\frac{\Delta S}{\Delta P} = 0.0001726$

7. Develop an average $\frac{\Delta S_o}{\Delta P}$ for the pressure interval 2,500-2,300 psi.

$$(\Delta S_o/\Delta p)_{av} = [(\Delta S_o/\Delta p)_{(n-1)} + (\Delta S_o/\Delta p)_n]/2$$

$$= \frac{0.0001456 + 0.0001726}{2}$$

$$= 0.0001591 \qquad (8)$$

8. Compute the change in reservoir-oil saturation for the pressure interval 2,500-2,300 psi.

$$\Delta S_o = (\Delta S_o/\Delta p)_{av}\, \Delta p \qquad (9)$$

$$= (0.0001591)\,(200) = 0.0318$$

9. Compute the reservoir residual-oil saturation at the end of the pressure interval (2,300 psi.).

$$S_o'_n = S_{oi} - \sum_{j=1}^{j=n} \Delta S_{oj}$$

$$= 0.8000 - 0.0318 = 0.7682$$

This value becomes the $S_{o\,(n-1)}$ for the next pressure interval.

10. Repeat steps 5 through 9 for successive pressure intervals.

11. Convert the results to cumulative oil recovery in stock-tank barrels.

$$N_p = N\,\{1.000 - [S_o'_n/(1-S_w)]\, B_{oi}/B_o\} \qquad (10)$$

At 2,300 psi.

$$N_p = 56 \times 10^6\,\{1.000 - [0.7682/(1.00 - 0.20)]\, 1.498/1.463\}$$

$$= 56 \times 10^6 \times [1.0000 - (0.9603)\,(1.024)]$$

$$= 56 \times 10^6\,[1.0000 - 0.9833]$$

$$= 935{,}200 \text{ St.-tk. bbl.}$$

Table 1 shows the calculations and results for all the pressure intervals. The first 24 columns contain the basic data and show calculation steps in the solution of Equation 1. Columns 25 through 28 show the computation of oil saturation and columns 29 through 33 show the computation of cumulative oil recovery.

Discussion. Muskat derived a material-balance equation by considering the stock-tank-oil content and gas content of a unit volume of reservoir pore space.[2 4 5] His final equation is in differential form and is applicable to elementary volumes of the reservoir between which pressure gradients are assumed negligible. The reservoir is considered a homogeneous medium with uniform pressure throughout. The reservoir volume is considered constant and each volume element of the reservoir is treated independently and is required to satisfy conservation requirements of the oil and gas contents. The equation is solved using a single reservoir unit element and average reservoir conditions. The results thus obtained are applied to all reservoir elements since it is assumed that they all behave similarly.

Equation 1 is a first-order ordinary differential equation that expresses the variation of oil saturation with pressure at any point in the history of the reservoir. Note that all the factors involved are functions of pressure with the exception of the relative-permeability ratio (k_g/k_o) and the oil and water saturations. Since the water saturation is considered constant, this equation can be solved at any pressure if the oil saturation is known.

Initial oil saturation is normally known and thus Equation 1 can be solved at this point. For subsequent points various different approaches can be used. If small pressure decrements are used, the error which results from the assumption of an oil saturation equal to that existing at the start of the pressure decrement will be small.[5] This characteristic makes the Muskat method particularly amenable to solution by either medium or high-speed computers.

A better solution can be obtained by assuming that the oil saturation will vary linearly with pressure throughout the pressure decrement. The oil saturation at the end of the pressure decrement is then computed with Equation 7 and Equation 1 then solved for this saturation. If preferred, still better solutions can be obtained by integrating Equation 1 numerically using the method of successive approximations or either the Runge-Kutta or Milne methods.[6 7] These methods are normally not used because they are tedious, and the improved accuracy is actually not warranted.

The results obtained are used with other factors such as net sand volume and porosity which are usually not as accurate. The solution used in this problem represents the first step of the method of successive approximations. This solution is recommended since it is more accurate and requires no more effort than supposedly simpler approaches. Table 1 shows this solution. Columns 1 through 24 contain basic data and show the steps in the solution of Equation 1. Columns 25 through 28 show the solution of residual-oil saturation. Correct solution of Equation 1 would show the same values of oil saturation in columns 14 and 28.

Columns 28 through 33 show the conversion of residual-oil saturation to cumulative oil recovery, or the solution of Equation 10. As the same data were used in this problem as in that on Page 18, a comparison can be made of the results obtained by the Schilthuis and Muskat material-balance approaches. Column 32 of Table 1 is comparable to column 9, Page 19, and column 33 of Table 1 can be compared with column 31, Page 20. The comparison shows, in this case, that the two methods give nearly identical results.

Muskat's method of predicting oil recovery and performance is particularly advantageous when a large number of computations are required, as is the case in theoretical studies concerning the influence of various factors, and where the reservoir rock and fluid properties remain the same. For such a case, the pressure factors defined by Equations 2, 3, and 4 can be determined at various pressures and graphs constructed to show their variation with pressure.

References

1. Guerrero, E. T., Part 40: The Oil and and Gas Journal, Sept. 11, 1961, p. 111.
2. Muskat, M., "Physical Principles of Oil Production": McGraw-Hill Book Co., Inc., first edition (1949).
3. "Standard Letter Symbols for Petroleum Reservoir Engineering and Electric Logging": Journal of Petroleum Technology, October 1956.
4. Pirson, S. J., "The Engineering Approach to Oil Reservoir Controls": Oil Weekly, Dec. 31, 1945, p. 22.
5. Pirson, S. J., "Oil Reservoir Engineering" second edition: McGraw-Hill Book Co., Inc. (1958).
6. Scarborough, J. B., "Numerical Mathematical Analysis," fourth edition: Johns-Hopkins Press (1958).
7. Hildebrand, F. B., "Advanced Calculus for Engineers": Prentice-Hall, Inc. (1949).